Proteomic Characterization of Oxidative Stress Related Alterations in Adult and Senescent Primary Hepatocytes

Dissertation

zur Erlangung des Grades
des Doktors der Naturwissenschaften
der Naturwissenschaftlich-Technischen Fakultät
der Universität des Saarlandes

von
Malina Orsini
Saarbrücken
2018

Tag des Kolloquiums:	11. Januar 2019
Dekan:	Prof. Dr. Guido Kickelbick
Berichterstatter:	Prof. Dr. Elmar Heinzle
	Prof. Dr. Gert-Wieland Kohring
Vorsitz:	Prof. Dr. Uli Müller
Akademischer Mitarbeiter:	Dr. Michael Kohlstedt

Im Grunde haben die Menschen nur zwei Wünsche:

Alt zu werden und dabei jung zu bleiben.

Peter Bamm,

deutscher Arzt und Journalist

Experience is what you get when

you didn't get what you wanted.

Randy Pausch,

US-amerikanischer Informatiker

Abstract

In this study the influence of oxidative stress on the proteome of primary rat hepatocytes (PRH) was analyzed. Our *in vitro* heat stress model included hepatocytes from middle-aged and old Wistar and Sprague Dawley (SD) rats. The efficacy of N-acetylcysteine (NAC) and quercetin as antioxidants was addressed using principal component analysis. Overall, old PRH were more susceptible to oxidative stress than middle-aged PRH. We identified potential biomarkers for age-related alterations in the secretome of old PRH. The analysis of hepatic function and oxidative stress markers in middle-aged PRH revealed a high biological variance in Wistar rats. They can be categorized into low- and high-responders. In low-responders quercetin and NAC had a beneficial effect on cell function and viability whereas in high-responders the toxic effect of these compounds outweighed their antioxidant properties. Therefore, we used SD rats exhibiting less inter-individual variances in the following proteomic study. The proteomic characterization showed that oxidative stress had the strongest influence in old PRH on proteins related to oxidative stress defense and enzymes of the urea cycle. Deficiencies in theses enzymes are strongly correlated to an impaired redox state and damaged antioxidant defense mechanisms. Comparative studies with primary mouse hepatocytes in sandwich and monolayer cultures revealed a higher level of oxidative stress in monolayer culture potentially causing dedifferentiation.

Zusammenfassung

In dieser Studie wurde der Einfluss von oxidativem Stress auf das Proteom von primären Rattenhepatozyten (PRH) untersucht. Unser *in vitro* Hitzestressmodell verwendete Hepatozyten von mittelalten und alten Wistar- und Sprague Dawley-Ratten (SD). Der Nutzen der Antioxidantien N-acetylcystein (NAC) und Quercetin wurde mit Hilfe der Hauptkomponentenanalyse untersucht. Alte PRH waren anfälliger für oxidativen Stress als mittelalte. Im Sekretom alter PRH konnten wir potentielle Biomarker für altersbedingte Veränderungen identifizieren. Die Analyse hepatischer Funktionen und oxidativer Stressmarker zeigte, dass Wistar-Ratten eine hohe biologische Varianz haben. Sie können in Bezug auf oxidativen Stress in low- und high-Responder unterteilt werden. Quercetin und NAC hatten in low-Respondern eine positive Wirkung auf Zellfunktionen und Viabilität, wohingegen in high-Respondern ihr toxischer Effekt überwog. Weger dieser Ergebnisse, wurden in folgenden Studien SD-Ratten verwendet, die weniger interindividuelle Unterschiede aufweisen. Proteomanalysen konnten zeigen, dass oxidativer Stress den größten Einfluss auf alte PRH hat, genauer auf antioxidative Enzyme und Enzyme des Harnstoffzyklus. Ein Mangel an diesen Enzymen korreliert mit einem gestörten Redox-Haushalt und einer Beeinträchtigung der Stressabwehr. Studien mit primären Maushepatozyten konnten weiterhin aufzeigen, dass oxidativer Stress eine Hauptursache für die Dedifferenzierung von Zellen in Monolayer Kulturen ist.

Table of Contents

1. General Introduction

1.1 Theories of aging

Aging is an inevitable and progressive process which is defined by a decline of various cellular and physiological functions. The increasing human life span and the resulting increase in age-related diseases make aging research an interesting and relevant topic. Therefore, it is not surprising that there are more than 300 different theories about the underlying mechanisms of aging (Vina et al., 2007). Theories of aging generally fall into one of two categories. The first category consists of theories claiming intrinsic, genetic reasons determine longevity. One of the most popular genetic aging theories postulates telomere shortening as the cause for aging processes (Hayflick & Moorhead, 1961). In 2003 it was discovered that individuals with longer telomeres have an increased longevity compared to individuals with shorter telomeres (Cawthon et al., 2003). However, it is not known whether short telomeres are just a symptom of cellular age or the cause of the aging process itself. Another theory, the "neuroendocrine aging theory", proposes that hormones and their influence on neurons are the key point to aging processes (Troen, 2003). Research studies revealed that the age-related decrease of growth hormone and the insulin-like signaling pathway play a role in regulating lifespan. The activity of the insulin-like signaling pathway was reported to be decreased in nematodes, mice and humans with a long lifespan (Kenyon, 2010). The "molecular inflammatory theory" associates the decline in the immune response and increasing levels of autoimmune diseases with senescence (Cornelius, 1972).

The second category of aging theories claims that accumulating damage to macromolecules and deficiencies in repair mechanisms cause senescence. Weisman first introduced the theory of accumulated damage in 1882 (Jin, 2010). His "wear and tear" theory compares biological senescence to the deterioration of a machine which is damaged over time by mechanical and environmental wearing. An example would be arthritis or the loss of dentin in aging teeth. However, this theory does not consider intra- and inter-cellular mechanisms as modern aging theories do. One of these more modern theories, the "cross-linking theory of aging" postulates that glycosylation of proteins which impairs protein function are the reason for the decline in

cellular function with increasing age. Previous studies revealed that patients with diabetes type 2 possess 2-3 times as many cross-linked proteins as healthy individuals of the same age group (Lipsky, 2015). Another theory is the DNA damage hypothesis (Freitas & de Magalhaes, 2011) which proposes that aging is the result of accumulating DNA damage due to insufficient repair mechanisms.

The most prominent hypothesis is the "free radical theory of aging" (Harman, 1956) which proposes that the damage to macromolecules induced by reactive oxygen species (ROS) is responsible for aging. Reactive oxygen species can either be a by-product of normal metabolism or have exogenous origins. As highly reactive species, they cause oxidative damage to lipids, DNA and proteins. Harman argued that this macromolecular damage accumulates over a life-span and eventually leads to a loss of metabolic function and ultimately death. In 1972, Harman revised his theory to include new insights about ROS generation by mitochondria leading to the "mitochondrial free radical theory of aging" (Speakman & Selman, 2011). Mitochondria generate reactive oxygen species as part of the electron transport chain. However, mitochondria lack DNA repair enzymes which make them susceptible to oxidative damage. This damage causes mutations which again lead to an increase in ROS production forming a damaging cycle. Ultimately, the resulting progressive decline in cellular function and the ability to counteract stress conditions lead to senescence. Overall, it can be assumed that all aging theories contain parts of the true reason behind aging. Aging research still meets the challenge to find the link between all of them.

1.2 Reactive oxygen species and their role in normal cellular function and oxidative stress

Intrinsic sources of ROS

Reactive oxygen species have various intrinsic and extrinsic sources. Endogenous ROS can be generated as the primary function of an enzyme system (e.g. NADPH oxidases, Cyp P450 oxidase), as a side reaction of other biological processes (e.g. the mitochondrial electron transport chain, lipid metabolism in peroxisomes), or by metal-catalyzed oxidations (Fenton reaction: $Fe^{2+} + H_2O_2 + H^+ \rightarrow Fe^{3+} + OH \bullet + OH^-$). The primary ROS species generated in a cell are the superoxide anion ($\bullet O_2^-$) and hydrogen peroxide (H_2O_2) (Nathan & Ding, 2010).

These molecules can then further react to form other ROS (Figure 1-1) like hydroxyl radicals (•OH) (Fransen et al., 2012).

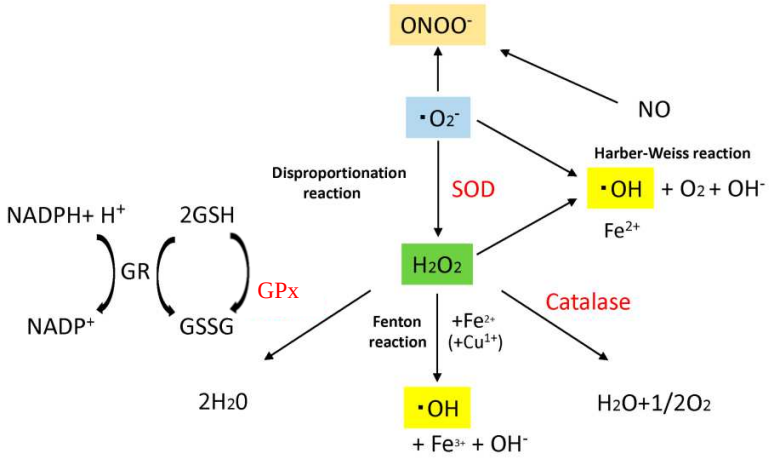

Figure 1-1: Major generative and eliminative reactions of reactive oxygen species (ROS). Superoxide dismutase (SOD) catalyzes the dismutation of superoxide ($\cdot O_2^-$) into H_2O_2 and O_2. Catalase dismutates H_2O_2 into water and molecular oxygen. Glutathione peroxidase (GPx) reduces H_2O_2 by oxidizing glutathione and generating water. The resulting disulfide is reduced by glutathione reductase (GR) using NADPH. Disproportionation reactions, Harber–Weiss reaction and Fenton reaction generate hydroxyl radicals ($^{\cdot}OH$) (Kayama et al., 2015).

The main source of intrinsic ROS can be found in the mitochondrial process of oxidative phosphorylation. Here, the controlled oxidation of NADH and FADH creates a mitochondrial membrane potential which allows ATP synthase to phosphorylate ADP to ATP. The electrons derived from NADH and FADH have to pass through the electron transport chain consisting of four membrane-bound complexes during oxidative phosphorylation. Approximately 90 % of cellular ROS, mainly superoxide anions (O_2^-), are generated in the mitochondria at complex I and III (Balaban et al., 2005) which have a high redox potential and where the electrons can directly react with molecular oxygen (Figure 1-2).

Previous studies showed that the ROS production in mitochondria increases with progressing age (Payne & Chinnery, 2015). Mitochondrial DNA is prone to oxidative damage due to the close proximity to the ROS source and the missing histones which protect nuclear DNA from damage. The DNA alterations result in an increased ROS production and decreased ATP production creating a vicious cycle.

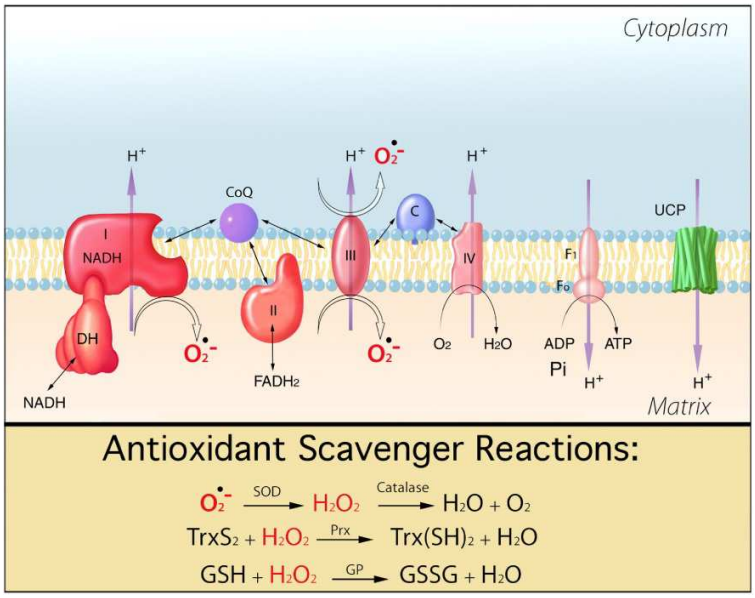

Figure 1-2: Illustration of the main sources of superoxide anions at complex I (NADH coenzyme Q reductase) and III (cytochrome bc_1 complex) of the mitochondrial electron transport chain. Below: major ROS scavenging pathways consisting of the enzymes superoxide dismutase, catalase, peroxiredoxin and glutathione peroxidase (Balaban et al., 2005).

To counteract these damaging effects of ROS, organisms have developed various defense mechanisms which accomplish a state of homeostasis in a healthy cell. These mechanisms include enzymatic and non-enzymatic ROS scavengers (Figures 1-1, 1-2).

Superoxide Dismutase (SOD)

There are three different forms of SOD found in mammals. SOD1 is a dimer containing copper and zinc (Cu-Zn-SOD) located in the cytoplasm. SOD2, with manganese in the reactive centre, is a tetramer located in the mitochondria (Mn-SOD). SOD3 is also a tretramer, but with copper and zinc which can be found extracellular.

SOD promotes the dismutation of two O_2^- molecules to H_2O_2 and O_2 (Reaction 1)

$$O_2\bullet^- + O_2\bullet^- + 2H+ \rightarrow O_2 + H_2O_2 \qquad (1)$$

SOD prevents the damaging effect of the highly reactive superoxide, which can act as an oxidant by itself, or combine with H_2O_2 to form the •OH radical.

Catalase

Catalase is a tetramer located in peroxisomes. It contains four iron-containing heme groups which allow the reaction with hydrogen peroxide. It efficiently detoxifies hydrogen peroxide to water and oxygen (Reaction 2) (Michiels et al., 1994). Additionally, it can use hydrogen peroxide to oxidize various other molecules, like phenols, formaldehyde, acetaldehyde and alcohols (Reaction 3).

$$2\ H_2O_2 \rightarrow 2\ H_2O + O_2 \qquad (2)$$

$$H_2O_2 + H_2R \rightarrow 2H_2O + R \qquad (3)$$

This reaction is important in liver and kidney cells, where the peroxisomes detoxify various toxic substances that enter the blood (e.g. 25% of ethanol humans drink) (Lamond, 2002)

Peroxiredoxin (Prx)

Peroxiredoxins are high-abundant enzymes with a redox-active cysteine in their reactive centre. It can reduce hydrogen peroxide to water (Rhee et al., 2001)(Reaction 4). The oxidized peroxiredoxin is inactive and requires thiols like thioredoxin (Trx) as an electron donor to regain its catalytic activity (Reaction 5) (Pillay et al., 2009).

$$\text{Prx (red.)} + H_2O_2 \rightarrow \text{Prx (ox.)} + 2H_2O \qquad (4)$$

$$\text{Prx (ox.)} + \text{Trx (red.)} \rightarrow \text{Prx (red.)} + \text{Trx (ox.)} \qquad (5)$$

Glutathione peroxidase (GPx)

Glutathione peroxidase is a tetrameric enzyme with a selenocysteine in the active centre. It catalyzes the reduction of free hydrogen peroxide to water (Reaction 6) in the GSH/GSSG redox system. Glutathione reductase recycles the oxidized glutathione to GSH (Reaction 7).

$2\ GSH + H_2O_2 \rightarrow GSSG + 2\ H_2O$ (6)

$GS–SG + NADPH + H^+ \rightarrow 2\ GSH + NADP^+$ (7)

GSH/GSSG redox system

The tripeptide glutathione (γ-l-glutamyl-l-cysteinyl-glycine (GSH)) is the most important low molecular weight antioxidant in aerobic cells. It is synthesized by the sequential addition of cysteine to glutamate followed by the addition of glycine (Forman et al., 2009). The average glutathione concentration in cells is 1–2 mM, while in hepatocytes, which export GSH, the concentration reaches up to 10 mM (Meister, 1988). About 90% of total GSH can be found in the cytosol, the remaining 10% in the mitochondria and the ER. Reduced GSH detoxifies hydrogen peroxide in the presence of glutathione peroxidase. The resulting oxidized GSSG is then again converted to reduced GSH by glutathione reductase (see Reactions 6/7).

Glutathione is the most prominent non-enzymatic ROS scavenger. However, there are other small molecular weight antioxidants like vitamins E (α-tocopherol) and C (ascorbic acid) which are obtained from the mammalian diet. Vitamin E reduces lipid hydroxyl radicals and lipid peroxides that are produced from polyunsaturated fatty acids. The oxidized vitamin E is then again reduced by vitamin C. The oxidized vitamin C can then be recycled using GSH as a substrate (Forman et al., 2009).

Cell signaling

The aforementioned defense mechanisms accomplish a redox homeostasis in cells. Nonetheless, a low amount of ROS “leak” from the mitochondrial electron chain. In the past, this leakage was thought to be a normal byproduct of oxidative phosphorylation. More recent studies could provide evidence that ROS release from mitochondria is part of a complex regulatory mechanism (Dröge, 2002). Reactive oxygen species play an important role in various cell signaling pathways. ROS regulates the function of key enzymes in signaling pathways mostly by oxidizing redox-reactive cysteine residues (known as redox switch) in these enzymes (Ray et al., 2012). This modification results in an altered structure and/or activity of the respective enzyme effectively modulating redox-sensitive signaling pathways. The most prominent modulating oxygen species is H_2O_2 because of its relative longevity and

stability compared to free radicals. ROS trigger different stress responses depending on the level of oxygen species present in the cell. For example, at low levels, H_2O_2 mainly modulates pathways associated with hormone release, steroidogenesis, T-cell activation or proliferation and differentiation processes (Kuksal et al., 2017). Accordingly, moderate levels of ROS are crucial in the innate and adaptive immune response for the production of NFAT (nuclear factor of activated T-cells) and interleukin-2 trough cysteine oxidation, two factors important for the T-cell activation and proliferation (Sena et al., 2013). Furthermore, ROS stimulate cell proliferation and differentiation through a growth-factor mediated activation of the mTOR pathway (Ricoult & Manning, 2013). Higher levels of H_2O_2 activate stress response signaling cascades (Nrf2 (nuclear factor like 2), HIF-1α (hypoxia inducable factor)) and, in extreme cases, induce apoptosis in extensively damaged cells. But every complex mechanism has its flaws. Extrinsic influences can disturb the often fragile balances in a cellular pathway. For instance, a permanently high exposure of pancreatic β-cells to glucose increases cellular ROS release which again stimulates insulin release. This cycle promotes insulin resistance and ultimately the development of diabetes mellitus type 2 (Ricoult & Manning, 2013).

Heat stress as an extrinsic source of ROS

Additional to the intrinsic ROS sources, there are also many environmental factors playing a role in the excessive generation of ROS. Some of them are exposure to air and water pollution, tobacco smoke, industrial pesticides and solvents, food (smoked meat, used oil, fat), xenobiotics, alcohol consume, ultraviolet light and high temperatures (Phaniendra et al., 2015).

In our study, we concentrated on the influence of heat on the oxidative stress reaction of primary hepatocytes. Hyperthermia and oxidative stress have a close connection. Heat exposure induces an accelerated mitochondrial respiration and consequently an increased production of reactive oxygen species (Slimen et al., 2014). Another sign of oxidative stress is the production of cytokines - like tumor necrosis factor alpha (TNF-α) - responsible for inflammatory processes. Furthermore, oxidative stress induces apoptosis or inflammation via the JNK (c-Jun N-terminal kinase) pathway (Kaneto et al., 2007). All these pathways are also triggered by acute heat exposure (Li, Wang, et al., 2014) indicating the overlapping mechanisms involved in both types of stress. Therefore, the induction of oxidative stress by

heat treatment seems the most suitable model to study oxidative damage in a controlled *in vitro* system. The connection of hyperthermia, oxidative stress and aging can be drawn by looking at the protein family of the heat shock proteins (HSP). Both, heat and oxidative stress, induce an overexpression of HSP genes (Ikwegbue et al., 2017). HSPs are molecular chaperones responsible for the refolding or degradation of misfolded proteins. Further, they play an important, but not well understood, role in the suppression of inflammation and apoptosis (Ikwegbue et al., 2017). Under the influence of extrinsic stress heat stress transcription factors (HSF) are activated which activate the production of HSP mRNA. Especially the HSP70 family is strongly induced by oxidative stress and plays a major role in damage control and cell survival (Kiang & Tsokos, 1998). Aging leads to an increased expression of HSP genes indicating a high intrinsic stress level (Muller et al., 2007). However, previous studies also showed that the response to acute extrinsic heat shock deteriorates with increasing age. This is due to a decline in the activity of transcription factor HSF1 (heat shock factor 1) leading to decreased heat shock protein abundance under acute stress conditions (Heydari et al., 2000). For instance, a previous study showed that the mitochondria of old male Fischer rats lost the ability to up-regulate HSP60 and HSP10 under heat stress conditions whereas young rats showed no impairment in the reaction to heat.

Role of ROS in aging and disease

According to the “free radical theory”, aging is the result of an imbalance of ROS generation and antioxidant defense. Cellular senescence and age-related diseases can be a direct result of an impairment in the enzymatic antioxidant defense. Studies were able to prove the correlation between specific enzymes and aging. So can the loss of SOD 1 lead to a shortened lifespan with a significant increase in hepatocellular carcinoma and accelerated aging phenotypes (Zhang et al., 2016). Overexpression of catalase in mice prevents the age-associated loss of spermatozoa, testicular germ and Sertoli cells seen in wild-type mice. (Selvaratnam & Robaire, 2016). Additionally, the overexpression of catalase targeted to mitochondria extends the lifespan of mice (Schriner et al., 2005) which locates the source of excess ROS production in the mitochondria as well as its effect on aging. The analysis of peroxiredoxin 1 knockout mice showed a 15% reduction in lifespan (Neumann et al., 2003).

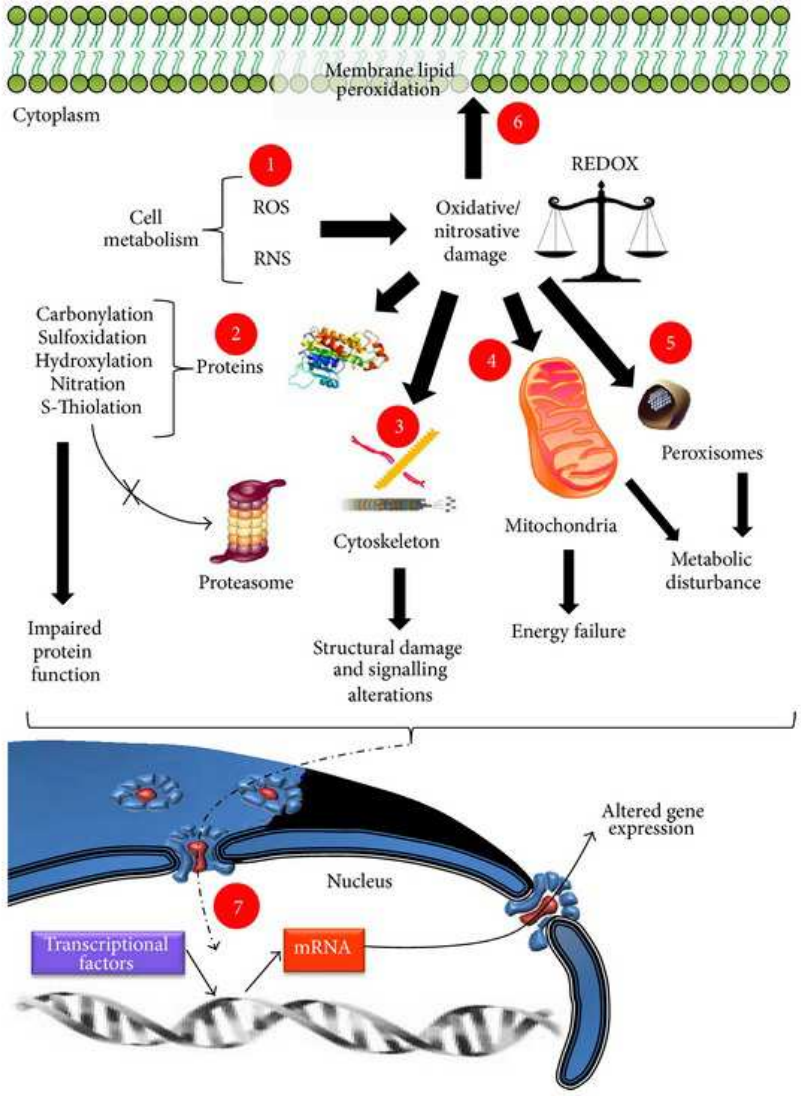

Figure 1-3: Cellular dysfunctions in aging or in age-related diseases by oxidative stress imbalance. (1) Cell metabolism generates reactive oxygen species (ROS) which in turn causes oxidative damage. (2) Macromolecular damage by oxidative stress results in impaired protein function and impairs refolding and degradation of damaged proteins in the proteasomes. (3) Damage of cytoskeletal proteins causes structural damage and signaling alterations. (4) In mitochondria, oxidative stress alters energy production and (5) affects peroxisomes; oxidative stress alters correct metabolic function. (6) Oxidative stress also affects the cellular membrane. (7) All cellular damages combined cause an alteration in the transcriptional activity of the cell, leading to an altered gene expression that in turn leads the cell to the aging process or to degenerative disease (Ortuno-Sahagun et al., 2014).

All these studies illustrate the importance of antioxidant enzymes in the prevention of cellular senescence and age-related diseases. However, loss of antioxidant activity in aged individuals is inevitable. Oxidative stress causes misfolding of proteins and oxidative alterations which impair protein function (Figure 1-3).

Additionally, chronic expression of unfolded, misfolded or aggregated proteins contributes to the development of some age-related diseases, such as Alzheimer's disease, Parkinson's disease and cataracts (Lopez-Otin et al., 2013). Deficiencies in refolding and degradation mechanisms via HSPs cause an accumulation of these impaired proteins.

In addition, the transcription factors responsible for the expression of antioxidant enzymes are also affected by oxidative damage. This results in an accumulation of damaged proteins and a further decline in cellular function. Another protein with a high impact on cellular function is actin (Figure 1-3). As the highest abundant protein in the cytoskeleton, oxidative alterations of actin can cause irreparable structural damages (Perez et al., 2006).

Furthermore, lipid peroxidation is disturbing the integrity of the cell membrane and signaling alterations (Wong-Ekkabut et al., 2007). These alterations are associated with several disorders and diseases, such as cardiovascular disease, cancer, neurodegenerative diseases, and aging, with increasing evidence showing the involvement of *in vivo* oxidation in these conditions (Halliwell, 2006).

All the aforementioned oxidative alterations are direct results of macromolecular damage. There is also more subtle damage by alterations of cellular pathways which are known to have a high impact on aging. The mechanistic target of rapamycin mTOR (formerly mammalian target of rapamycin) pathway is the most prominent modulator of the aging process and was first discovered in the 1970s (Johnson et al., 2013). mTOR is a highly conserved serine/threonine protein kinase and is part of the phosphatidylinositol-3-OH kinase (PI3K) kinase family. It consists of two complexes: mTOR complex 1 (mTORC1) and mTOR complex 2 (mTORC2). The mTOR pathway plays a major role in the aging process because of the various cellular functions it is involved in. Cell growth and proliferation, autophagy, apoptosis and protein homeostasis are all regulated by the mTOR pathway (Stanfel et al., 2009).Furthermore, mTOR is essential for the activity of HSF1 and therefore for the synthesis of heat shock proteins (Chou et al., 2012). mTORC2 has also been associated with the control of the actin cytoskeleton (Lipton & Sahin, 2014). Previous studies revealed that reduced

mTOR activity is associated with an increased lifespan in yeast (Medvedik et al., 2007), nematodes (Robida-Stubbs et al., 2012), fruitflies (Bjedov et al., 2010) and mice (Harrison et al., 2009). The mTOR pathway is activated by insulin (insulin/insulin growth factor-1 (IGF-1) signaling) and environmental nutrients like amino acids (Colman et al., 2009; Johnson et al., 2013). Accordingly, caloric restriction and methionine restriction can increase lifespan by decreasing mTOR activity (Powers et al., 2006). Some studies suggest that mTOR increases with age (Baar et al., 2016). The reason for this increased activity could be oxidative stress (Mercado et al., 2015). Hydrogen peroxide is known to activate PI3K (Figure 1-4) and therefore accelerates the mTOR pathway and ultimately the aging process (To et al., 2010).

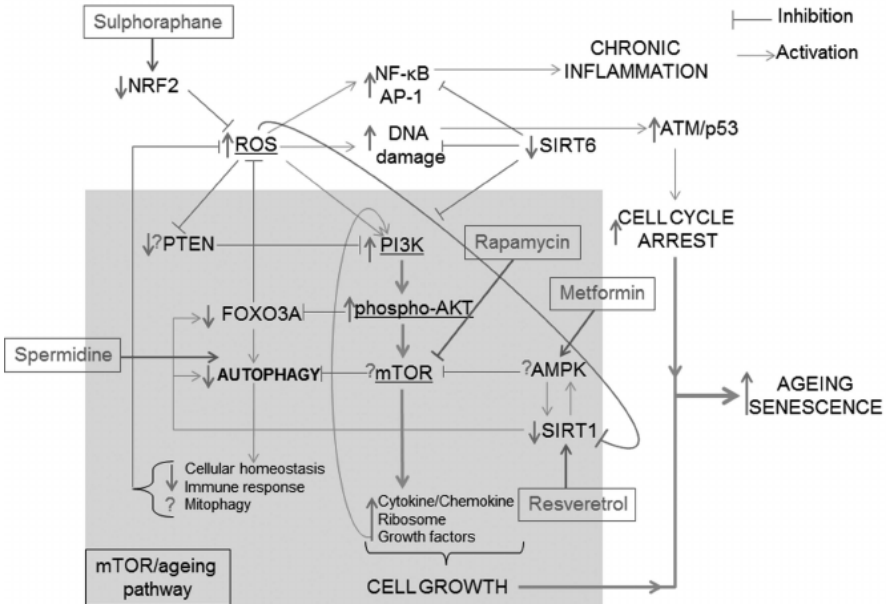

Figure 1-4: Oxidative stress accelerates the aging process by activating the mTOR pathway. ROS like hydrogen peroxide activate PI3K/phospho-AKT/ mTOR resulting in a loss of autophagy, immune response and cellular homeostasis. Excessive ROS also activates NF-κB/AP-1 and causes chronic inflammation. Abbreviations: AMPK, 5′-AMP-activated protein kinase; AP, activator protein; ATM, ataxia telangiectasia mutated; FOXO3A, forkhead box O3A; mTOR. mammalian target for rapamycin; NF-κB, nuclear factor-κB; Nrf2, Nuclear factor erythroid 2-related factor 2; PI3K, phosphatidylinositol-4,5-bisphosphate 3-kinase; PTEN, phosphatase and tensin homologue; ROS, reactive oxygen species; SIRT, Sirtuin (Mercado et al., 2015).

1.3 Model systems in aging research

1.3.1 The liver as a model organ for aging and oxidative stress research

The mammalian liver is an essential organ to maintain physiological body function. It is responsible for the synthesis of plasma proteins like albumin (Si-Tayeb et al., 2010), metabolic homeostasis, detoxification of ammonia via the urea cycle as well as synthesis of glutamine and alanine as non-toxic nitrogen containing compounds (Kuepfer, 2010). Most importantly, a wide range of endo- and xenobiotic compounds are metabolized by the liver (Gille et al., 2010). The liver consists of several cell types, being hepatocytes, endothelial cells, cholangiocytes, Kupffer cells, pit cells and hepatic stellate cells (HSC) (Maher & Friedman, 1993). Endothelial cells play an important role in hepatic blood flow regulation and fluid exchange (Poisson et al., 2017). Additionally, endothelial cells contribute to immune defense and signaling pathways by producing cytokines and presenting antigens (Jungermann & Kietzmann, 1996; Si-Tayeb et al., 2010). Cholangiocytes form the bile ducts and regulate the rate of bile flow and pH of the bile (Si-Tayeb et al., 2010). Kupffer cells represent the macrophages of the liver. Additionally, they produce cytokines, interleukins and nitric oxide and are therefore vital for cell development, immune response and regulation of signaling cascades (Dinarello, 2000). A dysregulation in Kupffer cells is associated with inflammation, schizophrenia, Alzheimer's disease (Swardfager et al., 2010) and cancer (Locksley et al., 2001). Pit cells are the killer cells in liver and are highly cytotoxic. Hepatic stellate cells store vitamin A in lipid droplets (Si-Tayeb et al., 2010). Because the HSC is the main source of extracellular matrix, they are the key to many liver diseases like cirrhosis and liver fibrosis (Eng & Friedman, 2000). Hepatocytes are the parenchymal cells of the liver. They account for 60% of all liver cells and 80% of the total liver volume (Gille et al., 2010). Hepatocytes are mainly responsible for the physiological functions of the liver, like glucose homeostasis and the production of CYPs and antioxidant proteins (Kim et al., 2008). Therefore the liver, and hepatocytes in particular, are interesting models for the study of diseases caused by age-related hepatic dysfunctions (see Figure 1-5).

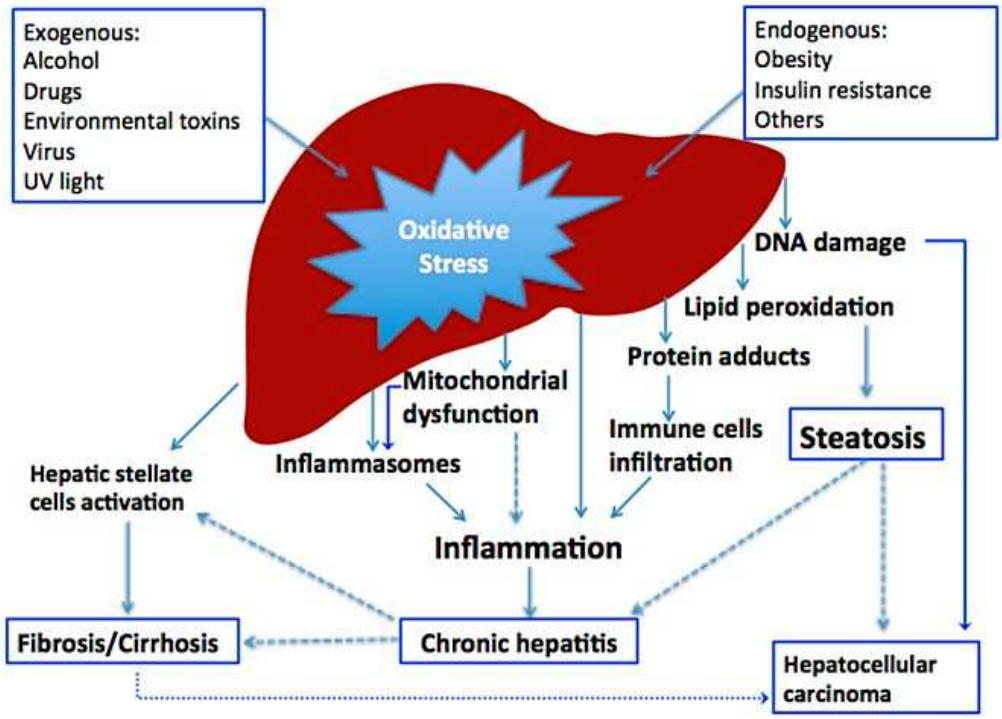

Figure 1-5: Exogenous and endogenous sources lead to increased ROS production in the liver. Oxidative damage of DNA can cause hepatocellular carcinoma (HCC) and lipid peroxidation leads to an accumulation of fatty acids causing steatosis. Accumulation of oxidatively damaged proteins and mitochondrial dysfunction affect signaling molecules and increase inflammation leading to chronic hepatitis. Hepatic stellate cell activation leads to fibrosis or cirrhosis as a pathological accumulation of extracellular matrix (Li et al., 2015).

Aging causes atrophy in the mammalian liver with a decreased blood flow and a reduction of weight by about 25-35% (Zeeh & Platt, 2002). Atrophy is the result of the accumulation of lipofuscin in hepatocytes. Lipofuscin are aggregates of highly oxidized insoluble proteins and lipid clusters. Their formation is a direct result of chronic oxidative stress and impairment in the degradation of damaged proteins (Grizzi et al., 2013). The livers of elderly mammals also take longer to regenerate because of the inhibition of cell cycle genes and the reduced ability of hepatocytes to proliferate (Sanchez-Hidalgo et al., 2012). In addition to these physiological changes, hepatocytes also show alterations on the molecular level due to aging. So is the expression of several CYP P450 enzymes (Cyp3a2 and Cyp2c11) drastically decreased in the liver of aged Fischer 344 rats which negatively affects the phase I of xenobiotic metabolism (Mori et al., 2007). Studies of the effect of aging on human livers are more diverse. Due to the

high polymorphism in humans, there is no clear trend in the expression profiles of CYP P450 in aged individuals (Zanger & Schwab, 2013). These results can show exemplary the challenges researchers have to face when choosing their model system.

1.3.2 *In vitro* cultivation systems in aging and oxidative stress research

The first decision a researcher has to make in choosing a model system is to decide whether to use an *in vivo* or *in vitro* model. In the pre-clinical phase of pharmaceutical testing and in the cosmetic industry *in vivo* animal models have always been the first choice. However, out of ethical reasons, it has become more and more important to reduce animal testing as much as possible (Holmes et al., 2010; Krewski et al., 2010). Additionally, *in vivo* models have certain drawbacks like high costs and a time-consuming maintenance of animal stocks. Therefore, primary hepatocytes are becoming the gold standard in liver research (Müller et al., 2014). Freshly isolated primary human hepatocytes (PHH) have the advantage that they retain most of their liver-specific functions and express the characteristic CYP enzymes which is essential for the study of pharmacological effects (Gerets et al., 2012). Because of the almost *in vivo* like conditions of PHH, they are also used in fundamental research (Liu et al., 2017) and research of inflammation (Bullone & Lavoie, 2017), age-related disease (Wiemann et al., 2002) and the discovery of drugs against oxidative stress (Rubiolo et al., 2008). The most common source of PHH are small parts from liver transplantations or biopsies of diseased livers (Zeilinger et al., 2016). However, patient material has several major disadvantages. First of all, PHH derived from diseased livers are difficult to assess regarding their comparability to healthy human livers. Comparability is also a key problem considering the many polymorphisms present in human populations (Zeilinger et al., 2016). Additionally, the limited availability of PHH could be problematic in hindsight to large-scale experiments.

In comparison, primary hepatocytes from inbred or outbred rodents (rat or mouse) have a strain dependent stable genetic background. Basic needs like sleep, nutrients and water can be tightly controlled minimizing the inter-individual differences. Regarding aging research, the short lifespan of rats and mice can be considered an additional advantage. Primary hepatocytes from rodents are therefore considered a useful tool to analyze age-related diseases (Czochra et al., 2006) and basic mechanisms of oxidative stress (Rubiolo et al., 2008; Shenvi et al., 2008). The possibility to induce mutations like SOD deficiency provides detailed

insights into very specific parts of a scientific question (Kokoszka et al., 2001). Nonetheless, inter-species differences between human and rodent in drug metabolism and compound toxicity susceptibility have always to be considered in discussing results (Jemnitz et al., 2008). So, rodents show differences in glucose metabolism (Kowalski & Bruce, 2014), insulin signaling (Bunner et al., 2014) and CYP activity (Martignoni et al., 2006) compared to human hepatocytes.

A problem regarding primary hepatocytes in general is the rapid dedifferentiation and loss of hepatic function in conventional 2D *in vitro* system. Primary hepatocytes in monolayer cultivation start to dedifferentiate into a fibroblast-like phenotype within the first 3 days after hepatocyte isolation (Godoy et al., 2009). Dedifferentiation of primary hepatocytes in *in vitro* cultures is a well-known problem hindering long-term studies, which are necessary for e.g. *in vitro* drug toxicity testing (Alepee et al., 2014). There are several approaches to delay this dedifferentiation process, ranging from media optimization and co-cultivation with other liver cells to cultivation of hepatocytes in scaffolds of extracellular matrix (ECM) (Klingmuller et al., 2006), (Kostadinova et al., 2013), (Müller et al., 2014). Cultivation of hepatocytes in a sandwich of the extracellular matrix protein collagen (SW) is one of these approaches. Cultivation of primary hepatocytes in collagen SW culture leads to improved hepatic functions such as albumin and urea production and activity of CYP enzymes (Iredale & Arthur, 1994). Morphologically, hepatocytes cultivated in the SW configuration regain a more *in vivo* like structure compared to hepatocytes cultivated as standard monolayers.

A way to avoid the problem of dedifferentiation processes is the use of immortalized human hepatic cell lines to study oxidative stress. Because of their high availability and low cost, cell lines are a widely used tool to research age-induced alterations. The main cell line used for oxidative stress studies is *HepG2* (Sakurai & Cederbaum, 1998; Manthey et al., 2005; Zhuang et al., 2017). The *HepG2* cell line originates from a hepatoma of a 15 year old Caucasian male. These cells are highly differentiated and exhibit a genotype comparable to normal human hepatocytes (Gerets et al., 2012). *HepG2* cells are suitable for cytotoxicity testing in early pre-clinical phases due to their human-like expression of phase II enzymes. However, their metabolic capacity is low compared to primary hepatocytes caused by a low CYP expression (Westerink & Schoonen, 2007).

A promising alternative to *HepG2* is the human hepatocellular carcinoma cell line *HepaRG* (Gripon et al., 2002), a co-culture of hepatocytes-like and biliary-like cells. They exhibit a xenobiotic metabolism comparable to primary hepatocytes and are stable in long-term cultivations (Lambert et al., 2009). However, Gerets et al. showed that both *HepG2* and *HepaRG* have a crucially lower sensitivity to hepatotoxins than primary human hepatocytes (Gerets et al., 2012). Overall, these findings show that cell lines are only suitable for very specific scientific questions and of course not suitable for aging studies at all. Therefore, we chose primary rat hepatocytes for our *in vitro* model for aging and oxidative stress.

1.4 Proteomics

The term “proteome” was first introduced in 1995 by Marc Wilkins (Wasinger et al., 1995) and means the entirety of all proteins expressed in a cell, tissue or organism at a certain time. Proteomics, a term chosen in analogy to genomics (James, 1997), includes all methods available for the identification, quantification and localization of the proteome.

The proteome is highly dynamic and therefore closer to the actual phenotype than the genome and still more stable than the metabolome (Schanstra & Mischak, 2015). Milestones in proteomic analysis were the development of soft ionisation procedures in mass spectrometry like electrospray-ionisation (ESI) (Meng et al., 1988) and matrix-assisted laser desorption/ionization (Karas & Hillenkamp, 1988) and the development of two-dimensional gel electrophoresis (O'Farrell, 1975). The generation of huge amounts of complex data made high-capacity bioinformatic tools necessary. This need resulted in the creation of databases and search algorithms like SEQUEST, Mascot or OMSSA which made a novel high-troughput protein identification possible (Kim & Pevzner, 2014).

Methods for the analysis of the proteome have to have a high resolution and sensitivity combined with a high reproducibility. Proteomic methods can be roughly divided in gel-based “top-down” and LC-based “bottom-up” approaches. The “top-down” analysis uses as a first step two-dimensional separation of intact proteins with chromatography or gel electrophoresis followed by a enzymatic digest to peptides. The peptides can than be identified with mass spectrometry and a database search. This allows for the analysis of a specific scientific

question without the generation of unnecessarily huge amounts of data. However, this approach requires the consideration of a more limited, targeted subproteomic analysis considering that gel electrophoresis is no high-troughput method. It is also limited to soluble proteins. Nevertheless, the complexity of the sample has to be reduced to obtain meaningful data, e.g. by restricting the pH range or concentrating on a specific organelle (Sharov & Schoneich, 2007).

The “bottom-up” or “shotgun” approach allows for a broader analysis of the proteome of interest. A complex protein mixture is first digested to peptides and then analyzed with high-resolution methods like HPLC. However, the analysis of this huge amount of data is extremely time-consuming and requires increasingly sophisticated bioinformatic tools (Qian et al., 2005).

1.4.1 Two-dimensional gel electrophoresis and DIGE

The principle of two-dimensional gel electrophoresis (2-DE) is based on the separation of complex protein mixtures via a two-step protocol (O'Farrell, 1975). In the first step proteins are separated according to their isoelectric point (IP) on a gel-strip with an immobilized pH gradient (Figure 1-6 A). Proteins are amphoteric in nature and migrate in an electric field to the pH where their net charge is zero. In the second step the proteins are separated according to their molecular weight using SDS-PAGE. SDS (Sodium dodecylsulfate) is a negatively charged anionic detergent which binds to the proteins. The negative charge of the SDS-protein-complexes allows for a consistent separation towards the anode in an electric field. The pore size of the polyacrylamide gel separates the proteins according to their molecular weight.

Both properties of a protein, IP and molecular weight, can be altered by post-translational modifications such as phosphorylation, glycosylation and oxidation. 2-D electrophoresis can therefore also be used to detect alterations in modifications (Nkuipou-Kenfack et al., 2014). After 2-D electrophoresis, there are various staining methods for in-gel protein detection (Steinberg, 2009). Most commonly, the proteins are stained with Coomassie Blue, which has a dynamic range of 10^1, and then digested with trypsin followed by MS identification (Toda, 2001; Dierick et al., 2002; Sharov & Schoneich, 2007).

2-D gel electrophoresis has certain drawbacks. The method it is time-consuming, the separation of hydrophobic and highly acidic or basic proteins is limited, it demands a relatively high amount of sample, and shows a considerable gel-to-gel variation (Magdeldin et al., 2014). The last two points can be overcome by two-dimensional difference gel electrophoresis (2-D DIGE) (Unlü et al., 1997) where two samples can be compared in one gel (Figure 1-6 B).

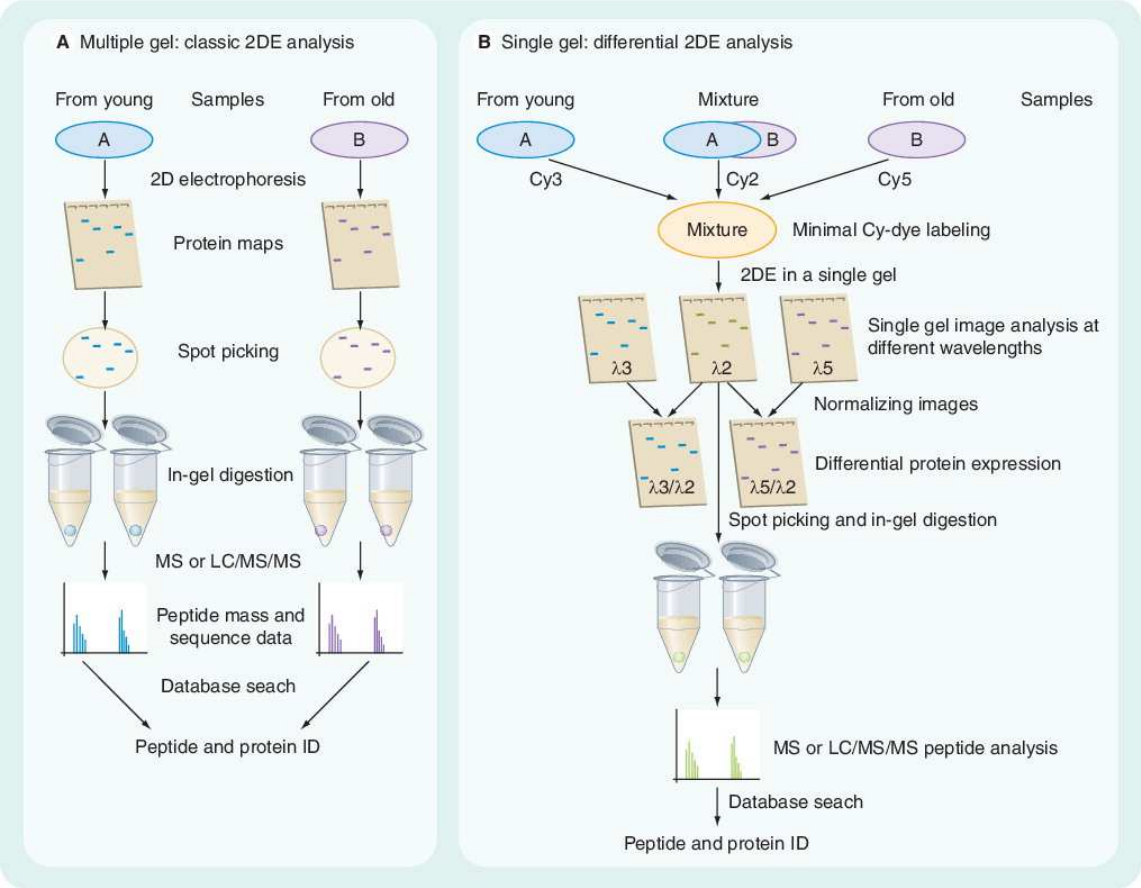

Figure 1-6: A) Classical two-dimensional gel electrophoresis coupled with MS for protein identification for aging research; B) Differential gel electrophoresis for relative quantification of protein abundance (Sharov & Schoneich, 2007).

DIGE is a highly sensitive method for relative quantification which is based on the use of fluorescent dyes (CyDyes). They are N-hydroxy succinimidyl ester reagents which bind to the ε-amine groups of lysine side-chains of proteins. The protein samples can be run on the same gel by using three differently fluorescing dyes (Cy 3 (blue), Cy 5 (red) and Cy 2 (yellow,

internal standard)) and therefore reducing the gel-to-gel variation. The internal standard consisting of 1:1 mix of protein from the compared samples enables intra- and inter-gel comparability (Lilley & Friedman, 2004).

1.4.2 "Shotgun" proteomics

Non-gel based "shotgun" approaches mostly use mass spectrometry for peptide separation and identification (Figure 1-7 A). One of the most commonly used quantification methods is SILAC (Stable isotope labeling by amino acids in cell culture). SILAC is a metabolic labeling method (Ong et al., 2002) which relies on the incorporation of stable isotopes. The isotope labeled amino acids ($(_{15})N_4$-arginine or $(_{13})C_6$-lysine) are supplemented to the media and incorporated into the intracellular proteins. The "heavy" isotopes can then be distinguished from the "light" non-labeled amino acids using mass spectrometry. With SILAC, similar to DIGE, a relative quantification of protein abundance is achieved. However, SILAC requires a high protein-turnover to ensure a sufficient labeling rate (Mann, 2006) limiting its application mostly to high-proliferating cells.

Other methods without this kind of limitation are chemical labeling methods like ICAT (isotope-coded affinity tag), iTraq (isobaric tags for relative and absolute quantitation) or ^{18}O-labeling.

ICAT was first introduced by Gygi et al. in 1999 (Gygi et al., 1999). ICAT consists of three elements: a reactive group for derivatizing an amino acid side chain, an external mass tag and isotopically coded linker. The reactive group is usually iodoacetamide to modify cysteine residues. The isotope linker can either be hydrogen as the "light" isotope control or deuterium as the "heavy" variant (Figure 1-7 B). The tag itself is biotin which is used for affinity purification to separate the labeled and unlabeled peptides in LC/MS. However, because cysteine is often a rare amino acid, application of ICAT is limited if the proteins of interest do not contain cysteines.

A popular alternative tag to ICAT is iTraq. Contrary to ICAT, isobaric mass tags all have the same total mass. The method is based on the covalent labeling of the amines of peptides from protein digestions. The mass differences in isobaric labels are only apparent after tandem MS fragmentation generating different reporter masses which are unique to each sample.

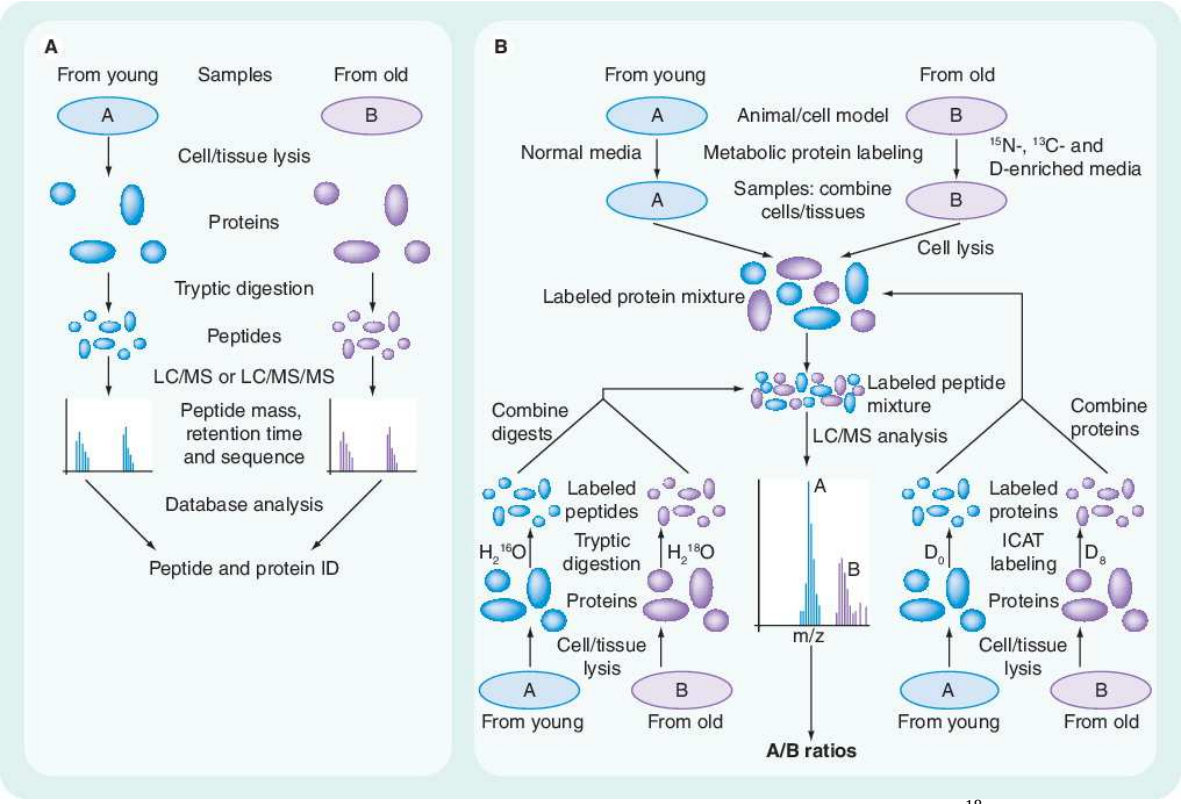

Figure 1-7: A) Classical workflow of a proteomic "shotgun" approach in aging research; B) ^{18}O labeling [bottom left]; SILAC [top]; ICAT (isotope-coded affinity tag) [bottom right]: quantitative differential proteomic analysis based on light/heavy isotope labeling (8 Da difference) (Sharov & Schoneich, 2007).

An alternative to ICAT and iTraq is ^{18}O labeling (Figure 1-6 B). This method is based on the incorporation of ^{18}O via isotopically altered H_2O. The isotope labelling of proteins takes place during trypic digest with trypsin being the catalyst for the reaction (Nkuipou-Kenfack et al., 2014). This procedure generates "heavy" and "light" peptides with a mass difference of 4 Da. However, this methods has some major disadvantages. First, incorporation of isotopes is often insufficient and second, the mass shift is too small for a reproducible analysis.

A completely different approach for the quantification of protein abundance is the label-free quantification. Thereby, signal intensity is compared for quantification. The major advantage of this method is that the number of conditions which can be compared to each other, is not limited (Bantscheff et al., 2012).

1.4.3 Mass spectrometry

All above mentioned quantification methods have in common that they rely on mass spectrometry for the identification of the analyzed proteins. MALDI ToF and ESI are two of the most commonly used ionization methods for MS proteomics (Meng et al., 1988; Hillenkamp et al., 1991).

ESI (electrospray ionization) is based on the generation of an aerosol by the application of a high voltage to a liquid sample under atmospheric pressure. During ESI, the analyte is dissolved in a volatile solvent. The strong electric filed applied leads to an accumulation of charges at the surface of the liquid sample. Highly charged, small droplets dissolve from the sample until the solvent is completely evaporated. The analytes are released as single and multiple charged ions into the high vacuum of the mass analyzer. For ESI, the most commonly used analyzers are the ion trap and the hybrid quadrupole time-of-flight (QTOF) instruments.

MALDI ToF is based on the co-crystallization of the trypsin digested peptides with a matrix which absorbs the laser energy to create ions from molecules with minimal fragmentation. The suitability of the matrix depends on the molecules of interest. α-Cyano-4-hydroxycinnamic acid is a matrix commonly used for peptides with a mass lower than 2.5 kDa.

The matrix is added at a high molar excess compared to the analyte to reduce the formation of analyte aggregates. The sample is brought into the high vacuum of the mass spectrometer and irradiated with a UV laser (usually nitrogen) leading to the desorption of the peptides into the gas phase and the generation of single charged ions.

MALDI is often coupled to a time-of-flight (TOF) analyzer. There, the ions are accelerated by an electric field. The time the ions need to pass the flight tube depends on their mass to charge ratio (m/z) considering that they are accelerated with the same kinetic energy. The tandem mass spectrometer contains a CID (collision-induced dissociation) chamber for fragmentation of the ions in MS/MS mode. This chamber can be flooded with an inert gas (e.g. helium). A selected precursor with a specific mass is isolated by the timed ion selector by deflecting all ions with the wrong mass. After fragmentation of the precursor in the CID chamber, the resulting fragment ions are accelerated again and separated in the second TOF analyzer to obtain the MS/MS spectrum.

1.5 Aim and outline of the thesis

The presented thesis was part of the BMBF funded project “Oxisys”. The aim of the project was to analyze ROS-induced proteomic alterations in primary hepatocytes from middle-aged (6 months) and old (> 23 months) rats. A lot is already known about oxidative stress response and mechanisms in aging cells. The changes in the proteome of age-accelerated mouse brain cells (Poon et al., 2004) and the influence of heat stress in *in vivo* rat models (Qian et al., 2004; Shen et al., 2007; Chen et al., 2017) was studied before. However, a detailed analysis of the *in vitro* proteome-wide changes in primary rat hepatocytes due to oxidative stress has not been done before. Additionally, the integrated analysis of the effect of quercetin on old heat-stressed PRH was not done before.

First in chapter 3, the secretomes of primary hepatocytes were studied to evaluate potential biomarkers and therapeutic targets that could allow prediction and diagnosis of ROS-induced cell aging. For that purpose, hepatocytes from middle-aged and old Wistar rats were analyzed under heat stress conditions compared to control conditions using 2-D DIGE and MALDI ToF MS/MS. Oxidative stress was induced by heat treatment at 42 °C for 30 min. The hepatic function and induction of oxidative damage was monitored by measuring albumin secretion, LDH- and AST-leakage and protein oxidation. In the following chapter 4, the influence of two antioxidant compounds, namely N-acetylcysteine and quercetin, was in the focus of the analysis. Therefore, hepatic function and oxidative stress response of primary hepatocytes from middle-aged Wistar rats and the human hepatoma cell line *HepG2* were analyzed under oxidative stress conditions. The cells were pre-treated with 500 µM NAC or 50 µM quercetin and the effect was compared 1 h, 5 h and 24 h after induction of oxidative stress by heat treatment at 42 °C or treatment with 2 mM H_2O_2. Hepatic function was monitored during the cultivation time by measuring albumin production and LDH release into the supernatant at the corresponding time-points. The oxidative stress response was examined by measuring ROS production, GSH/GSSG content, protein oxidation and SOD (superoxide dismutase) and CAT (catalase) activity. The aim of this study was to evaluate the properties of NAC (N-acetylcysteine) and quercetin in our *in vitro* heat stress model.

In chapter 5, the results from previous studies were used to establish a complete model for the identification of molecular targets for the prediction and diagnosis of ROS-induced cell aging and to analyze cellular mechanisms of the defense against oxidative stress. For that purpose,

cells were pre-treated with 50 µM quercetin and the effect was compared 1 h, 5 h and 24 h after induction of oxidative stress by heat treatment at 42 °C or treatment with 2 mM H_2O_2. The hepatic function, oxidative damage markers and the proteome of primary hepatocytes from middle-aged (6 months) and old (> 23 months) Sprague Dawley rats (SD) were analyzed under oxidative stress conditions compared to control conditions using 2-D DIGE and MALDI ToF MS/MS. The outbred rat stock Sprague Dawley was used because of the unavailability of old Wistar rats. In chapter 6, the focus was on the influence of cultivation methods on the proteome of primary mouse hepatocytes (PMH). This study was part of the BMBF funded project "Virtual Liver". Here, the intracellular proteome of middle-aged primary mouse hepatocytes in conventional monolayer cultures (ML) was compared to collagen sandwich culture (SW) after 1 day and 5 days of cultivation with 2-D DIGE and MALDI ToF MS/MS. Proteomic methods were supposed to reveal whether the choice of cultivation method has influence on specific protein markers related to oxidative stress.

2. Materials & Methods

2.1 Chemicals

William's medium E (WME) was purchased from Pan Biotech GmbH (Aidenbach, Germany). Dexamethasone, calcein AM, bovine serum albumin (BSA), trichloroacetic acid (TCA), tetrahydrofuran, N-laurylsarcosine, CHAPS, sodium dodecyl sulfate (SDS), glycerol, ammonia bicarbonate, bromophenol blue, N,N,N′,N′-tetramethylethylenediamine (TEMED), ammonium persulfate (APS), $DCFH_2$- DA, quercetin, N' acetylcysteine, iodoacetamide (IAA), hydrocortisone, DTNB and glutathione reductase (GR) were obtained from Sigma Aldrich (Steinheim, Germany). Insulin/transferrine/selenium (ITS) was purchased from Invitrogen (Karlsruhe, Germany) and lyophilized rat tail collagen from Roche (Penzberg, Germany). TRIS, 24eroxiredoxin24 (DTT), GSH, NADPH and urea were purchased from Carl Roth (Karlsruhe, Germany). Thiourea was purchased from Merck (Darmstadt, Germany) and Percoll from Biochrom (Berlin, Germany). Mineral oil, Bio-Lyte® 3/10 ampholyte 100x and 10x Tris/Glycine/SDS-buffer were bought from Bio-Rad Laboratories, Inc. (Hercules, CA, USA) and NaCl from VWR International GmbH (Bruchsal, Germany). LE Agarose was purchased from Biozym Scientific GmbH, Hessisch Oldendorf, Germany). HEPES, penicillin/streptomycin, gentamycin and insulin were obtained from cc-pro (Oberdorla, Germany). Fetal calf serum (FCS) was purchased from PAA Laboratories (Pasching, Austria).

2.2 Cell culture

2.2.1 Monolayer culture of primary rat hepatocytes

The isolation of primary rat hepatocytes was performed by Pharmacelsus GmbH (Saarbrücken, Germany). The cells were extracted from male Wistar (Janvier, Le Genest-St-Isle, France) and Sprague Dawley rats (Harlan Laboratories Inc., Indianapolis, USA) using two- step collagenase perfusion as previously described (Figliomeni & Abdel-Rahman, 1998). Animals were either middle- aged (6 months) or old (> 23 months). Viable hepatocytes were enriched with Percoll density gradient centrifugation (Pertoft et al., 1978). Percoll solutions contain silica particles coated with a layer of polyvinylpyrrolidone (PVP). Percoll solutions diluted

with water have high density, low osmolarity and low viscosity resulting in the generation of gradients during centrifugation of the colloid, resulting in the separation of viable hepatocytes from dead ones.

For enrichment of hepatocytes, a 25% Percoll solution (v/v with PBS) (Easycoll, Biochrom, Berlin, Germany) was overlaid with the cell suspension containing 35 × 10^6 viable cells (estimated with trypan blue staining, chapter 2.2.3) in a volume of 5 ml culture medium and centrifuged at 1000 × g for 20 min at 25 °C (Labofuge 400 R, Thermo Scientific, Waltham, USA). The supernatant with the dead cells was aspirated and the pellet was resuspended in 50 ml of PBS prior to centrifugation for 5 min at 50 × g and 25 °C. In the resulting pellet living hepatocytes were enriched. It was resuspended in Williams Medium E (WME) supplemented with 15 mM HEPES, 1% penicillin/streptomycin, 50 µg/ml gentamycin, 1.4 µM hydrocortisone and 1 µM insulin (WME 0). For adhesion of the cells, WME was supplemented with 10% fetal calf serum (WME 10).

The hepatocytes were seeded in culture vessels pre-coated with 7.5 µg/cm^2 of rat tail collagen as described in Table 2-1 and left to adhere at 37 °C in a humidified atmosphere containing 5% CO_2 for 4 hours. The medium was changed to WME0 and the cells were incubated over night before starting antioxidant treatment and heat stress.

Table 2-1: Number of seeded viable hepatocytes in different culture vessels

Culture vessel	Seeded cell number
6 well plate (assays)	1×10^6
6 cm petridish (intracellular proteome)	2×10^6
75 cm^2 flask (extracellular proteome)	10×10^6

2.2.2 Monolayer and sandwich culture of primary mouse hepatocytes

Culture of primary mouse hepatocytes (PMH) was carried out by Saskia Sperber. Primary mouse hepatocytes were isolated from livers of male C57/BL6 mice (Charles River Laboratories, Sulzfeld, Germany) using collagenase perfusion as previously described (Seglen, 1972). After over-night shipping in suspension or directly after isolation the transport medium was removed via centrifugation (Heraeus Laborfuge 400R Functionline, Thermo Scientific; 50 × g, 5 min, RT). The cells were seeded at a density of 600 000 cells per well on 6 well

plates pre-coated with a collagen solution of 1 mg/ml. The cultures were prepared as collagen sandwich (SW) and collagen monolayer (ML) cultures as previously described (Tuschl & Mueller, 2006). Hepatocytes were cultivated in Williams Medium E (WME) containing 100 U/ml penicillin, 100 µg/ml streptomycin, 0.00001% ITS and 100 nM dexamethasone at 37 °C in a humidified atmosphere containing 5% CO_2 for up to 5 days.

2.2.3 Monolayer culture of the hepatoma cell line *HepG2*

The human hepatoma cell line HepG2 (DSMZ, Braunschweig, Germany) was maintained in Williams Medium E (WME) supplemented with 15 mM HEPES, 1% penicillin/streptomycin, 50 µg/ml gentamycin, 1.4 µM hydrocortisone and 1 µM insulin (WME 0). For adhesion of the cells, WME was supplemented with 10% fetal calf serum (WME 10). *HepG2* were cultivated at 37 °C in a humidified atmosphere containing 5% CO_2 in an incubator and were subcultivated at 90% confluency. The cells were seeded in culture vessels without coating and left to adhere at 37 °C in a humidified atmosphere containing 5% CO_2 for 4 hours. The medium was changed to WME0 and the cells were incubated over night before starting antioxidant treatment and heat stress.

2.2.4 Determination of viable cell number

Trypan blue

To estimate viable cell number before seeding, 10 µl of cell suspension were mixed with an equal amount of trypan blue solution (Invitrogen, Karlsruhe, Germany). 10 µl of that mix were transferred into a Neubauer chamber and then counted under the microscope (IX70 microscope, Olympus, Hamburg, Germany). Trypan blue stains only dead cells blue, whereas living cells remain white.

Calcein AM

For the determination of viable cell number in culture, calcein AM (1 mg/ml in dimethyl sulfoxide) was diluted with serum free WME to a final concentration of 4 µg/ml. Adherent cells in culture were stained and analyzed as previously described (Priesnitz et al., 2016).

2.3 Induction of oxidative stress and administration of antioxidants

For induction of oxidative stress, the cells were exposed to heat stress for 30 min at 42 °C in a humidified atmosphere containing 5% CO_2. To reach a temperature of 42 °C inside the culture vessels, the incubator was set to a temperature of 41.5 °C (Figure 2-1). Temperature measurements were carried out with a PT100 FS-400P sensor and Labview 8.0 (National Instruments, Austin, SA). The temperature in the culture vessels reached 42.2 °C after 25 min of heating. Due to technical limitations, the actual temperature was slightly above the target temperature of 42.0 °C. However, this default temperature was reproducible in all experiments and adequate to induce oxidative stress in our experimental setup. The heating phase was followed by the 30 min heat stress phase (constant temperature at 42 °C) and a 5 min cool down to 37 °C.

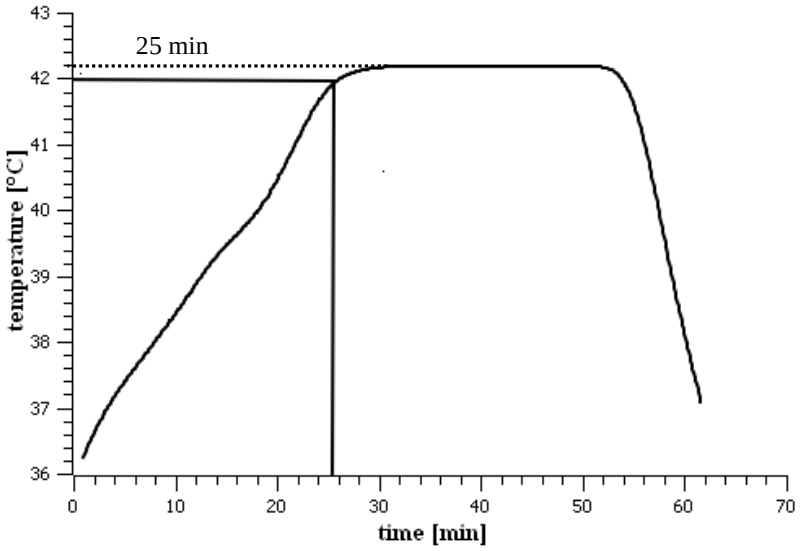

Figure 2-1: Temperature curve during the induction of oxidative stress through heat treatment; $Temp_{set}$: 41.5 °C, $Temp_{target}$: 42.0 °C (t = 25 min).

As a control, cells were treated with a subtoxic concentration (2 mM) of hydrogen peroxide (Conde de la Rosa et al., 2006) for 1 h to induce formation of reactive oxygen species. For antioxidant treatment, cells were incubated with 50 µM of quercetin (Liu et al., 2010) or 500 µM of N' acetylcysteine (Zaragoza et al., 2000) for 4 h prior to heat stress and H_2O_2-treatment.

2.4 Determination of hepatic function and oxidative stress response

2.4.1 Albumin secretion

The albumin release into the supernatant was determined using a highly sensitive two site enzyme linked immunoassay (ELISA) for measuring albumin in biological samples of rats (Immunoperoxidase for determination of albumin in rat samples (Genway Biotech, San Diego, CA)).

The principle of the assay is represented in Figure 2-2. Collected supernatants were diluted 1:30 or 1:80 depending on cultivation time. The albumin in the samples binds to the anti-albumin antibodies on the surface of the polystyrene microtiter plate. After removing unbound proteins, anti-albumin antibodies conjugated with horseradish peroxidase (HRP) are added. The resulting complexes are assayed by adding a chromogenic substrate, 3,3',5,5'-tetramethylbenzidine (TMB) and measuring the absorbance with an iEMS absorbance Reader MF (Labsystems, Helsinki, Finland) at 450 nm.

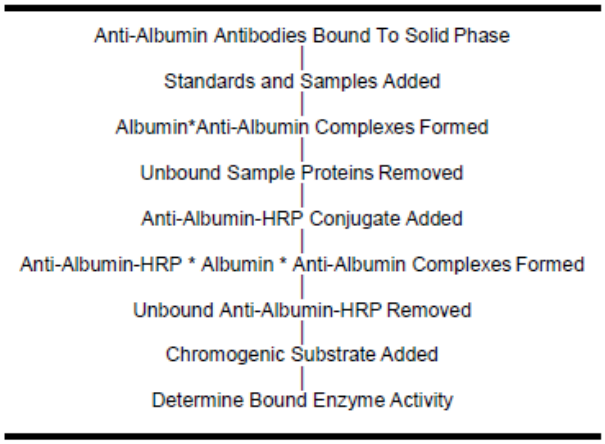

Figure 2-2: Principle of the two site enzyme linked immunoassay (ELISA) for measuring albumin production of primary rat hepatocytes (http://www.genwaybio.com).

2.4.2 AST release

Aspartate aminotransferase (AST) is a liver specific enzyme only present in the supernatant, if the integrity of the cell membranes is disturbed. Therefore it is commonly used as a viability marker in *in vitro* hepatocyte cultures. AST activity was determined using the Fluitest® GOT

AST test kit from Analyticon Biotechnologies AG (Lichtenfels, Germany). AST catalyzes the conversion of aspartate and α-ketoglutarate to oxaloacetate and glutamate. Oxaloacetate is then reduced to malate while NADH is consumed. The absorbance of NADH was measured with an iEMS absorbance Reader MF (Labsystems, Helsinki, Finland) at 340 nm. The AST activity was interpolated from the standard curve using a multi-calibrator (Bio Cal® E, Analyticon Biotechnologies AG, Lichtenfels, Germany).

2.4.3 LDH release

Lactate dehydrogenase (LDH) is a stable cytoplasmic enzyme catalyzing the conversion of lactate to pyruvate, as it converts NAD^+ to NADH. It is present in all cells and rapidly released into the cell culture supernatant upon damage of the plasma membrane. LDH release was determined using the LDH Cytotoxicity Detection Kit from Roche Diagnostics GmbH (Mannheim, Germany). Collected supernatants were diluted 1:5 or 1:20 depending on cultivation time. The principle of the assay is represented in Figure 2-3. In the first step NAD^+ is reduced to NADH by the LDH-catalyzed conversion of lactate to pyruvate. In the second step the catalyst (diaphorase) transfers H/H^+ to the tetrazolium salt, which is reduced to formazan. The absorbance of the formazan dye was measured with an iEMS absorbance reader MF at 490 nm. The LDH release was interpolated from the standard curve using a multi-calibrator (Bio Cal® E, Analyticon Biotechnologies AG, Lichtenfels, Germany).

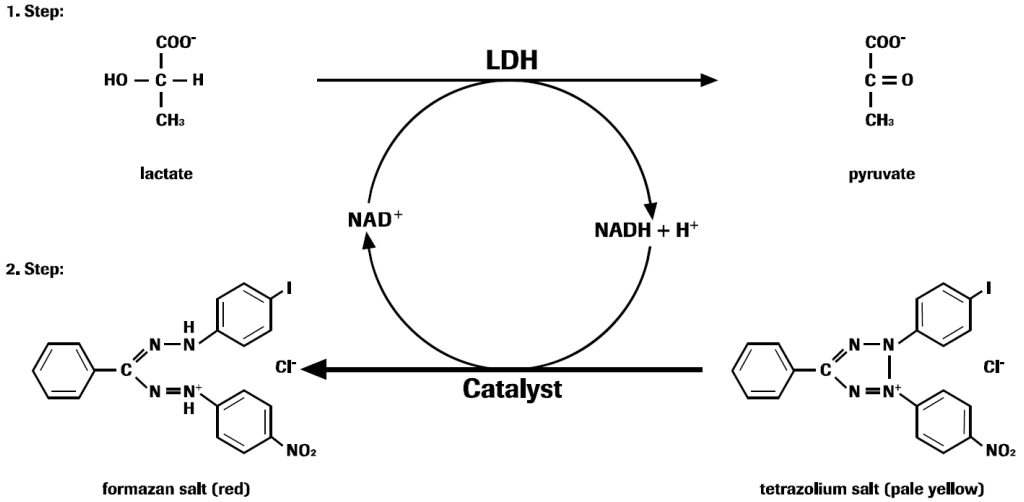

Figure 2-3: Assay principle of the LDH Cytotoxicity Detection Kit (Sigma-Aldrich). Abbreviations: LDH: lactated dehydrogenase; $NAD^+/H+H^+$: nicotinamide adenine dinucleotide.

2.4.4 Superoxide dismutase activity

Superoxide dismutase (SOD) catalyzes the dismutation of superoxide radicals to hydrogen peroxide. The SOD activity was determined using the OxiSelect™ Superoxide Dismutase Activity Assay from Cell Biolabs (San Diego, USA). Intracellular samples were concentrated 7-fold using centrifugal filter devices according to manufacturer's instructions (Amicon® Ultra- 0.5, 10 kDa MWCO, Merck Millipore, Darmstadt, Germany) to reach the detection limit of the assay. The SOD activity assay uses a xanthine/xanthine oxidase (XOD) system to generate superoxide anions. The included chromagen produces a water-soluble formazan dye upon reduction by superoxide anions. The activity of SOD is determined as the inhibition of chromagen reduction (Figure 2-4). The absorbance of the formazan dye was measured with an iEMS absorbance reader MF at 490 nm.

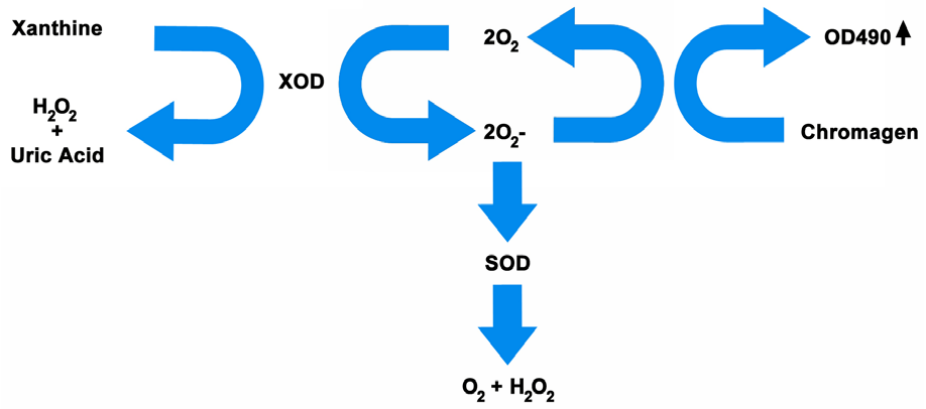

Figure 2-4: Assay principle of the OxiSelect™ Superoxide Dismutase Activity Assay (Cell Biolabs (San Diego, USA)). Abbreviations: SOD: Superoxide dismutase; XOD: xanthine oxidase

2.4.5 Catalase activity

The catalase activity was determined using the fluorometric OxiSelect™ Catalase Activity Assay Kit (Cell Biolabs, San Diego, USA). Catalase is an antioxidant heme enzyme that removes hydrogen peroxide by dismutation. Hydrogen peroxide is toxic to eukaryotic cells and initiates oxidation of DNA, lipids, and proteins. The principle of the assay is presented in Figure 2-5. Catalase induces decomposition of H_2O_2 to produce water and oxygen. In the presence of horseradish peroxidase (HRP), non-fluorescent ADHP (10-Acetyl-3,7-dihydroxyphenoxazine) is oxidized to the highly fluorescent resorufin. As the catalase activity increases, the resorufin signal decreases. The absorbance of resorufin is measured

fluorometrically with Fluoroscan Ascent CF (Labsystems, Helsinki, Finnland) with a 544/590 nm filter set.

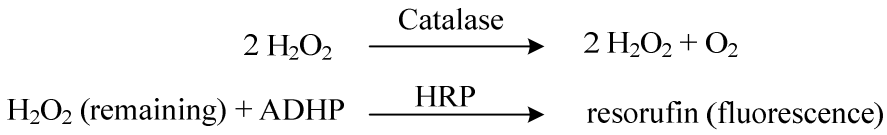

Figure 2-5: Assay reactions of the OxiSelectTM Catalase Activity Assay. Abbreviations: ADHP: 10-Acetyl-3,7-dihydroxyphenoxazine; HRP: horseradish peroxidase

2.4.6 Protein carbonyl content

Protein oxidation is the covalent modification of a protein by reactive oxygen species (ROS) or by reaction with secondary by-products of oxidative stress. The most common products of protein oxidation in biological samples are the protein carbonyl derivatives of proline, arginine, lysine, and threonine (Berlett & Stadtman, 1997). These derivatives are chemically stable and serve as markers of oxidative stress.

Carbonyl content in protein samples was determined using the OxiSelect™ Protein Carbonyl Fluorometric Assay (Cell Biolabs, San Diego, USA). The carbonyl residues are first derivatized with a protein carbonyl fluorophore, which binds to the protein carbonyl group in a 1:1 ratio. Proteins are then TCA precipitated and free fluorophore is removed by washing the protein pellet with acetone. After dissolving the protein pellet in guanidine hydrochloride, the absorbance of the protein- fluorophore is measured fluorometrically with Fluoroscan Ascent with a 485/538 nm filter set.

2.4.7 Reactive oxygen species (ROS)

For detection of ROS, an assay initially developed for H_2O_2 detection (Brandt & Keston, 1965) was used.

The principle of the assay is represented in Figure 2-6. The cells were treated with 10 µM 2′,7′-dichlorofluorescin diacetate ($DCFH_2$ –DA) at 37 °C in a humidified atmosphere containing 5% CO_2 for 30 min. The nonfluorescent lipophilic $DCFH_2$ –DA diffuses through the cell membrane. Intracellular esterases deacetylate $DCFH_2$ –DA to form $DCFH_2$, which is membrane-impermeable (Chen et al., 2010). $DCFH_2$ reacts with intracellular ROS to produce the fluorescent DCF, which can be measured with a 485/538 nm filter set.

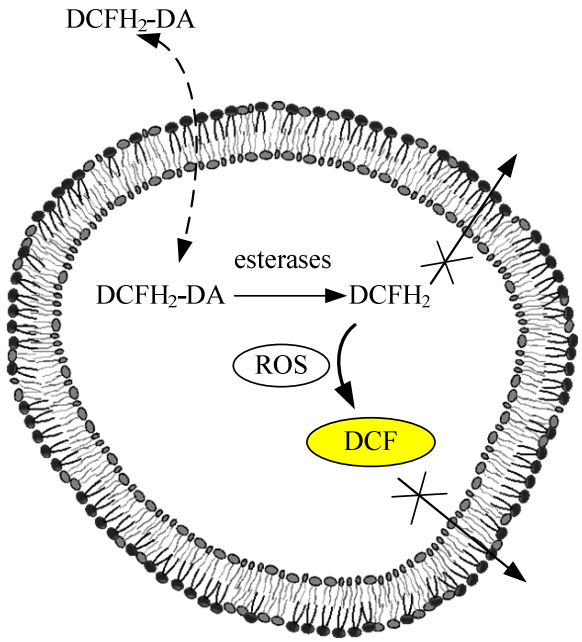

Figure 2-6: The generally accepted formation mechanism of DCF in cell. Abbreviations: $DCFH_2$ –DA: 2′,7′-dichlorofluorescin diacetate

2.4.8 Determination of total cellular glutathione

The quantitative determination of total glutathione (GSH/GSSG) was carried out as previously described (Rahman et al., 2006). The principle of the kinetic recycling assay is shown in Figure 2-7. Reduced glutathione (GSH) reacts with DTNB (5,5'–dithiobis-(2-nitrobenzoic acid)) to form free TNB, which can be measured with an iEMS absorbance reader MF at 412 nm. Oxidized glutathione (GSSG) is reduced by glutathione reductase (GR). Therefore, the determined concentration represents the total amount of glutathione in the sample. The adherent cells were washed twice with 2 ml cold PBS, collected with a cell scraper and resuspended in 1 ml PBS. After centrifugation (1000 × g/5 min/4 °C), the cell pellet was resuspended in 100 µl 3 % (w/v) metaphosphoric acid. The sample was frozen, defrosted and centrifuged at 3000 × g and 4 °C for 10 min. The protein content in the pellet was analyzed using a Bradford assay (see chapter 2.5.1). The supernatant was used for total glutathione measurement. 20 µl of supernatant were mixed with 120 µl of a 1:1 solution of DTNB/GR (1.7 mM DTNB and 6.8 units GR) and incubated for 30 seconds. Then, 60 µl of 0.8 mM NADPH were added and the absorbance at 412 nm was measured. GSH values were interpolated from a GSH standard curve. During the assay oxidized GSH (GSSG) is reduced by

GSH reductase (GR) in the presence of NADPH. Therefore, the measured values represent the total amount of cellular GSH. For data analysis GSH values are expressed as nmol per mg protein.

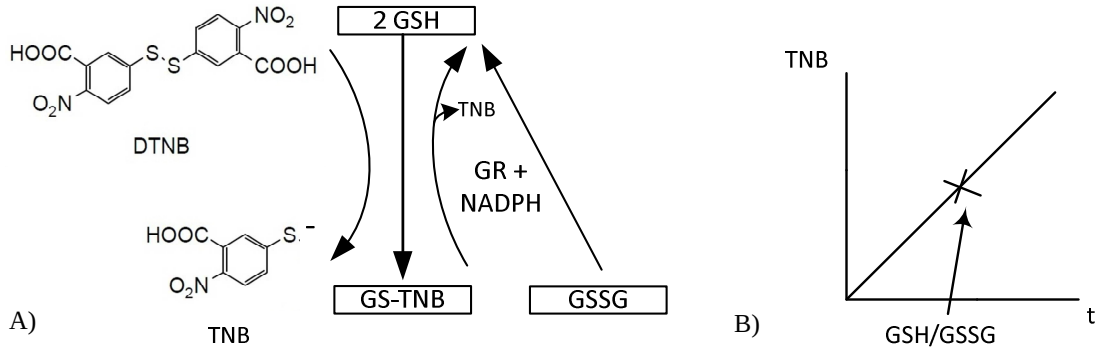

Figure 2-7: A) Schematic representation of the glutathione recycling assay for quantitative determination of total cellular glutathione. B) Principle of the kinetic assay for determination of total glutathione. Abbreviations: GR: glutathione reductase; DTNB: 5,5'–dithiobis-(2-nitrobenzoic acid); GSH: reduced glutathione; GSSG: oxidized glutathione

2.5 Proteome analysis

2.5.1 Bradford assay

The protein content of the samples was determined using a Bradford assay (Bradford, 1976). Bovine serum albumin (BSA) in a concentration range of 0-1 mg/ml served as calibrator. Samples were diluted with MilliQ water to be within calibration range. 10 µl of BSA or protein samples were mixed with 200 µl assay reagent (1:5 with MilliQ water, Bio-Rad Laboratories, Inc., Hercules, USA) in a 96-well plate and incubated for 10 min on a rocking table. The absorbance was measured at 595 nm with an iEMS absorbance Reader.

2.5.2 Extracellular proteome

Ultrafiltration and purification of extracellular proteins

Cell culture supernatants were collected 24 h and 48 h after heat stress and centrifuged for 20 min at 3000 × g and 4 °C (Labofuge 400R, Heraeus, Thermo Fisher Scientific, Waltham, USA) to remove dead cells and cell debris.

The samples were 20fold concentrated, desalted and the buffer exchanged using Vivaspin 15 ml ultrafiltration devices (10 kDa MWCO, Sartorius Stedim Biotech GmbH, Göttingen,

Germany). The filter devices were first sterilized with 70% ethanol and then washed with MilliQ water at 3000 × g and 4 °C (Labofuge 400R, Heraeus, Thermo Fisher Scientific, Waltham, USA). 10 ml of cell culture supernatant were concentrated for 45 minutes at 3000 × g at 4 °C to a volume of 500 µl. The filter devices were then filled up twice with 40 mM NH_4HCO_3 (pH 9.5) containing 0.4 mM Pefabloc® SC Plus (Roche Diagnostics, Mannheim) and centrifuged as described before.

Immunodepletion for the removal of highly abundant proteins

Selective immunodepletion enables the removal of seven highly abundant proteins from rat serum. 60-70% of total protein was depleted resulting in the enrichment of low-abundant proteins for downstream proteomic analyses. The depletion of albumin, transferrin, haptoglobin, α_1 antitrypsin, fibrinogen, IgG and IgM was carried out using Seppro® Rat Spin Columns (Sigma Aldrich, Steinheim, Germany).

Samples containing 600 µg of protein were transferred to the spin columns and incubated on a rocking table for 15 min at room temperature. The columns were then centrifuged at 2300 × g for 30 s (Heraeus Biofuge Fresco, Thermo Fisher Scientific, Waltham, USA) to obtain the first fraction (F1) of flow-through proteins. This centrifugation step was repeated with 500 µl of dilution buffer to obtain the second fraction (F2) of flow- through. Bound proteins (B) were eluted by washing four times with stripping buffer as described above. All bound fractions were pooled and neutralized with neutralization buffer for further analysis of highly abundant proteins.

Afterwards, the depleted samples were filtered with Vivaspin 4 ml to exchange buffer to 40 mM NH_4HCO_3 (same procedure as Vivaspin 15 ml, chapter 2.5.2). Respective fractions were separated with 1-D gel electrophoresis (Figure 2-8) and proteins were identified with MALDI ToF/ToF mass spectrometry to verify successful immunodepletion. Albumin, transferrin and haptoglobin were identified in the bound fraction, but not in the flow-through fraction.

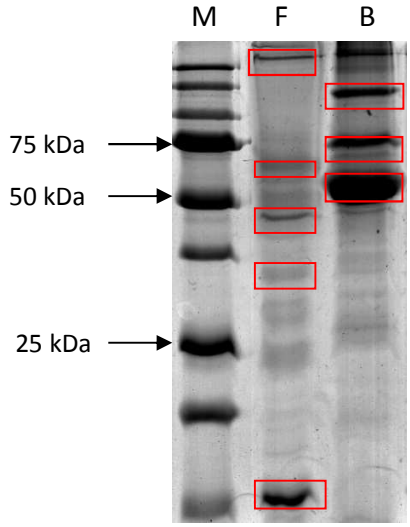

Figure 2-8: 1-D SDS PAGE with 10 µg protein after 24 h of cell culture, EZBlue Coomassie staining; protein identification with MALDI ToF/ToF. M: molecular weight marker, F: flow- through fraction with extracellular proteins (high to low molecular weight: α1-inhibitor 3, hemopexin, vitamin D-binding protein, major urinary protein), B: specifically bound fraction with highly abundant proteins (high to low molecular weight: haptoglobin, albumin, transferrin)

Acetone precipitation

Acetone precipitation is a widely used method for concentrating and purifying most soluble proteins. Salts and many lipid soluble contaminants are removed. Four volumes of prechilled (4 °C) acetone were mixed with one volume of concentrated protein solution and incubated for 2 h at -20 °C. Afterwards, the samples were centrifuged at 12300 × g and 4 °C for 10 min (Heraeus Biofuge Fresco, Thermo Fisher Scientific, Waltham, USA). The supernatant was discarded and the pellet left to dry for 30 min at room temperature. The pellet was resuspended in 125 µl of rehydration buffer (7 M urea; 2 M thiourea; 4% CHAPS (w/v); 0.6% Bio-Lyte® 3/10 ampholyte 100x (v/v); 40 mM DTT) prior to 2-D gel electrophoresis.

2.5.3 Intracellular proteome

Extraction of intracellular proteins

Cells were washed twice with PBS (4 °C) followed by the addition of cold lysis buffer (50 mM Tris, pH 7.4; 150 mM NaCl; 0.1% N-laurylsarcosine (w/v); 1 mM EDTA; 0.4 mM Pefabloc® SC Plus). Cells were incubated for 30 min at 4 °C. Collagen and cells were scraped of the dishes, transferred into Eppendorf reaction tubes and centrifuged at 12300 × g and 4 °C for 10

min (Heraeus Biofuge Fresco, Thermo Fisher Scientific, Waltham, USA). TCA (7.5% v/v) was added to the supernatant to precipitate proteins and the mixture was incubated for 2 h on ice followed by another centrifugation step at 12300 × g and 4 °C for 10 min. The pellet was washed twice with 2 ml tetrahydrofuran (4 °C), centrifuged as mentioned above and resuspended in 125 µl rehydration buffer (7 M urea; 2 M thiourea; 4% CHAPS (w/v); 0.6% Bio-Lyte® 3/10 ampholyte 100x (v/v); 40 mM DTT) by sonication for 30 min. The determination of the intracellular protein content was carried out using the previously described (chapter 2.5.1) Bradford assay (Bradford, 1976).

Intracellular protein extracts were cleaned from ionic detergents, salts, lipids and nucleic acids prior to 2-D gel electrophoresis using the ReadyPrep 2-D cleanup kit (Bio-Rad Laboratories, Inc., Hercules, CA, USA) according to manufacturer's instructions. Resulting protein pellets were resuspended in 100 µl of rehydration buffer (7 M urea; 2 M thiourea; 4% CHAPS; 0.6% Bio-Lyte® 3/10 ampholyte 100x; 40 mM DTT).

Protein purification

Protein extracts were purified using the ReadyPrep 2-D cleanup kit (Bio-Rad Laboratories, Inc., Hercules, USA) prior to 2-D gel electrophoresis. The procedure works by quantitatively recipitating and concentrating proteins in a sample while washing away ionic detergents, salts, nucleic acids, lipids, and plant-derived phenolic compounds, all of which are known to interfere with IEF.

Up to 500 µg protein in a final volume of 100 µl were mixed with 300 µl of agent 1 to precipitate proteins. After 15 min incubation on ice, 300 µl of agent 2 were added and the samples centrifuged at 12300 × g for 10 min at 4 °C (Heraeus Biofuge Fresco, Thermo Fisher Scientific, Waltham, USA). The resulting pellet was first washed with 40 µl of wash reagent 1 and then with 25 µl MilliQ water. 1 ml of wash reagent 2 (pre-chilled at -20 °C) and 5 µl of wash 2 additive were added to the pellet. The mix was incubated for 30 min on ice and vortexed every 10 min for 30 sec. After centrifugation at 12300 × g for 10 min at 4 °C (Heraeus Biofuge Fresco, Thermo Fisher Scientific, Waltham, USA), protein pellets were resuspended in 125 µl of rehydration buffer (7 M urea; 2 M thiourea; 4% CHAPS (w/v); 0.6% Bio-Lyte® 3/10 ampholyte 100x (v/v); 40 mM DTT) prior to 2-D gel electrophoresis.

2.5.4 Two-dimensional SDS-PAGE

In the first dimension, the protein samples were separated by isoelectric focusing (IEF) using immobilized pH gradient (IPG) strips (7 cm, pH 3-10, non-linear for intracellular proteins and pH 5-8, linear for extracellular proteins) (Bio-Rad Laboratories, Inc., Hercules, USA) in a Protean® IEF cell (Bio-Rad Laboratories, Inc., Hercules, CA, USA). IPG strips were thawed for 1 h at room temperature prior to use. The samples containing 100 µg of protein in a volume of 125 µl rehydration buffer (7 M urea; 2 M thiourea; 4% CHAPS (w/v); 0.6% Bio-Lyte® 3/10 ampholyte 100x (v/v); 40 mM DTT) were pipetted in a loading tray and carefully covered with the IPG strip avoiding air bubbles. The samples were overlaid with mineral oil and left inside the Protean® IEF cell for 16 h at 20 °C for passive rehydration. IEF was carried out using the program described in Table 2-2 with a total of 46 000 volt-hours.

Table 2-2: Program for isoelectric focusing of protein samples

Stage	Voltage [V]	Duration [h]
S 1	100	1
S 2	200	1
S 3	500	2
S 4	700	1
S 5	2500 ↗	6 (linear)
S 6	2500	14
S 7	500	unlimited

After IEF, the focused strips were equilibrated on a rocking table in equilibration buffer I (6 M urea; 2% SDS; 0.375 M TRIS; 30% glycerol; 1% DTT) for 15 min followed by 15 min incubation in equilibration buffer II (6 M urea; 2% SDS; 0.375 M TRIS; 30% glycerol; 2.5% IAA). For the second dimension, the samples were separated on a 12.5% SDS Laemmli gel (Laemmli, 1970) overlaid with agarose (1% low-melt agarose (w/v), 0.4% bromphenol blue in 5 × Tris/glycine/SDS-buffer) in a Mini- PROTEAN Tetra cell (Bio-Rad Laboratories, Inc., Hercules, CA, USA). The chamber was filled with 1.5 l of 1 × Tris/Glycine/SDS-buffer. A constant current of 15 mA per gel was applied until the bromophenol blue tracking lane reached the end of the gel. For protein identification gels were stained with EZBlue™ according to the manufacturer's instructions (Bio-Rad Laboratories, Inc., Hercules, CA, USA).

2.5.5 Colloidal Coomassie staining (EZBlue™)

SDS gels were stained with EZBlue™ Coomassie Brilliant Blue G-250 colloidal protein stain (Bio-Rad Laboratories, Inc., Hercules, CA, USA). After SDS- PAGE, the gels were first washed 3 x 5 min with deionized water to remove excess SDS. Protein spots were fixed in 50% methanol, 10% acetic acid for 15 min followed by a washing step with deionized water for another 15 minutes. Gels were stained with EZBlueTM staining for 45 – 60 min.

As a colloidal stain, it interacts only with proteins, not the gel itself. Therefore, background staining is reduced. Additionally, a washing step with deionized water for 2 h further intensifies the protein spots.

2.5.6 In-Gel digest

For the identification of proteins which show significantly changed abundance in DIGE analysis, EZBlue^{TM}- stained protein spots were picked and destained completely by washing 3-5 times with 100 µl 50% acetonitrile for 5 min at 37 °C. The destained gel-pieces were dehydrated with 100% acetonitrile, 5 µl of sequencing-grade modified trypsin (0.15 µg/µl in 40 mM ammonium bicarbonate buffer; Promega Corp., Madison, USA) was added and incubated overnight at 37 °C for digestion. Trypsin proteolysis was stopped by adding 0.5 µl of 10% trifluoroacetic acid (TFA). For further peptide extraction, gel pieces were covered with 60% acetonitrile, 0.1% TFA and sonicated for 15 min. This step was repeated with 100% acetonitrile. All supernatants were pooled and the volume was reduced in a SpeedVac (Jouan RC 10.22). The peptide samples were concentrated and purified using ZipTip C18 (Merck Millipore, Billerica, USA) according to manufacturer's instructions.

2.5.7 Desalting and concentrating with ZipTip C18

For desalting and concentrating of peptides, ZipTip C18 (Millipore Corporation, Billerica, USA) were used. The tips were wetted with 10 µl of 100% ACN and equilibrated with 10 µl of 0.1% TFA. Afterwards, the peptides were bound to the C18 material by pipetting the samples up and down ten times. Bound peptides were washed with 10 µl of 0.1% TFA and eluted in 5 µl matrix solution (5 mg/ml α-cyano-4-hydroxycinnamic acid (CCA) in 70% acetonitrile, 0.1% TFA) prior to spotting onto a MALDI-target plate (384 well Opti-TOF, Applied Biosystems, Darmstadt, Germany).

2.5.8 Matrix assisted laser desorption/ionization (MALDI) mass spectrometry

MS and MS/MS analysis was performed on an Applied Biosystems 4800 MALDI TOF/TOF Analyzer (Applied Biosystems). The analyzer was calibrated using the 4700 Proteomics Analyzer Calibration Mixture (Applied Biosystems). MS-data was generated in positive reflector-mode in a mass range of 700-4000 m/z with 50 shots per subspectrum accumulating 1000 shots in total. Common fragments of the calibrant and matrix were added to an exclusion list. Laser frequency was set to 200 Hz using a Nd:YAG laser operating at 355 nm and laser intensity was adjusted according to spectrum quality (usually 2700 – 3000). For MS/MS analysis a total of 5 precursor ions per fraction were selected by the software (4000 series explorer software, version 3.5.1, Applied Biosystems) for MS/MS-analysis.

The threshold criteria for MS/MS were a minimum signal-to-noise ratio of 20 and a precursor mass tolerance between spots of 100 ppm. MS/MS data was produced with 100 shots per subspectrum with 2000 shots in total or after achieving stop criteria of a signal-to-noise ratio of 20 for at least 10 peaks in the MS/MS spectrum and accumulation of at least 12 subspectra. Peptides were fragmented by 1 kV collisions via collision-induced dissociation (CID).

Generated spectra were searched with MASCOT search algorithm (Perkins et al., 1999) (version 2.1.03) (http://www.matrixscience.com) against the Swiss-Prot database with mouse taxonomy using GPS explorer software v. 3.6 (Applied Biosystems). Search parameters were: maximum missed cleavages: 1; precursor mass tolerance: 100 ppm; MS/MS fragment tolerance: 0.3 Da; variable modifications allowed: oxidation of methionine and carbamidomethylation of cysteine. Protein scores were significant above a value of 55 or 85 depending on the measurement. The function of the identified proteins was retrieved from Uniprot Knowledge Base (Bateman et al., 2017) .

2.5.9 Difference gel electrophoresis (DIGE)

The CyDye^{TM} DIGE Fluor (minimal dye) labeling kit (GE Healthcare, Little Chalfont, UK) was used to quantify significant differences in abundance of proteins. The DIGE method was previously described (Unlü et al., 1997). The minimal labeling ensures that the dyes label approximately 1– 2% of the available lysines and that only a single lysine per protein molecule is labeled. CyDyes were reconstituted in 99.8% anhydrous dimethylformamide (DMF) to give a stock solution of 1 mM. For each of the three replicate gels 15 µg of untreated sample (Cy3),

treated sample (Cy5) and internal standard (Cy2) were diluted with lysis buffer (30 mM TRIS; 7 M urea; 2 M thiourea; 4% CHAPS (w/v)) to a final volume of 7.5 µl and incubated with 120 pmol of the respective CyDye for 30 min on ice. To stop the labeling reaction, 1 µl of 10 mM lysine was added to the samples and the mix was incubated for another 30 min on ice. After the protein samples have been CyDye labeled, an equal volume of 2 × sample buffer (8 M urea; 4% CHAPS (w/v); 2% Bio-Lyte® 3/10 ampholyte 100x (v/v); 130 mM DTT) was added and left on ice for 10 min. The protein samples that were going to be separated on the same gel were pooled.

2-D gel electrophoresis was carried out using special low-fluorescence glass plates (NHDyeagnostics, Halle, Germany). Fluorescence images of the gels were obtained using Typhoon Trio Variable Mode Imager (GE Healthcare, Little Chalfont, UK) and analyzed with DeCyder 2-D v 7.0 software according to developer's instructions. Statistical evaluation was accomplished by applying one-way ANOVA and Student's t-test. Only proteins with a threshold change of at least 1.5 or -1.5 and a minimum significance level of p=0.05 were accepted as significantly changed in the treated group.

3. Secretome analysis of primary hepatocytes from middle-aged and old Wistar rats under oxidative stress conditions for biomarker discovery

3.1 Introduction

The inevitable process of aging is defined as a time-dependent decline in the maintenance of homeostasis and hence an increasing disposition to degenerative diseases and death (Hayflick, 1998). There are various theories of aging (see Chapter 1). The most prominent is the free radical theory of aging (Harman, 1956) which proposes that the damage to macromolecules induced by reactive oxygen species is responsible for aging. Consequently, the search for potential therapeutic biomarkers that could allow diagnosis and protection from ROS-induced cell aging is of wide interest.

According to the National Institutes of Health (NIH) a biomarker is "a characteristic that is objectively measured and evaluated as an indicator of normal biological processes, pathogenic processes, or pharmacologic responses to a therapeutic intervention" (2001). For clinical purposes, a biomarker candidate requires a high specificity and reproducibility and is, ideally, easy to access and robust. One approach for biomarker discovery is the analysis of the entirety of the proteins secreted by an *in vitro* hepatocyte culture into a conditioned medium. Secreted, soluble proteins are likely to be present in bodily fluids and therefore easy to measure with non-invasive methods. Active secretion of proteins is divided into the classical and the non-classical secretory pathway. Classically secreted proteins contain a N-terminal signal sequence which can be processed via endoplasmic reticulum and Golgi apparatus (Klee & Sosa, 2007). All secretion pathways of proteins without signal sequence are referred to as non-classical, including transport in lysosomes and exosomes, shedding of plasma membrane vesicles and direct secretion through membrane transporters (Nickel & Seedorf, 2008).

The totality of proteins secreted actively from living cells is referred to as the secretome, a term first introduced in 2000 (Tjalsma et al., 2000). Secretome analysis already revealed many

promising biomarker candidates, e.g. oxidized albumin for type 2 diabetes (Jun et al., 2017) or other proteins related to diabetes (Dowling et al., 2008; Song et al., 2009), several types of cancer (Kulasingam & Diamandis, 2008; Gunawardana et al., 2009; Srisomsap et al., 2010), (Gunawardana et al., 2009) and neurodegenerative diseases (Jeon et al., 2010) such as Parkinson's disease (Pan et al., 2014).

In this study the secretomes of primary hepatocytes from middle-aged (6 months) and old (> 23 months) Wistar rats (PRH) were analyzed under oxidative stress conditions compared to control conditions using 2-D DIGE and MALDI ToF MS/MS. Oxidative stress was induced by heat treatment at 42 °C for 30 min. Heat stress induces the formation of ROS through various mechanisms (see Chapter 1). For instance, hyperthermia causes an increase in superoxide anions (Mujahid et al., 2006), hydrogen peroxide (Zhao et al., 2006) and hydroxyl radicals (Zhao et al., 2006). Additionally, heat stress activates NADPH oxidase, an enzyme which generates ROS by converting NADPH to NADP (Slimen et al., 2014). The advantage of using heat stress for induction of oxidative stress is that the method is chemically non-invasive and therefore also suitable for *in vivo* studies (Hall et al., 2000; Zhang et al., 2003; Slimen et al., 2014).
The aim of the study was to evaluate potential biomarkers and therapeutic targets that could allow prediction and diagnosis of ROS-induced cell aging.

3.2 Results

The secretomes of primary hepatocytes of middle-aged and old Wistar rats were compared 24 h after induction of oxidative stress by heat treatment at 42 °C. Hepatic function was monitored during the cultivation time by measuring albumin production and AST and LDH release into the supernatant at 24 h (Figure 3-1).

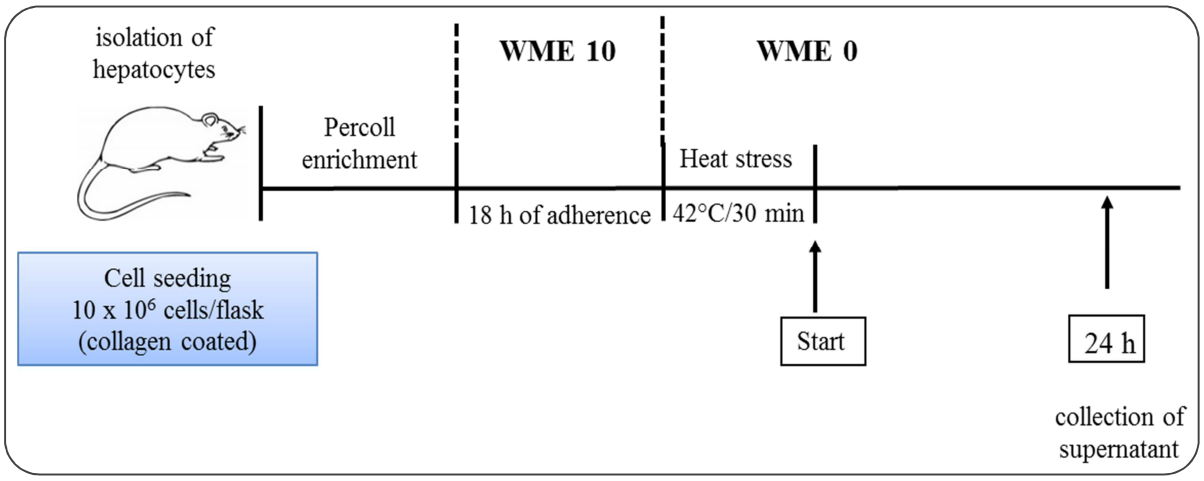

Figure 3-1: Experimental setup of the secretome analysis of primary hepatocytes from middle-aged and old Wistar rats (isolation at Pharmacelsus GmbH, Saarbrücken) and sampling of extracellular proteins after heat induction of oxidative stress; Abbreviations: WME 0 (Williams Medium E w/o FCS), WME 10 (Williams Medium E with 10% FCS); dashed lines: medium change.

After isolation, viable hepatocytes were enriched with Percoll density gradient centrifugation (Pertoft et al., 1978). After Percoll enrichment, 5 x 10^6 cells were lysed and the intracellular protein content was measured with a Bradford assay. The cells were seeded in 75 cm^2 culture flasks pre-coated with 7.5 µg/cm^2 of rat tail collagen and left to adhere in WME 10 at 37 °C for 18 h. After the adherence phase, medium was changed to WME 0 and an oxidative stress response was induced by heat treatment. The supernatants were collected 24 h after induction of oxidative stress. High-abundant proteins like albumin were removed via immunodepletion prior to secretome analysis with 2-D DIGE and MALDI ToF MS/MS to intensify the low-abundant proteins. The 24 h time point for the collection of supernatant was chosen for two reasons: First, because the time is needed for the accumulation of secreted proteins in the supernatant and second, because primary hepatocytes in monolayer cultivation dedifferentiate

into a fibroblast-like phenotype within the first 3 days after hepatocyte isolation (Godoy et al., 2009).

3.2.1 Influence of oxidative stress on cell viability, protein oxidation and albumin secretion of primary hepatocytes from Wistar rats

The degree of heat-induced oxidative stress in primary rat hepatocytes was estimated by determining the carbonylation status of the intracellular proteins after 24 h of incubation (Figure 3-2).

Hepatocytes from middle-aged rats show an overall lower protein oxidation level than old hepatocytes. Moreover, the influence of oxidative stress on middle-aged cells is contrary to old hepatocytes with respect to carbonyl content. They show a significantly decreased carbonyl content compared to the control, whereas old hepatocytes exhibit an increase in protein oxidation by heat exposure. These results were confirmed in further studies (see Chapter 4).

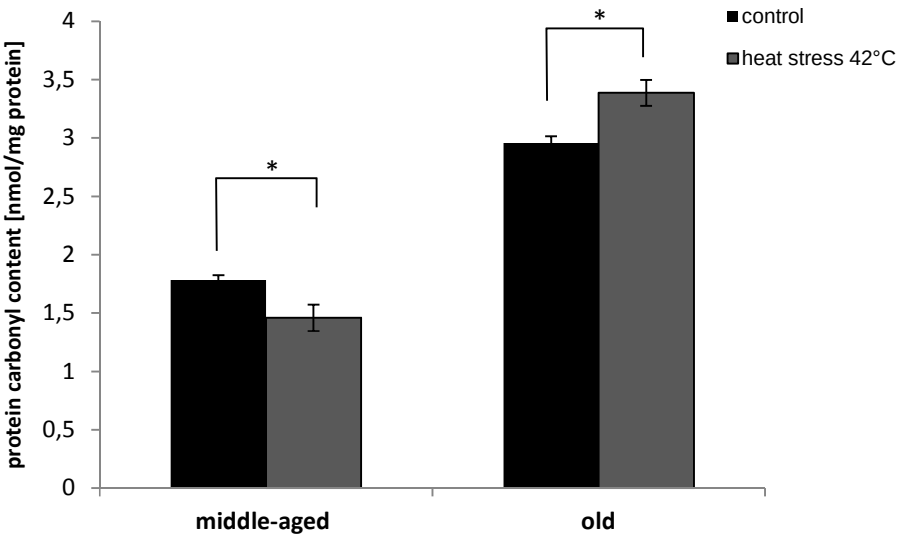

Figure 3-2: Protein carbonyl content of PRH from middle-aged and old Wistar rats under control and heat stress conditions after 24 h of cultivation. The amount of oxidized proteins as a marker for oxidative stress is given as nmol per mg protein (protein content determined with Bradford assay). Error bars indicate standard deviations (N=2, n=6).* indicate significance at p=0.05.

The level of hepatic function was determined 24 h after induction of oxidative stress by measuring albumin production and AST and LDH release.

The measurement of albumin secretion into the supernatant of primary hepatocytes serves as an indicator for cell viability and hepatocyte-specific function. However, in middle-aged hepatocytes a 40% lower basic albumin secretion than in old hepatocytes was observed (Figure 3-3). Assuming that, in this case, albumin secretion and viability do not correlate, we determined the intracellular protein content of middle-aged PRH (429 pg/cell ± 30 pg/cell) and old PRH (687 pg/cell ± 63 pg/cell). The measurements confirmed an inherently higher protein content of about 60% in old hepatocytes (~1.5-fold) which could be associated with the higher albumin secretion.

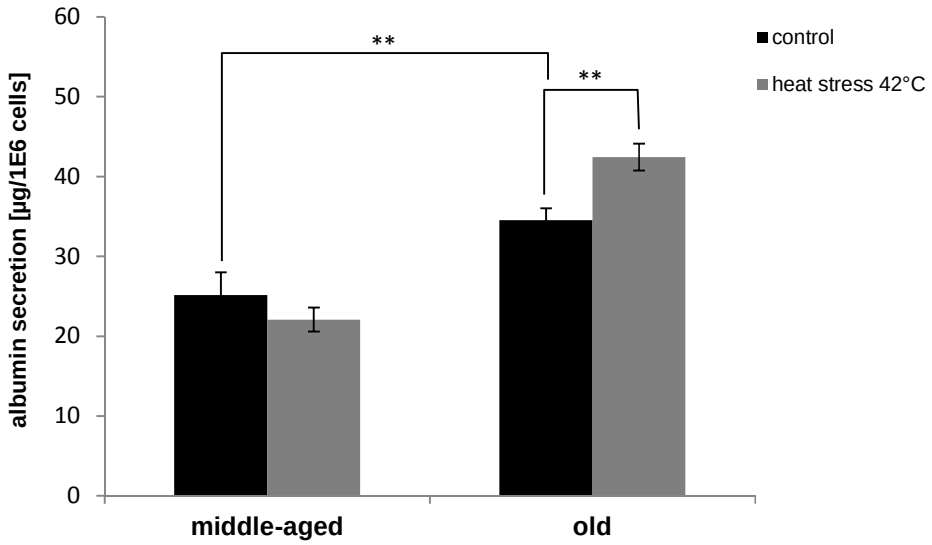

Figure 3-3: Albumin production of PRH from middle-aged and old Wistar rats under control and heat stress conditions within 24 h of cultivation. Albumin production is given as µg per million seeded cells. Error bars indicate standard deviations (N=2, n=6). ** indicate significance at p=0.01.

In old PRH the albumin secretion increased due to heat stress whereas in middle-aged PRH no significant differences were detected. The enzymes AST and LDH are only released into the supernatant if the integrity of the cell membrane is compromised. Therefore, LDH is used as a general viability marker in cell culture, whereas AST is a liver-specific viability marker.

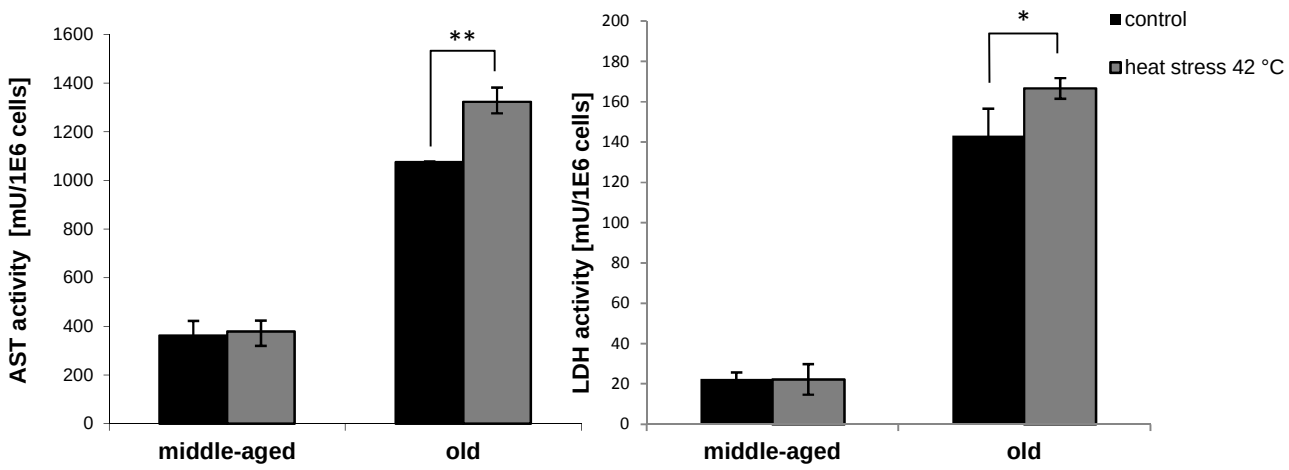

Figure 3-4: LDH and liver-specific AST activity of PRH from middle-aged and old Wistar rats under control and heat stress conditions within 24 h of cultivation. The amount of released enzyme is given as milliunits (mU) per million seeded cells. Error bars indicate standard deviations (N=2, n=6).* and ** indicate significance at p=0.05 and p=0.01.

The measurements of AST and LDH activity of middle-aged and old hepatocytes under control and oxidative stress conditions are illustrated in Figure 3-4. As was expected, a comparable trend for each age group and stress condition can be observed for both enzymes. Old hepatocytes exhibit a higher level of oxidative stress already under control conditions as was indicated by the higher protein carbonyl content. Consequently, it is not surprising that the level of AST and LDH in the supernatant is elevated due to dying cells and compromised cell membranes. The results for the cells under oxidative stress coincide with the protein oxidation level. Middle-aged hepatocytes show no differences in viability, whereas old hepatocytes show an increase in cell death markers.

3.2.2 Influence of oxidative stress on the secretome of primary rat hepatocytes

The samples were immunodepleted to remove high-abundant serum proteins. They were further concentrated and desalted with an ultrafiltration device with a MWCO of 10 kDa prior to 2-D gel electrophoresis. 2-D gel electrophoresis was executed as EZBlue-stained preparative gels for further identification with MALDI ToF MS/MS (Supplementary Figure 3-1) and as fluorescence-labeled DIGE gels for relative quantification (Figure 3-5).

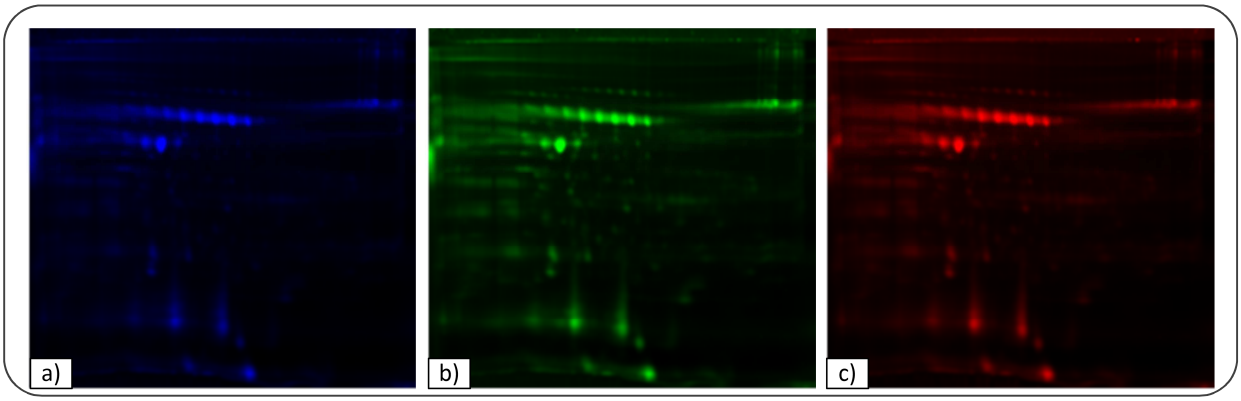

Figure 3-5: representative 2-D DIGE gel images (pH 5-8) of secreted proteins from Wistar PRH after exposure to heat stress. Proteins were labeled with (a) Cy2 containing equal amounts of control (37°C) and treated (42°C) sample as an internal standard for the quantitative comparison (473/530 nm), (b) Cy3 containing the control (37°C) sample (532/570 nm) and (c) Cy5 containing the treated sample (635/665 nm).

DIGE allows the comparison of two different conditions at a time. In this experimental setup, the control condition (cultivation at 37 °C) was compared to the heat stress condition (42 °C for 30 minutes) for each age group. Representative gels are shown in Figure 3-6.
In total 58 protein spots were identified on the preparative gels (Supplementary Table 3-1 and 3-2). For some proteins several isoforms were found resulting in 28 different proteins. The identified proteins are involved in various biological processes like transport (GO:0006810), lipid metabolism (GO:0006629), catabolic processes (GO:0009056), iron homeostasis (GO:0006879) and regulation of catalytic activity (GO:0050790). Almost half of the identified proteins can also be associated with processes involved in aging and oxidative stress (GO:0006950), illustrating the importance of the secretome as a source for biomarker discovery.

When the extracellular proteomes of middle-aged PRH under control and heat stress conditions were compared (Figure 3-6 a), it was observed that most spots were white which indicates a similar proteomic profile. Confirming this assumption, statistical analysis revealed no significant changes in the secretion of proteins from middle-aged primary hepatocytes due to heat stress.
In total 144 protein spots were detected on the fluorescent DIGE gels in the pH range 5-8. Primary hepatocytes from old Wistar rats show clear differences between control and heat

stress condition (Figure 3-6 b). Statistical evaluation of the DIGE-gels revealed 63 significantly (≥ 1.5-fold) altered spots. These results compared with the alterations in hepatic functions indicate a stronger effect of heat stress on old hepatocytes than middle-aged ones and prove the basic applicability of the heat stress model to study oxidative stress.

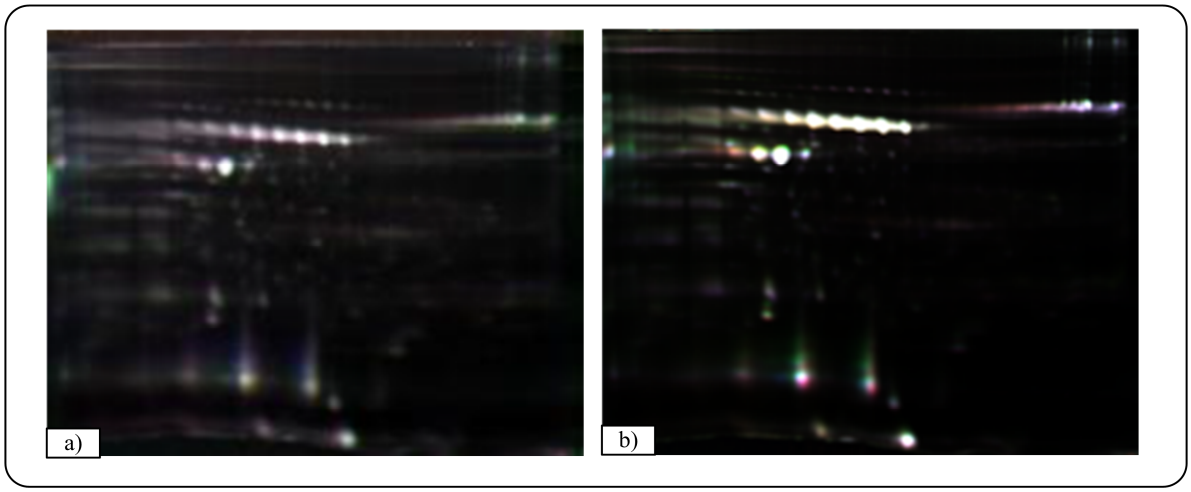

Figure 3-6: Overlay of representative DIGE gels (pH 5-8) showing differential protein abundance in the secretome of Wistar PRH 24 h after exposure to heat stress. Comparison between control (37 °C) and heat-stressed (42 °C) PRH samples (a) of middle-aged (b) and old rats. Spots that are only present in control: green; heat-stressed: red; same abundance: white; (n=3).

Comparing the number of proteins identified with MALDI ToF/ToF from EZBlue-stained gels (58) and the number of detected spots on DIGE gels (144) there is a noticeable discrepancy. Hence, it can be assumed that some spots, which were identified as differentially expressed under oxidative stress, could not be identified. The main reason for this is the higher sensitivity of the fluorescent DIGE labeling compared to EZBlue staining. Additionally, MALDI ToF/ToF measurements revealed that several spots contained isoforms of the same proteins.

Figure 3-7 (a) represents the detailed distribution of the altered protein abundance in old PRH under oxidative stress. Out of 144 detected spots 43 contained proteins with higher abundance and 20 contained proteins with lower abundance than the control samples. As can be expected, a high fold change is less likely. Accordingly, only 3 spots exhibited a fold change above 4-fold of which only one spot could be assigned to a protein (SOD [Cu/Zn], Table 3-1).

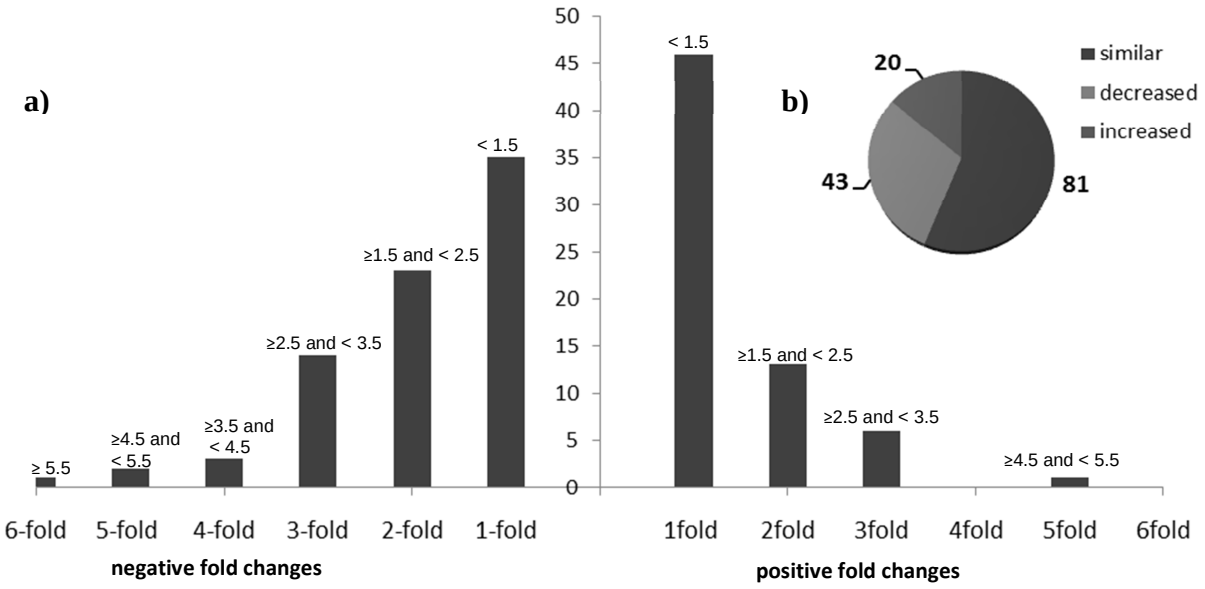

Figure 3-7: Graphical representation of a) the number of secreted proteins with a certain fold change and b) the total number of proteins with an altered (> 1.5-fold) abundance in PRH from old Wistar rats after induction of oxidative stress. Positive fold changes represent higher differential abundance compared to the control and negative values represent lower differential abundance compared to the control.

In Table 3-1, the results of the comparison of control and heat stress conditions in old rat primary hepatocytes are listed. From the 2-D gels 23 spots per gel could be assigned to differentially expressed spots on the according DIGE gels**.** For hemopexin, transthyretin, vitamin D-binding protein, apolipoprotein E and regucalcin several isoforms were found. Shown are the averages of all isoforms of a single protein which show comparable behavior to the stress conditions. In total we identified 12 differentially expressed proteins in old PRH under oxidative stress compared to the control conditions.

Table 3-1: Identified extracellular proteins with significantly different abundance in PRH of old Wistar rats 24 h after induction of oxidative stress (at 42 °C). The secretome of the PRH cultivated at 37 °C served as control to which the secretome of the PRH heat-stressed at 42 °C was compared. Positive values indicate a higher abundance of the detected protein due to heat stress compared to the control condition, whereas negative values indicate a lower abundance. Shown are the means of the fold change from the different gels (N=2, n=6). * In case of isoforms the average of all spots is shown. Swiss-Prot database information is derived from http://www.uniprot.org.

Swiss-Prot Accession no.	Protein	Secretion status	Fold change	Std. dev.	GO molecular function
P02650	**Apolipoprotein E***	secreted	-2.34	0.28	GO:0005319: lipid transporter activity GO:0007568: aging
P80254	**D-dopachrome decarboxylase**	secreted	-1.95	0.33	GO:0006954: inflammatory response GO:0042438: melanin biosynthetic process
P07632	**Superoxide dismutase [Cu-Zn]**	secretion via exosomes	4.63	0.47	GO:0006979: response to oxidative stress
P70619	**Glutathione reductase**	secretion via exosomes	3.47	0.25	GO:0006979: response to oxidative stress
P02767	**Transthyretin***	secreted	-1.89	0.12	GO:0042562: hormone binding
P04276	**Vitamin D-binding protein***	secreted	3.01	0.86	GO:0003779: actin binding GO:0005499: vitamin D-binding
P02651	**Apolipoprotein A-IV**	secreted	-2.11	0.06	GO:0017127: cholesterol transporter activity
P02761	**Major urinary protein**	secreted	-2.23	0.51	GO:0005550: pheromone binding
P20059	**Hemopexin***	secreted	2.09	0.17	GO:0015232: heme transporter activity
Q64240	**Protein AMBP**	secreted	3.26	0.65	GO:0004867: serine-type endopeptidase inhibitor activity
P04916	**Retinol-binding protein 4**	secreted	-1.96	0.03	GO:0005215: transporter activity
Q03336	**Regucalcin***	secreted	-2.78	0.16	GO:1901671: positive regulation of SOD activity GO:0007568: aging

Most of the detected proteins are directly or indirectly related to oxidative stress, aging or age-related diseases. One protein responsible for the removal of reactive oxygen species, namely SOD [Cu/Zn], and glutathione reductase responsible for upkeep of the GSH/GSSG redox state, showed the overall highest increase in abundance (+4.63-fold and +3.47-fold) after heat treatment. The regucalcin and protein AMBP expression was also increased 24 h after heat stress (+2.78-fold and +3.26). Contrarily, D-dopachrome decarboxylase expression, also known for its role in the defense against oxidative stress, was decreased almost 2-fold. The amounts of most of the proteins with transporter function were clearly lower under oxidative stress conditions. Specifically, the serum levels of the lipoprotein transporters ApoE and ApoA-IV, transthyretin, major urinary protein and retinol-binding protein 4 were significantly decreased. Hemopexin and vitamin D-binding protein, on the other hand, showed a significantly higher abundance under stress conditions. The highest difference was found for vitamin D-binding protein, which was more than 3 times as abundant as in the control sample.

3.3 Discussion

In this study the extracellular proteomes of primary hepatocytes from middle-aged and old Wistar rats were analyzed under control and oxidative stress conditions.

The determination of the AST and LDH levels, as markers for hepatic injury, revealed that the PRH from old rats show impaired hepatic function already under control conditions. AST levels were 3-fold and LDH levels even 7-fold higher than in PRH of middle-aged Wistar rats (Figure 3-4). This is most likely not an artifact of the prevailing cultivation but a long-lasting effect of the stress induced by the liver perfusion even after the adherence phase and the subsequent washing step. The average cell viability after perfusion was about 10% smaller in old than in middle-aged PRH. Additionally, heat stress had no impact on middle-aged PRH, whereas old PRH were highly susceptible to cellular damage through oxidative stress. AST and LDH levels were both significantly increased in old PRH. Additionally, the carbonyl protein content, known as a marker for oxidative stress (Dalle-Donne et al., 2003), was elevated in old hepatocytes (Figure 3-2).

Contrary to this observation we determined an increased albumin production in senescent PRH under control conditions (Figure 3-3). Usually, a high albumin production is considered

as correlated to high cell viability. This is the case in studies of xenobiotic metabolism (Soldatow et al., 2013), but is not applicable for *in vitro* models of aging and oxidative stress. *In vivo* studies confirm the higher albumin production in senescent animals under control conditions (Schmucker, 1990). The higher albumin secretion of PRH from old rats may be correlated to the higher intracellular protein content of old PRH (687 pg/cell) compared to middle-aged PRH (429 pg/cell). This may be due the higher level of oxidative stress they are exposed to even under control cultivation conditions. Aging lowers the expression of antioxidant enzymes in primary hepatocytes (Hall et al., 2001). Elevated albumin levels could be a cellular mechanism to counteract this decrease in stress protein expression. Previous works have shown that more than 70% of the ROS scavenging ability of serum was due to serum albumin (Bourdon & Blache, 2001). In old PRH, the induction of heat stress resulted in a further increase in albumin secretion demonstrating the impact of heat treatment as a source of oxidative damage.

PRH from middle-aged rats showed no signs of oxidative stress in the hepatic function or in the expression level of secreted proteins under heat stress conditions. The amount of protein carbonyls was even significantly decreased after heat treatment. This effect could be explained if we presume fully intact defense mechanisms against oxidative stress in hepatocytes from middle-aged rats. In this case, heat exposure at 42 °C would cause only a mild physiological heat stress that initiates two processes. First, the induction of Hsp72 suppresses apoptosis via the inhibition of the JNK pathway (Gabai et al., 1998). Second, the activation of the HSP70 recovery system may reduce protein aggregation by activating refolding and degradation processes (Verbeke et al., 2000) as illustrated in Figure 3-8. Since heat shock proteins are intracellular proteins, we could not confirm this speculation in this experiment. However, there is strong evidence that this theory is accurate because there was a significant increase in the abundance of HSP70s in the hepatocytes from middle-aged Sprague Dawley rats after heat exposure (see chapter 5).

Primary hepatocytes from old Wistar rats, on the other hand, show a clear increase in protein carbonylation under heat stress. Furthermore, the induction of HSP70 transcription by heat shock was significantly reduced in hepatocytes isolated from old rats compared to hepatocytes isolated from young/adult rats as reported previously (Heydari et al., 2000).

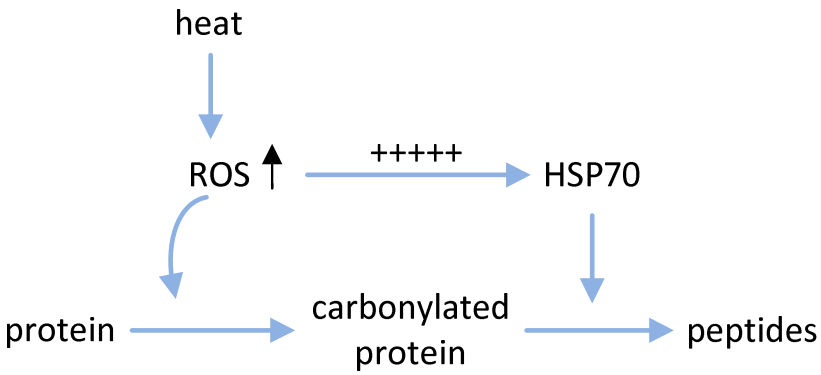

Figure 3-8: HSP70 recovery system protects against protein damage caused by oxidative stress; heat shock proteins are overexpressed under oxidative stress conditions; HSP70 initiates refolding or degrading of oxidized proteins to provide peptides and amino acids for the cell.

These observations indicate impaired defense mechanisms against oxidative stress in aged cells. On the secretome level, old PRH showed significant differences in the abundance of proteins after heat treatment (Table 3-1). However, heat exposure evoked contradictive effects on the expression of stress-related proteins. Some proteins showed a lower abundance, whereas others showed a significantly higher abundance after heat exposure.

The expression of retinol-binding protein 4 (RBP) is 2-fold decreased. It is mainly produced in the liver and is a transport protein for vitamin A. Additionally, it plays an important role in the modulation of the glucose metabolism. Previous human *in vivo* studies proved a positive correlation of RBP and the development of adipositas and insulin resistance (Li, Wongsiriroj, et al., 2014). Transthyretin (TTR) stands in close relation to RBP. Under oxidative stress, TTR forms tetramers with thyroxine and RBP which aggregate to amyloidogenic plaques. Therefore, oxidative stress is a major factor in the development of Alzheimer's disease (Ando et al., 1997). The decrease in abundance of free RBP and TTR in heat-stressed old rat hepatocytes could be due to the formation of aggregates. It is known that carbonylated TTR has a higher affinity to form aggregates than non-carbonylated TTR (Zhao et al., 2013).

D-dopachrome decarboxylase (alternative name D-dopachrome tautomerase, DDT), is an inherently intracellular protein. However, it is reported to be secreted into the serum (Merk et al., 2011) as a protection mechanism against oxidative stress (Hiyoshi et al., 2009). Its expression in old PRH after heat exposure is 2-fold decreased. DDT catalyzes the conversion of D-dopachrome to 5,6-dihydroxyindole which is a melanin precursor. Melanin has an

antioxidant activity in liver which is however not clearly understood (Hung et al., 2003). The expression of both detected and identified apolipoproteins is also significantly decreased. Both proteins have an antioxidant activity, in addition to their important role in the transport and metabolism of lipids. Apolipoprotein E protects cells against hydrogen peroxide (Miyata & Smith, 1996; Tarnus et al., 2009), whereas apolipoprotein A-IV is protecting against oxidative modifications of lipoproteins (Qin et al., 1998).

In case of regucalcin (also known as SMP-30, senescence marker protein 30), the almost 3-fold decrease supports our previous conclusion. Regucalcin is known to decrease in age, causing inflammation and elevated levels of oxidative stress due to its importance for the vitamin C biosynthesis pathway (Kondo & Ishigami, 2016). Regucalcin deficiency is suspected to cause glucose intolerance, impaired lipid metabolism and elevated carbonylation of proteins (Sato et al., 2014). All of the above-mentioned stress-related proteins showed a decreased abundance which confirms impaired defense mechanisms in PRH from old rats. However, several other stress proteins were increased in abundance. Proteins involved in detoxification of heme, namely hemopexin and protein AMBP, showed an increased abundance under heat stress conditions. Free heme promotes oxidative stress by catalyzing free radical reactions (Kumar & Bandyopadhyay, 2005). Hemopexin is necessary to mediate heme-iron recovery and detoxification in hepatocytes (Vinchi et al., 2008). Protein AMBP has several antioxidant properties. It scavenges heme and other pro-oxidants, inhibits oxidation reactions and catalyzes the reduction of oxidation products (Akerstrom et al., 2000). Though, the decrease of protein AMBP in serum could be, at least in part, due to its affinity to bind to albumin. Normally, 7% of protein AMBP in serum is bound to albumin (Berggard et al., 1997). The higher secretion of albumin into the serum could therefore reduce the amount of free protein AMBP. The proteins showing the highest increase in abundance after heat exposure are [Cu-Zn] superoxide dismutase (+4.63-fold) and glutathione reductase (+3.47-fold). Both enzymes catalyze important reactions in the detoxification of reactive oxygen species. Compared to the previously discussed effects of heat stress on old PRH, this increase in the expression of crucial antioxidant enzymes seems contradictory. Nonetheless, other studies confirm that some antioxidant enzymes (namely [Cu-Zn] SOD, catalase, glutathione peroxidase and glutathione reductase) of hepatocytes from 30 months old rats underwent increases in their specific enzyme activities as well as in their mRNA compared to 6 months old Wistar rats (Sanz et al., 1997). These results imply that the expression of SOD and

glutathione reductase increase with age but are still insufficient to compensate the highly increased generation of ROS, resulting in oxidative injury (see also Chapter 5).

Proteomic analyses of the rat secretome revealed several potential biomarkers to determine the risk of oxidative stress-dependent diseases like diabetes, arteriosclerosis and cardiovascular diseases. As a result of this study, the amount of regucalcin and the ratio of RBP/TTR are promising serum marker candidates for assessing the extent of oxidative injury in elderly patients and their long-term prognosis for age-dependent diseases.

4. Comparison of the antioxidant effect of N-acetylcysteine and quercetin on middle-aged Wistar primary rat hepatocytes and *HepG2*

4.1 Introduction

Reactive oxygen species (ROS) are constantly generated in cells during metabolic processes. The main source is hereby the mitochondrial respiratory chain. In normal cellular metabolism, ROS play an important role in cell signaling and homeostasis (Gil Del Valle, 2010). However, as highly reactive molecules, they have the potential to cause damage to macromolecules like DNA, proteins and lipids. Therefore, organisms developed various defense mechanisms to prevent oxidative damage. The major endogenous antioxidant system includes the enzymes superoxide dismutase (SOD), catalase (CAT), glutathione peroxidase (GPx), glutathione reductase (GR) and the GSH/GSSG redox system. These systems are widely responsible for the redox homeostasis in the cell. However, the addition of exogenous sources of reactive oxygen species (ROS), e.g. UV-light, pathogens, xenobiotics, extensive exercise and hyperthermia, can cause oxidative stress, an imbalance of pro- and antioxidants that leads to diseases and aging (Finkel & Holbrook, 2000) by damaging macromolecules. Therefore, supplementation of exogenous antioxidants has become increasingly popular to improve health and prevent oxidative stress related chronic diseases and premature aging (Poljsak et al., 2013). The used antioxidants vary from natural parts of the human diet such as the vitamins C and E (Lobo et al., 2010) and polyphenols (Urquiaga & Leighton, 2000) to synthetic compounds (e.g. EUK134, NAC) (Augustyniak et al., 2010).

Previous research explored the effect of various antioxidants on diseases caused by oxidative stress like Alzheimer's disease (Scarmeas et al., 2007), COPD (Cerda et al., 2006), diabetes (Johansen et al., 2005) and cancer (Yasueda et al., 2016). These studies confirm a positive influence of antioxidants on prevention and treatment of the aforementioned diseases. However, there are also studies which revealed no (Farouque et al., 2006) or even an adverse effect on human health (Bardia et al., 2008; Sesso et al., 2008). Therefore, more research is needed to specify the impact of antioxidant treatment on aging and oxidative stress related

diseases. A highly promising candidate for the prevention of oxidative stress is the polyphenol quercetin (3,3′,4′,5,7-pentahydroxyflavone). Quercetin is the most abundant flavonoid in the human diet with an average intake of 25 mg/d (Dajas et al., 2003). It occurs in fruits and vegetables such as onions, apples (Wach et al., 2007), berries, broccoli, tea and red wine (Dajas et al., 2003). Quercetin (Figure 4-1 A) has five hydroxyl groups which account for its role as a ROS scavenger with anti-inflammatory, hypolipidemic and anti-fibrotic properties (Yoon et al., 2012; Li et al., 2016). Moreover, quercetin chelates metal ions, effectively inhibiting fenton reaction (Cheng & Breen, 2000) and thus limiting the formation of hydroxyl radicals. Due to its antioxidative properties, the therapeutic potential of quercetin in the treatment of oxidative stress related diseases like atheriosclerosis (Hung et al., 2015), several types of cancer (Szatrowski & Nathan, 1991; Zhou et al., 2003), ishemic heart disease (Perez-Vizcaino & Duarte, 2010) and COPD (Tabak et al., 2001) is discussed. Quercetin is also discussed to have hepatoprotective effects *in vivo* (Ansar et al., 2016; Tang et al., 2016; Barros et al., 2017) and *in vitro* (Gao et al., 2009; Liu et al., 2010; Ji et al., 2015).

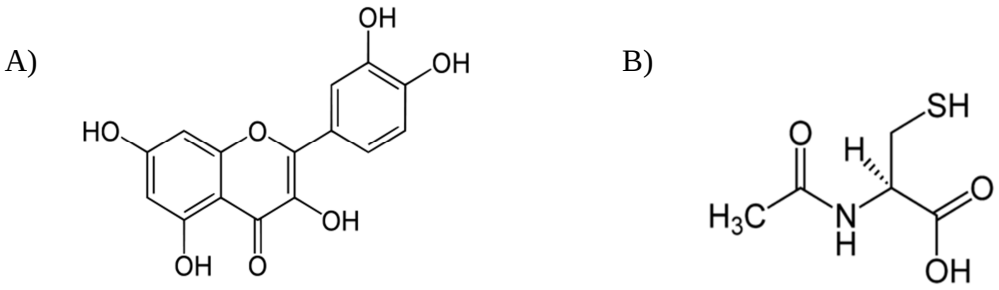

Figure 4-1: Chemical structure of the antioxidants A) quercetin and B) N-acetylcysteine

Another promising candidate for the defense against oxidative stress is N-acetylcysteine (NAC, Figure 4-1 B). The NAC molecule contains a thiol group which serves as a scavenger of free radicals and prevents oxidative damage to proteins, lipids and DNA. Additionally, NAC is a direct precursor for the biosynthesis of glutathione. Disturbances in the GSH biosynthetic pathway are associated with various diseases such as cystic fibrosis, diabetes, heart attack and cancer (Wu et al., 2004) and hepatic injuries such as alcoholic liver disease (Hirano et al., 1992), non-alcoholic fatty liver disease and drug-induced liver toxicity (Pessayre et al., 2012). NAC is already widely used in the treatment of respiratory diseases

(Bolser, 2010; Santus et al., 2014) and as a non-toxic antidote for acetaminophen overdose (Mahmoudi et al., 2015).

In the present study the influence of these two antioxidant compounds, namely Nacetylcysteine and quercetin, was the focus of the analysis. Therefore, hepatic function and oxidative stress response of primary hepatocytes from middle-aged (6 months) Wistar rats and the human hepatoma cell line *HepG2* were analyzed under heat stress conditions. PRH were pre-treated with 500 µM NAC or 50 µM quercetin to evaluate their effect on the oxidative stress response. The aim of the study was to evaluate the properties of NAC and quercetin in our *in vitro* heat stress model.

4.2 Results

The influence of the antioxidant compounds quercetin and N-acetylcysteine was analyzed using primary hepatocytes from two individual middle-aged Wistar rats (PRH) and the hepatoma cell line *HepG2*. The effect was compared 1 h, 5 h and 24 h after induction of oxidative stress by heat treatment at 42 °C or treatment with 2 mM H_2O_2. Hepatic function was monitored during the cultivation time by measuring albumin production and LDH release into the supernatant at the corresponding time points (Figure 4-2). The oxidative stress response was examined by measuring ROS production, glutathione content, protein oxidation and SOD and CAT activity.

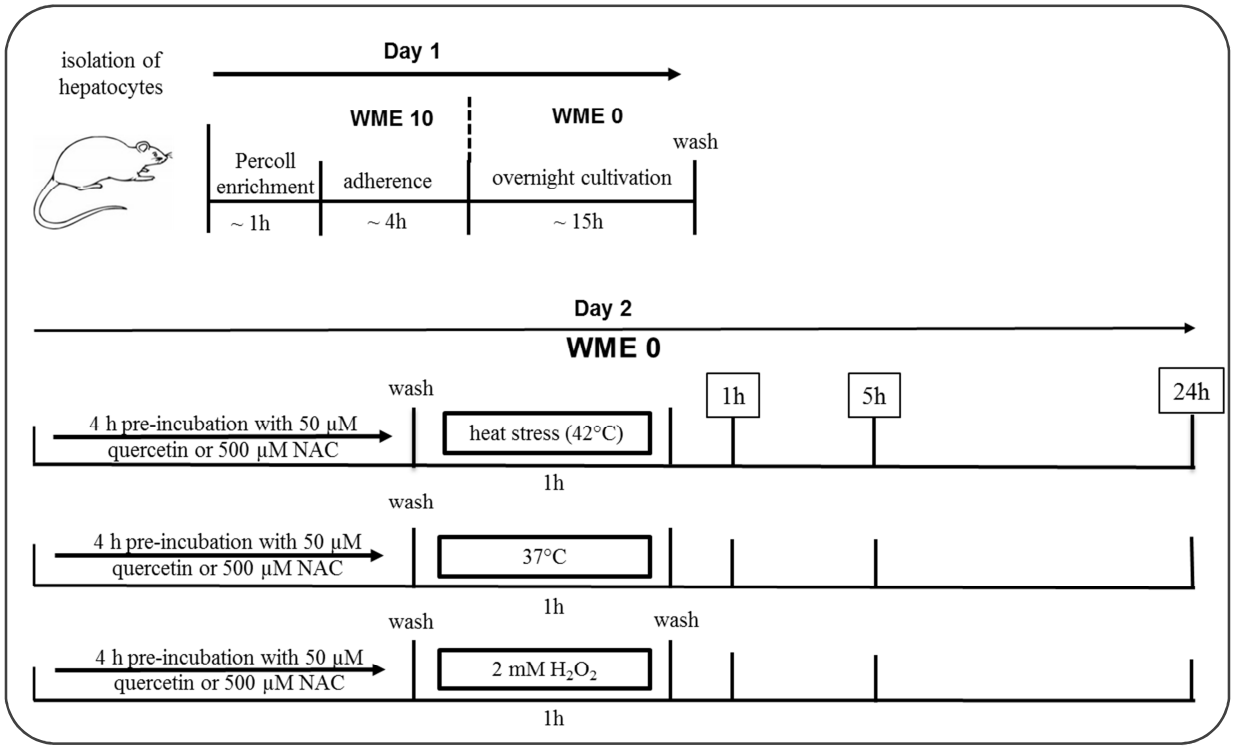

Figure 4-2: Experimental setup for the analysis of the influence of the antioxidants NAC and quercetin; PRH of two individual middle-aged Wistar rats and the hepatoma cell line HepG2 were pre-incubated with 50 µM quercetin or 500 µM NAC for 4 h; induction of oxidative stress was achieved by heat (42 °C) or treatment with 2 mM H_2O_2; supernatants and cell lysates for enzyme assays were collected 1 h, 5 h and 24 h after oxidative stress.

Viable hepatocytes and *HepG2* were seeded in 6 well plates either pre-coated (PRH) with rat tail collagen or without coating (*HepG2*) and left to adhere in WME 10 at 37 °C for 4 h.

Afterwards, the cells were left to adapt to serum-free medium at 37 °C overnight. After the adaptation phase, the cells were pre-treated with 500 µM NAC or 50 µM quercetin for 4 h. Afterwards, the medium was changed to WME 0 and an oxidative stress response was induced by heat treatment at 42 °C or treatment with 2 mM H_2O_2 for 1 h. The supernatants and intracellular proteins were collected 1 h, 5 h and 24 h after induction of oxidative stress.

Primary hepatocytes of two individual middle-aged Wistar rats were analyzed separately to demonstrate the variance within this outbred rat stock. The addition of *HepG2* in the experimental setup allows a comparison of rodent and human cells and provides a consistent *in vitro* model unaffected by stress due to liver perfusion. The major disadvantage of the *HepG2* cell line is its inherently lower metabolic capacity due to its low levels of cytochromes (Westerink & Schoonen, 2007).

The dose of hydrogen peroxide of 2 mM significantly increases ROS production without impairing cell viability (Garg, 2016). For the antioxidants a treatment was chosen that balances antioxidant effect and cytotoxicity. After 4 h of treatment, a dose of 50 µM of quercetin was reported to significantly increase the concentration of glutathione without reducing cell viability of hepatocytes. A longer incubation period of 24 h increases LDH leakage about 4-5-fold and lower concentrations have no effect on intracellular glutathione content (Alia et al., 2006). Previous studies showed also that pre-treatment with NAC rather than co-treatment results in protection of hepatocytes against oxidative stress caused by acetaminophen (Pawlowska-Goral et al., 2013) and cocaine (Zaragoza et al., 2000).

4.2.1 Influence of oxidative stress and antioxidant treatment on cell viability and albumin secretion of primary hepatocytes from Wistar rats and *HepG2*

The level of hepatic function was determined 1 h, 5 h and 24 h after induction of oxidative stress by measuring albumin production and LDH release. Previous studies (see Chapter 3) already assessed the influence of heat stress on middle-aged PRH after 24 h of incubation. Including time points closer to the actual stress induction, provides the opportunity to gain insights into time-dependent mechanisms of the defense against oxidative stress.

The measurement of albumin secretion of PRH revealed significant differences between the two individual Wistar rats (Figure 4-3). The PRH of both rats showed an increased albumin secretion after heat treatment in general. However, Wistar 1 reached a peak 5 h after heat stress

with almost 4-fold higher values than the control, whereas Wistar 2 showed no such peak (Figure 4-3 A and B).

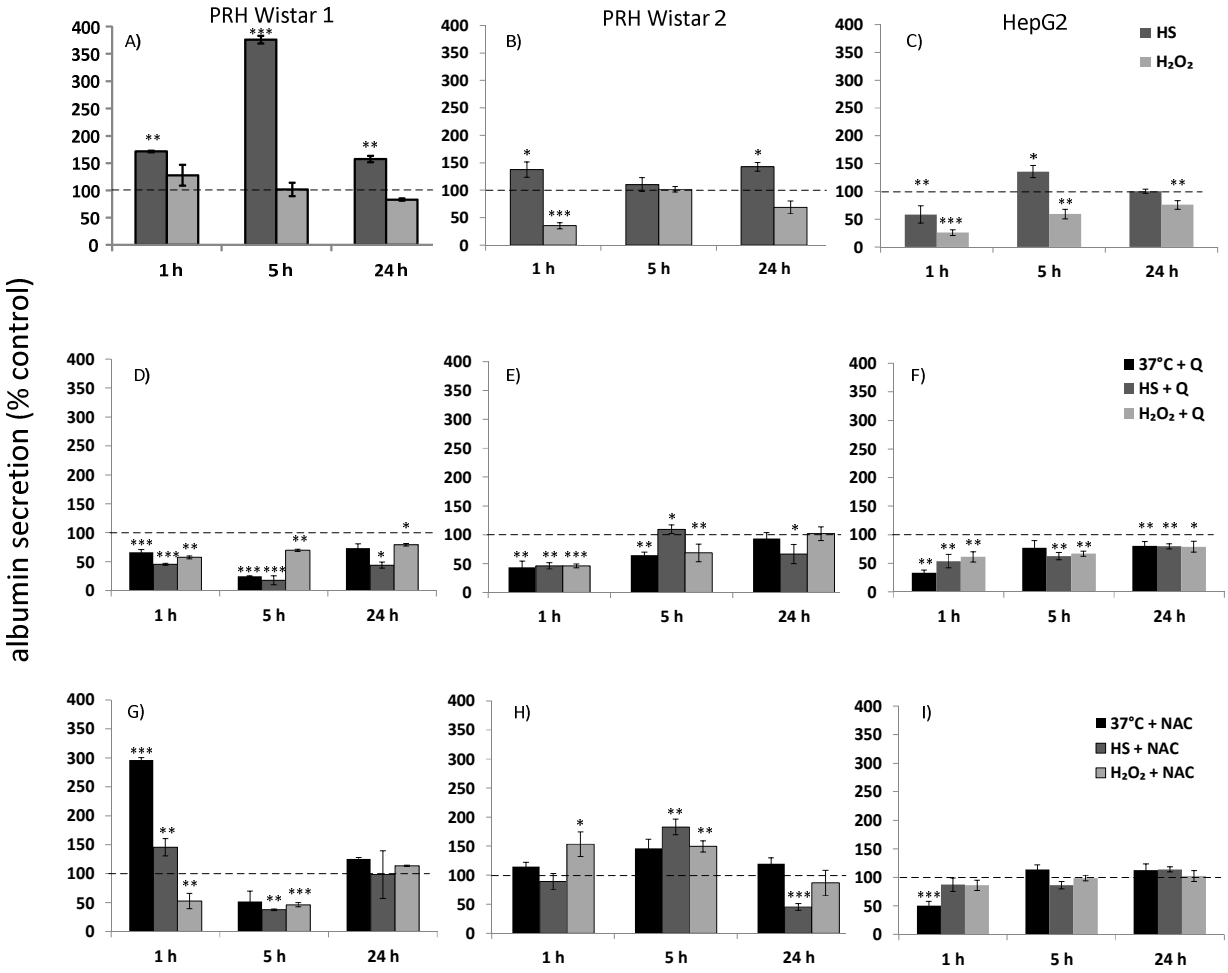

Figure 4-3: Albumin secretion of A) primary hepatocytes from Wistar rat 1, B) Wistar rat 2 and C) hepatoma cell line *HepG2* under heat stress and H_2O_2 stress related to untreated control (dashed line). Albumin production of D) PRH Wistar 1 E) PRH Wistar 2 and F) *HepG2* after 4 h pre-incubation with 50 µM quercetin in relation to the corresponding untreated and treated cells. Albumin production of G) PRH Wistar 1, H) PRH Wistar 2 and I) *HepG2* after 4 h pre-incubation with 500 µM NAC in relation to untreated and treated cells (dashed line). Error bars indicate standard deviation (PRH Wistar 1: n=3; PRH Wistar 2: n=3; *HepG2*: n=3). Statistical significance was determined with student's t-test. *, ** and *** indicate significance at p=0.05, p=0.01 and p=0.001. All results were correlated to the living cell number after 1 h, 5 h and 24 h of cultivation determined using calcein AM staining. Abbreviations: HS: heat stress; NAC: N-acetylcysteine; Q: quercetin.

The albumin secretion of *HepG2* first decreased 1 h after heat stress. After 5 h the albumin secretion increased above control levels, before coming back to control levels after 24 h (Figure 4-3 C).

The treatment with 2 mM H_2O_2 revealed that *HepG2* cells are more sensitive to this chemical stress than Wistar PRH. They exhibited a reduced albumin secretion at all time-points. Only Wistar 2 showed a significant decrease in albumin secretion 1 h after chemical oxidative stress. The pre-treatment with quercetin consistently evoked a highly decreased albumin secretion in all cell types and under all cultivation conditions (Figure 4-3 D-F). In contrast, the treatment with NAC showed no unequivocal effect on PRH. Cells originating from the two Wistar rats showed a significant reaction to NAC, however, there is no trend connecting both individuals (Figure 4-3 G-H). NAC seems to have a time-dependent effect. Hepatocytes from Wistar 1 responded 1 h after the start of the experiment, whereas Wistar 2 responded with a delay after 5 h. Only *HepG2* were unsusceptible to NAC pre-treatment.

The enzyme LDH is used as a general viability marker in cell culture which is only released into the supernatant if the integrity of the cell membrane is compromised. LDH release was determined to estimate the influence of stress and antioxidant treatment on cell viability. Primary hepatocytes from Wistar rat 1 showed a clearly significant increase in LDH release due to heat stress, whereas hydrogen peroxide caused only a slight increase 1 h after stress (Figure 4-4 A). The LDH leakage of PRH from Wistar 2 was less distinct between heat and H_2O_2 treatment. Both types of stress induced a significant LDH release after 5 h which lasted until the end of the cultivation after 24 h. Interestingly, in *HepG2* heat and chemical stress resulted in a decreased LDH release compared to the control cells (Figure 4-4 C). The cells under control conditions exhibited a higher stress level than the cells which were treated with heat and hydrogen peroxide. Accordingly, untreated *HepG2* cells showed a more beneficial reaction to antioxidant treatment than treated cells (Figure 4-4 F/I). In treated cells, both antioxidants seemed to even induce LDH leakage and thus cell death. Primary hepatocytes reacted in a similar way. Both antioxidants led to an increase in LDH release. Administration of NAC and quercetin was only beneficial for the cells in case of heat stress, considering the high LDH values under this condition. In case of PRH from Wistar 1, the LDH release was more than 2-fold increased compared to the control so that the cells could benefit from the antioxidants (see Figure 4-4 D/G).

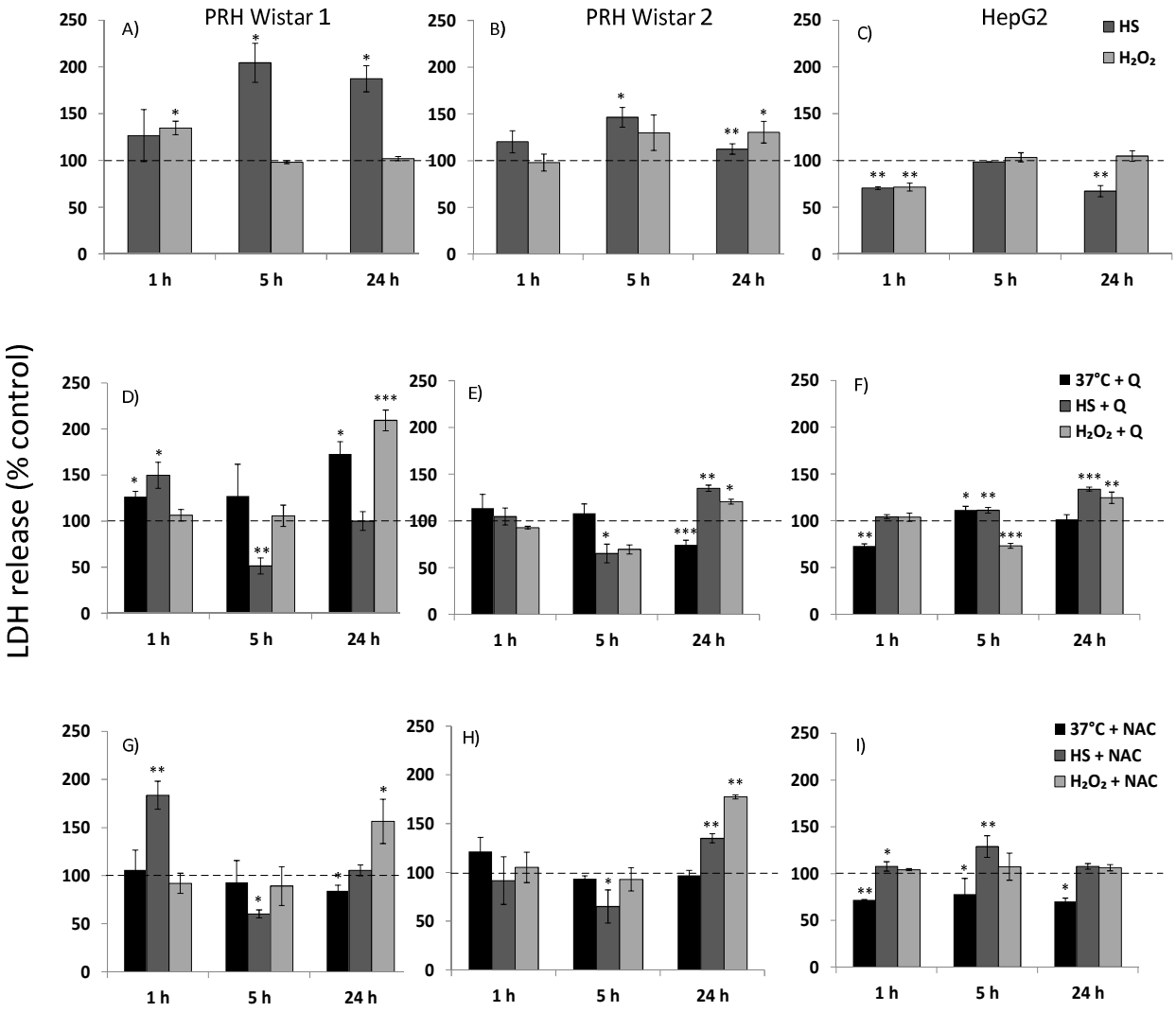

Figure 4-4: LDH release of A) primary hepatocytes from Wistar rat 1, B) Wistar rat 2 and C) hepatoma cell line *HepG2* under heat stress and H_2O_2 stress related to untreated control (dashed line). LDH release of D) PRH Wistar 1 E) PRH Wistar 2 and F) *HepG2* after 4 h pre-incubation with 50 µM quercetin in relation to the corresponding untreated and treated cells. LDH release of G) PRH Wistar 1, H) PRH Wistar 2 and I) *HepG2* after 4 h pre-incubation with 500 µM NAC in relation to untreated and treated cells (dashed line). Error bars indicate standard deviation (PRH Wistar 1: n=3; PRH Wistar 2: n=3; *HepG2*: n=3). Statistical significance was determined with student's t-test. *, ** and *** indicate significance at p=0.05, p=0.01 and p=0.001. All results were correlated to the living cell number after 1 h, 5 h and 24 h of cultivation determined using calcein AM staining. Abbreviations: LDH: lactate dehydrogenase; HS: heat stress; NAC: N-acetylcysteine; Q: quercetin.

4.2.2 Influence of oxidative stress and antioxidant treatment on generation of reactive oxygen species (ROS) and protein oxidation of primary hepatocytes from Wistar rats and *HepG2*

To accurately characterize the stress response induced by heat and H_2O_2 treatment, the actual ROS production and the ROS-associated protein oxidation were measured with a DCFH2 –DA assay. The ROS data obtained from PRH from two individual Wistar rats was comparable and therefore discussed as average values of both rats (Figure 4-5). Heat stress and H_2O_2 both induced a significant ROS production of comparable magnitude in PRH directly after treatment. The amount of ROS returned to about control level after 5 h. The reaction of heat stress on *HepG2* showed a clear delay. The peak of ROS production was reached 5 h after heat stress, whereas hydrogen peroxide induced an immediate reaction which lasted until the end of the experiment (Figure 4-5 B). This time delay could also be observed in the reaction of the cells to antioxidant treatment. Additionally, there was a clear separation between PRH and *HepG2* regarding the effectiveness of NAC and quercetin. Whereas PRH showed reduced ROS production due to quercetin pre-treatment at 1 h and 5 h, *HepG2* showed decreased ROS levels 5 h after NAC pre-treatment. NAC treatment also reversed the decrease in ROS production 24 h after heat stress in *HepG2* (Figure 4-5 B and F).

In addition to ROS generation, the degree of oxidative stress in PRH and *HepG2* was estimated by determining the carbonylation status of the intracellular proteins after 1 h, 5 h and 24 h of incubation (Figure 4-6 A-C). Primary hepatocytes from Wistar rat 1 showed a decrease in protein oxidation 24 h after heat stress, an effect that was already observed in previous studies (see Chapter 3). A similar result could be detected in PRH from Wistar 2, but the effect occurred already after 5 h of incubation and came back to control level at 24 h. The same time delay in Wistar 1 was measured in case of hydrogen peroxide treatment. However, in contrast to heat stress, there was a reverse effect of H_2O_2 on the PRH of Wistar 1 and 2. In Wistar 1, it caused a decrease in protein oxidation, whereas Wistar 2 showed increased protein oxidation. To further determine the cause of these differences, the protein oxidation of the control cells over the 24 h time course was examined (Supplementary Figure 4-3). This data revealed a significantly higher protein oxidation (> 2fold) in PRH from Wistar 2 compared to Wistar 1 under control conditions.

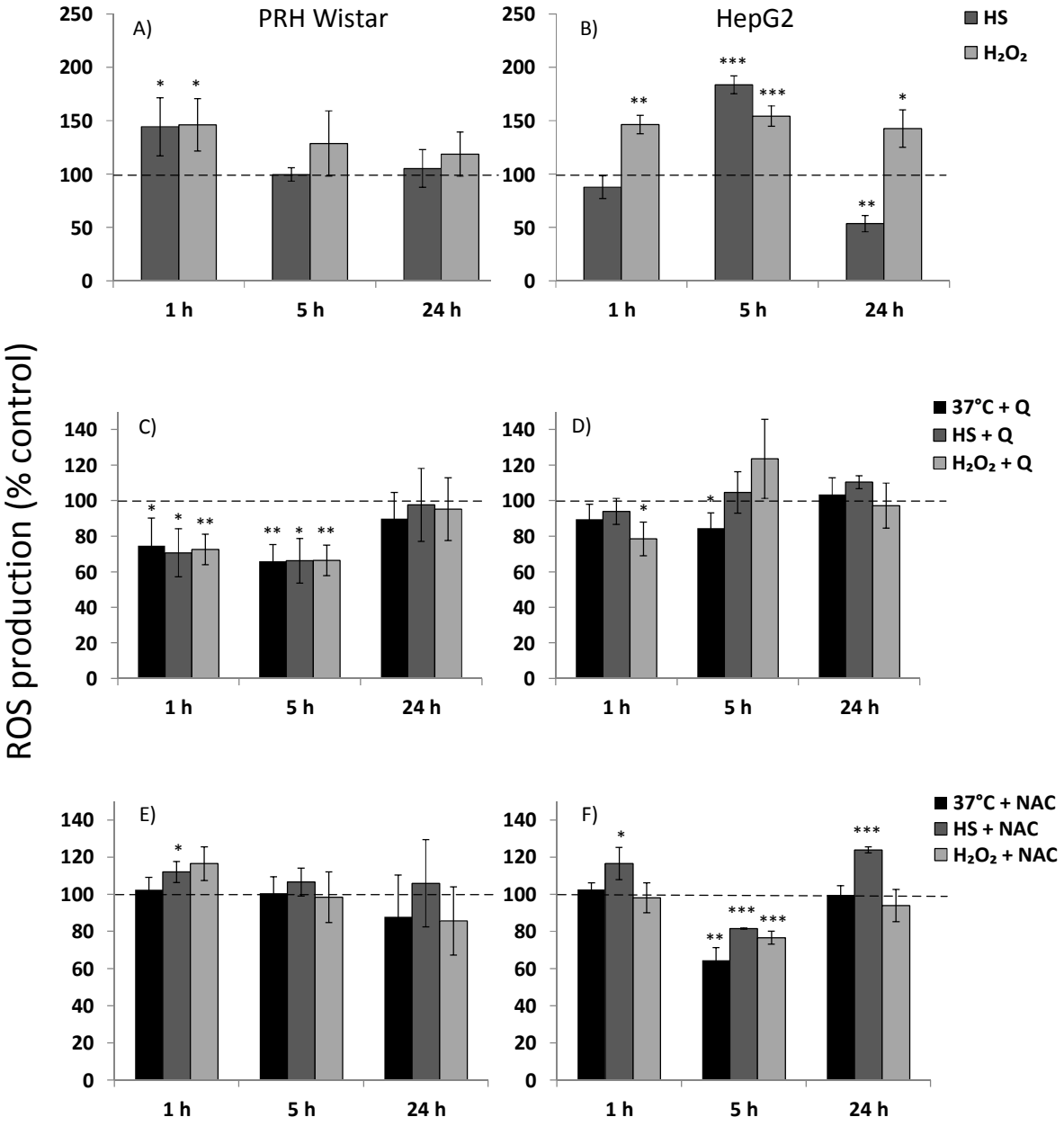

Figure 4-5: ROS production of A) primary hepatocytes from Wistar rats and B) hepatoma cell line *HepG2* under heat stress and H_2O_2 stress related to untreated control (dashed line). ROS production of C) Wistar PRH and D) *HepG2* after 4 h pre-incubation with 50 µM quercetin in relation to the corresponding untreated and treated cells. ROS production of E) Wistar PRH and F) *HepG2* after 4 h pre-incubation with 500 µM NAC in relation to untreated and treated cells (dashed line). Error bars indicate standard deviation (PRH: N=2; n=6; *HepG2*: n=3. Statistical significance was determined with student's t-test. *, ** and *** indicate significance at p=0.05, p=0.01 and p=0.001. All results were correlated to the living cell number after 1 h, 5 h and 24 h of cultivation determined using calcein AM staining. Abbreviations: ROS: reactive oxygen species; HS: heat stress; NAC: N-acetylcysteine; Q: quercetin.

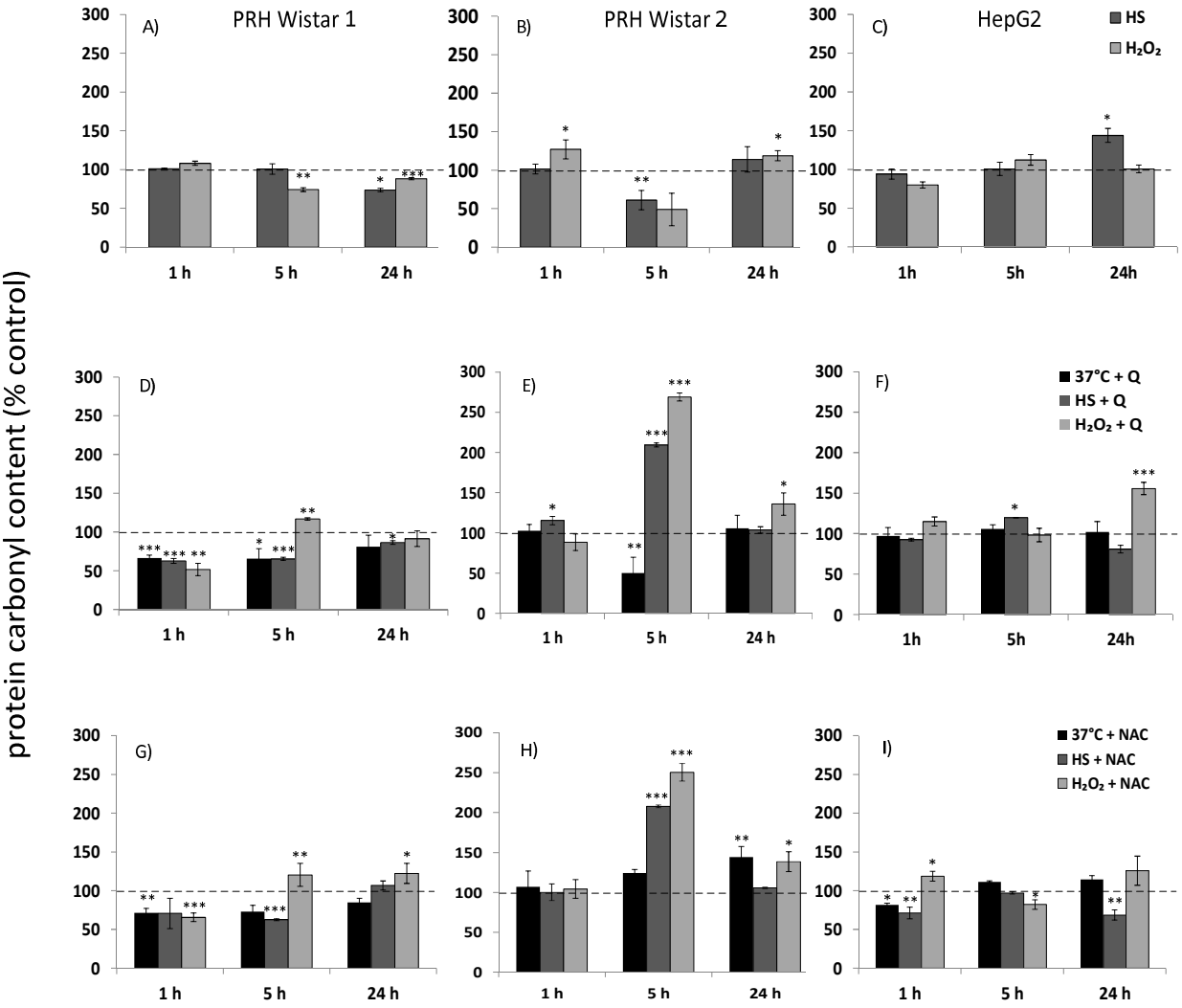

Figure 4-6: Protein carbonyl content of A) primary hepatocytes from Wistar rat 1, B) Wistar rat 2 and C) hepatoma cell line *HepG2* under heat stress and H_2O_2 stress related to untreated control (dashed line). Protein carbonyl content of D) PRH Wistar 1 E) PRH Wistar 2 and F) *HepG2* after 4 h pre-incubation with 50 µM quercetin in relation to the corresponding untreated and treated cells. Protein carbonyl content of G) PRH Wistar 1, H) PRH Wistar 2 and I) *HepG2* after 4 h pre-incubation with 500 µM NAC in relation to untreated and treated cells (dashed line). Error bars indicate standard deviation (PRH Wistar 1: n=3; PRH Wistar 2: n=3; *HepG2*: n=3). Statistical significance was determined with student's t-test. *, ** and *** indicate significance at p=0.05, p=0.01 and p=0.001. All results were correlated to the protein content after 1 h, 5 h and 24 h of cultivation determined using Bradford assay. Abbreviations: HS: heat stress; NAC: N-acetylcysteine; Q: quercetin.

Overall (PRH and *HepG2*) the protein oxidation levels in the control cells decreased over the time period of 24 h indicating a high basic stress level at the beginning of the cultivation independent of oxidative stress treatment. In accordance with these results, the PRH from the

two rats showed different reactions to the administration of antioxidants. Remarkably, PRH from each rat showed a similar protein oxidation profile independent of the kind of the used antioxidant (Figure 4-6 D/G and E/H). Hence, Wistar 1 reacted to NAC and quercetin with a decrease in protein oxidation after 1 h of cultivation under treated and untreated conditions. In case of H_2O_2, this effect reversed 5 h after treatment. Contrarily, antioxidant treatment of Wistar 2 resulted in an increase in protein oxidation after 5 h. *HepG2* were, accordingly to the aforementioned ROS values, more susceptible to NAC than quercetin.

4.2.3 Influence of oxidative stress and antioxidant treatment on antioxidant defense mechanisms of primary hepatocytes from Wistar rats and *HepG2*

Glutathione is the most important non-enzymatic antioxidant system to counteract oxidative stress in cells. The total amount of glutathione characterizes the antioxidant potential of the system. The glutathione data obtained from PRH from two individual Wistar rats was comparable and therefore discussed as average values of both rats (Figure 4-7). The measurement of the intracellular content of reduced glutathione revealed opposite reactions of PRH and *HepG2* towards heat and chemical stress. Primary hepatocytes treated with H_2O_2 showed a decreased glutathione (GSH/GSSG) content already 1 h after treatment. In contrast, heat stress provoked a time-delayed increase in the GSH/GSSG content at 5 h. *HepG2* responded exactly the other way around. Heat stress provoked a drastic decrease in the amount of glutathione (~20 % of control) immediately after treatment and glutathione increased due to H_2O_2 treatment. The influence of antioxidants on the different cell types was diverse. In PRH, antioxidant treatment further decreased glutathione content in the control cells (Figure 4-7 C/E). Under oxidative stress conditions, antioxidants showed no significant effect. In *HepG2*, control cells cultivated at 37 °C reacted differently to NAC compared to quercetin. Here, pre-treatment with quercetin increased GSH/GSSG, NAC pre-treatment decreased GSH/GSSG content (Figure 4-7 D/F). The treatment of cells treated with heat or H_2O_2 with both NAC and quercetin caused an adjustment of GSH/GSSG content towards the control values (Figure 4-7 D/F). This means, heat stress decreased GSH/GSSG content (Figure 4-7 B) and antioxidant treatment increased GSH/GSSG relative to this heat stress condition. In the same way, H_2O_2 increased GSH/GSSG content (Figure 4-7 B) and antioxidant treatment decreased GSH/GSSG

relative to this H_2O_2 stress condition (see Supplemetary Table 4-1 for measured values in nmol/mg protein).

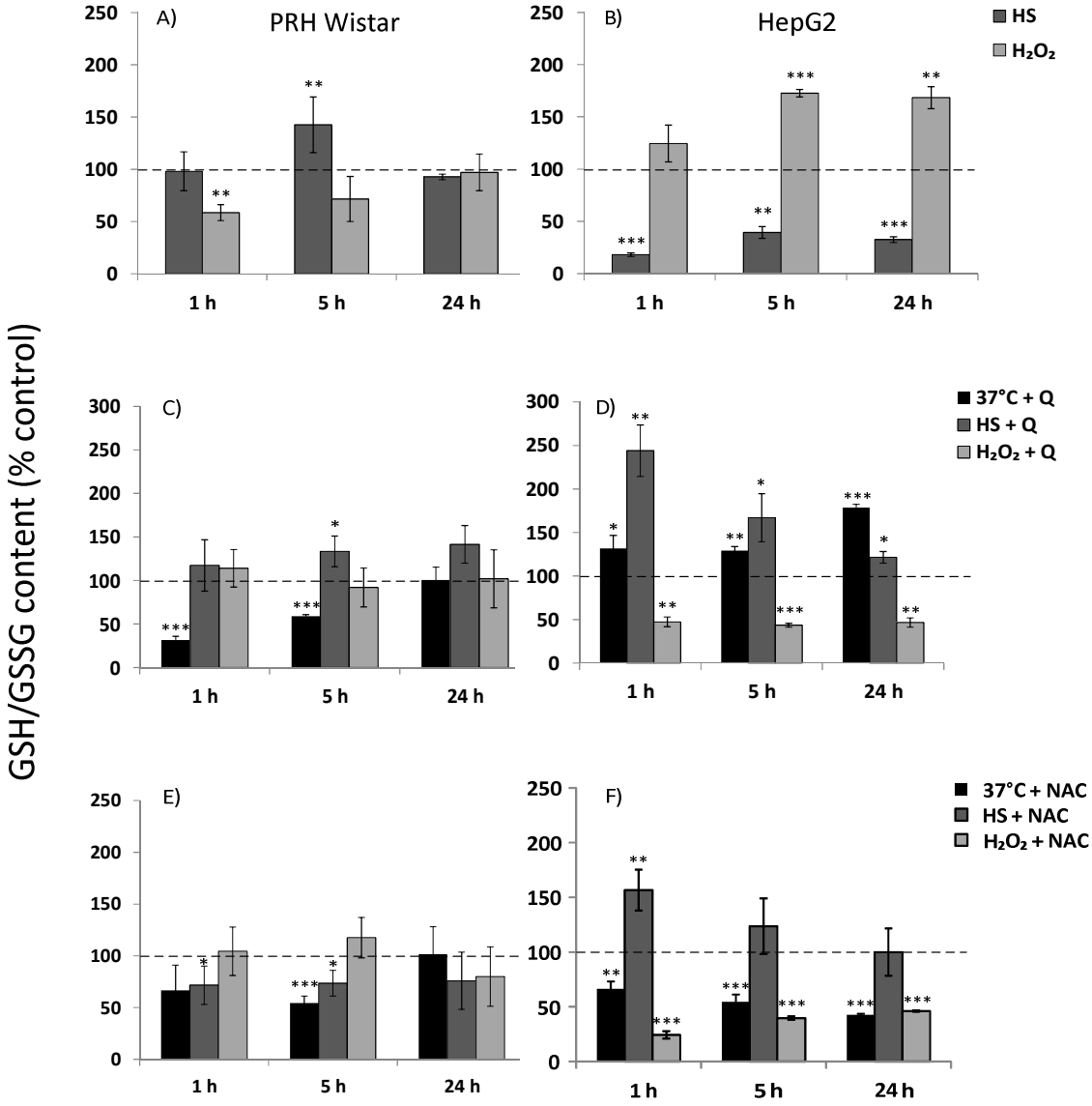

Figure 4-7: GSH content of A) primary hepatocytes from Wistar rats and B) hepatoma cell line *HepG2* under heat stress and H_2O_2 stress related to untreated control (dashed line). GSH content of C) Wistar PRH and D) *HepG2* after 4 h pre-incubation with 50 µM quercetin in relation to the corresponding untreated and treated cells. ROS production of E) Wistar PRH and F) *HepG2* after 4 h pre-incubation with 500 µM NAC in relation to untreated and treated cells (dashed line). Error bars indicate standard deviation (PRH: N=2; n=6; *HepG2*: n=3). Statistical significance was determined with student's t-test. *, ** and *** indicate significance at p=0.05, p=0.01 and p=0.001. All results were correlated to the living cell number after 1 h, 5 h and 24 h of cultivation determined using calcein AM staining. Abbreviations: GSH/GSSG: glutathione; HS: heat stress; NAC: N-acetylcysteine; Q: quercetin.

In addition to glutathione as a central part of enzymatic defense mechanism against oxidative stress, it was examined in which way the activities of the endogenous antioxidant enzymes catalase and superoxide dismutase were influenced in our experimental setup.

Heat and chemical stress had only a minimal influence on catalase activity in both PRH and *HepG2* (Figure 4-8 A-C). Nonetheless, catalase activity was affected by treatment with NAC and quercetin. Primary hepatocytes from Wistar rat1 showed a rapid increase in catalase activity due to NAC and quercetin which abated over time. Cells which were heat stressed after antioxidant treatment showed an especially strong reaction compared to chemically stressed cells (Figure 4-8 D/G). In contrast, PRH from Wistar 2 were remarkably unsusceptible to changes in their catalase activity. This different reaction to antioxidants is surprising, considering that both Wistar rats showed the same catalase activity in their control cells. In hepatocytes from both rats the activity increased over time independent of oxidative stress or antioxidant treatment (Supplementary Figure 4-1 A). *HepG2* control cells showed a peak in catalase activity 5 h after the start of the experiment (Supplementary Figure 4-1 B). Treatment with NAC showed a remarkable effect in *HepG2* cells which were incubated with H_2O_2 (Figure 4-8 I). Here, catalase activity increased to about 140% compared to untreated cells at 1 h, then decreased to only 60% at 5 h and came back to about control levels at 24 h.

In contrast to catalase, the measurement of superoxide dismutase activity showed a constant activity in PRH at all time-points (Supplementary Figure 4-2 A). In *HepG2* cells, the SOD activity dropped after 5 h of cultivation and recovered after 24 h (Supplementary Figure 4-2 B). Comparable to catalase, all cell types were relatively unsusceptible to heat and chemical stress concerning SOD activity. PRH from Wistar 1 showed a small decline at 1 h and 5 h after heat stress, whereas PRH from Wistar 2 showed no significant changes (Figure 4-9 A/B). In *HepG2*, the effect was much more pronounced (Figure 4-9). Hydrogen peroxide caused a clear increase in SOD activity already after 1 h. Heat stressed cells followed with a time delay after 5 h with an activity of about 140% compared to control. After 24 h the values dropped back to about control level. PRH from Wistar 2 showed no measurable reaction to antioxidant treatment (Figure 4-9 E/H). In PRH from Wistar 1, quercetin caused a general decline in SOD activity. NAC had a similar effect at 1 h which was however reversed at 5 h (Figure 4-9 G). In *HepG2*, untreated control cells showed a decreased SOD activity after 5 h of incubation (see Supplementary Figure 4-2). The treatment with quercetin resulted in a increase of SOD activity (Figure 4-9 F) towards the level of the control at 1 h and 24 h. SOD activity of control cells

increased and that of oxidatively stressed cells decreased towards the control level. In *HepG2* treated with NAC this effect was also observed but less pronounced for heat stress (Figure 4-9 I).

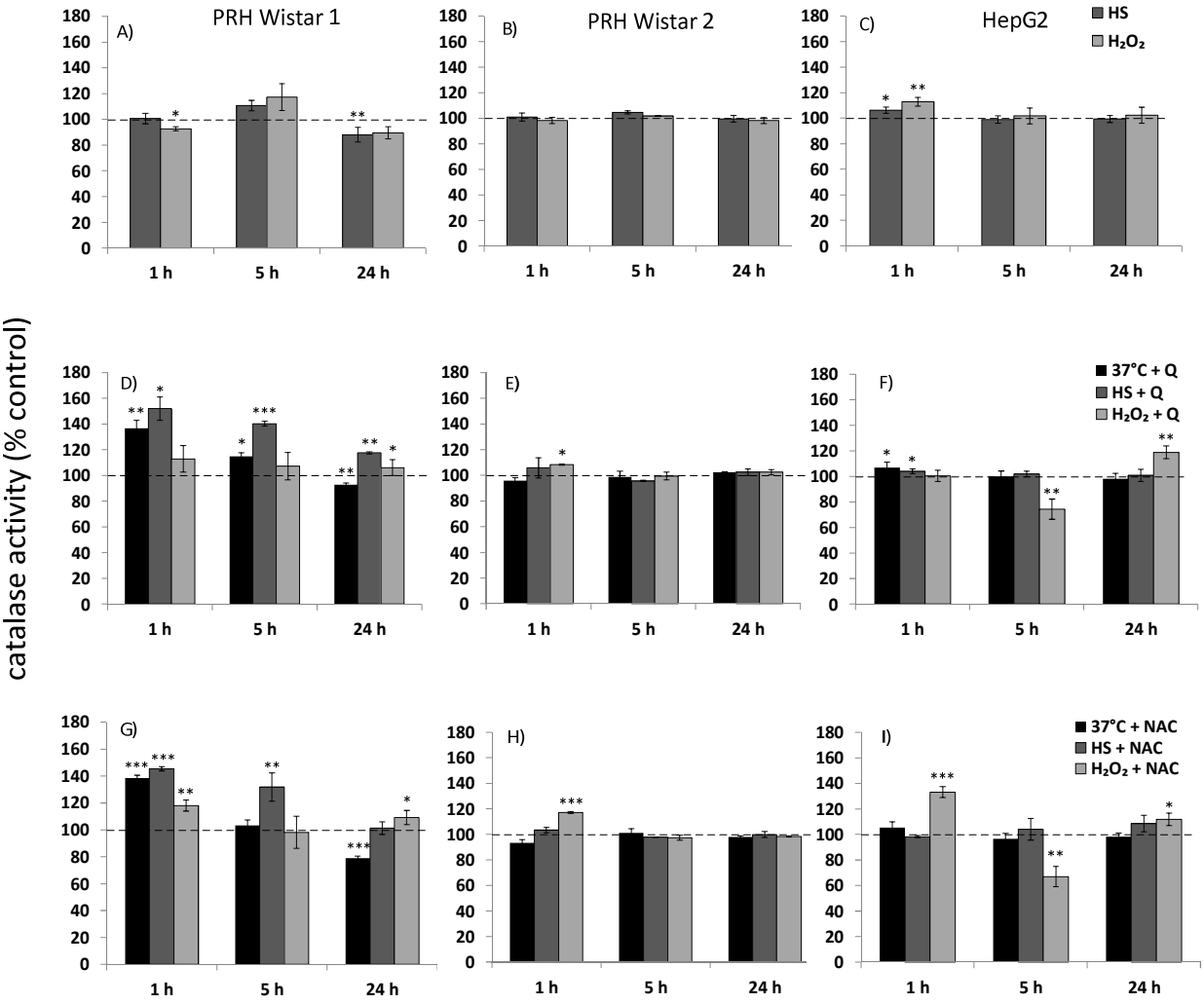

Figure 4-8: Catalase activity of A) primary hepatocytes from Wistar rat 1, B) Wistar rat 2 and C) hepatoma cell line *HepG2* under heat stress and H_2O_2 stress related to untreated control (dashed line). Catalase activity of D) PRH Wistar 1 E) PRH Wistar 2 and F) *HepG2* after 4 h pre-incubation with 50 µM quercetin in relation to the corresponding untreated and treated cells. Catalase activity of G) PRH Wistar 1, H) PRH Wistar 2 and I) *HepG2* after 4 h pre-incubation with 500 µM NAC in relation to untreated and treated cells (dashed line). Error bars indicate standard deviation (PRH Wistar 1: n=3; PRH Wistar 2: n=3; *HepG2*: n=3. Statistical significance was determined with student's t-test. *, ** and *** indicate significance at p=0.05, p=0.01 and p=0.001. All results were correlated to the living cell number after 1 h, 5 h and 24 h of cultivation determined using calcein AM staining. Abbreviations: HS: heat stress; NAC: N-acetylcysteine; Q: quercetin.

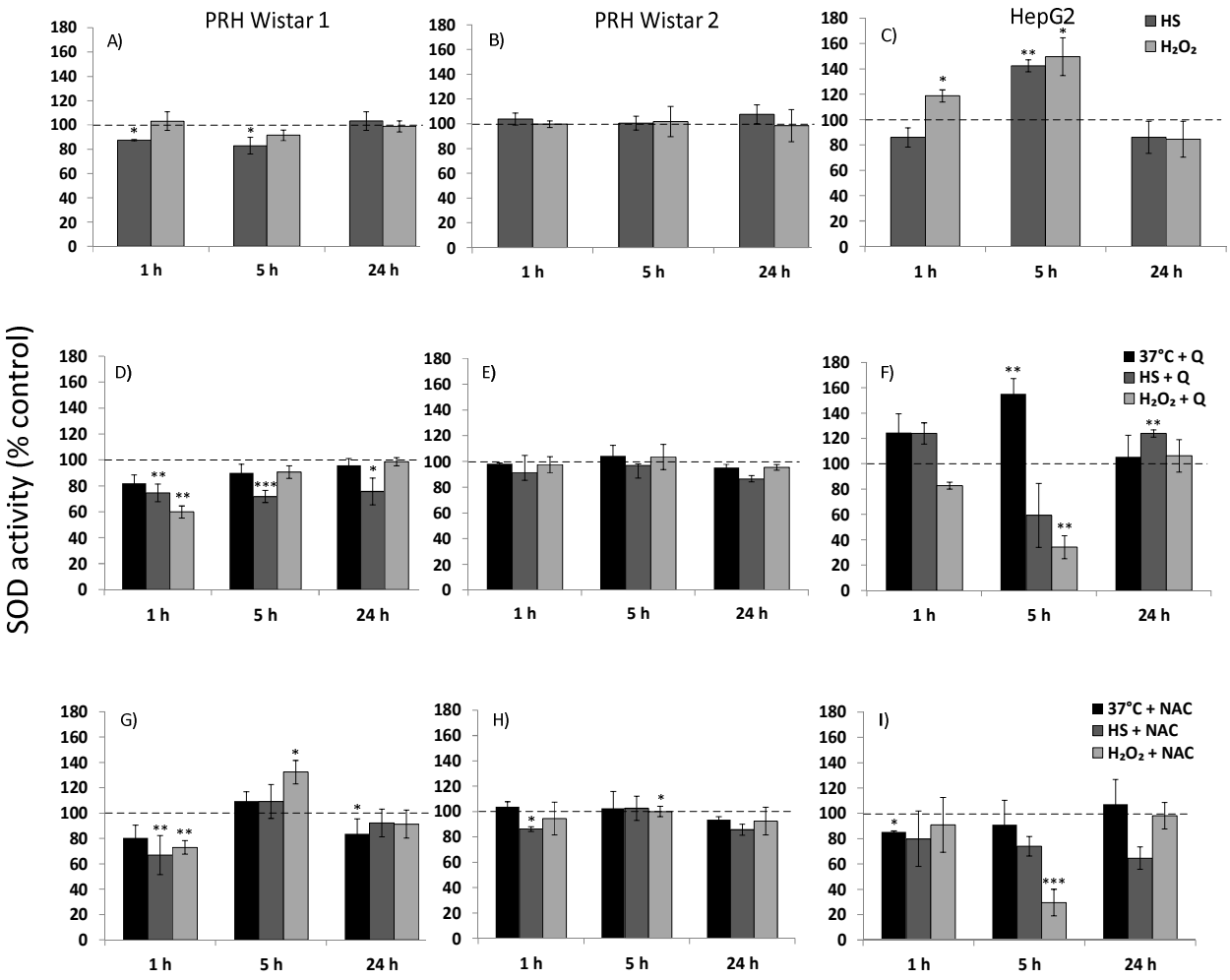

Figure 4-9: Superoxide dismutase activity of A) primary hepatocytes from Wistar rat 1, B) Wistar rat 2 and C) hepatoma cell line *HepG2* under heat stress and H_2O_2 stress related to untreated control (dashed line). SOD activity of D) PRH Wistar 1 E) PRH Wistar 2 and F) *HepG2* after 4 h pre-incubation with 50 µM quercetin in relation to the corresponding untreated and treated cells. SOD activity of G) PRH Wistar 1, H) PRH Wistar 2 and I) *HepG2* after 4 h pre-incubation with 500 µM NAC in relation to untreated and treated cells (dashed line). Error bars indicate standard deviation (PRH Wistar 1: n=3; PRH Wistar 2: n=3; *HepG2*: n=3). Statistical significance was determined with student's t-test. *, ** and *** indicate significance at p=0.05, p=0.01 and p=0.001. All results were correlated to the living cell number after 1 h, 5 h and 24 h of cultivation determined using calcein AM staining. Abbreviations: SOD: superoxide dismutase; HS: heat stress; NAC: N-acetylcysteine; Q: quercetin.

4.2.4 Estimation of biological variance of Wistar rats and *HepG2* by Principal Component Analysis (PCA)

In order to determine if there are clear separations between the PRH of the two individual Wistar rats and the human hepatoma cell line *HepG2* a Principal Component Analysis (PCA) with all available assay data was performed using MatLab 2017a (MathWorks, Nattick, MA, USA). The results are illustrated in Figure 4-12.

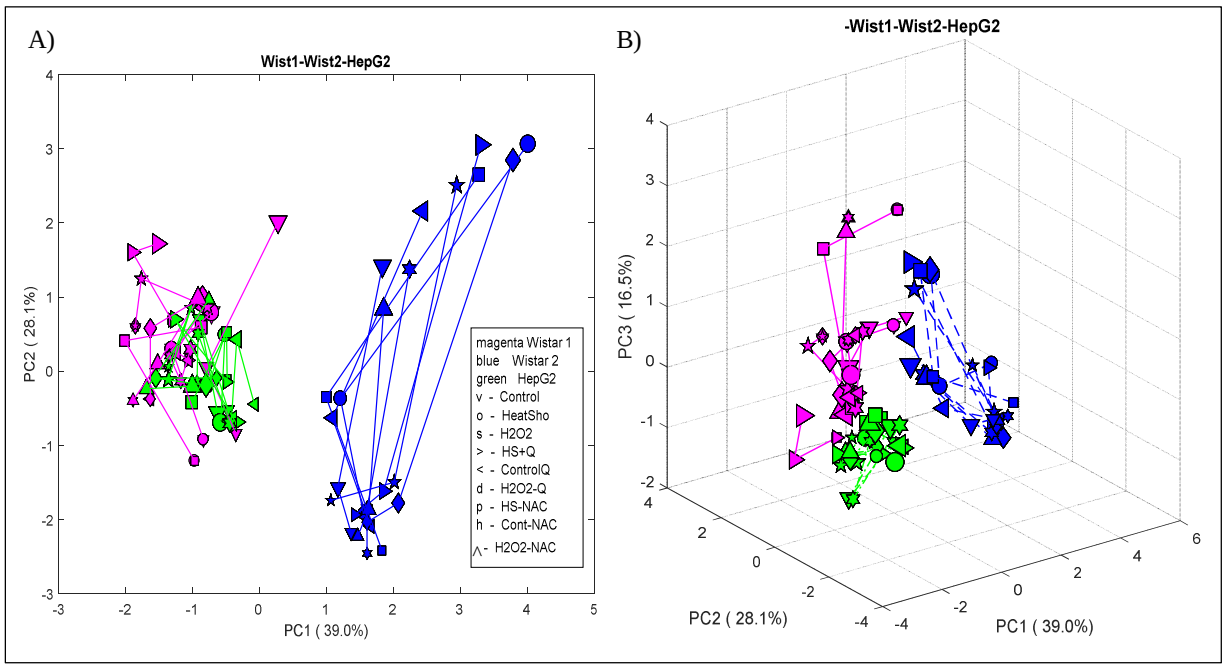

Figure 4-12: Principal component analysis (PCA) of the assay data for albumin, LDH, ROS, protein oxidation, GSH, catalase and SOD from PRH of two individual Wistar rats (magenta: Wistar1, blue: Wistar2) and *HepG2* (green) (n=3). The data was normalized to Z-score. A) PCA with two principal components, B) 3D plot with three principal components. Hepatocytes were exposed to oxidative stress by heat or H_2O_2. Antioxidant effect of NAC and quercetin were normalized to the respective control. Increasing size of the data symbol represents the progressing time after treatment.

The PCA is a widely used method for multivariate statistics, which was first invented 1901 by Pearson. PCA concentrates linear combinations of the original variables to a new variable, the principal component, which explains most of the observed variation in the data and therefore reduces dimensions and brings out patterns in large data sets. The data is transferred to a new

coordinate system, where the first principal component (PC1) is the variable which stands for the highest data variance and the second principal component (PC2) the second highest variance. Including a third principal component (PC3) increases the coverage of the variance of the first and second component (see Figure 4-12 B). For PCA the measured data was normalized using the average and standard deviation resulting in the Z-score (in-built MatLab PCA routine). Z-score is defined as $z_i = \frac{x_i - \mu}{\sigma}$, where x_i is a measured value, μ the average of all the measurements and σ the standard deviation of all the measurements.

Because of the low significance level of the obtained data groups, it was refrained from inserting confidence ellipses into the plot. Interestingly, for all chosen conditions a clear separation of PRH of Wistar 2 from Wistar 1 and *HepG2* was observed (Figure 4-12). In this PCA plot, PC1 represents 39% and PC2 28.1% of the data variance. PRH from Wistar 1 and *HepG2*, on the other hand, showed many overlapping regions. To further examine a potential difference of data from Wistar 1 and *HepG2*, the third principal component (PC3) was added to create a 3D plot (Figure 4-12 B). The addition of PC3, which represents 16.5% of the data variance, revealed that there is also a separation between PRH of Wistar 1 and *HepG2*. However, the variance of data was much less pronounced than expected considering the human origin of the *HepG2* cell line. A closer look at the data using 3D plots of only two cell types confirmed this first impression (see Supplementary Figure 4-4 E).

The influence of individual measured variables on the variance between the three cell types is expressed as the loading coefficient (Figure 4-13). According to this figure, SOD is most influential on PC1. Loadings for PC2 showed similar contribution of catalase on the positive axis and protein oxidation on the negative axis. PC3 was clearly dominated by ROS.

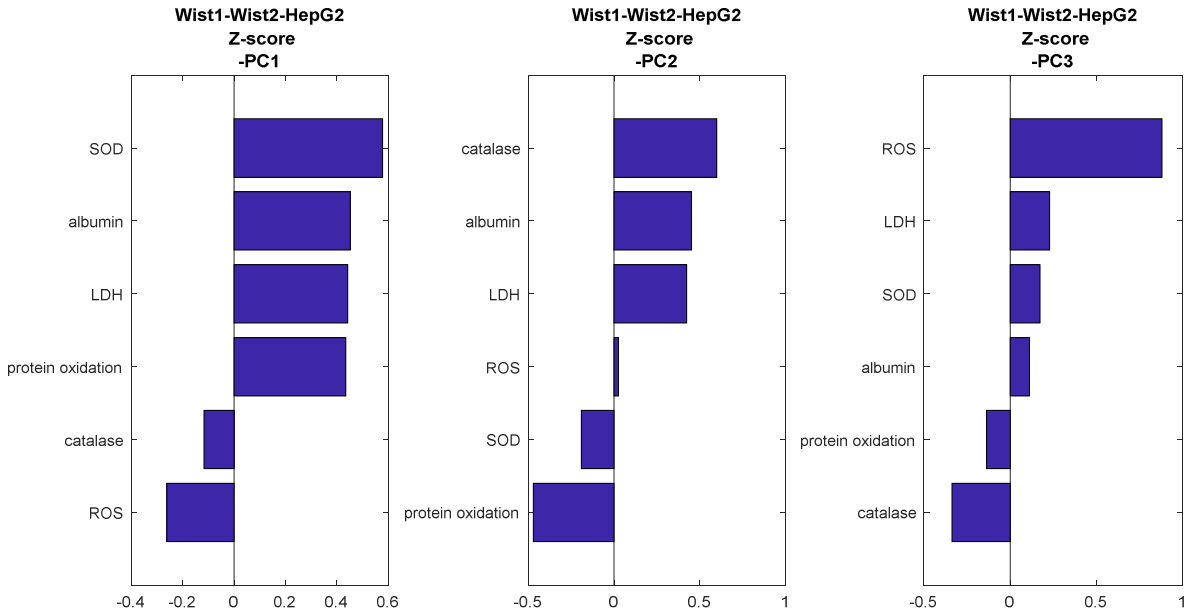

Figure 4-13: Loading coefficients for PC1, PC2 and PC3 corresponding to the principle component analysis (see Figure 4-12). Assay data with the greatest influence on separation between PRH from Wistar 1, PRH from Wistar 2 and *HepG2*.

PCA revealed a clear separation between control and heat stress pre-treated with quercetin in PRH from Wistar 1 (Figure 4-14 B) and Wistar 2 (Supplementary Figure 4-6 A). Furthermore, both NAC and quercetin pre-treatment of untreated control cells results in a separation between control and antioxidants in Wistar 1 (Figure 4-14 A). The influence of antioxidant treatment on PRH from Wistar 1 is illustrated in Figure 4-14 B. It shows a trend towards separation between heat stress and heat stress after quercetin pre-treatment in PRH from Wistar which was not observed in Wistar 2 and *HepG2* (Supplementary Figure 4-6 E). *HepG2* showed a similar trend towards separation between heat stress and NAC treatment (Figure 4-16 B and Supplementary Figure 4-6 F). This observation corresponds to the ROS and protein oxidation data presented in chapter 4.2.2. The experimental data for the treatment with 2 mM H_2O_2 did not allow for a clear conclusion regarding PCA. For PRH from Wistar 1, the untreated control condition seems to be separated from all other conditions (Figure 4-14 C), whereas for Wistar 2 and *HepG2* the H_2O_2 treatment shows no obvious systematic difference to the other conditions (Figure 4-15 C and 4-16 C).

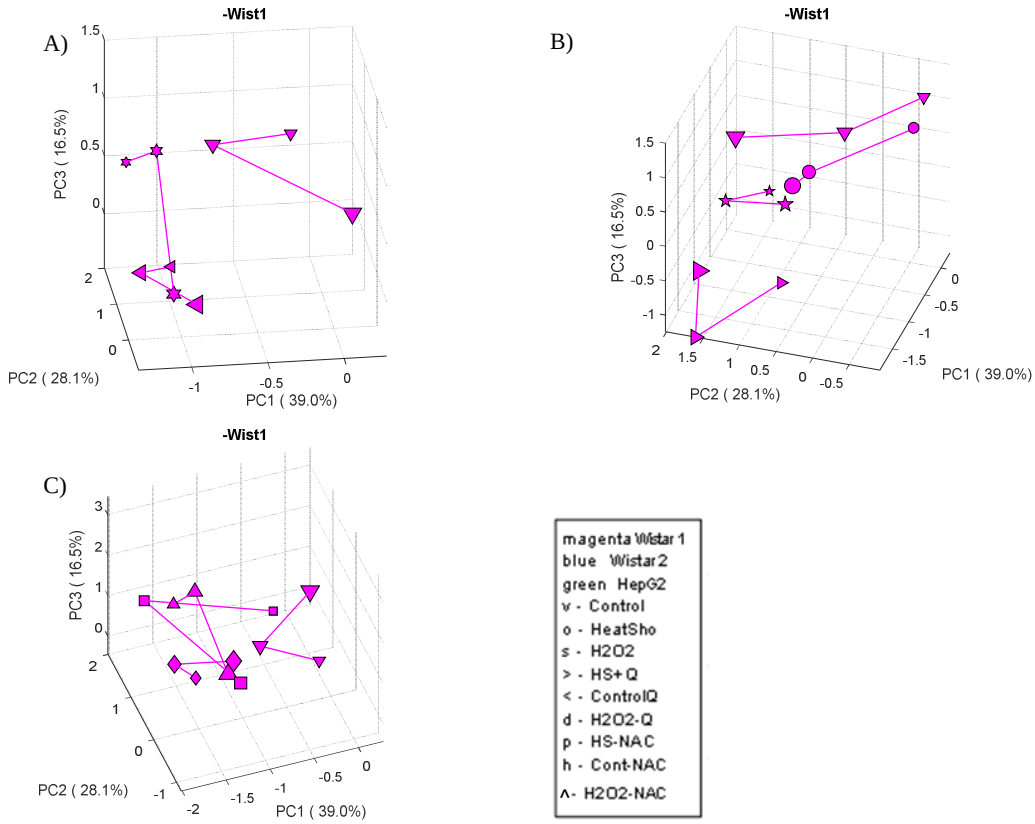

Figure 4-14: 3D plots of the principal component analysis of the assay data for albumin, LDH, ROS, protein oxidation, GSH/GSSG, catalase and SOD from PRH of Wistar rat 1 (magenta) (n=3). A) Comparison of untreated hepatocytes (control) from Wistar 1 with PRH pre-treated with quercetin (ControlQ) or NAC (ControlNAC); B) comparison of untreated hepatocytes (control) from Wistar 1 with PRH under heat shock (HS) and PRH pre-treated with quercetin (HS+Q) or NAC (HS+NAC) prior to HS; C) comparison of untreated hepatocytes (control) from Wistar 1 with PRH after hydrogen peroxide treatment (H2O2) and PRH pre-treated with quercetin (H2O2-Q) or NAC (H2O2-NAC) prior to H_2O_2. Increasing size of the data symbol represents the progressing time after treatment.

PCA for Wistar 2 showed no separation regarding antioxidant effect of quercetin or NAC (Figure 4-15). However, PCA revealed a strong time-dependent pattern for Wistar 2 compared to Wistar 1 or *HepG2*. This is clearly shown in the 2D plots (Supplementary Figure 4-5) with long lines between the three time-points which are dominated by PC2. Additionally, an also time-dependent v-pattern can be observed in the plots which appears in all experiments (Figure 4-15).

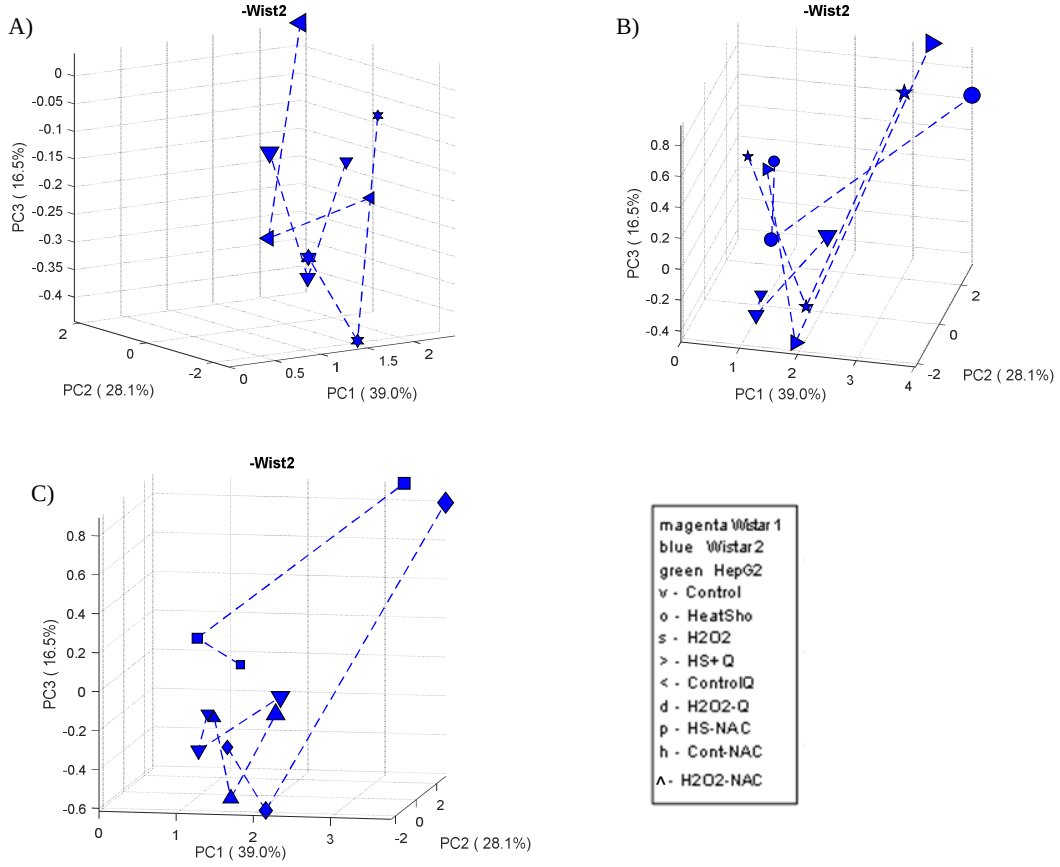

Figure 4-15: 3D plots of the principal component analysis of the assay data for albumin, LDH, ROS, protein oxidation, GSH/GSSG, catalase and SOD from PRH of Wistar rat 2 (blue) (n=3). A) Comparison of untreated hepatocytes (control) from Wistar 2 with PRH pre-treated with quercetin (ControlQ) or NAC (ControlNAC); B) comparison of untreated hepatocytes (control) from Wistar 2 with PRH under heat shock (HS) and PRH pre-treated with quercetin (HS+Q) or NAC (HS+NAC) prior to HS; C) comparison of untreated hepatocytes (control) from Wistar 2 with PRH after hydrogen peroxide treatment (H2O2) and PRH pre-treated with quercetin (H2O2-Q) or NAC (H2O2-NAC) prior to H_2O_2. Increasing size of the data symbol represents the progressing time after treatment.

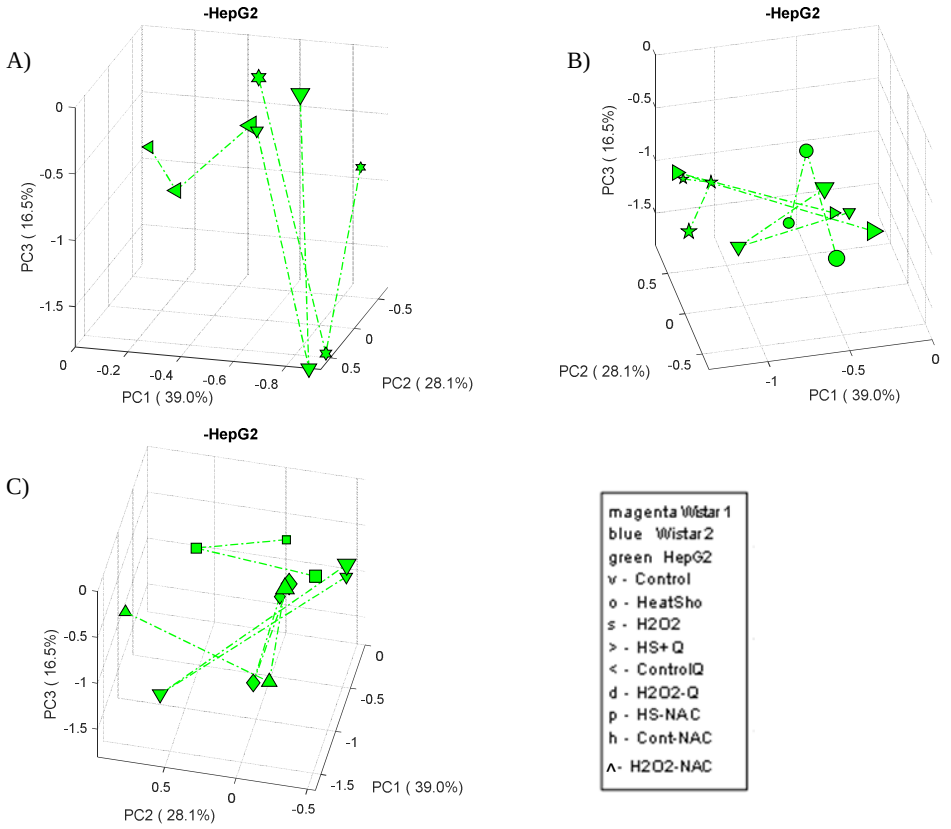

Figure 4-16: 3D plots of the principal component analysis of the assay data for albumin, LDH, ROS, protein oxidation, GSH/GSSG, catalase and SOD from hepatoma cell line *HepG2* (green) (n=3). A) Comparison of untreated hepatocytes (control) from *HepG2* with cells pre-treated with quercetin (ControlQ) or NAC (ControlNAC); B) comparison of untreated hepatocytes (control) from *HepG2* with cells under heat shock (HS) and cells pre-treated with quercetin (HS+Q) or NAC (HS+NAC) prior to HS; C) comparison of untreated hepatocytes (control) from *HepG2* with cells after hydrogen peroxide treatment (H2O2) and cells pre-treated with quercetin (H2O2-Q) or NAC (H2O2-NAC) prior to H_2O_2. Increasing size of the data symbol represents the progressing time after treatment.

4.3 Discussion

In this study the influence of the two antioxidant compounds N-acetylcysteine and quercetin on primary hepatocytes of two individual middle-aged Wistar rats and on the cell line *HepG2* was analyzed under oxidative stress conditions. The aim of the study was to evaluate the effectiveness of NAC and quercetin in our in vitro heat stress model. However, data evaluation showed different reactions of PRH from two individual Wistar rats to diverse stress stimuli and antioxidant treatment. Principal component analyses confirmed a high diversity of primary hepatocytes of the two individual Wistar rats (Chapter 4.2.4). As an outbred rat stock, Wistar rats are not genetically uniform (Festing, 1993), but genetically heterogeneous (Kacew & Festing, 1996), which e.g. results in a different disposition for obesity (Harrold et al., 2000). Another study revealed that individuals of outbred rat stocks show a varying response to hypoxia. Individual rats could be divided in groups of high-, middle- and low-responders to hypoxia due to inter-individual differences in cytochrome P450 activity, an enzyme family which crucially contributes to xenobiotic metabolism (Bayanov & Brunt, 1999). Because of this diversity, the results from primary hepatocytes of the two individual middle-aged Wistar rats were discussed separately. To summarize the rather complex results of this chapter, Table 4-1 is given as a condensed overview. The presentation of the data in color scales illustrates the differences between the PRH of the two individual Wistar rats and *HepG2*.

Albumin, normally used as a specific marker for liver function, was measured under all oxidative stress conditions and under antioxidant treatment (Chapter 4.2.1). PRH from Wistar 1 reacted to heat treatment with a strong increase in albumin secretion, whereas hydrogen peroxide induced no changes in albumin secretion compared to control conditions. This higher albumin secretion due to heat stress was already observed in previous studies (see Chapter 3) as a result of increased antioxidant defense. However, in these cases only PRH from old rats were affected after 24 h. Previous works showed that more than 70% of the ROS scavenging ability of serum was due to serum albumin (Bourdon & Blache, 2001). Therefore, a high serum concentration of albumin in PRH from this individual middle-aged Wistar 1 could indicate long-lasting oxidative stress effects due to heat treatment. Quercetin pre-treatment induced a decrease in albumin secretion. This reaction to antioxidant treatment is possibly due to the ROS scavenging activity of quercetin (Boots et al., 2008) which causes reduced

Table 4-1: Summary of all quantitative data sets (see Figure 4-3 – Figure 4-9) related to oxidative stress and antioxidant treatment of PRH and *HepG2* relative to control conditions. Trends for all significantly altered categories according to the color scale below.

			PRH Wistar 1			PRH Wistar 2			*HepG2*		
	time –point		1 h	5 h	24 h	1 h	5 h	24 h	1 h	5 h	24 h
albumin	heat		+++	+ ++	- -	+			< 85%		
	H_2O_2					- - -			- - -	- -	- -
	Q	37 °C	-	- - -		- -	-		- - -		-
		heat	- -	- - -	- -	- -			- -	-	-
		H_2O_2	- -	-	-	- -	-		-	-	-
	NAC	37 °C	+++						-		
		heat	+	- -			++	-			
		H_2O_2	-	- -		++	++				
LDH	heat			++	++		+	+	-		-
	H_2O_2		+					+	-		
	Q	37 °C	+		++			-	-	+	
		heat	++	-			-	+		+	+
		H_2O_2			+++			+		-	+
	NAC	37 °C			-				-	-	-
		heat	++	-	++		-	+		+	
		H_2O_2			++			++			
ROS	heat		+			+				++	-
	H_2O_2		+			+			+	++	++
	Q	37 °C	-	-		-	-			-	
		heat	-	-		-	-				
		H_2O_2	-	-		-	-		-		
	NAC	37 °C								-	
		heat								-	+
		H_2O_2								-	
protein oxidation	heat				-		-				+
	H_2O_2			-	-	+					
	Q	37 °C	-	-		+	- -				
		heat	-	-			+++				
		H_2O_2	-	+			+++	+			++
	NAC	37 °C	-					+	-		
		heat		-			+++		-		-
		H_2O_2	-	+	+		+++	+	+	-	
GSH/GSSG	heat			+			+		- - -	- -	- -
	H_2O_2		-			-				++	++
	Q	37 °C	- -	-		- -	-		+	+	++
		heat		+			+		+++	++	+
		H_2O_2							- -	- -	-
	NAC	37 °C		-			-		-	-	- -
		heat	-	-		-	-		++		
		H_2O_2							- - -	- -	- -
catalase	heat				-				+		
	H_2O_2		-						+		
	Q	37 °C	+	+							
		heat	++	++	+						
		H_2O_2			+					-	+
	NAC	37 °C	+		-						
		heat	++	+							
		H_2O_2	+			+			+	-	
SOD	heat		-	-			-			+	
	H_2O_2								+	+	
	Q	37 °C								++	
		heat	-	-	-						+
		H_2O_2	-							- -	
	NAC	37 °C			-				-		
		heat	-								
		H_2O_2	-	+						- -	

< 50%
< 25%
> 115%
> 150%
> 200%

oxidative stress and therefore a limitation of albumin production to control levels. Additionally, ROS-oxidized quercetin binds covalently to serum albumin with a high affinity (Kaldas et al., 2005), leading to reduced serum levels of unbound albumin. NAC pre-treatment resulted in a similar but less pronounced reaction. Interestingly, NAC showed a beneficial effect on control cells. Albumin production was significantly increased 1 h after NAC treatment, indicating an improved hepatic function of untreated cells *in vitro*. This assumption is supported by the reduced LDH leakage after 24 h of incubation in monolayer culture. Previous studies showed that culture media can catalyse oxidation processes which lead to oxidative stress in monolayer cultures (Halliwell, 2003). Our own studies of the proteome of primary mouse hepatocytes revealed significantly higher abundance of proteins related to oxidative stress in monolayer culture compared to sandwich culture (Orsini et al., 2018). The present study indicates a beneficial role of NAC pre-treatment for reducing oxidative stress processes in monolayer cell culture under control conditions.

Similar to the albumin data, PRH from Wistar 1 showed a higher LDH leakage after heat stress than after treatment with hydrogen peroxide. The overall higher impact of heat stress on PRH from Wistar 1 compared to H_2O_2 was also confirmed by principal component analysis (Figure 4-14). Contrary to our expectations, both the treatment with NAC and quercetin increased LDH leakage in oxidatively stressed PRH, indicating cell death. This was unexpected, considering the simultaneous reduction of ROS, the decrease in protein oxidation and the increase in catalase activity caused by quercetin treatment (Table 4-1). This paradoxical effect of quercetin treatment was already described in the literature. Quercetin is an efficient ROS scavenger and protects macromolecules against oxidative damage. However, by doing that, quercetin is converted into the oxidation products o-quinone and o-semiquinone which act as cytotoxic pro-oxidants leading to LDH leakage (Boots et al., 2007; Halliwell, 2008). Additionally, oxidized quercetin is highly reactive towards thiol groups and therefore toxic. Quercetin can form adducts in its oxidized form. Its targets are, e.g. proteins, but also glutathione resulting in a reduction of free glutathione (Boots et al., 2003). Furthermore, quercetin is known to inhibit the expression of heat shock proteins (HSP) (Jakubowicz-Gil et al., 2002) as confirmed in our own studies with Sprague Dawley rats (see Chapter 5). Heat shock proteins play an important role in the heat shock response which consists of the induction of gene expression of proteins, like chaperones, proteases and antioxidant enzymes, essential for maintenance of cell homeostasis by counteracting heat stress related damage

(Mustafi et al., 2009). In this context, HSPs function as molecular chaperones, initiating the refolding or degradation of stress-damaged proteins, thus protecting cells from potential damaging effects. HSP expression is initiated by the binding of the transcription factor HSF1 (heat shock factor 1) to the heat-shock element in the promotor region of the HSP family (Jolly & Morimoto, 2000). Quercetin suppresses the heat shock response by inhibiting HSF1 (Nagai et al., 1995) which is compromising the beneficial antioxidant effect of quercetin. Nonetheless, quercetin pre-treatment still showed positive effects on middle-aged PRH from Wistar 1. The production of ROS under heat stress and H_2O_2 stress was reduced after pre-treatment with quercetin (Table 4-1). Furthermore, quercetin reduced the protein oxidation level in PRH from middle-aged Wistar 1. As discussed in Chapter 3, PRH from middle-aged Wistar rats possess highly efficient defense mechanisms against oxidative damage. Protein oxidation was observed to be lower in heat stressed cells than in control cells at 24 h (see HSP70 recovery system, Chapter 3). In this study, similar results were found. Protein oxidation decreased over time under control conditions, indicating an adaptation to the culture conditions (Supplementary Figure 4-3). Heat stress and H_2O_2 treatment resulted in a further decrease in protein oxidation and in case of heat an increase in glutathione (Table 4-1) confirming the thesis that the defense mechanisms of PRH from middle-aged rats is stimulated under stress conditions. Quercetin further decreased protein oxidation which indicates the supporting effect for the antioxidant defense of middle-aged PRH. Further evidence of the beneficial role of quercetin is supported by the catalase activity. Contrary to SOD, catalase activity needs time to adapt at the beginning of the cultivation (Richert et al., 2002). Therefore, catalase activity increased over time under control conditions (Supplementary Figure 4-1). This adaptation process was supported by pre-treatment with quercetin resulting in increased catalase activity 1 h and 5 h after the start of the culture (Table 4-1). However, the SOD activity showed only slight changes under stress conditions and no positive effect of quercetin.

Similar, but less pronounced effects were also shown for NAC treatment. Cells under heat stress were shown to exhibit a slightly reduced expression of HSP72 and HSP27 after NAC treatment (Gorman et al., 1999) resulting in an increased caspase activity and ultimately apoptosis. In our own study, NAC pre-treatment resulted in an increased LDH leakage, but contrary to quercetin, was not able to reduce ROS production. Surprisingly, NAC, as an acetylated cysteine residue, was not able to restore glutathione (Table 4-1). Additionally,

NAC-treated PRH even showed a slight increase in protein oxidation. All these data imply a less beneficial effect of NAC on PRH from Wistar 1 compared to quercetin. Principal component analysis supported this assumption (Figure 4-14 B/C). PCA showed no separation between stress conditions and NAC pre-treatment for Wistar 1.

Compared to Wistar 1, hepatocytes from Wistar 2 seemed to show only a low response to heat stress. The reaction to H_2O_2 treatment was more pronounced as confirmed by PCA (Figure 4-15). Remarkably, PRH from Wistar 2 reacted prevalently with a time-delay compared to Wistar 1 which resulted in a strong time-dependent pattern in PCA (see Chapter 4.2.4). This condition is possibly related to the high basic level of oxidative stress PRH from Wistar 2 were exhibiting, especially at 5 h. Protein oxidation of hepatocytes from Wistar 2 was 3-fold higher than in Wistar 1 at the beginning of the experiment (Supplementary Figure 4-3). After 24 h, the protein oxidation values decreased to a level comparable to Wistar 1 at 1 h. Additionally, LDH leakage was more than 5-fold higher in Wistar 2 (Supplementary Table 4-2). Other measurements, like glutathione, ROS and albumin were similar to Wistar 1. However, the significantly increased protein oxidation under antioxidant treatment with NAC or quercetin and the lack of changes in catalase and SOD activity suggest that PRH from Wistar 2 reached the limit of their ability to defend against oxidative damage due to their high basic stress level. These results are surprising regarding the standardized culture conditions and the comparable start viability of the hepatocytes from both rats (Wistar 1: 78%; Wistar 2: 82%). An explanation for these differences could possibly be found in the previously discussed biological variance of the outbred Wistar rats. As shown in the previous study about hypoxia (Bayanov & Brunt, 1999), Wistar rats can be divided in low-, middle- and high-responders. Our data suggest possible analogous properties of PRH from Wistar rats regarding basic oxidative stress under cell culture conditions. Under this premise, Wistar 1 is supposed to be a middle- to low-responder, whereas Wistar 2 would qualify as a high-responder. Thus, PRH from Wistar 1 show low levels of oxidative stress under control conditions and PRH from Wistar 2 exhibit signs of high basic oxidative stress. Naturally, this assumption is only a theoretical categorization which would have to be further studied with a high number of biological replicates.

HepG2 is a cell line derived from human hepatoblastoma. As cancer cells, it can be expected that they react significantly different to oxidative stress than primary hepatocytes. The advantage of using a cell line is that it provides a consistent *in vitro* model unaffected by

stress due to liver perfusion. The HepG2 cell line is known to have a low expression of cytochrome P450 enzymes (Gerets et al., 2012) which results in a low metabolism of xenobiotics. However, *HepG2* were previously described as susceptible to heat-induced apoptosis when treated at 42 °C for 1 h to 6 h (Basile et al., 2008) which makes it an interesting candidate in our present *in vitro* heat stress model.

First of all, our data suggest that the reaction of *HepG2* to heat stress mainly occurred within the first 5 h after the start of the experiment. Heat treatment provoked an increase in ROS production and catalase and SOD activity (Table 4-1). Despite this evidence of an oxidative stress reaction, heat stress had no negative effect on cell viability (see LDH, Table 4-1). This suggests that *HepG2* were able to counteract the oxidative stress induced by heat in our setup. The strongest impact of heat treatment on *HepG2* could be observed in the GSH/GSSG measurements. Heat treatment induced a significant decrease in glutathione which is surprising considering the successful defense against oxidative stress. This reduction of glutathione could possibly also be responsible for the increase in protein oxidation after 24 h of cultivation. Principal component analysis confirmed that *HepG2* were more susceptible to H_2O_2 stress than heat stress (Figure 4-16). This observation is in accordance with previous studies which proved that tumor cells, like *HepG2,* have lower ability to metabolize H_2O_2 than healthy cells (Doskey et al., 2016). In our study, hydrogen peroxide treatment resulted in a strong decrease in albumin production and increased ROS values (Table 4-1). Protein oxidation increased with a time-delay at 24 h. Comparable to heat stress, H_2O_2 treatment caused an increase in catalase and SOD activity and did not compromise cell viability. In summary, *HepG2* exhibit signs of oxidative stress. However, their antioxidant defense mechanisms prevent loss of cell viability. Pre-treatment with quercetin resulted in a decreased ROS production but still appeared to have a negative impact on *HepG2*. Albumin production was drastically decreased and increase in LDH leakage indicated loss of cell viability (Table 4-1).

That is surprising, considering the beneficial effect quercetin had on GSH/GSSG content and catalase and SOD activity. Therefore, it can be assumed that another cellular mechanism is responsible for the reduction of cell viability. As a cancer cell line, *HepG2* reacts differently to many exogenous stimuli and xenobiotics. In this case, quercetin fulfilled its function as a ROS scavenger but simultaneously induced cell death. Treatment of *HepG2* with 50 µM quercetin, as used in our study, was already known to inhibit fatty acid biosynthesis and

induce apoptosis (Zhao et al., 2014). The reaction of *HepG2* to pre-treatment with NAC resulted in similar observations. The underlying mechanisms regarding toxicity in *HepG2* are not known but previous studies confirmed the inefficiency of NAC to protect *HepG2* from oxidative stress induced damage (Manov et al., 2004).

In summary, *HepG2* exhibited signs of oxidative stress. The reaction to heat treatment was detectable but did not cause a significant deviation from the control. The treatment of *HepG2* with 2 mM H_2O_2 caused a strong oxidative stress response. However, their antioxidant defense mechanisms prevented loss of cell viability. The pre-treatment of *HepG2* with NAC or quercetin reduced ROS and enhanced antioxidant defense mechanisms but had no beneficial effect on cell viability. Antioxidant treatment rather induced toxic reactions leading to apoptosis.

Wistar rats used in this study can be divided in low- and high-responders to oxidative stress. PRH from Wistar 1 would categorize as low-responder. Heat treatment provoked the activation of antioxidant defense mechanisms counteracting long-lasting damaging effects. Hydrogen peroxide treatment caused less pronounced effects. Quercetin pre-treatment supported these defense mechanisms, despite causing an increased LDH leakage. NAC treatment showed no significant beneficial effect. PRH from Wistar 2 would fall in the category of high-responders to oxidative stress. Their basic stress level was significantly higher than in PRH from Wistar 1 leading to a limitation in antioxidant defense capability. They were more prone to hydrogen peroxide stress than heat and the toxic effect of NAC and quercetin outweighed their antioxidant properties.

5. Quantitative proteome analysis of primary hepatocytes from middle-aged and old Sprague Dawley rats under oxidative stress conditions

5.1 Introduction

Proteomic approaches are widely used in aging research. The proteome is highly dynamic and therefore more closely related to the actual phenotype than the transcriptome but still more stable than the metabolome (Schanstra & Mischak, 2015). The analysis of the proteome can reveal qualitative and quantitative changes during the aging process and in the development of age-related diseases like diabetes (Prewit, 2018), neurodegenerative diseases (Mirzaei et al., 2017) and cardiovascular diseases (Herzog et al., 2006; Koser et al., 2014). Also, there are many studies focusing on the basic mechanisms of aging (I et al., 2005; de Graff et al., 2016; Guevara et al., 2016), revealing potential therapeutic targets against age-related alterations. High-throughput mass spectrometry methods allow the global characterization of complex protein compositions leading to huge data sets with thousands of identified proteins. Proteomic shotgun methods such as ICAT, SILAC and iTRAQ (see Chapter 1) allow the quantitation of these global proteome profiles in biofluids, cells and tissues. However, the analysis of this information requires increasingly complicated bioinformatics tools such as homology search engines, like FAST and BLAST (Altschul et al., 1990) and databases, like the UniProt Knowledge Base. Frequently, these elaborate studies only generate very specific answers for specific biological questions (Sharov & Schoneich, 2007). Therefore, the complexity of an experimental setup should be adapted to the analytical purpose. Many research topics require only a targeted proteomic approach. One way to successfully reduce the complexity of a cellular proteome is the use of 2-D gel electrophoresis prior to mass spectrometry. Most proteome analysis in aging research was therefore performed with classic and differential 2-D gel electrophoresis and MALDI ToF MS/MS similar to our own approach (Ortuno-Sahagun et al., 2014). With these methods, previous studies revealed the involvement of dysfunctional protein degradation mechanisms in aging (Baraibar et al., 2013). Furthermore, it was proven that a low generation rate of macromolecular damage and the resistance of proteins against oxidative modifications are directly related to longevity (Barja,

2013). These results emphasize the relevance of our own research regarding the proteomic characterization of age-related alterations under oxidative stress conditions in primary hepatocytes.

In our study the hepatic function, oxidative damage markers and the proteome of primary hepatocytes from middle-aged (6 months) and old (> 23 months) Sprague Dawley rats (SD) were analyzed under oxidative stress conditions compared to control conditions using 2-D DIGE and MALDI ToF MS/MS. The outbred rat stock Sprague Dawley was used because of the unavailability of old Wistar rats. Oxidative stress was induced by heat treatment at 42 °C for 30 min or treatment with 2 mM H_2O_2 for 1 h. PRH were pre-treated with 50 µM quercetin for 4 h to induce antioxidant reactions as a protection against oxidative damage.
The aim of the study was to analyze cellular mechanisms of the defense against oxidative stress and the influence of advanced age on these mechanisms. The identification of molecular targets could allow the prediction and diagnosis of ROS-induced cell aging. The antioxidant quercetin was tested as a candidate for the prevention of age- and oxidative stress- related alterations and diseases.

5.2 Results

The influence of aging and the antioxidant effect of quercetin were analyzed using primary rat hepatocytes (PRH) from three individual middle-aged and three individual old Sprague Dawley rats. The effect was compared at 1 h, 5 h and 24 h after induction of oxidative stress by heat treatment at 42 °C or treatment with 2 mM H_2O_2. Hepatic function was monitored during the cultivation time by measuring albumin production and LDH release into the supernatant at the corresponding time points (Figure 5-1). The oxidative stress response was examined by measuring protein oxidation and SOD and catalase activity.

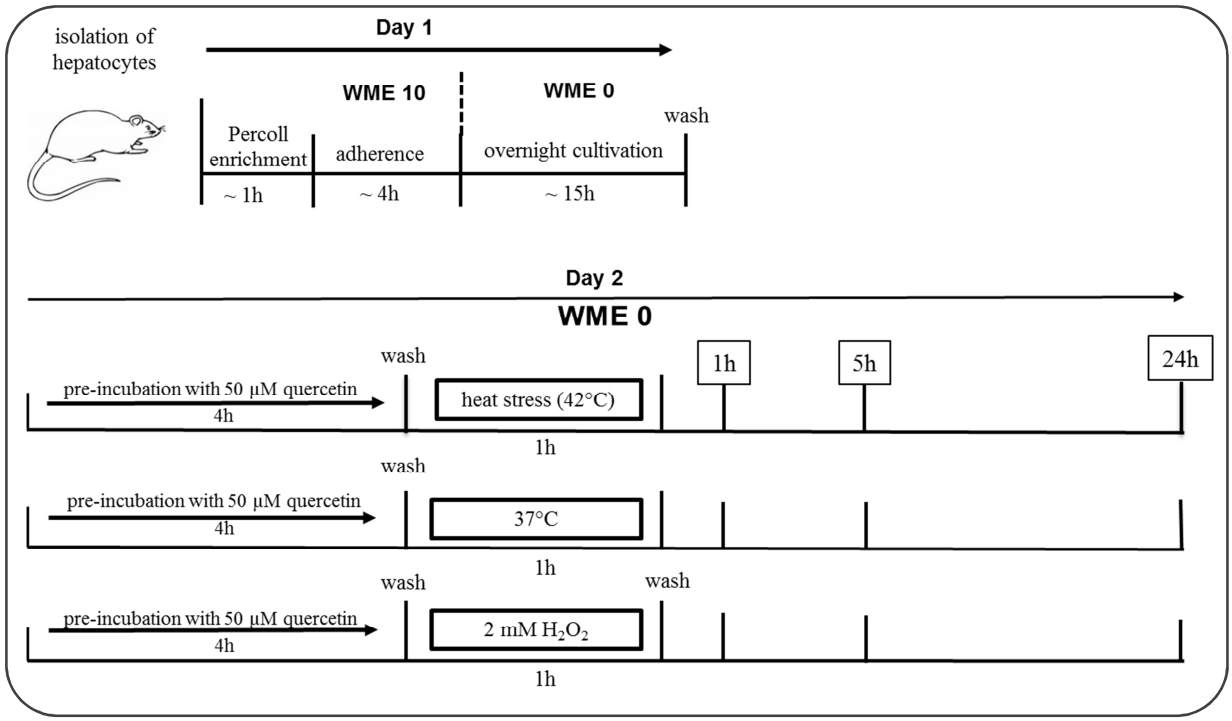

Figure 5-1: Experimental setup for the analysis of the influence of aging and the antioxidant effect of quercetin; PRH of two individual middle-aged or old Sprague Dawley rats were pre-incubated with 50 µM quercetin for 4 h; induction of oxidative stress was achieved by heat (42 °C) or treatment with 2 mM H_2O_2; supernatants and cell lysates for enzyme assays and intracellular proteome analysis were collected 1 h, 5 h and 24 h after oxidative stress.

Viable hepatocytes were seeded in 6 well plates pre-coated with rat tail collagen and left to adhere in WME 10 at 37 °C for 4 h. Afterwards, the cells were left to adapt to serum-free medium (WME0) at 37 °C overnight. After the adaptation phase, the cells were pre-treated with 50 µM quercetin for 4 h. Afterwards, the medium was changed to WME 0 and an oxidative stress response was induced by heat treatment at 42 °C or treatment with 2 mM

H_2O_2 for 1 h. The supernatants and intracellular proteins were collected at 1 h, 5 h and 24 h after induction of oxidative stress.

The dose of hydrogen peroxide of 2 mM significantly increases ROS production without a strong impairment of cell viability (see Chapter 4). Oxidative stress was induced by heat treatment at 42 °C for 30 min. Heat stress induces the formation of ROS through various mechanisms. For instance, hyperthermia causes an increase in superoxide anions (Mujahid et al., 2006), hydrogen peroxide (Zhao et al., 2006) and hydroxyl radicals (Zhao et al., 2006). Additionally, heat stress activates NADPH oxidase, an enzyme which generates ROS by converting NADPH to NADP (Slimen et al., 2014). The advantage of using heat stress also for induction of oxidative stress is that the method is chemically non-invasive and therefore suitable for *in vivo* studies (Hall et al., 2000; Zhang et al., 2003; Slimen et al., 2014). For the antioxidant treatment, a setup was chosen that considers the observations made in our previous studies (see Chapter 4). Our data provided evidence that NAC pre-treatment had no significant beneficial effect on primary rat hepatocytes under heat stress conditions. In contrast, quercetin pre-treatment was proven to have a high ROS scavenging capacity, but without exhibiting significant toxic effects. Therefore, quercetin pre-treatment was chosen to induce antioxidant reactions in primary rat hepatocytes.

Interestingly, primary hepatocytes from Sprague Dawley rats (SD), contrary to Wistar rats, showed no significant inter-individual variance regarding the response to oxidative stress and antioxidant treatment. Therefore, it can be assumed that primary hepatocytes from Sprague Dawley rats are a more suitable model for oxidative stress research than hepatocytes from Wistar rats.

5.2.1 Influence of oxidative stress and quercetin antioxidant treatment on cell viability and albumin secretion of primary hepatocytes from middle-aged and old Sprague Dawley rats

The level of hepatic function was determined 1 h, 5 h and 24 h after induction of oxidative stress by measuring albumin production and LDH release. Previous studies (see Chapter 3 and 4) already assessed the influence of heat stress on middle-aged and old Wistar PRH after 24 h of incubation.

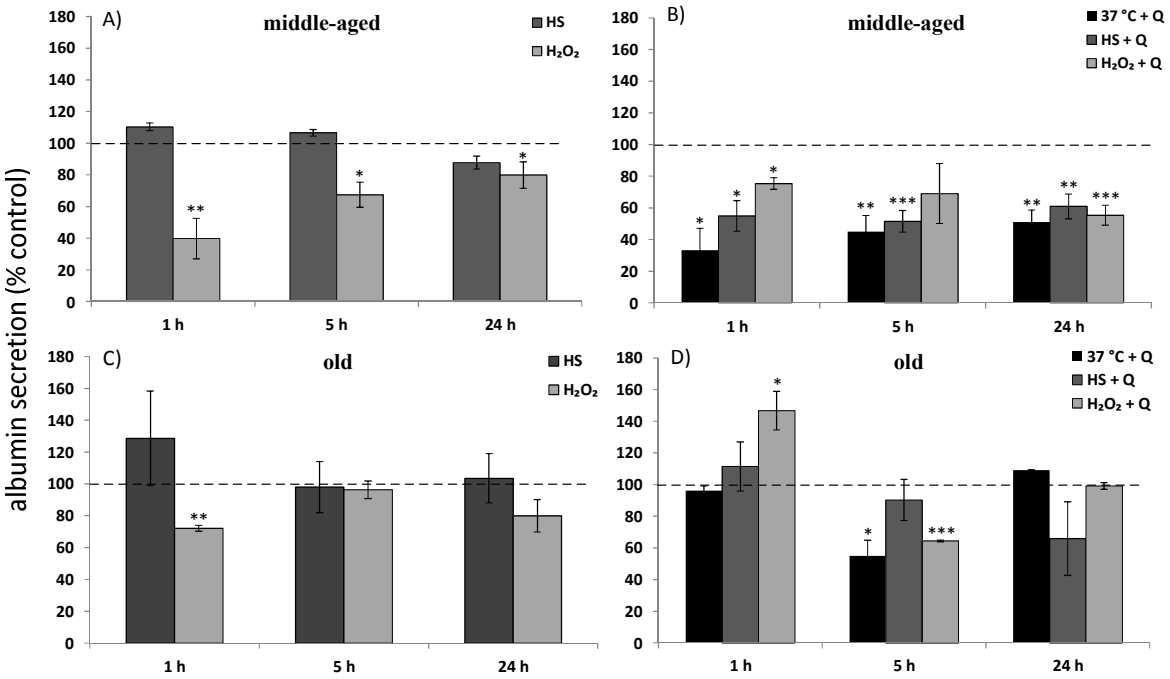

Figure 5-2: Albumin secretion of A) primary hepatocytes from middle-aged Sprague Dawley rats under heat stress and H_2O_2 stress related to untreated control, B) primary hepatocytes from middle-aged Sprague Dawley rats after 4 h pre-incubation with 50 µM quercetin in relation to the corresponding untreated and treated cells, C) primary hepatocytes from old Sprague Dawley rats under heat stress and H_2O_2 stress related to untreated control and D) primary hepatocytes from old Sprague Dawley rats after 4 h pre-incubation with 50 µM quercetin in relation to the corresponding untreated and treated cells. Error bars indicate standard deviation (N=3, n=9). The dashed lines represent the respective control. Statistical significance was determined with student's t-test. *, ** and *** indicate significance at p=0.05, p=0.01 and p=0.001. All results were correlated to the living cell number after 1 h, 5 h and 24 h of cultivation determined using calcein AM staining. Abbreviations: HS: heat stress; Q: quercetin.

For Wistar rats studied earlier, the trend regarding albumin secretion of PRH from middle-aged rats 24 h after heat stress was contradictory. The Wistar rats used in Chapter 3 exhibited

a decreased, the Wistar rats in Chapter 4 an increased albumin secretion. As mentioned before, PRH from SD rats were much more consistent in their reaction to oxidative stress and antioxidant treatment. Interestingly, PRH from SD rats also showed differences in albumin secretion compared to Wistar rats under control conditions. PRH from old Wistar rats secreted more albumin into the supernatant than PRH from middle-aged animals. PRH from SD rats showed exactly the opposite reaction (Supplementary Figure 5-1). The data obtained from the measurement of albumin secretion in PRH from SD rats confirmed the previous observation that cells from middle-aged animals responded to heat stress with a decrease in albumin secretion over time (Figure 5-2 A). PRH from old SD rats showed no significant reaction to heat stress regarding albumin secretion. However, a trend towards an initial increase in albumin can be observed (Figure 5-2 C). The treatment of cells with 2 mM H_2O_2 clearly caused a reduced albumin secretion in both middle-aged and old PRH. Antioxidant pre-treatment of PRH from middle-aged SD rats with 50 µM quercetin resulted in a decrease in albumin, as observed in previous studies (Chapter 4). Contrary, in old hepatocytes quercetin treatment resulted in a time-dependent reaction. Directly after the stress induction albumin increased, whereas this effect reversed over time (Figure 5-2 D).

As mentioned before, albumin secretion does not correlate to hepatocyte-specific cell viability in our heat stress model. However, the data obtained from SD rats suggest a closer correlation of albumin secretion to viability in SD rats compared to Wistar rats. Nonetheless, the activity of the enzyme LDH was measured as a general viability marker which is only released into the supernatant if the integrity of the cell membrane is compromised. The quantification of LDH activity was the only parameter that differed strongly in PRH from the individual SD rats. In both groups, middle-aged and old, LDH data from one individual rat (in the following called middle-aged and old SD rat 3) had to be eliminated to obtain meaningful data (for details see Supplementary Figures 5-2 and 5-3). Because of this behavior middle-aged and old SD rat 3 were also excluded from proteome analysis.

The analysis of the remaining data showed a trend towards increased LDH leakage in middle-aged and old PRH after stress induction (Figure 5-3). Only in old PRH 1 h after hydrogen peroxide treatment the LDH activity was reduced compared to the untreated control.

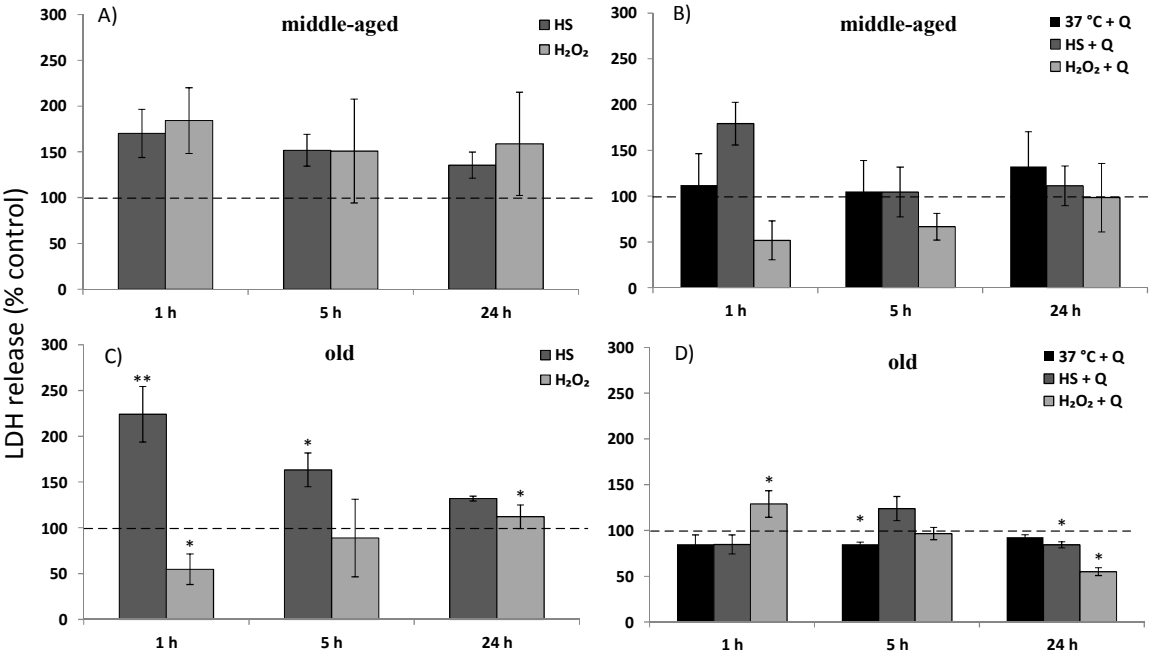

Figure 5-3: LDH release of two A) primary hepatocytes from middle-aged Sprague Dawley rats under heat stress and H_2O_2 stress related to untreated control, B) primary hepatocytes from middle-aged Sprague Dawley rats after 4 h pre-incubation with 50 µM quercetin in relation to the corresponding untreated and treated cells, C) primary hepatocytes from old Sprague Dawley rats under heat stress and H_2O_2 stress related to untreated control and D) primary hepatocytes from old Sprague Dawley rats after 4 h pre-incubation with 50 µM quercetin in relation to the corresponding untreated and treated cells. Error bars indicate standard deviation (N=2, n=6). The dashed lines represent the respective control. Statistical significance was determined with student's t-test. *, ** and *** indicate significance at p=0.05, p=0.01 and p=0.001. All results were correlated to the living cell number after 1 h, 5 h and 24 h of cultivation determined using calcein AM staining. Abbreviations: HS: heat stress; Q: quercetin.

The effect of pre-treatment with quercetin differed between the age groups (Figure 5-3 B/D). Because of the high standard deviations, it is difficult to draw a clear conclusion. Nonetheless, the obtained data showed meaningful trends which stand in accordance with the results generated in previous studies. In PRH from middle-aged SD rats, quercetin pre-treatment caused an increased LDH leakage in cells under heat stress conditions. In hydrogen peroxide treated cells the influence of quercetin was more beneficial, resulting in a lower LDH release. Contrary to middle-aged cells, in hepatocytes from old SD rats, quercetin treatment showed a time-dependent decrease in LDH leakage. However, the LDH activity in cells under hydrogen peroxide stress first increased at 1 h before significantly decreasing again over the cultivation time.

5.2.2 Influence of oxidative stress and quercetin antioxidant treatment on protein oxidation and the activity of antioxidant enzymes of primary hepatocytes from middle-aged and old Sprague Dawley rats

The content of protein carbonyl was measured as a marker for oxidative damage to macromolecules. Under control conditions, the protein oxidation state of hepatocytes from middle-aged SD rats was relatively stable over the whole cultivation period (Supplementary Figure 5-4). The protein carbonyl content in PRH from old SD rats was overall higher than in middle-aged PRH and showed in addition a drastic increase over time, indicating a high level of oxidative stress under control conditions. The influence of the addition of exogenous stress and antioxidant treatment with quercetin is depicted in Figure 5-4.

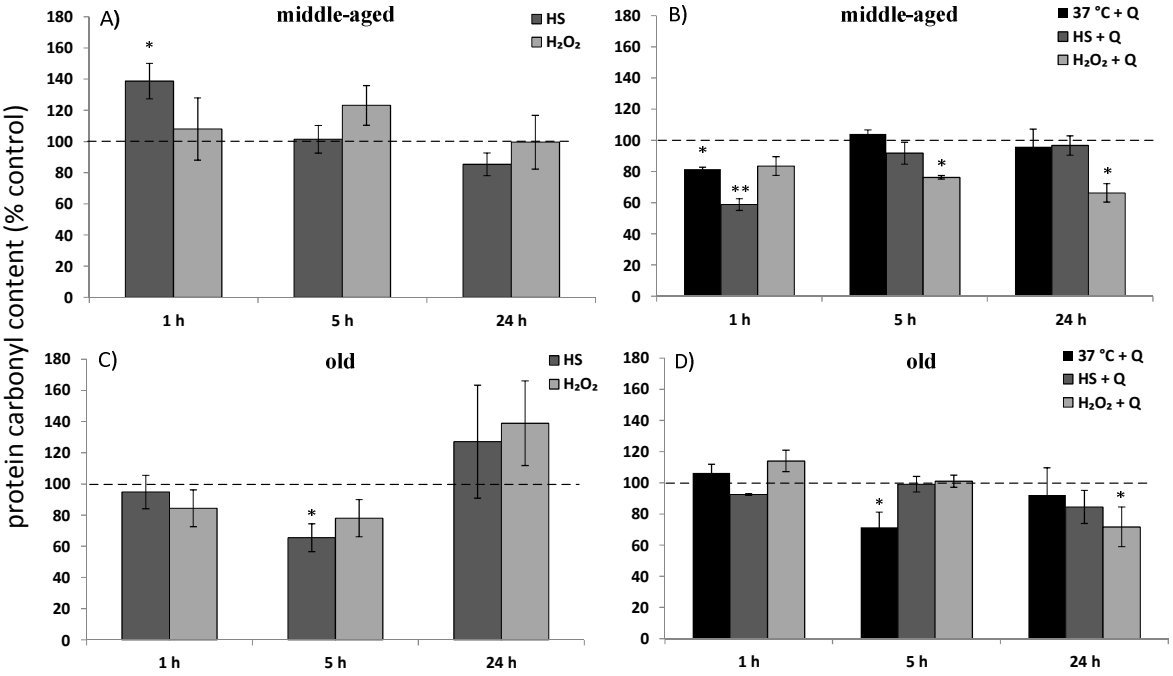

Figure 5-4: Protein carbonyl content of A) primary hepatocytes from middle-aged Sprague Dawley rats under heat stress and H_2O_2 stress related to untreated control, B) primary hepatocytes from middle-aged Sprague Dawley rats after 4 h pre-incubation with 50 µM quercetin in relation to the corresponding untreated and treated cells, C) primary hepatocytes from old Sprague Dawley rats under heat stress and H_2O_2 stress related to untreated control and D) primary hepatocytes from old Sprague Dawley rats after 4 h pre-incubation with 50 µM quercetin in relation to the corresponding untreated and treated cells. Error bars indicate standard deviation (N=3, n=9). The dashed lines represent the respective control. Statistical significance was determined with student's t-test. *, ** and *** indicate significance at p=0.05, p=0.01 and p=0.001. All results were correlated to the living cell number after 1 h, 5 h and 24 h of cultivation determined using calcein AM staining. Abbreviations: HS: heat stress; Q: quercetin.

Heat treatment caused an increase in protein oxidation in PRH from middle-aged SD rats directly after the induction of stress (Figure 5-4 A). 24 h after heat stress, the protein oxidation was lower than under control conditions which confirms the observations made in previous studies (Wistar rats, Chapter 4). Hydrogen peroxide treatment showed no significant effect on middle-aged PRH but showed a trend towards an increased carbonyl content. The treatment of PRH with quercetin resulted in a reduction of protein oxidation in both middle-aged and old cells (Figure 5-4 B/D). However, the effect was more pronounced in middle-aged than old PRH and occurred already 1 h after stress induction whereas old PRH expressed a beneficial reaction to quercetin only after 24 h.

In addition to the measurement of the protein oxidation as a marker for oxidative stress, it was examined if there are age-dependent differences in the way the activities of the endogenous antioxidant enzymes catalase and superoxide dismutase were influenced by oxidative stress. Interestingly, age had no influence on the catalase activity in primary hepatocytes from SD rats (Supplementary Figure 5-5). Catalase activity was on the same constant level over the whole cultivation period in both middle-aged and old PRH. Additionally, catalase activity was stable under all stress conditions and antioxidant treatment in middle-aged and old PRH (Supplementary Figure 5-7).

Superoxide dismutase activity is much more susceptible to age- and oxidative stress-related changes than catalase activity. In cultures under control conditions SOD activity in hepatocytes from old SD rats was significantly higher than in middle-aged SD rats (Supplementary Figure 5-6). These results are in accordance with the results from the extracellular SOD content in the supernatant from middle-aged and old Wistar rats analyzed with DIGE and MALDI ToF MS/MS (see Chapter 3). The influence of oxidative stress by heat and hydrogen peroxide treatment on SOD activity in PRH from middle-aged rats did not follow a clear trend (Figure 5-5 A). The obtained data, however, suggests a slight increase in SOD activity due to oxidative stress treatment. In contrast, PRH from old rats responded to heat and H_2O_2 with a significant increase of about 60% in SOD activity after 24 h but showed no changes within the first 5 h of the cultivation (Figure 5-5 C). Pre-treatment with quercetin caused a reduction of SOD activity in untreated and heat-treated middle-aged PRH at 5 h and 24 h. Contrary, the activity slightly increased in cells treated with H_2O_2. In PRH from old SD rats the most pronounced effect of quercetin was a significant increase of SOD activity at 24 h in untreated control cells. The reduced SOD activity observed in middle-aged PRH after heat stress could not be observed in old PRH.

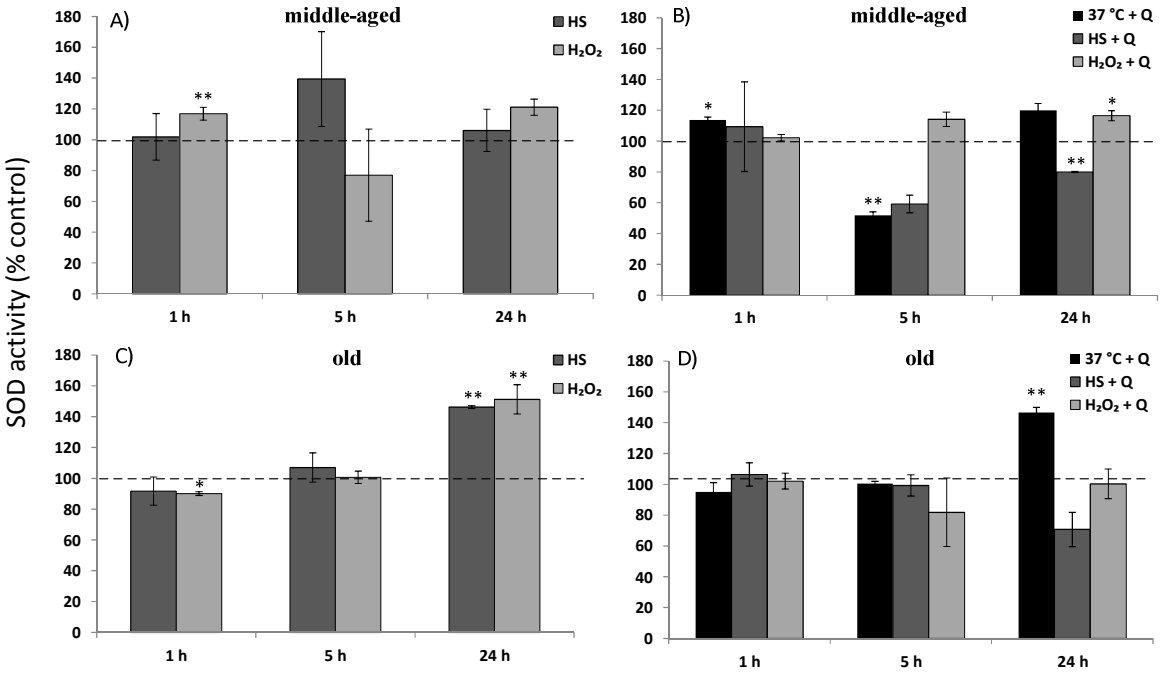

Figure 5-5: Superoxide dismutase activity of A) primary hepatocytes from middle-aged Sprague Dawley rats under heat stress and H_2O_2 stress related to untreated control, B) primary hepatocytes from middle-aged Sprague Dawley rats after 4 h pre-incubation with 50 µM quercetin in relation to the corresponding untreated and treated cells, C) primary hepatocytes from old Sprague Dawley rats under heat stress and H_2O_2 stress related to untreated control and D) primary hepatocytes from old Sprague Dawley rats after 4 h pre-incubation with 50 µM quercetin in relation to the corresponding untreated and treated cells. Error bars indicate standard deviation (N=3, n=9). The dashed lines represent the respective control. Statistical significance was determined with student's t-test. *, ** and *** indicate significance at p=0.05, p=0.01 and p=0.001. All results were correlated to the living cell number after 1 h, 5 h and 24 h of cultivation determined using calcein AM staining. Abbreviations: HS: heat stress; Q: quercetin.

5.2.3 Proteomic characterization of the influence of oxidative stress and quercetin antioxidant treatment on primary hepatocytes from middle-aged and old Sprague Dawley rats

The proteomic characterization of Sprague Dawley rats focused on the differences between the two age groups under control conditions and heat treatment. Intracellular protein extracts were cleaned from ionic detergents, salts, lipids and nucleic acids prior to 2-D gel electrophoresis using the ReadyPrep 2-D cleanup kit. Afterwards, the protein samples were concentrated and desalted with an ultrafiltration device with a MWCO of 10 kDa prior to 2-D gel electrophoresis. 2-D gel electrophoresis was executed as EZBlue-stained preparative gels for further identification with MALDI ToF MS/MS (Supplementary Figure 5-8) and as fluorescence-labeled DIGE gels for relative quantification. DIGE allows the comparison of two different conditions at a time. In the first experimental setup, the proteome of PRH from middle-aged and old SD rats was compared. Representative gels are shown in Figure 5-6.

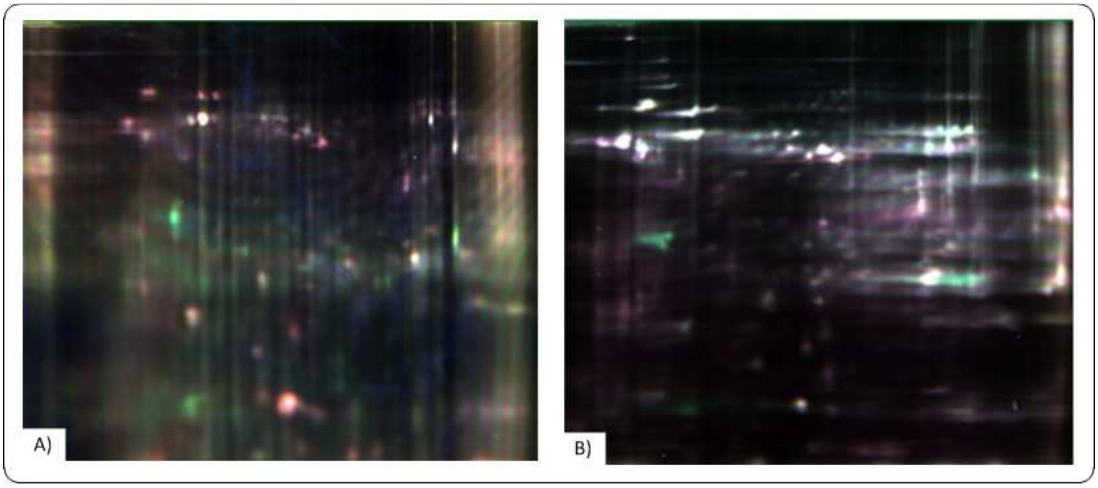

Figure 5-6: Overlay of representative DIGE gels (pH 3-10) showing differential protein abundance in the intracellular proteome of old Sprague Dawley PRH compared to middle-aged PRH. Proteome after A) 5 h of cultivation and B) 24 h of cultivation. Spots that are only present in middle-aged: green; old: red; same abundance: white; (N=2, n=6).

In total 80 protein spots were identified on the preparative gels (Supplementary Figure 5-8 and Table 5-1). For some proteins several isoforms were found, resulting in 62 different proteins. The identified proteins are involved in various biological processes like transporter acivity (GO:0006810), lipid metabolism (GO:0006629), catabolic processes (GO:0009056),

iron homeostasis (GO:0006879) and regulation of catalytic activity (GO:0050790). Almost a third of the identified proteins can also be associated with processes involved in aging (GO:0007568) and oxidative stress (GO:0006950).

When the intracellular proteomes of middle-aged and old PRH from SD rats were compared under control conditions (Figure 5-6), it was observed that many spots were red or green which indicates prominent differences in the proteomic profile of the two age groups. An average of 186 protein spots was detected on the fluorescent DIGE gels in the pH range 3-10. Statistical evaluation of the DIGE-gels revealed 63 significantly (≥ 1.5-fold) altered spots. These results compared with the alterations in hepatic functions indicate a stronger effect of heat stress on old hepatocytes than middle-aged ones and prove the basic applicability of the heat stress model to study oxidative stress.

The number of proteins identified with MALDI ToF/ToF from EZBlue-stained gels (80) was considerably less than the number of detected spots on DIGE gels (186). Hence, it can be assumed that some spots, which were identified as differentially expressed under oxidative stress, could not be identified. The main reason for this is the higher sensitivity of the fluorescent DIGE labeling compared to EZBlue staining. Additionally, MALDI ToF/ToF measurements revealed that several spots contained isoforms of the same proteins.

In Table 5-1, the results of the comparison of primary hepatocytes from middle-aged and old SD rats under control conditions are listed. From the 2-D gels 23 spots per gel could be assigned to differentially expressed spots on the according DIGE gels. For some proteins, like heat shock proteins, regucalcin, SOD and carbamoyl-phosphate synthase several isoforms were found. Shown are the averages of all isoforms of a single protein. In total we identified up to 15 (depending on time-point) differentially expressed proteins in old PRH under control conditions compared to the middle-aged PRH.

Table 5-1: Identified proteins with significantly different abundance in PRH from old Sprague Dawley rats cultivated at 37 °C after 1 h, 5 h and 24 h of incubation. The proteome of middle-aged PRH served as control to which the proteome of the old PRH was compared. Positive values indicate a higher abundance of the detected protein in old PRH compared to middle-aged PRH, whereas negative values indicate a lower abundance. Shown are the means of the fold change from the different gels (N=2, n=6). Abbreviations: Std.dev.=Standard deviation. Swiss- Prot database information (http://www.uniprot.org).

Swiss-Prot Accession no.	Protein	1h Fold change (Std. Dev.)	5 h Fold change (Std. Dev.)	24 h Fold change (Std. Dev.)
P06761	**78kDa glucose regulated protein**	3.66 (1.15)	3.47 (0.22)	2.12 (0.34)
P63039	**60 kDa heat shock protein, mitochondrial**	1.92 (0.36)	--	1.61 (0.28)
P63018	**Heat shock cognate 71 kDa protein**	1.91 (0.24)	2.68 (0.46)	2.59 (0.06)
P48721	**Stress-70 protein, mitochondrial (Hspa9)**	-1.81 (0.08)	--	--
P07756	**Carbamoyl-phosphate synthase**	-2.14 (0.21)	-2.21 (0.33)	-4.65 (1.32)
P04041	**Glutathione peroxidase 1**	2.35 (0.58)	2.87 (0.35)	3.68 (0.78)
P35704	**Peroxiredoxin-2**	2.59 (0.18)	3.21 (0.61)	3.02 (0.39)
P00481	**Ornithine carbamoyltransferase, mitochondrial**	-2.71 (0.18)	-3.80 (0.29)	-3.92 (0.14)
P10860	**Glutamate dehydrogenase**	1.77 (0.01)	--	--
P02650	**Apolipoprotein E**	3.78 (0.97)	5.69 (1.78)	4.36 (0.67)
Q64380	**Argininosuccinate synthase**	--	-1.62 (0.56)	-1.81 (0.32)
P41562	**Isocitrate dehydrogenase, cytoplasmic**	--	1.81 (0.04)	1.91 (0.15)
P10719	**ATP synthase**	-1.96 (0.36)	-2.56 (0.03)	-2.12 (0.16)
Q03336	**Regucalcin**	-1.69 (0.17)	-2.63 (0.46)	-3.12 (0.11)
P07632	**Superoxide dismutase [Cu-Zn]**	1.56 (0.31)	2.43 (0.05)	2.74 (0.13)

Most of the detected proteins are directly or indirectly related to oxidative stress, aging or age-related diseases. Interestingly, old PRH showed a higher abundance in heat shock proteins compared to middle-aged PRH. Heat shock proteins play an important role in the heat shock response which consists of the induction of gene expression of proteins like chaperones, proteases and antioxidant enzymes, essential for maintenance of cell homeostasis counteracting heat stress related damage (Mustafi et al., 2009). In this context, HSPs function as molecular chaperones, initiating the refolding or degradation of stress-damaged proteins, thus protecting cells from potential damaging effects. Therefore, this increase in HSP expression is highly surprising, considering the overall reduced hepatic function in older hepatocytes compared to middle-aged PRH (see Chapter 5.2.1 and 5.2.2). In total, three proteins from the HSP70 family and HSP60 were altered. The highest differences in abundance were detected for the two cytoplasmic HSPs (78 kDa glucose regulated protein, heat shock cognate 71 kDa protein), whereas the mitochondrial HSP60 and Hspa9 had a lower and less long-lasting increase in abundance. Furthermore, the abundance of enzymes related to oxidative stress was significantly increased in hepatocytes from old SD rats. Superoxide dismutase [Cu/Zn] was more than 2-fold increased over the whole cultivation period. Glutathione peroxidase and peroxiredoxin-2, both enzymes responsible for the reduction of hydrogen peroxide to water, even showed an increase in abundance over the cultivation time (up to 4-fold and 3-fold). The lipid transport protein apolipoprotein E showed the overall highest increase in protein abundance in the comparison between the age groups. After 5 h of cultivation, ApoE expression was almost 6-fold higher in old PRH. The regucalcin expression was also increased in old PRH and showed an additional increase over time (+1.6-fold at 1 h and +3.1 at 24 h). Contrarily, the abundance of several enzymes involved in the urea cycle was lower than in middle-aged PRH. Carbamoyl-phosphate synthase and ornithine carbamoyltransferase showed the largest decrease in abundance (-4.7-fold and -3.9-fold). The abundance of ATP synthase was also 2-fold lower in old PRH compared to middle-aged PRH.

When the intracellular proteomes of middle-aged PRH under control and heat stress conditions were compared (Figure 5-7), it was observed that most spots were white which indicates a similar proteomic profile. Statistical analysis revealed only 8 significantly changed proteins in middle-aged primary hepatocytes due to heat stress (Table 5-2), confirming this assumption.

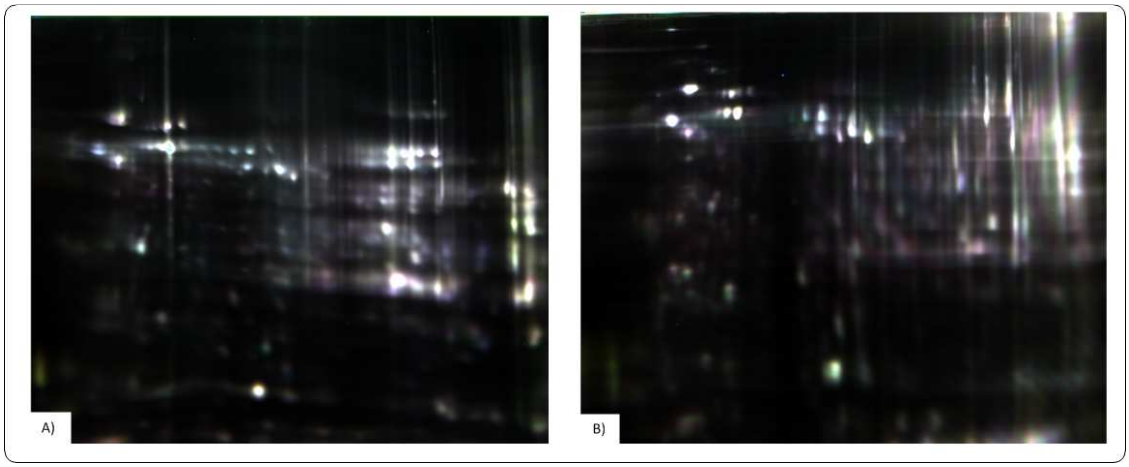

Figure 5-7: Overlay of representative DIGE gels (pH 3-10) showing differential protein abundance in the intracellular proteome of middle-aged Sprague Dawley PRH after heat exposure. Comparison between control (37 °C) and heat-stressed (42 °C) PRH samples after (A) 5 h of cultivation and (B) 24 h of cultivation. Spots that are only present in control: green; heat-stressed: red; same abundance: white; (N=2, n=6).

Table 5-2: Identified proteins with significantly different abundance in PRH from middle-aged Sprague Dawley rats after heat treatment (42 °C) after 1 h, 5 h and 24 h of incubation. The proteome of middle-aged PRH under control conditions served as control to which the proteome of the heat-stressed PRH was compared. Positive values indicate a higher abundance of the detected protein in middle-aged heat-stressed PRH compared to middle-aged control PRH, whereas negative values indicate a lower abundance. Shown are the means of the fold change from the different gels (N=2, n=6). Abbreviations: Std.dev.=Standard deviation. Swiss- Prot database information (http://www.uniprot.org).

Swiss-Prot Accession no.	Protein	1h Fold change (Std. Dev.)	5 h Fold change (Std. Dev.)	24 h Fold change (Std. Dev.)
P63039	**60 kDa heat shock protein, mitochondrial**	1.94 (0.02)	2.18 (0.21)	2.01 (0.05)
P06761	**78kDa glucose regulated protein**	1.98 (0.26)	2.04 (0.17)	2.18 (0.12)
P63018	**Heat shock cognate 71 kDa protein**	1.64 (0.14)	2.22 (0.07)	2.12 (0.07)
P48721	**Stress-70 protein, mitochondrial**	1.88 (0.10)	1.52 (0.14)	--
P07632	**Superoxide dismutase [Cu-Zn]**	--	1.69 (0.08)	--
P11884	**Aldehyde dehydrogenase**	-1.66 (0.02)	--	--
P10719	**ATP synthase**	1.89 (0.11)	1.69 (0.13)	--
P00884	**Fructose bisphosphate aldolase B**	--	1.78 (0.35)	--

Primary hepatocytes from middle-aged Wistar rats exhibited no alterations in the secretome due to heat stress (see Chapter 3). It is not surprising that most of the detected proteins with a change in abundance in middle-aged Sprague Dawley PRH were heat shock proteins (Table 5.2). Their abundance was 1.6-fold to 2-fold increased after heat treatment and further increased over time. SOD expression increased slightly after 5 h of cultivation, whereas other antioxidant enzymes were not significantly altered. ATP synthase and fructose bisphosphate aldolase B were significantly increased up to 5 h after heat treatment indicating an increased energy metabolism. Quantification of the changes in PRH from middle-aged SD rats revealed a noticeable time-dependent change in protein abundance. HSPs were increased over the whole cultivation period. All other influenced proteins came back to control levels after 24 h of cultivation.

When the intracellular proteomes of primary hepatocytes from old SD rats under control and heat stress conditions were compared (Supplementary Figure 5-9), the changes observed were much more pronounced than in PRH from middle-aged SD rats. Statistical analysis revealed only 18 significantly changed proteins in old primary hepatocytes due to heat stress at different time-points after heat treatment (Table 5-3). Strikingly, heat shock cognate 71 kDa protein was the only HSP significantly altered in its abundance due to heat stress in old PRH. During the cultivation period its abundance came back to control levels.

The abundance of enzymes related to oxidative stress was significantly increased due to heat stress in hepatocytes from old SD rats. Superoxide dismutase [Cu/Zn] was more than 2-fold increased 5 h and 24 h after treatment. Glutathione peroxidase and glutathione S-transferase, both enzymes responsible for the reduction of hydrogen peroxide to water, showed higher abundance over the cultivation time (up to 1.7-fold and 1.9-fold). The abundance of regucalcin increased over time, the expression of retinol-binding protein 4 decreased over time due to heat stress. These results are comparable to the changes in the secretome of old Wistar PRH (see Chapter 3). Actin, the only identified structural protein, was increased after heat stress in old hepatocytes up to 3.5-fold. On the proteomic level, expression of enzymes involved in the urea cycle (P07756, P09034) decreased in old PRH due to heat stress, whereas an enzyme involved in glycolysis (P00884) increased in abundance. ATP synthase abundance was decreased at 5 h and 24 h after heat stress. Old PRH already show a decreased ATP synthase abundance compared to middle-aged PRH. Ferritin, an enzyme responsible for cellular iron homeostasis, increased over time in old PRH up to 2.3-fold.

Table 5-3: Identified proteins with significantly different abundance in PRH from old Sprague Dawley rats after heat treatment (42 °C) after 1 h, 5 h and 24 h of incubation. The proteome of old PRH under control conditions served as control to which the proteome of the heat-stressed PRH was compared. Positive values indicate a higher abundance of the detected protein in old heat-stressed PRH compared to old control PRH, whereas negative values indicate a lower abundance. Shown are the means of the fold change from the different gels (N=2, n=6). Abbreviations: Std.dev.=Standard deviation. Swiss-Prot database information (http://www.uniprot.org).

Swiss-Prot Accession no.	Protein	1h Fold change (Std. Dev.)	5 h Fold change (Std. Dev.)	24 h Fold change (Std. Dev.)
P60711	**Actin, cytoplasmic 1**	1.61 (0.31)	2.57 (0.32)	3.55 (0.23)
P02650	**Apolipoprotein E**	--	-1.72 (0.11)	-2.3 (0.39)
Q8VIF7	**Selenium-binding protein 1**	1.91 (0.20)	1.52 (0.02)	--
P04041	**Glutathione peroxidase 1**	1.55 (0.23)	1.68 (0.21)	1.72 (0.06)
P63018	**Heat shock cognate 71 kDa protein**	--	1.76 (0.01)	--
P07632	**Superoxide dismutase [Cu-Zn]**	--	2.02 (0.31)	3.02 (0.28)
Q03336	**Regucalcin**	--	1.70 (0.15)	2.31 (0.10)
P04916	**Retinol-binding protein 4**	--	-2.21 (0.21)	-2.28 (0.04)
P11884	**Aldehyde dehydrogenase**	-1.81 (0.30)	-1.87 (0.22)	-1.85 (0.16)
P07756	**Carbamoyl-phosphate synthase**	--	-1.77 (0.03)	--
P04906	**Glutathione-S-transferase**	1.75 (0.21)	1.88 (0.35)	1.78 (0.11)
P09034	**Argininosuccinate synthase**	--	-1.67 (0.02)	--
Q64380	**Sarcosine dehydrogenase, mitochondrial**	--	--	1.63
P02793	**Ferritin light chain 1**	--	1.74 (0.14)	2.54 (0.23)
P19132	**Ferritin heavy chain**	1.69 (0.02)	1.77 (0.26)	1.95 (0.29)
P10719	**ATP synthase**	--	-1.56 (0.35)	-1.87 (0.19)
P00884	**Fructose bisphosphate aldolase B**	1.51 (0.28)	--	--
P02761	**Major urinary protein**	-1.59 (0.12)	-2.00 (0.33)	-2.30 (0.14)

In the following experiment, the influence of treatment of primary rat hepatocytes with 50 µM quercetin prior to heat stress on the proteome was analyzed (Supplementary Figure 5-10).
In Table 5-4, the results of the comparison of primary hepatocytes from middle-aged SD rats under heat stress conditions with and without pre-treatment with quercetin and old SD rats under control conditions are listed.

Table 5-4: Identified proteins with significantly different abundance in PRH from middle-aged Sprague Dawley rats after heat stress and pre-treated with 50 µM quercetin after 1 h, 5 h and 24 h of incubation. The proteome of middle-aged PRH under heat stress conditions (42 °C) served as control to which the proteome of the quercetin-treated PRH was compared. Positive values indicate a higher abundance of the detected protein in middle-aged quercetin-treated PRH compared to middle-aged heat-stressed PRH, whereas negative values indicate a lower abundance. Shown are the means of the fold change from the different gels (N=2, n=6). Abbreviations: Std.dev.=Standard deviation. Swiss-Prot database information (http://www.uniprot.org).

Swiss-Prot Accession no.	Protein	1h Fold change (Std. Dev.)	5 h Fold change (Std. Dev.)	24 h Fold change (Std. Dev.)
P63018	**Heat shock cognate 71 kDa protein**	-1.54 (0.05)	-3.07 (0.63)	-2.87 (0.32)
P63039	**60 kDa heat shock protein, mitochondrial**	-1.65 (0.17)	-1.97 (0.11)	-2.81 (0.49)
P48721	**Stress-70 protein, mitochondrial**	-1.91 (0.35)	-1.89 (0.27)	-2.12 (0.58)
P06761	**78kDa glucose regulated protein**	-2.03 (0.13)	-1.81 (0.06)	-1.99 (0.14)
P04785	**Protein disulfide-isomerase 1**	1.79 (0.03)	1.88 (0.23)	1.67 (0.07)
P04797	**Glyceraldehyde-3-phosphate dehydrogenase**	--	1.66 (0.28)	1.75 (0.36)
P04764	**Alpha-enolase**	--	1.56 (0.31)	1.55 (0.11)
P12928	**Pyruvate kinase PKLR**	-1.69 (0.33)	-1.64 (0.04)	-1.52 (0.26)
P00884	**Fructose bisphosphate aldolase B**	-1.69 (0.09)	-3.66 (1.12)	-3.62 (0.65)
P07756	**Carbamoyl-phosphate synthase [ammonia]**	1.66 (0.10)	1.58 (0.04)	1.91 (0.13)

From the 2-D gels 17 spots per gel could be assigned to differentially expressed spots on the according DIGE gels. For some proteins, like heat shock proteins, carbamoyl-phosphate synthase and alpha-enolase several isoforms were found. Shown are the averages of all isoforms of a single protein. In total we identified up to 10 (depending on time-point) differentially expressed proteins in quercetin pre-treated middle-aged PRH compared to PRH under heat stress without quercetin. These results suggest that quercetin treatment has a stronger effect on middle-aged PRH than heat stress itself. Quercetin treated cells exhibited a strong decrease in HSP expression over the whole cultivation time. In this experiment, no clear conclusion about the effect of quercetin treatment on glycolytic processes could be drawn. Pyruvate kinase and fructose bisphosphate aldolase were decreased up to 2-fold, however glyceraldehyde-3-phosphate dehydrogenase was increased in quercetin treated cells. Interestingly, quercetin treatment could not reverse the changes in protein expression due to heat stress in middle-aged PRH.

At last, the influence of treatment of old primary rat hepatocytes with 50 µM quercetin prior to heat stress on the proteome was analyzed (Supplementary Figure 5-10). From the 2-D gels 25 spots per gel could be assigned to differentially expressed spots on the according DIGE gels. For some proteins, like heat shock proteins, regucalcin, carbamoyl-phosphate synthase and alpha-enolase several isoforms were found. Shown are the averages of all isoforms of a single protein. In total we identified up to 16 (depending on time-point) differentially expressed proteins in quercetin pre-treated old PRH compared to PRH under heat stress without quercetin.

In Table 5-5, the results of the comparison of primary hepatocytes from old Sprague Dawley rats under heat stress conditions with and without pre-treatment with quercetin and old SD rats under control conditions are listed. Comparable to middle-aged PRH, quercetin treatment caused a decrease in HSP expression in hepatocytes of old rats. This result is interesting considering that heat treatment alone did not increase HSP abundance in old PRH. The abundance of heat shock cognate 71 kDa protein even decreased 5-fold after quercetin treatment. The only antioxidant enzymes influenced by quercetin were glutathione S-transferase (GST) and peroxiredoxin-6. GST was slightly decreased at 5 h and 24 h after the start of the cultivation. Contrary, peroxiredoxin-6 was strongly increased up to 3.5-fold. Contrary to middle-aged PRH, enzymes in glycolysis (P04797, P12928, P00884) clearly

decreased, whereas enzymes in the urea cycle (P20673, P07756) increased. All other influenced proteins behaved the same way as PRH from middle-aged cells.

Table 5-5: Identified proteins with significantly different abundance in PRH from old Sprague Dawley rats after heat stress and pre-treated with 50 µM quercetin after 1 h, 5 h and 24 h of incubation. The proteome of old PRH under heat stress conditions (42 °C) served as control to which the proteome of the quercetin-treated PRH was compared. Positive values indicate a higher abundance of the detected protein in old quercetin-treated PRH compared to old heat-stressed PRH, whereas negative values indicate a lower abundance. Shown are the means of the fold change from the different gels (N=2, n=6). Abbreviations: Std.dev.=Standard deviation. Swiss-Prot database information (http://www.uniprot.org).

Swiss-Prot Accession no.	Protein	1h Fold change (Std. Dev.)	5 h Fold change (Std. Dev.)	24 h Fold change (Std. Dev.)
P63018	**Heat shock cognate 71 kDa protein**	-2.02 (0.15)	-3.41 (0.36)	-5.11 (1.13)
P63039	**60 kDa heat shock protein, mitochondrial**	--	-1.69 (0.04)	-1.97 (0.18)
P48721	**Stress-70 protein, mitochondrial**	--	-1.79 (0.27)	-2.15 (0.36)
P06761	**78kDa glucose regulated protein**	-1.61 (0.07)	-1.53 (0.19)	-1.87 (0.11)
P04906	**Glutathione S-transferase**	--	-1.75 (0.21)	-1.78 (0.12)
P20673	**Argininosuccinate lyase**	1.67 (0.02)	1.68 (0.15)	1.54 (0.01)
P04797	**Glyceraldehyde-3-phosphate dehydrogenase**	-1.63 (0.08)	-1.88 (0.23)	-2.03 (0.14)
P07756	**Carbamoyl-phosphate synthase [ammonia]**	1.54 (0.03)	--	1.92 (0.22)
P12928	**Pyruvate kinase PKLR**	-1.69 (0.16)	-1.64 (0.03)	-1.76 (0.13)
P50137	**Transketolase**	-2.30 (0.44)	-1.78 (0.21)	--
P00884	**Fructose bisphosphate aldolase B**	-1.80 (0.17)	-2.11 (0.10)	-1.93 (0.08)
P48500	**Triosephosphate isomerase**	--	-1.53 (0.01)	-1.77 (0.12)
P04785	**Protein disulfide-isomerase 1**	1.79 (0.03)	1.88 (0.23)	1.67 (0.07)
Q03336	**Regucalcin**	--	-1.74 (0.05)	-1.93 (0.17)
P04764	**Alpha-enolase**	1.67 (0.09)	1.88 (0.20)	2.62 (0.38)
O35244	**Peroxiredoxin-6**	3.51 (0.34)	3.53 (0.41)	3.08 (0.09)

5.3 Discussion

In this study the effect of heat- and H_2O_2-induced oxidative stress on primary hepatocytes from middle-aged and old Sprague Dawley rats was analyzed. Additionally, the influence of the treatment with the ROS scavenging compound quercetin prior to heat stress was studied. The aim of the study was to evaluate the age-dependent alterations in the response to oxidative stress and the identification of intracellular protein targets for the prediction and diagnosis of ROS-induced cell aging. Quercetin was tested as a potential therapeutic candidate for the prevention of age-related diseases. The analysis of stress-induced alterations included the estimation of hepatic function (albumin and LDH), protein oxidation and the activity of the endogenous antioxidant enzymes SOD and catalase. The detailed characterization of the intracellular proteome alterations concentrated on the influence of heat stress and antioxidant effect of quercetin. Additionally, the proteomes of hepatocytes from middle-aged and old SD rats was compared at different cultivation time-points.

Albumin, normally used as a specific marker for liver function, was measured under all oxidative stress conditions and under antioxidant treatment (Chapter 5.2.1). The comparison of middle-aged and old PRH revealed an inherently higher albumin secretion of middle-aged hepatocytes over the whole cultivation period. These results are opposed to the albumin secretion profiles of Wistar rats, where old PRH showed a higher albumin secretion (Chapter 3). Furthermore, heat stress did not induce significant changes in albumin secretion in any of the age groups (Figure 5-2). However, treatment with 2 mM hydrogen peroxide caused a reduction of albumin secretion. All these data suggest that Sprague Dawley rats differ significantly from Wistar rats in their reaction to hyperthermia. Therefore, albumin can be considered a valid marker for hepatic function in SD PRH. The effect of quercetin pre-treatment on albumin secretion was especially strong in middle-aged PRH. Here, albumin measurements revealed a significant decrease under all conditions. In old PRH the effect was less pronounced and time-delayed. Nonetheless, quercetin was able to reduce the increased LDH leakage in oxidatively stressed hepatocytes (Figure 5-3). This paradoxical effect of quercetin treatment was already discussed in Chapter 4. Quercetin is an efficient ROS scavenger and protects macromolecules against oxidative damage. However, by doing that, quercetin is oxidized to cytotoxic pro-oxidants leading to LDH leakage (Boots et al., 2007; Halliwell, 2008). Additionally, oxidized quercetin is highly reactive towards thiol groups and

therefore toxic. Quercetin can form adducts in its oxidized form. Its targets are, e.g. proteins, but also glutathione resulting in a reduction of free glutathione levels (Boots et al., 2003). Hydrogen peroxide treatment, surprisingly, caused a decrease in LDH in old PRH. This observation is possibly not correlated to the actual LDH leakage but to the LDH activity which is known to be reduced by hydrogen peroxide treatment (Kendig & Tarloff, 2007). It can be speculated that middle-aged PRH did not exhibit this effect due to a faster metabolization of hydrogen peroxide. Quercetin treatment had a more beneficial effect on old PRH compared to middle-aged PRH regarding LDH leakage. The protein carbonyl content in old hepatocytes was significantly higher than in middle-aged PRH under control conditions (Supplementary Figure 5-4). This indicates a high basic stress level and a high degree of macromolecular damage in old PRH already under control cultivation conditions. Middle-aged PRH reacted to heat treatment the same way as already observed before (Chapters 3 and 4). After an initial increase in protein oxidation, the values decreased beneath the control level after 24 h (Figure 5-4). It was already speculated that these reduced values in oxidized proteins could be due to the HSP70 recovery system, as discussed in Chapter 3 (see Figure 3-8). HSPs function as molecular chaperones, initiating the refolding or degradation of stress-damaged proteins, thus protecting cells from potential damaging effects. This theory implies that middle-aged primary hepatocytes possess a potent defense mechanism against oxidative stress. Heat treatment, therefore, activates the expression of heat shock proteins leading to the degradation of oxidized proteins and, hence, an even better oxidation status than under control conditions. In this study, we could confirm this hypothesis with our obtained proteomic data (see following discussion on proteomic results). Interestingly, protein oxidation was reduced in old PRH 5 h after heat stress before increasing again after 24 h. This observation could also be related to the expression of heat shock proteins, as discussed later. Quercetin had a beneficial effect on both age groups resulting in a decreased protein carbonyl content.

The effect of oxidative stress on the activity of SOD and catalase was contradictory. Catalase activity was not susceptible to any kind of treatment in both age groups. However, SOD activity was unexpectedly high in old PRH compared to middle-aged PRH (Supplementary Figure 5-5). Heat treatment even further increased the activity after 24 h of cultivation. Compared to the previously discussed effects of heat stress on old PRH, this increase in the expression of SOD activity could be correlated to the reduced LDH leakage observed in old PRH after 24 h preventing loss of viability. Other studies confirm that SOD activity of

hepatocytes from 30 months old rats underwent increases in their specific enzyme activities as well as in their mRNA compared to 6 months old Wistar rats (Sanz et al., 1997). Middle-aged PRH reacted to oxidative stress with only slight changes in SOD activity. In case of SOD activity, quercetin treatment had no beneficial effect on primary hepatocytes from old and middle-aged rats. Activity was reduced under oxidative stress conditions.

The following part of the study concentrated on the proteomic characterization of age-dependent alterations in response to oxidative stress.

First, we investigated the differences in protein abundance between primary hepatocytes from middle-aged and old SD rats. Interestingly, old PRH showed a high abundance in heat shock proteins compared to middle-aged PRH (Table 5-1). Especially the two identified cytosolic HSPs were more than 3-fold more abundant whereas mitochondrial Hspa9 was even slightly lower. These observations could possibly be an indication for a high basic oxidative stress level and hence, oxidative damage to proteins which is counteracted by the HSP70 system. However, reduced albumin production and higher LDH leakage of old PRH suggest that antioxidant defense mechanisms exhibit deficiencies in the protection against cellular damage. Previous studies showed that the continuous generation of ROS by mitochondria plays an important role in aging processes (see Chapter 1, mitochondrial theory of aging). During aging processes, oxidative damage to mitochondria accumulates resulting in an impairment of mitochondrial redox homeostasis (Starkov, 2008). Decreased mitochondrial HSP abundance could indicate such a dysfunction of mitochondria. In this case, also a high abundance of cytosolic HSPs would not be sufficient to counteract oxidative damage to proteins. Furthermore, DIGE quantification only provides information about the abundance of a protein not about their condition. In aged cells, damaged and non-functional proteins tend to accumulate due to impaired proteasome functionality (Grune et al., 2001). Therefore, part of the higher abundance of HSPs could be due to damaged proteins which can no longer function as chaperones.

Primary hepatocytes also showed drastically higher abundances in several antioxidant enzymes (SOD [Cu-Zn], peroxiredoxin, glutathione peroxidase). These results imply that the expression of antioxidant enzymes increases with age but is still insufficient to compensate the highly increased generation of ROS, resulting in oxidative injury (Hung et al., 2003). Another protein involved in antioxidant defense mechanisms is apolipoprotein E. The

expression of ApoE was, similar to the antioxidant enzymes, significantly increased. In addition to its important role in the transport and metabolism of lipids, apolipoprotein E protects cells against hydrogen peroxide (Miyata & Smith, 1996; Tarnus et al., 2009) oxidative modifications of lipoproteins (Qin et al., 1998).

Regucalcin (also known as SMP-30, senescence marker protein 30) decreased in aged hepatocytes from SD rats. It is known that a decrease in SMP-30 causes inflammation and elevated levels of oxidative stress due to its importance for the vitamin C biosynthesis pathway (Kondo & Ishigami, 2016). Regucalcin deficiency is suspected to cause glucose intolerance, impaired lipid metabolism and elevated carbonylation of proteins (Sato et al., 2014). The comparison of the proteome from middle-aged and old SD rats also revealed significant changes in metabolic pathways due to aging. ATP synthase was strongly decreased, indicating a deficiency in energy metabolism in aged cells. The influence of aging was most pronounced in the urea cycle. The urea cycle is the main pathway for the detoxification of ammonia, consisting of five enzymes: carbamoyl phosphate synthetase, ornithine carbamoyltransferase, argininosuccinate synthase, argininosuccinate lyase and arginase-1. In our study, all five enzymes could be identified with MALDI ToF MS/MS. Three of the enzymes were significantly decreased in abundance in old PRH. The possible intracellular implications of these deficiencies are illustrated in Figure 5-8.

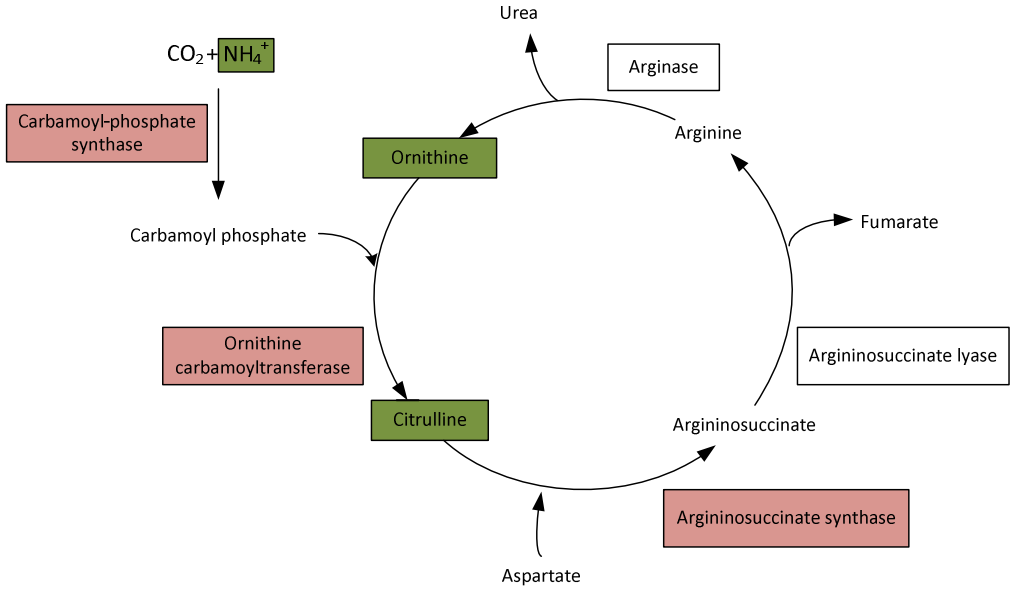

Figure 5-8: Influence of aging on the urea cycle; red: enzymes with decreased abundance in primary hepatocytes from old SD rats compared to middle-aged rats; white boxes: unaffected enzymes; green: intermediates accumulating due to enzyme deficiency.

First of all, carbamoyl-phosphate synthase deficiency in urea cycle causes an accumulation of toxic ammonia leading to a loss of viability. Interestingly, ammonia is reported to increase SOD activity (Prestes et al., 2006). This could partly explain the high SOD activity in old PRH compared to middle-aged PRH. Ornithine carbamoyltransferase deficiency causes an accumulation of ornithine which induces lipid oxidative damage (Zanatta et al., 2015). Argininosuccinate synthase deficiency results in an accumulation of citrulline which impairs cellular antioxidant response (Prestes et al., 2006). All these results demonstrate the highly impaired redox state and antioxidant defense mechanisms due to aging.

The next part of the study included the induction of endogenous oxidative stress in middle-aged and old primary rat hepatocytes via heat stress. As expected (see also Chapter 3), PRH from middle-aged SD rats showed only a few changes in protein abundance due to heat stress. Expression of HSPs increased strongly over the whole cultivation period (Table 5-2) indicating the activation of the HSP70 recovery system. These increases in abundance explain the reduced protein oxidation 24 h after heat treatment in middle-aged PRH (Figure 5-4). Increased ATP synthase and fructose bisphosphate aldolase B suggest that cells under heat stress conditions have a slightly higher energy demand. Superoxide dismutase was the only antioxidant enzyme with an altered abundance due to heat stress. SOD increased slightly after 5 h and came back to control levels at 24 h. These data correlate also with the SOD activity measured in middle-aged PRH (Figure 5-5 A).

The analysis of heat stress induced changes in the protein abundance of old hepatocytes (Table 5-3) revealed that they were much more susceptible to oxidative stress than middle-aged PRH. Interestingly, heat shock cognate 71 kDa protein was the only altered HSP. After 5 h of cultivation the expression was back to control levels. Actin expression was also significantly increased indicating the formation of actin stress fibers in the cytoplasm which is typical in aging cells (Doshi et al., 2010). The higher abundance in regucalcin as a biomarker for senescence is an indication for a strong decline in cellular function in old PRH due to heat stress. The increased abundance of antioxidant enzymes (SOD, glutathione S-transferase and glutathione peroxidase) and ferritin over the cultivation time (increase from 1 h to 24 h) could possibly be the reason for the decrease in cell death 24 h (see LDH, Figure 5-3) after heat stress. An upregulated ferritin biosynthesis prevents necrotic cell death (Omiya et al., 2009). The analysis also revealed changes in energy metabolism in old PRH due to heat stress. ATP

synthase decreased in abundance, whereas enzymes involved in glycolysis increased. Enzymes from urea cycle decreased. This is a trend already observed in old PRH compared to middle-aged PRH which is intensified by oxidative stress conditions.

The influence of the ROS-scavenging compound quercetin on primary hepatocytes of middle-aged and old rats under heat stress conditions was analyzed in the next part of the study.
These results suggest that quercetin treatment has a stronger effect on middle-aged PRH than heat stress itself. Quercetin treated cells exhibited a strong decrease in HSP expression over the whole cultivation time. In middle-aged PRH, quercetin treatment had a higher influence on protein abundance than heat stress itself (Table 5-4). The expression of all heat shock proteins was 1.5-fold to 3-fold decreased, whereas the effect intensified over the cultivation period. Quercetin was reported to inhibit the heat shock response. HSP expression is initiated by the binding of the transcription factor HSF1 (heat shock factor 1) to the heat-shock element in the promotor region of the HSP family (Jolly & Morimoto, 2000). Quercetin suppresses the heat shock response by inhibiting HSF1 (Nagai et al., 1995) which is compromising the beneficial antioxidant effect of quercetin as already discussed in Chapter 4. Nonetheless, quercetin treatment had beneficial effects on hepatocytes under heat stress conditions. Quercetin seems to decrease glycolysis related enzymes which reverses the effect of heat treatment. Reduced glycolytic activity could indicate that the energy demand of the cells came back to control levels due to quercetin. Additionally, protein disulfide isomerase showed an increase in abundance. It is known to protect cells against apoptosis (Ko et al., 2002) and could be involved in the protection mechanism of quercetin. In old hepatocytes treated with quercetin prior to heat stress, protein disulfide isomerase was also increased. Overall, old PRH exhibited clearly more signs of a beneficial effect of quercetin on the proteome than middle-aged PRH (Table 5-5). The antioxidant enzyme peroxiredoxin increased significantly in abundance. Enzymes involved in urea cycle increased in abundance allowing the detoxification of ammonia and reducing the accumulation of toxic intermediates. The increased anaerobic glycolytic activity was reversed in old PRH due to quercetin. *In vivo* studies showed a causality between the increase in anaerobic glycolytic activity and senescence (Guerrieri et al., 1994). However, quercetin induced a decreased HSP expression also in old PRH. Nonetheless, quercetin seems to have a regulating effect on heat-induced proteomic alterations resulting in cell survival and a reduction of oxidative damage.

6. Proteomic Characterization of Primary Mouse Hepatocytes in Collagen Monolayer and Sandwich Culture[1]

Abstract

Dedifferentiation of primary hepatocytes in vitro makes their application in long-term studies difficult. Embedding hepatocytes in a sandwich of extracellular matrix is reported to delay the dedifferentiation process to some extent. In this study, we compared the intracellular proteome of primary mouse hepatocytes (PMH) in conventional monolayer cultures (ML) to collagen sandwich culture (SW) after 1 day and 5 days of cultivation. Quantitative proteome analysis of PMH showed no differences between collagen SW and ML cultures after 1 day. Glycolysis and gluconeogenesis were strongly affected by long-term cultivation in both ML and SW cultures. Interestingly, culture conditions had no effect on cellular lipid metabolism. After 5 days, PMH in collagen SW and ML cultures exhibit characteristic indications of oxidative stress. However, in the SW culture the defense system against oxidative stress is significantly up-regulated to deal with this, whereas in the ML culture a down-regulation of these important enzymes takes place. Regarding the multiple effects of ROS and oxidative stress in cells, we conclude that the down-regulation of these enzymes seems to play a role in the loss of hepatic function observed in the ML cultivation. In addition, enzymes of the urea cycle were clearly down-regulated in ML culture. Proteomics confirms lack in oxidative stress defense mechanisms as the major characteristic of hepatocytes in monolayer cultures compared to sandwich culture.

[1] This chapter was adapted from "Proteomic characterization of primary mouse hepatocytes in collagen monolayer and sandwich culture" (Orsini et al., 2018) published in J. Cell. Biochem. 2018 Jan;119(1):447-454. doi: 10.1002/jcb.26202. Epub 2017 Jul 14. Dr. Saskia Sperber contributed equally to this work.

6.1 Introduction

The mammalian liver is an essential organ to maintain physiological body function. It is responsible for the synthesis of plasma proteins like albumin (Si-Tayeb et al., 2010), metabolic homeostasis, detoxification of ammonia via the urea cycle as well as synthesis of glutamine and alanine as non-toxic nitrogen containing compounds (Kuepfer, 2010). Most importantly, a wide range of endo- and xenobiotic compounds are metabolized by the liver (Gille et al., 2010). Cultured primary hepatocytes are not only used in pharmaceutical industry in drug metabolism studies, enzyme induction and hepatotoxicity, but they are also used to study molecular mechanisms involved in liver diseases and regeneration (Nussler et al., 2006), (Brulport et al., 2007), (Hohme et al., 2007), (Lilienblum et al., 2008), (Schug et al., 2008).

Dedifferentiation of primary hepatocytes in *in vitro* cultures is a well-known problem hindering long-term studies, which are necessary for e.g. *in vitro* drug toxicity testing (Alepee et al., 2014). There are several approaches to delay this dedifferentiation process, ranging from media optimization and co-cultivation with other liver cells to cultivation of hepatocytes in scaffolds of extracellular matrix (ECM) (Klingmuller et al., 2006), (Kostadinova et al., 2013), (Müller et al., 2014). Cultivation of hepatocytes in a sandwich of the extracellular matrix protein collagen (SW) is one of these approaches. Cultivation of primary hepatocytes in collagen SW culture leads to improved hepatic functions such as albumin and urea production and activity of CYP enzymes (Iredale & Arthur, 1994). Morphologically, hepatocytes cultivated in the SW configuration regain a more *in vivo* like structure compared to hepatocytes cultivated as standard monolayers (ML). In addition, the SW cultivation method is known to lead to changes in gene expression (Dunn et al., 1992), (Schug et al., 2008). However, proteome changes do not necessarily correlate with the transcriptomic changes (Slany et al., 2010), (Altelaar et al., 2013). This can be due to differences in synthesis rates and half-lives of mRNA and proteins, phenotypic modifications of proteins, e.g. numerous post-translational modifications, interaction of proteins with other proteins or molecules as well as the subcellular distribution of these (Diamond et al., 2006). As such, the proteome is closer connected to the actual phenotype than the transcriptome.

In this study we used 2-D DIGE and MALDI ToF MS/MS to analyze the intracellular proteome of primary mouse hepatocytes (PMH) cultivated in collagen SW and ML cultures. In 2-D gel electrophoresis proteins were separated in the first dimension based on the

isoelectric point (pI). The separation in the second dimension is based on the molecular weight of the protein. Matrix assisted laser desorption/ionization time of flight mass spectrometry (MALDI Tof MS/MS) was then used to identify the respective proteins based on the mass of derived peptides. The technique of differential gel electrophoresis (DIGE) was established by the lab of Jon Minden (Unlü et al., 1997). The proteins of the samples are labeled with fluorescent dyes and an internal standard consisting of a mixture of all samples, also labeled with a fluorescent dye. Two samples and the internal standard were then run on the same gel, enabling a direct quantitative comparison of the protein samples. Our results show, that on a proteomic level, PMH in collagen SW culture are closer to the *in vivo* phenotype than in ML culture, but still show signs of dedifferentiation.

6.2 Results

The intracellular proteome of primary mouse hepatocytes in monolayer and sandwich culture was compared one day and five days after the start of the experiment (Figure 6-1). The experimental phase started after 24 h of cultivation because the polarized status of the cells is known to be lost during the isolation process (LeCluyse et al., 1994; Vinken et al., 2006) and gained again during the first 24 hours of cultivation in the collagen sandwich culture.

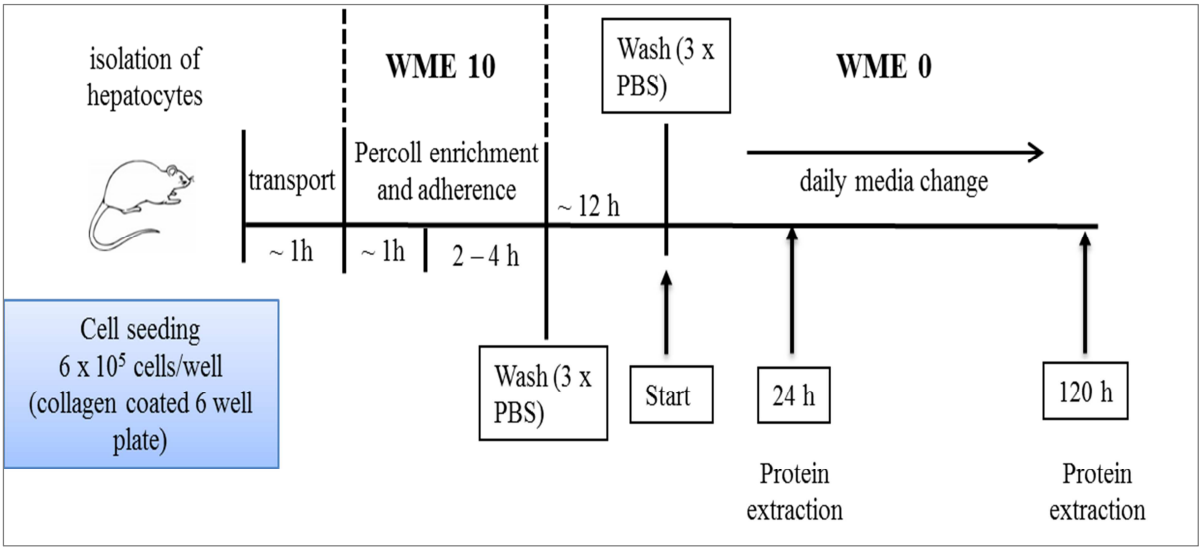

Figure 6-1: Experimental setup of the proteomic characterization of primary mouse hepatocytes in collagen monolayer and sandwich culture. The intracellular proteome was extracted 1 and 5 days after the start of the experiment.

The samples were purified and proteins further concentrated before 2-D gel electrophoresis. 2-D gel electrophoresis was accomplished in two variants: First as preparative EZBlue-stained gels to separate proteins for further identification with MALDI ToF MS/MS (Supplementary Figure 6-1 - 6-4–. In total 91 protein spots were identified on the preparative 2-D Coomassie-stained gels (Supplemetary Figure 6-5 and Supplementary Table 6-1). The second variant was with fluorescent labeled proteins for quantification (2-D DIGE). DIGE enables a quantitative comparison between two different conditions at a time. In this experimental setup, all available conditions were compared to each other. The samples from monolayer cultures (ML) at day 1 (ML d1) were compared to sandwich cultures (SW) at day 1(SW d1), as well as

at day 5 (ML d5 & SW d5) for three individual mice. Representative gels are shown in Figure 6-2.

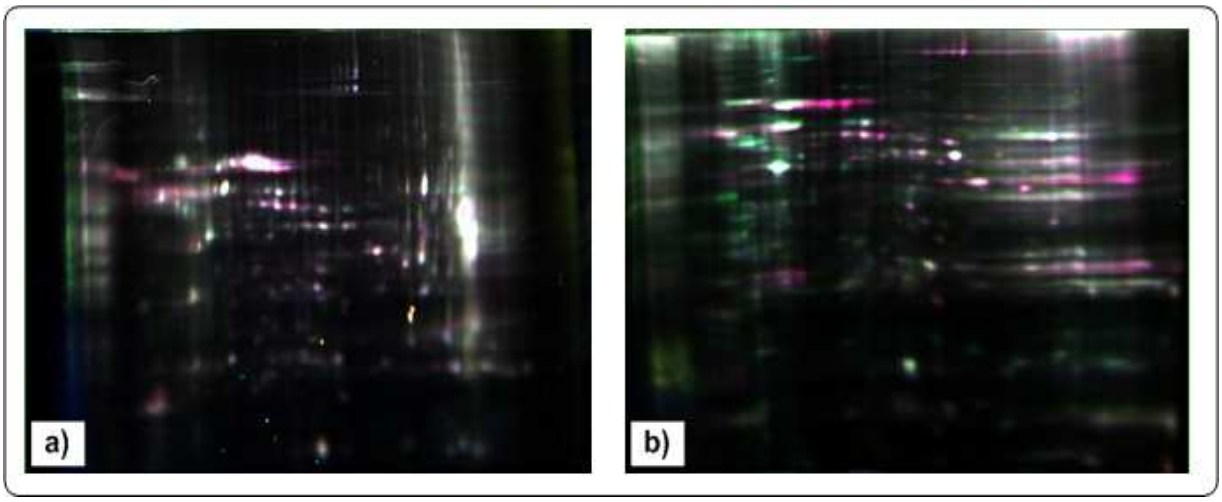

Figure 6-2: Overlay of representative DIGE gels showing differential protein abundance between PMH in collagen ML and SW culture. Comparison between samples at day 1 (ML d1/SW d1) (a) and at day 5 (ML d5/SW d5) (b). Spots that are only originating from the ML culture: green; SW culture: red; same abundance under ML and SW culture conditions: white; (n=3).

6.2.1 Influence of culture condition on the proteome (monolayer vs. sandwich culture)

When the intracellular proteomes of PMH in collagen SW and ML from day 1 of cultivation were compared to each other (Figure 6-2 a), it was observed that only few spots were only present in one of the conditions and most spots were white. This indicates a good overlap of the proteomic profiles. After statistical evaluation it was confirmed that there were no differentially expressed proteins 1 d after the start of the experiment. After 5 days of cultivation (Figure 6-2 b), clear differences between the two culture types were observed. Statistical evaluation of the DIGE-gels revealed 51 significantly altered spots.

The differentially expressed proteins, which were detected and quantified with DIGE, were identified with MALDI ToF MS/MS. To achieve this, the intracellular proteins were first separated with 2-D gel electrophoresis. The according spots on the gels were digested by trypsin and then identified using MALDI ToF MS/MS and a Swiss-Prot database search.

Using conventional 2-D gel electrophoresis with EZBlue staining of the protein spots, significantly less spots were detectable on the gels compared to the DIGE gels. This also implicated, that some spots, which were identified as differentially expressed under certain

conditions, could not be found on those gels. The major reason for this is the higher sensitivity, which is reached by using fluorescent dyes, as in DIGE, compared to EZBlue staining. Spot identification with MALDI ToF MS/MS showed that for some proteins, e.g. albumin, several isoforms could be found. In addition, only proteins are listed for which MALDI ToF MS/MS identification was clearly unequivocal. These two facts, in combination with the reduced sensitivity of EZBlue staining compared to fluorescence staining, explain, why the number of differentially expressed proteins identified with MALDI ToF MS/MS is significantly lower than with DIGE.

In Table 6-1, the results of the comparison of the expressed proteins at day 5 (ML d5/ SW d5) are listed.

Table 6-1: Identified proteins with significantly different abundance in PMH cultivated in collagen ML and SW culture after 5 days of incubation. The proteome of the ML culture served as control to which the proteome of the cells in SW culture was compared. Positive values indicate a higher abundance of the detected protein in the SW culture compared to the ML culture, whereas negative values indicate a lower abundance. Shown are the means of the fold change from the different gels (n=3). Abbreviations: Std. dev. = Standard deviation. Swiss-Prot database information (http://www.uniprot.org).

Swiss-Prot Accession no.	Protein	Fold change	Std. dev.	Protein function
Q03265	**ATP synthase**	-2.02	0.07	ATP formation (proton gradient)
P11588	**Major urinary protein**	-1.95	0.13	Male pheromone
Q64374	**Regucalcin**	-1.88	0.34	Calcium-binding protein; oxidative stress defense
P60710	**Actin**	-1.53	0.01	Cytoskeleton
P11725	**Ornithine carbamoyltransferase**	1.71	0.01	Urea cycle
Q91Y97	**Fructose-bisphosphate aldolase B**	1.82	0.19	Glycolysis and gluconeogenesis
P08226	**Apolipoprotein E**	2.45	1.09	Binding, internalization, and catabolism of lipoprotein particles and oxidative stress
P07724	**Serum albumin**	2.52	0.39	Main plasma protein produced by liver; ligand for macromolecules and for antioxidant defense

No significant (≥ 1.5-fold) differences were detected when PMH in collagen ML and SW culture were compared at day 1 (ML d1/ SW d1) of cultivation. From the 2-D gels 24 spots per gel could be assigned to differentially expressed spots on the according DIGE gels. For albumin, ATP synthase and actin several isoforms were found. In total we identified 8 differentially expressed proteins in PMH cultivated in ML compared to SW culture after 5 days of cultivation. The detected proteins covered different metabolic pathways such as the urea cycle, glycolysis and gluconeogenesis as well as the formation of ATP during oxidative phosphorylation. However, no proteins involved in TCA cycle were significantly changed in abundance (Supplementary Table 6-2). In addition to metabolic pathways, the cytoskeleton, Ca2+-signaling and pheromone production were concerned as well.

The amounts of major urinary protein, regucalcin and actin were clearly lower in the SW culture with the highest difference found for ATP synthase. Ornithine carbamoyltransferase, fructose-bisphosphate aldolase B, apolipoprotein E, on the other hand, showed a significantly higher abundance in the SW culture. The highest difference was found for serum albumin, which was more than twice as abundant as in the ML culture.

6.2.2 Influence of cultivation time in monolayer cultures on the proteome

In addition to the comparison of collagen SW and ML culture, incubation time influence on the protein expression in both cultivation conditions was analyzed by comparing samples from ML d1 with ML d5 and SW d1 with SW d5 (Figure 6-3 a and 6-3 b). Both DIGE gels revealed major differences in protein expression after visual inspection. One-way ANOVA and student's t-test ($p \leq 0.05$) confirmed that the duration of incubation has a strong influence on the intracellular proteome. In collagen ML culture 75 significantly altered spots could be detected.

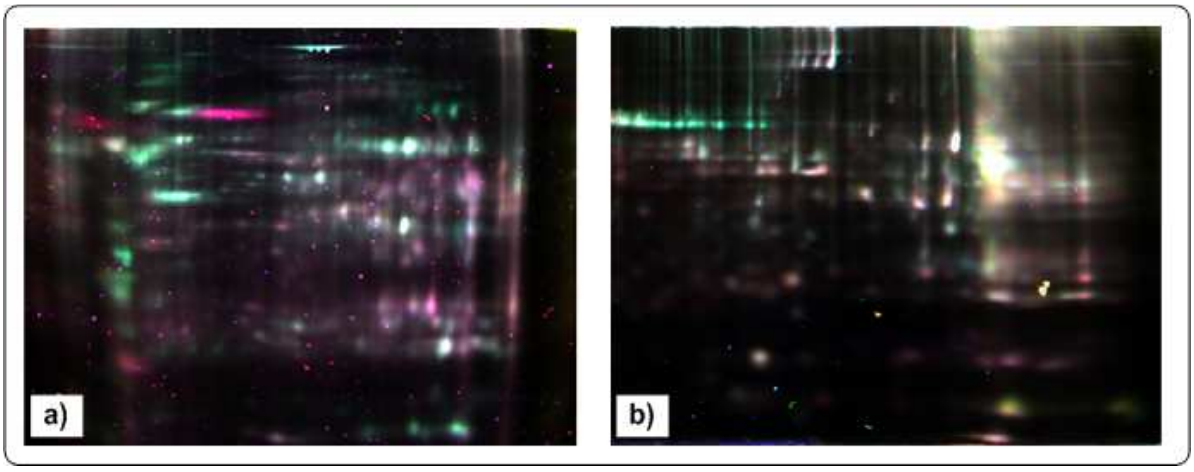

Figure 6-3: Overlay of representative DIGE-gels showing differential protein abundance of PMH in collagen ML and SW culture due to cultivation time. Comparison between ML samples from day 1 and day 5 (ML d1/ML d5) (a) as well as for SW day 1 and day 5 (SW d1/SW d5) (b). Spots that are only present at day 1: green; day 5: red; same abundance at day 1 and day 5: white; (n=3).

The results found for the comparison of day 1 and day 5 in collagen ML culture (ML d1/ ML d5) are listed in Table 6-2.

Table 6-2: Identified proteins with significantly different abundance in PMH cultivated in collagen ML culture after 1 and 5 days of incubation. The proteome of the ML culture at day 1 served as control to which the proteome of the cells of day 5 was compared. Positive values indicate a higher abundance of the detected protein at day 5 compared to day 1, whereas negative values indicate a lower abundance. Shown are the means of the fold change from the different gels (n=3). Abbreviations: Std. dev. = Standard deviation. Swiss-Prot database information (http://www.uniprot.org).

Swiss-Prot Accession no.	Protein	Fold change	Std. dev.	Protein function
P07724	**Serum albumin**	-5.07	1.10	Main plasma protein produced by liver; ligand for macromolecules and for antioxidant defense
P38647	**75kD glucose regulated protein**	-1.97	0.02	Binds estrogens, fatty acids and metals/heat shock or stress proteins
P17563	**Selenium-binding protein**	-1.91	0.29	Involved in Golgi transport, sensing of reactive xenobiotics
P30416	**Aldehyde dehydrogenase**	-1.81	0.28	Detoxification of alcohol-derived acetaldehyde
Q8C196	**Carbamoyl-phosphate synthase**	-1.77	0.14	Urea cycle
P13745	**Glutathione-S-transferase**	-1.75	0.04	Conjugation of reduced glutathione
P16460	**Argininosuccinate synthase**	-1.67	0.13	Urea cycle
Q99LB7	**Sarcosine dehydrogenase, mitochondrial**	-1.63	0.13	Reduction of electron transfer proteins
Q3SXD2	**Ferritin**	1.54	0.01	Iron storage
Q03265	**ATP synthase**	1.56	0.06	ATP formation (proton gradient)
Q01853	**Transitional ER ATPase**	1.69	0.14	Role in fragmentation of Golgi stacks
P11588	**Major urinary protein**	2.30	0.02	Pheromone binding protein

From the 2-D gels 34 spots per gel could be assigned to differentially expressed spots on the according DIGE gels. More than 1 spot were detected for albumin, ATP synthase and actin. In total we identified 12 differentially expressed proteins in PMH cultivated in ML culture after 1 and 5 days of cultivation. In this case as well, the detected proteins covered different

metabolic pathways like the urea cycle, detoxification as well as the formation of ATP during oxidative phosphorylation.

In addition to metabolic pathways, proteins involved in the cytoskeleton formation, serum protein production, iron storage, Golgi transport, oxidative stress and pheromone production were also affected. Specifically, Sarcosine dehydrogenase, argininosuccinate synthase, glutathione-S-transferase, carbamoyl-phosphate synthase, aldehyde dehydrogenase, selenium-binding protein and 75kD glucose regulated protein showed a significantly lower abundance after 5 days of cultivation in ML culture. Regucalcin expression was increased after 5 days of cultivation but not above our significance threshold (+ 1.42-fold). The highest difference was again found for serum albumin, which was reduced more than fivefold. Ferritin, ATP synthase and transitional ER ATPase were upregulated with increasing cultivation time. The highest increase was found for the major urinary protein, a male pheromone binding protein, which showed a two times higher abundance compared to the culture at day 1 after seeding.

Out of the found proteins, albumin, ATP synthase and the major urinary protein were detected as changed in the comparison of ML and SW culture at day 5 of cultivation as well. Not exactly the same enzymes of the urea cycle were detected in both approaches, but the urea cycle was a common target.

6.2.3 Influence of cultivation time in sandwich cultures on the proteome

The results found for the comparison of day 1 and day 5 in collagen SW culture (SW d1/ SW d5) are listed in Table 6-3.

From the 2-D gels 32 spots per gel could be assigned to differentially expressed spots on the according DIGE gels. More than one spot was detected for albumin, carbamoyl-phosphate synthase and ATP synthase. In total we identified 8 differentially expressed proteins in PMH cultivated in SW culture after 1 and 5 days of cultivation.

In this case as well, the detected proteins covered different metabolic pathways as the urea cycle, glycolysis and gluconeogenesis as well as the formation of ATP during oxidative phosphorylation.

Table 6-3: Identified proteins with significantly different abundance in PMH cultivated in collagen SW culture after 1 and 5 days of incubation. The proteome of the SW culture at day 1 served as control to which the proteome of the cells of day 5 was compared. Positive values indicate a higher abundance of the detected protein at day 5 compared to day 1, whereas negative values indicate a lower abundance. Shown are the means of the fold change from the different gels (n=3) and if more than 1 spot per protein was available (n=variable). Abbreviations: Std. dev. = Standard deviation. . Swiss-Prot database information (http://www.uniprot.org).

Swiss-Prot Accession no.	Protein	Fold change	Std. dev.	Protein function
P07724	**Serum albumin**	-3.08	1.06	Main plasma protein produced by liver; ligand for macromolecules and for antioxidant defense
Q8C196	**Carbamoyl-phosphate synthase**	-2.00	0.22	Urea cycle
P09103	**Protein disulfide-isomerase**	-1.83	0.06	Rearrangement of -S-S-–bonds in proteins
P13745	**Glutathione S-transferase**	1.71	0.12	Conjugation of reduced glutathione
Q03265	**ATP synthase**	1.71	0.24	ATP formation (proton gradient)
P08228	**Superoxide dismutase**	1.88	0.02	Destroys superoxide anion
P05064	**Fructose-bisphosphate aldolase**	1.90	0.18	Glycolysis and gluconeogenesis
Q64374	**Regucalcin**	2.00	0.04	Calcium-binding protein; oxidative stress defense

In addition to metabolic pathways serum protein production, Ca^{2+}-signaling, oxidative stress and protein rearrangement were also concerned. In contrary no proteins involved in lipid metabolism were significantly changed in abundance (Supplementary Table 6-2).

Glutathione S-transferase, ATP synthase, superoxide dismutase and fructose-bisphosphate aldolase showed a significantly higher abundance after 5 days of cultivation in SW culture with the highest difference found for regucalcin, which showed a two times higher abundance after 5 days. Protein disulfide-isomerase and carbamoyl-phosphate synthase were downregulated with increasing cultivation time. The highest decrease was found for the serum albumin, which showed a three times lower abundance compared to the culture at day 1 after seeding. ATP synthase, regucalcin, fructose-bisphosphate aldolase and serum albumin were also detected as differentially expressed in the comparison between SW and ML culture.

However, although not the same enzymes were found, urea cycle, which was differential in ML and SW culture after 5 days of cultivation, was also effected over time in the SW culture. However, in the case of regucalcin, we have to consider the relatively high standard deviation between the individual mice.

In both culture conditions we observed that after 5 days of cultivation ATP synthase, carbamoyl-phosphate synthase and serum albumin were differentially expressed with comparable abundance.

Table 5-5: Identified proteins with significantly different abundance in PRH from old Sprague Dawley rats after heat stress and pre-treated with 50 µM quercetin after 1 h, 5 h and 24 h of incubation. The proteome of old PRH under heat stress conditions (42 °C) served as control to which the proteome of the quercetin-treated PRH was compared. Positive values indicate a higher abundance of the detected protein in old quercetin-treated PRH compared to old heat-stressed PRH , whereas negative values indicate a lower abundance. Shown are the means of the fold change from the different gels (N=2, n=6). Abbreviations: Std.dev.=Standard deviation. Swiss- Prot database information (http://www.uniprot.org).

Swiss-Prot Accession no.	Protein	1h Fold change (Std. Dev.)	5 h Fold change (Std. Dev.)	24 h Fold change (Std. Dev.)
P63018	**Heat shock cognate 71 kDa protein**	-2.02 (0.15)	-3.41 (0.36)	-5.11 (1.13)
P63039	**60 kDa heat shock protein, mitochondrial**	--	-1.69 (0.04)	-1.97 (0.18)
P48721	**Stress-70 protein, mitochondrial**	--	-1.79 (0.27)	-2.15 (0.36)
P06761	**78kDa glucose regulated protein**	-1.61 (0.07)	-1.53 (0.19)	-1.87 (0.11)
P04906	**Glutathione S-tranferase**	--	-1.75 (0.21)	-1.78 (0.12)
P20673	**Argininosuccinate lyase**	1.67 (0.02)	1.68 (0.15)	1.54 (0.01)
P04797	**Glyceraldehyde-3-phosphate dehydrogenase**	-1.63 (0.08)	-1.88 (0.23)	-2.03 (0.14)
P07756	**Carbamoyl-**	1.54	--	1.92

	phosphate synthase [ammonia]	(0.03)		(0.22)
P12928	**Pyruvate kinase PKLR**	-1.69 (0.16)	-1.64 (0.03)	-1.76 (0.13)
P50137	**Transketolase**	-2.30 (0.44)	-1.78 (0.21)	--
P00884	**Fructose bisphosphate aldolase B**	-1.80 (0.17)	-2.11 (0.10)	-1.93 (0.08)
P48500	**Triosephosphate isomerase**	--	-1.53 (0.01)	-1.77 (0.12)
P04785	**Protein disulfide-isomerase 1**	1.79 (0.03)	1.88 (0.23)	1.67 (0.07)

6.3 Discussion

6.3.1 Influence of culture condition on the proteome (monolayer vs. sandwich culture)

In this study the intracellular proteome of primary mouse hepatocytes in collagen SW and ML culture was compared after 1 and 5 days of cultivation.

The concentration of ornithine carbamoyltransferase, which catalyzes the formation of L-citrulline from L-ornithine in the urea cycle, was about 70% higher in the SW culture. However, carbamoyl-phosphate synthase and argininosuccinate synthase, two other enzymes of the urea cycle, were down-regulated after 5 days of cultivation in ML. Interestingly, also in PMH cultivated in collagen SW carbamoyl-phosphate synthase was down-regulated after 5 days of cultivation. The formation of carbamoyl-phosphate and thereafter the formation of argininosuccinate represent the rate limiting steps of the urea cycle. However, the actual formation rate seems mostly limited by substrate availability and not by enzyme activity (Shambaugh, 1977). Since in both cultivation conditions the enzyme is down-regulated to about the same extent, other factors might play a role. These could involve post-translational modifications, leading to a lower activity of the enzymes, or a lower formation rate of ammonia. An example could be the acetylation status. SIRT5, a protein induced by oxidative stress, is known to lead to the deacetylation of carbamoylphosphate synthase, which is then activated (Nakagawa et al., 2009), (Bellei et al., 2011). The expression of actin was also influenced by the cultivation condition. The amount of the cytoskeletal protein was slightly lower (factor 1.53 in Table 1) in PMH cultivated in collagen SW at day 5 but no difference was seen at day 1. Actin could not be confirmed as differentially expressed with respect to

time of cultivation neither in SW nor in ML culture. Values might be slightly below the threshold ratio of 1.5. Therefore no clear conclusion could be drawn, if the protein was up-regulated in the ML culture or down-regulated in the SW culture. However, Beigel et al. showed that actin was up-regulated in primary rat hepatocytes cultivated in ML culture already after 48 h of cultivation (Beigel et al., 2008). This supports an up-regulation of the protein in PMH in collagen ML culture as well. The reason for this might be found in the differential distribution of actin in the cell. We showed in other studies (Sperber, 2016), that in SW culture actin was accumulated close to the cell-cell contacts, where bile canaliculi are formed. In the ML culture actin stress fibers were found throughout the cytoplasm. Stress fiber formation may therefore go along with increased actin production. The higher abundance in regucalcin in monolayer cultivation, as a biomarker for acute liver cell damage (Yamaguchi, 2014), is an indication for increased hepatocyte damage compared to the SW culture.

6.3.2 Influence of cultivation time on the proteome

In addition to the influence of the cultivation condition on the proteome, also the influence of the duration of the cultivation was analyzed.

It was shown that besides typical hepatic functions and cellular morphology also carbon and energy metabolism were affected. Fructose-bisphosphate aldolase, the glycolytic enzyme which catalyzes the split of fructose 1,6-bisphosphate into glyceraldehyde 3-phosphate and dihydroxyacetone phosphate, was up-regulated over time in the collagen SW culture. This enzyme does not catalyze an irreversible step in glycolysis and gluconeogenesis. This is why it cannot be said, whether glycolysis or gluconeogenesis activity were stimulated by this overexpression in PMH in SW culture. However, it gives us a strong hint, that these pathways may be affected. Thereby, enzymes catalyzing reversible steps of the respective pathways do not necessarily have to be altered regarding the total amount of their protein, but can also be strongly regulated by post-translational modification. However, the higher abundance in regucalcin after 5 days of sandwich cultivation is an indication for the suppression of gluconeogenesis. Regucalcin has been shown to inhibit fructose 1,6-diphosphatase activity which catalyzes an irreversible step of gluconeogenesis (Yamaguchi & Yoshida, 1985).

ATP synthase was up-regulated over time in SW and ML culture, but if the proteome was compared at day 5 of cultivation, the amount in the SW was lower compared to the ML culture. The most prominent effects were found with proteins dealing with oxidative stress. Reactive oxygen species (ROS) are constantly produced by aerobic metabolic processes such as respiration (Apel & Hirt, 2004). ROS cause oxidative damage to proteins, DNA, and lipids. Therefore, cells have devised defense systems, which prevent the formation of ROS or which repair the damage created by it (Halliwell, 1991). However, our results indicate that, with the exception of superoxide dismutase, no proteins directly scavenging free radicals are changed in abundance (Supplementary Table 6-2). In the ML culture proteins involved in oxidative stress defense were down-regulated, whereas in the SW proteins counteracting oxidative stress were up-regulated. PMH in collagen SW and ML culture seem to be confronted with oxidative stress. Regarding the multiple effects of ROS and oxidative stress in cells, one can assume that the down-regulation of these enzymes might also play a role in the loss of hepatic function observed in ML cultivation. Surprisingly, no changes of enzymes involved in phase I and II metabolism of xenobiotics were detected. Three proteins involved in xenobiotic metabolism, specifically bifunctional epoxide hydrolase 2, carboxylesterase 3A and alcohol dehydrogenase were identified, but showed no changes in abundance (Supplemetary Table 6-2). However, many other of these proteins are only weakly expressed and information on low abundant proteins are often lost on protein gels (Natarajan et al., 2009), (Beigel et al., 2008).
Overall, the most protein changes were induced by the cultivation in ML culture. Proteins involved in multiple pathways were concerned. The loss of hepatic function could be confirmed by this study. However, protein expression was also changed to a certain extent in PHM cultivated in collagen SW culture, although the changes were not as pronounced as in the ML culture. Still also in SW culture various pathways were affected. This is in accordance with the results gained by Farkas et al. with primary rat hepatocytes in collagen SW cultivation (Farkas et al., 2005). In that study it was shown, that also the secretome of primary hepatocytes is changed over time towards dedifferentiation. Other studies, which were conducted with primary rat hepatocytes found similar results for hepatocytes cultivated in ML over time, if the two cultivation methods were compared (Rowe et al., 2010), (Beigel et al., 2008). In these studies oxidative stress, cytoskeletal remodeling and glucose metabolism were identified as major disturbed pathways.

In conclusion, in collagen SW culture an increased abundance of proteins counteracting oxidative stress was seen at day 5. ML culture showed increased actin stress fiber formation and decreased activity in enzymes of the urea cycle. Overall, signs of dedifferentiation were stronger in the ML culture than in the SW culture. PMH in collagen SW culture retain *in vivo* function on the proteomic level that is at least in part linked to the observed stronger defense against oxidative stress, so far not studied on the proteomic level (Figure 6-4).

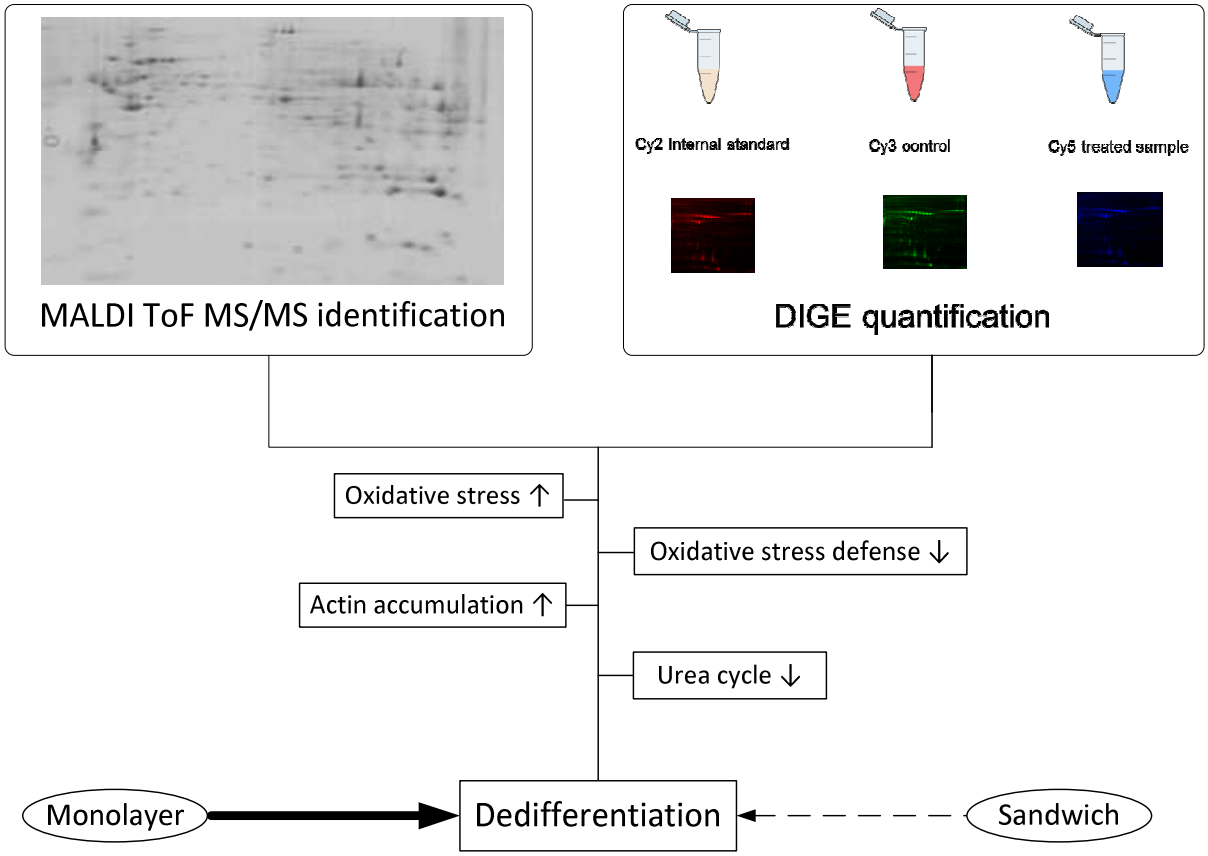

Figure 6-4: Graphical abstract of the proteomic analyses with primary mouse hepatocytes in collagen monolayer and sandwich culture. Hepatocytes in monolayer culture show more signs of dedifferentiation than in sandwich culture due to their deficiency in oxidative stress defense, actin accumulation and downregulation of the urea cycle.

ACKNOWLEDGMENTS

This presented research was funded by BMBF in the framework of the project Virtual Liver (contract grant number 0315738), the project OxiSys (contract grant number 031 5891 B), and the project Liver Systems Medicine (contract grant number 031L0051). We thank Annika Bohner for the isolation of the primary mouse hepatocytes. We thank Dr. Klaus Hollemeyer for technical support with MALDI ToF MS/MS and Prof. Karin Römisch for providing access to the Typhoon Trio Variable Mode Imager.

7. Summary and Outlook

Aging is an inevitable and progressive process which is defined by a decline of various cellular and physiological functions. The increasing human life span and the resulting increase in age-related diseases make aging research an interesting and necessary topic. *Reactive oxygen species* (ROS) are constantly generated in cells during metabolic processes. The "free radical theory of aging" (Harman, 1956) proclaims that ROS-induced macromolecular damage to DNA, proteins and lipids is the major factor responsible for aging and age-related diseases. There are various analytical approaches in aging research like proteomics, metabolomics and transcriptomics. The proteome is dynamic and therefore the ideal target for the analysis of qualitative and quantitative alterations during the aging process and in the development of age-related diseases. Especially, the liver proteome can give insights into a wide range of processes involved in protein secretion, metabolic homeostasis and xenobiotic detoxification. Therefore, we chose a liver model with heat treatment as a ROS source to analyze the influence of oxidative stress on the proteome of aged rats.

In the first part of this thesis (Chapter 3), the secretomes of primary hepatocytes from middle-aged and old Wistar rats were compared under oxidative stress conditions compared to control conditions. The secretome is easily accessible by taking blood samples and analyzing the serum proteins. Therefore, it is considered the first choice for biomarker discovery. Several liver-specific serum markers are already known. Therefore, enzymatic assays for monitoring albumin, AST and LDH are standard procedures in clinical and scientific analysis of liver function. The determination of the AST and LDH levels revealed that the PRH from old rats show impaired hepatic function already under control conditions. The addition of heat-induced oxidative stress resulted in significant cellular damage and elevated protein oxidation, a clear marker for macromolecular damage (Figure 3-2). Contrary to this observation we determined an increased albumin production in senescent PRH under control conditions (Figure 3-3). Elevated albumin levels could be a cellular mechanism to counteract the decrease in stress protein expression. In old PRH, the induction of heat stress resulted in a

further increase in albumin secretion demonstrating the impact of heat treatment as a source of oxidative damage.

PRH from middle-aged rats showed no signs of oxidative stress in the hepatic function or in the expression level of secreted proteins under heat stress conditions. The amount of protein carbonyls was even significantly decreased after heat treatment, an effect which was also observed in later studies (see Chapter 5) and which could be due to the HSP70 recovery sytem. These observations indicate impaired defense mechanisms against oxidative stress in aged cells. Quantifiying the secreted proteins confirmed a decrease in various proteins related to stress defense. The expression of retinol-binding protein 4 (RBP) is 2-fold decreased. It plays an important role in the modulation of the glucose metabolism. Transthyretin (TTR) stands in close relation to RBP. It is known that carbonylated TTR has a high affinity to form aggregates with RBP (Zhao et al., 2013). The decrease in abundance of free RBP and TTR in heat-stressed old rat hepatocytes could be due to the formation of such aggregates. Another protein with a reduced abundance was regucalcin. Regucalcin, also known as SMP-30 (senescence marker protein 30) was almost 3-fold decreased in aged hepatocytes, a phenomenon which is known to be associated with age-related inflammation and elevated levels of oxidative stress due to its importance for the vitamin C biosynthesis pathway (Kondo & Ishigami, 2016). Regucalcin deficiency is suspected to cause glucose intolerance and impaired lipid metabolism. Additionally, a decreased SMP-30 level results in an elevated carbonylation of proteins (Sato et al., 2014) causing further cellular damage and cell death. In contrast to the results discussed above, several other stress proteins (e.g. SOD, glutathione reductase, hemopexin) were increased in abundance, but are still insufficient to handle the vastly increased amount of ROS.

Regarding these results, proteomic analyses revealed several potential biomarkers in the hepatic rat secretome which could determine the risk of oxidative stress-dependent diseases. Therefore, the amount of regucalcin and the ratio of RBP/TTR are promising serum marker candidates for assessing the extent of oxidative injury in elderly patients and their long-term prognosis for age-dependent diseases. Future studies have to validate these biomarker candidates in the human model.

The second part of the thesis (Chapter 4) analyzed the influence of the antioxidant compounds N-acetylcysteine and quercetin on the cellular stress levels of middle-aged Wistar PRH and the hepatoma cell line *HepG2*. The aim of this research was to find an adequate antioxidant compound for our *in vitro* heat stress model.

Supplementation of exogenous antioxidants has become increasingly popular to improve health and prevent oxidative stress related chronic diseases and premature aging (Poljsak et al., 2013). However, the results generated in various studies range from a positive influence of antioxidants to no effect (Farouque et al., 2006) or even an adverse effect on prevention and treatment of the aforementioned diseases (Bardia et al., 2008; Sesso et al., 2008). Therefore, more research is needed to specify the impact of antioxidant treatment on aging and oxidative stress related diseases. Our study concentrated on the ROS scavenging polyphenol quercetin (3,3′,4′,5,7-pentahydroxyflavone) and the glutathione precursor N-acetylcysteine. Principal component analysis was used as a statistical tool to find variances in the experimental groups. It was revealed that Wistar rats show a high biological variance despite being an outbred rat stock. It was shown that the two individual middle-aged Wistar rats can be divided in low- and high- responders to oxidative stress. PRH from Wistar 1 would categorize as low-responders. Heat treatment provoked the activation of antioxidant defense mechanisms counteracting long-lasting damaging effects. Hydrogen peroxide treatment caused less pronounced effects. Quercetin pre-treatment supported these defense mechanisms, despite causing an increased LDH leakage. This paradoxical effect of quercetin was already discussed in previous studies (Boots et al., 2007; Halliwell, 2008). Quercetin is an efficient ROS scavenger and protects macromolecules against oxidative damage. However, by doing that, quercetin is oxidized to cytotoxic pro-oxidants leading to LDH leakage. Additionally, oxidized quercetin is highly reactive towards thiol groups and therefore toxic. Quercetin can form adducts in its oxidized form. Its targets are, e.g. proteins, but also glutathione resulting in a reduction of free glutathione (Boots et al., 2003). NAC treatment showed no significant beneficial effect but showed also a low toxicity. PRH from Wistar 2 would fall in the category of high-responders to oxidative stress. Their basic stress level was significantly higher than in PRH from Wistar 1 exceeding their capacity to prevent macromolecular damage. They were more prone to hydrogen peroxide stress than heat stress and the toxic effect of quercetin

outweighed its antioxidant properties. Future studies have to verify the categorization in low- and high-responders by analyzing a high number of biological replicates.

HepG2, a cell line derived from human hepatoblastoma, reacted to heat mainly within the first 5 h after stress induction. Heat treatment caused an increase in ROS production and catalase and SOD activity indicating an oxidative stress reaction without reducing cell viability (Table 4-1). This suggests that *HepG2* were able to counteract the oxidative stress. The reaction to heat treatment was detectable but did not cause a significant deviation from the control. However, the treatment of *HepG2* with 2 mM H_2O_2 caused a strong oxidative stress response, but also without loss of cell viability. The pre-treatment of *HepG2* with NAC or quercetin reduced ROS and enhanced antioxidant defense mechanisms but had no beneficial effect on cell viability. Antioxidant treatment rather induced toxic reactions leading to apoptosis. It would be interesting to further research the underlying mechanisms of this toxicity to *HepG2*.

The third part of the thesis (Chapter 5) analyzed the cellular mechanisms of the defense against oxidative stress and the influence of advanced age on these mechanisms. Experimental data included the hepatic function, oxidative damage markers and the proteome of primary hepatocytes from middle-aged (6 months) and old (> 23 months) Sprague Dawley rats (SD) under oxidative stress conditions compared to control conditions using 2-D DIGE and MALDI ToF MS/MS. The antioxidant quercetin was tested as a candidate for the prevention of age- and oxidative stress- related alterations and diseases.

Overall, hepatocytes from individual Sprague Dawley rats showed more consistent results than cells from Wistar rats. There was no categorization in high- and low-responders observed. Therefore, it could be concluded that SD rats are more suitable as an *in vitro* test model than Wistar rats.

A higher LDH leakage and protein carbonyl content in old PRH under control conditions compared to middle-aged PRH indicates a high basic stress level and a high degree of macromolecular damage in old PRH. Primary hepatocytes from old SD rats also showed drastically higher abundances in HSPs and several other antioxidant enzymes (SOD [Cu-Zn], peroxiredoxin-2, glutathione peroxidase). These results imply that the expression of antioxidant enzymes increases with age but is still insufficient to compensate the highly increased generation of ROS, resulting in oxidative injury. Proteomic analysis revealed

impaired central metabolic pathways due to aging. The influence of aging was most pronounced in the urea cycle. Carbamoyl phosphate synthetase, ornithine carbamoyltransferase, argininosuccinate synthase, three of the five enzymes in the urea cycle, were significantly decreased in old PRH. Deficiencies in theses enzymes are known to be strongly correlated to an impaired redox state and damaged antioxidant defense mechanisms.

The analysis of the influence of heat stress on middle-aged PRH showed that adult cells are able to counteract oxidative stress. An increasing abundance of HSPs during the whole cultivation period confirmed the assumption that the HSP70 recovery system defends the cells from macromolecular damage. An increase in SOD abundance and a higher energy metabolism further support the defense mechanisms against oxidative stress.

Hepatocytes from old SD rats were much more susceptible to oxidative stress than middle-aged PRH. Heat shock cognate 71 kDa protein was the only altered HSP indicating that the HSP expression was already at maximum under control conditions and could not be further increased. Actin expression was also significantly increased indicating the formation of actin stress fibers in the cytoplasm which is typical in aging cells (Doshi et al., 2010). The higher abundance in regucalcin as a biomarker for senescence is an indication for a strong decline in cellular function in old PRH due to heat stress. The increased abundance of antioxidant enzymes (SOD, glutathione S-transferase and glutathione peroxidase) and ferritin over the cultivation time could possibly be the reason for the decrease in cell death 24 h after heat stress (see LDH, Figure 5-3). Ferritin is involved in the negative regulation of necrotic cell death (Omiya et al., 2009). The analysis also revealed changes in energy metabolism in old PRH due to heat stress. ATP synthase decreased in abundance, whereas enzymes involved in glycolysis increased. Enzymes from urea cycle decreased. This is a trend already observed in old PRH compared to middle-aged PRH which is intensified by oxidative stress conditions.

Quercetin treatment of middle-aged PRH had a higher influence on protein abundance than heat stress itself. Quercetin inhibited HSP expression, an effect already discussed in other studies (Nagai et al., 1995). Nonetheless, quercetin treatment had beneficial effects on hepatocytes under heat stress conditions. Quercetin seems to decrease glycolysis related enzymes which reverses the effect of heat treatment. Additionally, protein disulfide isomerase showed an increase in abundance. It is known to protect cells against apoptosis (Ko et al., 2002) and could be involved in the protection mechanism of quercetin. In old PRH the

beneficial effect of quercetin on the proteome was more pronounced than in middle-aged PRH. The antioxidant enzyme peroxiredoxin increased significantly in abundance. Enzymes involved in the urea cycle increased in abundance allowing the detoxification of ammonia and reducing the accumulation of toxic intermediates. The increased anaerobic glycolytic activity was reversed in old PRH due to quercetin. Overall, quercetin seems to have a regulating effect on heat-induced proteomic alterations resulting in cell survival and a reduction of oxidative damage in all age groups. It would be interesting to further research the effect of quercetin on oxidative stress caused by other compounds like BSO or iron. A larger data set would allow a clearer differentiation between ROS- and heat-induced alterations. Additionally, it would be interesting to use rapamycin as an mTOR inhibitor to study the influence of the mTOR pathway in aging and oxidative stress (see Chapter 1).

In the last part of this thesis (Chapter 6) the proteome of primary mouse hepatocytes in collagen monolayer and sandwich culture was compared over a time period of 5 days. Cultivation in a sandwich of extracellular matrix is an approach to delay dedifferentiation in *in vitro* cultures.

Our study revealed the importance of oxidative stress in the dedifferentiation process. After 5 days, PMH in collagen SW and ML cultures exhibited characteristic indications of oxidative stress. However, in the SW culture the defense system against oxidative stress was significantly up-regulated to deal with this, whereas in the ML culture a down-regulation of these important enzymes was observed. Regarding the multiple effects of ROS and oxidative stress in cells, it can be concluded that the down-regulation of these enzymes seem to play a role in the loss of hepatic function observed in the ML cultivation. In addition, enzymes of the urea cycle were clearly down-regulated in ML culture. Glycolysis and gluconeogenesis were strongly affected by long-term cultivation in both ML and SW cultures. Interestingly, the culture condition had no effect on cellular lipid metabolism. To verify these results, it would be interesting to include enzyme assays related to lipid and glucose metabolism or to determine the activity of glycolytic enzymes with ^{13}C quantification. Additionally, the influence of antioxidants in monolayer and sandwich culture could give insights into the different states of the defense mechanisms against oxidative stress. The analysis of primary rat

hepatocytes in sandwich culture would be an adequate way to verify the importance of oxidative stress in the dedifferentiation of rodent primary hepatocytes.

8. Abbreviations

°C	Degree centigrade
µA	Microampere
µg	Microgram
µl	Microliter
µM	Micromolar
2-D	Two-dimensional
ACN	Acetonitrile
ADHP	10-Acetyl-3,7-dihydroxyphenoxazine
ANOVA	Analysis of variance
ApoA-IV	Apolipoprotein A-IV
ApoE	Apolipoprotein E
APS	Ammonium persulfate
AST	Aspartate aminotransferase
BSA	Bovine serum albumin
CAT	Catalase
CHAPS	3-[(3-cholamidopropyl)dimethylammonio]-1-propanesulfonate hydrate
CHCA	α-cyano-4-hydroxycinamic acid
CID	Collision-induced dissociation
CO_2	Carbon dioxide
COPD	Chronic obstructive pulmonary disease
$DCFH_{2\text{-}D}A$	2′,7′-Dichlorofluorescin diacetate
DDT	D-dopachrome tautomerase
DIGE	Difference gel electzrophoresis
DMF	Dimethylformamide
DTNB	5,5’-dithiobis-(2-nitrobenzoic acid)

DTT	Dithiothreitol
ELISA	Enzyme-linked immunosorbent assay
ESI	Electrospray-ionisation
FCS	Fetal calf serum
GPx	Glutathione peroxidase
GR	Glutathione reductase
GSH	Reduced glutathione
GSSG	Oxidized glutathione
h	Hour
H_2O_2	Hydrogen peroxide
HCM	Hepatic stellate cells
HEPES	4-(2-hydroxyethyl)-1-iperazineethanesulfonic acid
HRP	Horseradish peroxidase
HSP	Heat shock protein
IAA	Iodoacetamide
ICAT	Isotope-coded affinity tag
IEF	Isoelectric focusing
IPG	Immobilized pH gradient
iTraq	Isobaric tags for relative and absolute quantitation
ITS	Insulin/transferrine/selenium
kDa	Kilodalton
LDH	Lactate dehydrogenase
M	Molar
mA	Milliampere
MALDI	Matrix assisted laser desorption/ionization
mg	Milligram
MilliQ	Ultrapure water
min	Minute

ml	Milliliters
ML	Monolayer culture
ml	Milliliter
mM	Millimolar
MS	Mass spectrometry
MW	Molecular weight
MWCO	Molecular weight cut-off
NaCl	Sodium chloride
NAD^+/NADH	Nicotinamide adenine dinucleotide
NH_4HCO_3	Ammonium bicarbonate
nm	Nanometer
nM	Nanomolar
PAGE	Polyacrylamide gel electrophoresis
PBS	Phosphate-buffered saline
PC	Principal component
PCA	Principal component analysis
pg	Picogram
pI	Isoelectric point
PI3K	phosphatidylinositol-3-OH kinase
PHH	Primary human hepatocytes
PMH	Primary mouse hepatocytes
PRH	Primary rat hepatocytes
RBP	Retinol-binding protein
ROS	Reactive oxygen species
RT	Room temperature
SDS	Sodium dodecyl phosphate
SMP-30	Senescence marker protein 30
SOD	Superoxide dismutase

SW	Sandwich culture
TCA	Trichloroacetic acid
TEMED	*N*,*N*,*N*,*N*-tetramethylethylenediamine
TFA	Trifluoroacetic acid
TMB	3,3’,5,5’-tetramethylbenzidine
ToF	Time of Flight
TTR	Transthyretin
v/v	Volume/volume percent
w/v	Weight per volume
WME	William’s Medium E

9. References

Akerstrom, B., Logdberg, L., Berggard, T., Osmark, P. and Lindqvist, A. (2000). "alpha(1)-Microglobulin: a yellow-brown lipocalin." Biochim Biophys Acta **1482**(1-2): 172-184.

Alepee, N., Bahinski, A., Daneshian, M., De Wever, B., Fritsche, E., Goldberg, A., Hansmann, J., Hartung, T., Haycock, J., Hogberg, H., Hoelting, L., Kelm, J. M., Kadereit, S., McVey, E., Landsiedel, R., Leist, M., Lubberstedt, M., Noor, F., Pellevoisin, C., Petersohn, D., Pfannenbecker, U., Reisinger, K., Ramirez, T., Rothen-Rutishauser, B., Schafer-Korting, M., Zeilinger, K. and Zurich, M. G. (2014). "State-of-the-art of 3D cultures (organs-on-a-chip) in safety testing and pathophysiology." ALTEX **31**(4): 441-477.

Alia, M., Mateos, R., Ramos, S., Lecumberri, E., Bravo, L. and Goya, L. (2006). "Influence of quercetin and rutin on growth and antioxidant defense system of a human hepatoma cell line (HepG2)." Eur J Nutr **45**(1): 19-28.

Altelaar, A. F., Munoz, J. and Heck, A. J. (2013). "Next-generation proteomics: towards an integrative view of proteome dynamics." Nat Rev Genet **14**(1): 35-48.

Altschul, S. F., Gish, W., Miller, W., Myers, E. W. and Lipman, D. J. (1990). "Basic Local Alignment Search Tool." J Mol Biol **215**(3): 403-410.

Ando, Y., Nyhlin, N., Suhr, O., Holmgren, G., Uchida, K., el Sahly, M., Yamashita, T., Terasaki, H., Nakamura, M., Uchino, M. and Ando, M. (1997). "Oxidative stress is found in amyloid deposits in systemic amyloidosis." Biochem Biophys Res Commun **232**(2): 497-502.

Ansar, S., Siddiqi, N. J., Zargar, S., Ganaie, M. A. and Abudawood, M. (2016). "Hepatoprotective effect of Quercetin supplementation against Acrylamide-induced DNA damage in wistar rats." BMC Complement Altern Med **16**(1): 327.

Apel, K. and Hirt, H. (2004). "Reactive oxygen species: metabolism, oxidative stress, and signal transduction." Annu Rev Plant Biol **55**: 373-399.

Augustyniak, A., Bartosz, G., Cipak, A., Duburs, G., Horakova, L., Luczaj, W., Majekova, M., Odysseos, A. D., Rackova, L., Skrzydlewska, E., Stefek, M., Strosova, M., Tirzitis, G., Venskutonis, P. R., Viskupicova, J., Vraka, P. S. and Zarkovic, N. (2010). "Natural and synthetic antioxidants: an updated overview." Free Radic Res **44**(10): 1216-1262.

Baar, E. L., Carbajal, K. A., Ong, I. M. and Lamming, D. W. (2016). "Sex- and tissue-specific changes in mTOR signaling with age in C57BL/6J mice." Aging Cell **15**(1): 155-166.

Balaban, R. S., Nemoto, S. and Finkel, T. (2005). "Mitochondria, oxidants, and aging." Cell **120**(4): 483-495.

Bantscheff, M., Lemeer, S., Savitski, M. M. and Kuster, B. (2012). "Quantitative mass spectrometry in proteomics: critical review update from 2007 to the present." Anal Bioanal Chem **404**(4): 939-965.

Baraibar, M. A., Ladouce, R. and Friguet, B. (2013). "Proteomic quantification and identification of carbonylated proteins upon oxidative stress and during cellular aging." J Proteomics **92**: 63-70.

Bardia, A., Tleyjeh, I. M., Cerhan, J. R., Sood, A. K., Limburg, P. J., Erwin, P. J. and Montori, V. M. (2008). "Efficacy of antioxidant supplementation in reducing primary cancer incidence and mortality: systematic review and meta-analysis." Mayo Clin Proc **83**(1): 23-34.

Barja, G. (2013). "Updating the Mitochondrial Free Radical Theory of Aging: An Integrated View, Key Aspects, and Confounding Concepts." Antioxid Redox Signal **19**(12): 1420-1445.

Barros, P. P., da Silva, G. H., Goncalves, G. M. S., Oliveira, J. C., Pagnan, L. G. and Arco-e-Flexa, L. (2017). "Hepatoprotective Effect of Quercetin Pretreatment Against Paracetamol-Induced Liver Damage and Partial Hepatectomy in Rats." Braz Arch Biol Technol **60**.

Basile, A., Biziato, D., Sherbet, G. V., Comi, P. and Cajone, F. (2008). "Hyperthermia inhibits cell proliferation and induces apoptosis: Relative signaling status of p53, S100A4, and notch in heat sensitive and resistant cell lines." J Cell Biochem **103**(1): 212-220.

Bateman, A., Martin, M. J., O'Donovan, C., Magrane, M., Alpi, E., Antunes, R., Bely, B., Bingley, M., Bonilla, C., Britto, R., Bursteinas, B., Bye-A-Jee, H., Cowley, A., Da Silva, A., De Giorgi, M., Dogan, T., Fazzini, F., Castro, L. G., Figueira, L., Garmiri, P., Georghiou, G., Gonzalez, D., Hatton-Ellis, E., Li, W. Z., Liu, W. D., Lopez, R., Luo, J., Lussi, Y., MacDougall, A., Nightingale, A., Palka, B., Pichler, K., Poggioli, D., Pundir, S., Pureza, L., Qi, G. Y., Rosanoff, S., Saidi, R., Sawford, T., Shypitsyna, A., Speretta, E., Turner, E., Tyagi, N., Volynkin, V., Wardell, T., Warner, K., Watkins, X., Zaru, R., Zellner, H., Xenarios, I., Bougueleret, L., Bridge, A., Poux, S., Redaschi, N., Aimo, L., Argoud-Puy, G., Auchincloss, A., Axelsen, K., Bansal, P., Baratin, D., Blatter, M. C., Boeckmann, B., Bolleman, J., Boutet, E., Breuza, L., Casal-Casas, C., de Castro, E., Coudert, E., Cuche, B., Doche, M., Dornevil, D., Duvaud, S., Estreicher, A., Famiglietti, L., Feuermann, M., Gasteiger, E., Gehant, S., Gerritsen, V., Gos, A., Gruaz-Gumowski, N., Hinz, U., Hulo, C., Jungo, F., Keller, G., Lara, V., Lemercier, P., Lieberherr, D., Lombardot, T., Martin, X., Masson, P., Morgat, A., Neto, T., Nouspikel, N., Paesano, S., Pedruzzi, I., Pilbout, S., Pozzato, M., Pruess, M., Rivoire, C., Roechert, B., Schneider, M., Sigrist, C., Sonesson, K., Staehli, S., Stutz, A., Sundaram, S., Tognolli, M., Verbregue, L., Veuthey, A. L., Wu, C. H., Arighi, C. N., Arminski, L., Chen, C. M., Chen, Y. X., Garavelli, J. S., Huang, H. Z., Laiho, K., McGarvey, P., Natale, D. A., Ross, K., Vinayaka, C. R., Wang, Q. H., Wang, Y. Q., Yeh, L. S., Zhang, J. and Consortium, U. (2017). "UniProt: the universal protein knowledgebase." Nucleic Acids Res **45**(D1): D158-D169.

Bayanov, A. A. and Brunt, A. R. (1999). "Role of hypoxia and constitutionally different resistance to hypoxia/stress as the determiners of individual profile of cytochrome P450 isozyme activity." Gen Pharmacol **33**(4): 355-361.

Beigel, J., Fella, K., Kramer, P. J., Kroeger, M. and Hewitt, P. (2008). "Genomics and proteomics analysis of cultured primary rat hepatocytes." Toxicol In Vitro **22**(1): 171-181.

Bellei, E., Bergamini, S., Monari, E., Fantoni, L. I., Cuoghi, A., Ozben, T. and Tomasi, A. (2011). "High-abundance proteins depletion for serum proteomic analysis: concomitant removal of non-targeted proteins." Amino Acids **40**(1): 145-156.

Berggard, T., Thelin, N., Falkenberg, C., Enghild, J. J. and Akerstrom, B. (1997). "Prothrombin, albumin and immunoglobulin A form covalent complexes with alpha1-microglobulin in human plasma." Eur J Biochem **245**(3): 676-683.

Berlett, B. S. and Stadtman, E. R. (1997). "Protein oxidation in aging, disease, and oxidative stress." J Biol Chem **272**(33): 20313-20316.

Bjedov, I., Toivonen, J. M., Kerr, F., Slack, C., Jacobson, J., Foley, A. and Partridge, L. (2010). "Mechanisms of life span extension by rapamycin in the fruit fly Drosophila melanogaster." Cell Metab **11**(1): 35-46.

Bolser, D. C. (2010). "Pharmacologic Management of Cough." Otolaryng Clin North America **43**(1): 147.

Boots, A. W., Haenen, G. R. M. M. and Bast, A. (2008). "Health effects of quercetin: From antioxidant to nutraceutical." Eur J Pharmacol **585**(2-3): 325-337.

Boots, A. W., Kubben, N., Haenen, G. R. M. M. and Bast, A. (2003). "Oxidized quercetin reacts with thiols rather than with ascorbate: implication for quercetin supplementation." Biochem Biophys Res Commun **308**(3): 560-565.

Boots, A. W., Li, H., Schins, R. P. F., Duffin, R., Heemskerk, J. W. M., Bast, A. and Haenen, G. R. M. M. (2007). "The quercetin paradox." Toxicol Appl Pharmacol **222**(1): 89-96.

Bourdon, E. and Blache, D. (2001). "The importance of proteins in defense against oxidation." Antioxid Redox Signal **3**(2): 293-311.

Bradford, M. M. (1976). "A rapid and sensitive method for the quantitation of microgram quantities of protein utilizing the principle of protein-dye binding." Anal Biochem **72**: 248-254.

Brandt, R. and Keston, A. S. (1965). "Synthesis of diacetyldichlorofluorescin: A stable reagent for fluorometric analysis." Anal Biochem **11**: 6-9.

Brulport, M., Schormann, W., Bauer, A., Hermes, M., Elsner, C., Hammersen, F. J., Beerheide, W., Spitkovsky, D., Hartig, W., Nussler, A., Horn, L. C., Edelmann, J., Pelz-Ackermann, O., Petersen, J., Kamprad, M., von Mach, M., Lupp, A., Zulewski, H. and Hengstler, J. G. (2007). "Fate of extrahepatic human stem and precursor cells after transplantation into mouse livers." Hepatology **46**(3): 861-870.

Bullone, M. and Lavoie, J. P. (2017). "The Contribution of Oxidative Stress and Inflamm-Aging in Human and Equine Asthma." Int J Mol Sci **18**(12).

Bunner, A. E., Chandrasekera, P. C. and Barnard, N. D. (2014). "Knockout mouse models of insulin signaling: Relevance past and future." World J Diabetes **5**(2): 146-159.

Cawthon, R. M., Smith, K. R., O'Brien, E., Sivatchenko, A. and Kerber, R. A. (2003). "Association between telomere length in blood and mortality in people aged 60 years or older." Lancet **361**(9355): 393-395.

Cerda, B., Soto, C., Albaladejo, M. D., Martinez, P., Sanchez-Gascon, F., Tomas-Barberan, F. and Espin, J. C. (2006). "Pomegranate juice supplementation in chronic obstructive pulmonary disease: a 5-week randomized, double-blind, placebo-controlled trial." Eur J Clin Nutr **60**(2): 245-253.

Chen, X., Zhong, Z., Xu, Z., Chen, L. and Wang, Y. (2010). "2',7'-Dichlorodihydrofluorescein as a fluorescent probe for reactive oxygen species measurement: Forty years of application and controversy." Free Radic Res **44**(6): 587-604.

Chen, X. J., Tang, Z. Z., Zhu, G. G., Cheng, Q., Zhang, W. K., Li, H. M., Fu, W. and Lu, Q. P. (2017). "JNK signaling is required for the MIP-1 alpha-associated regulation of Kupffer cells in the heat stroke response." Mol Med Rep **16**(3): 2389-2396.

Cheng, I. F. and Breen, K. (2000). "On the ability of four flavonoids, baicilein, luteolin, naringenin, and quercetin, to suppress the fenton reaction of the iron-ATP complex." Biometals **13**(1): 77-83.

Chou, S. D., Prince, T., Gong, J. and Calderwood, S. K. (2012). "mTOR is essential for the proteotoxic stress response, HSF1 activation and heat shock protein synthesis." PLoS One **7**(6): e39679.

Colman, R. J., Anderson, R. M., Johnson, S. C., Kastman, E. K., Kosmatka, K. J., Beasley, T. M., Allison, D. B., Cruzen, C., Simmons, H. A., Kemnitz, J. W. and Weindruch, R. (2009). "Caloric restriction delays disease onset and mortality in rhesus monkeys." Science **325**(5937): 201-204.

Conde de la Rosa, L., Schoemaker, M. H., Vrenken, T. E., Buist-Homan, M., Havinga, R., Jansen, P. L. and Moshage, H. (2006). "Superoxide anions and hydrogen peroxide induce hepatocyte death by different mechanisms: involvement of JNK and ERK MAP kinases." J Hepatol **44**(5): 918-929.

Cornelius, E. (1972). "Increased Incidence of Lymphomas in Thymectomized Mice - Evidence for an Immunological Theory of Aging." Experientia **28**(4): 459-&.

Czochra, P., Klopcic, B., Meyer, E., Herkel, J., Garcia-Lazaro, J. F., Thieringer, F., Schirmacher, P., Biesterfeld, S., Galle, P. R., Lohse, A. W. and Kanzler, S. (2006). "Liver

fibrosis induced by hepatic overexpression of PDGF-B in transgenic mice." J Hepatol **45**(3): 419-428.

Dajas, F., Rivera-Megret, F., Blasina, F., Arredondo, F., Abin-Carriquiry, J. A., Costa, G., Echeverry, C., Lafon, L., Heizen, H., Ferreira, M. and Morquio, A. (2003). "Neuroprotection by flavonoids." Braz J Med Biol Res **36**(12): 1613-1620.

Dalle-Donne, I., Rossi, R., Giustarini, D., Milzani, A. and Colombo, R. (2003). "Protein carbonyl groups as biomarkers of oxidative stress." Clin Chim Acta **329**(1-2): 23-38.

de Graff, A. M. R., Hazoglou, M. J. and Dill, K. A. (2016). "Highly Charged Proteins: The Achilles' Heel of Aging Proteomes." Structure **24**(2): 329-336.

Diamond, D. L., Proll, S. C., Jacobs, J. M., Chan, E. Y., Camp, D. G., 2nd, Smith, R. D. and Katze, M. G. (2006). "HepatoProteomics: applying proteomic technologies to the study of liver function and disease." Hepatology **44**(2): 299-308.

Dierick, J. F., Dieu, M., Remacle, J., Raes, M., Roepstorff, P. and Toussaint, O. (2002). "Proteomics in experimental gerontology." Exp Gerontol **37**(5): 721-734.

Dinarello, C. A. (2000). "Proinflammatory cytokines." Chest **118**(2): 503-508.

Doshi, B. M., Hightower, L. E. and Lee, J. (2010). "HSPB1, actin filament dynamics, and aging cells." Ann Ny Acad Sci **1197**: 76-84.

Doskey, C. M., Buranasudja, V., Wagner, B. A., Wilkes, J. G., Du, J., Cullen, J. J. and Buettner, G. R. (2016). "Tumor cells have decreased ability to metabolize H2O2: Implications for pharmacological ascorbate in cancer therapy." Redox Biol **10**: 274-284.

Dowling, P., Shields, W., Rani, S., Meleady, P., Henry, M., Jeppesen, P., O'Driscoll, L. and Clynes, M. (2008). "Proteomic analysis of conditioned media from glucose responsive and glucose non-responsive phenotypes reveals a panel of secreted proteins associated with beta cell dysfunction." Electrophoresis **29**(20): 4141-4149.

Dröge, W. (2002). "Free radicals in the physiological control of cell function." Physiol Rev **82**(1): 47-95.

Dunn, J. C., Tompkins, R. G. and Yarmush, M. L. (1992). "Hepatocytes in collagen sandwich: evidence for transcriptional and translational regulation." J Cell Biol **116**(4): 1043-1053.

Eng, F. J. and Friedman, S. L. (2000). "Fibrogenesis I. New insights into hepatic stellate cell activation: the simple becomes complex." Am J Physiol-Gastr L **279**(1): G7-G11.

Farkas, D., Bhat, V. B., Mandapati, S., Wishnok, J. S. and Tannenbaum, S. R. (2005). "Characterization of the secreted proteome of rat hepatocytes cultured in collagen sandwiches." Chem Res Toxicol **18**(7): 1132-1139.

Farouque, H. M., Leung, M., Hope, S. A., Baldi, M., Schechter, C., Cameron, J. D. and Meredith, I. T. (2006). "Acute and chronic effects of flavanol-rich cocoa on vascular function in subjects with coronary artery disease: a randomized double-blind placebo-controlled study." Clin Sci (Lond) **111**(1): 71-80.

Festing, M. F. W. (1993). "Genetic-Variation in Outbred Rats and Mice and Its Implications for Toxicological Screening." J Exp Anim Sci **35**(5-6): 210-220.

Figliomeni, M. L. and Abdel-Rahman, M. S. (1998). "Ethanol does not increase the hepatotoxicity of cocaine in primary rat hepatocyte culture." Toxicology **129**(2-3): 125-135.

Finkel, T. and Holbrook, N. J. (2000). "Oxidants, oxidative stress and the biology of ageing." Nature **408**(6809): 239-247.

Forman, H. J., Zhang, H. Q. and Rinna, A. (2009). "Glutathione: Overview of its protective roles, measurement, and biosynthesis." Mol Aspects Med **30**(1-2): 1-12.

Fransen, M., Nordgren, M., Wang, B. and Apanasets, O. (2012). "Role of peroxisomes in ROS/RNS-metabolism: Implications for human disease." Bba-Mol Basis Dis **1822**(9): 1363-1373.

Freitas, A. A. and de Magalhaes, J. P. (2011). "A review and appraisal of the DNA damage theory of ageing." Mutat Res **728**(1-2): 12-22.

Gabai, V. L., Meriin, A. B., Yaglom, J. A., Volloch, V. Z. and Sherman, M. Y. (1998). "Role of Hsp70 in regulation of stress-kinase JNK: implications in apoptosis and aging." FEBS Lett **438**(1-2): 1-4.

Gao, W. N., Guo, C. J. and Wu, J. Q. (2009). "The Protective Effects of Quercetin on Rat Hepatocytes against Oxidative Stress in Metabolomics." Ann Nutr Metab **55**: 431-431.

Garg, R. (2016). "Oxidative stress induced alterations during aging: Quantifying the metabolic changes associated with aging and oxidative stress." Naturwissenschaftlich-Technische Fakultät der Universität des Saarlandes **PhD**(Dissertation): 43-44.

Gerets, H. H. J., Tilmant, K., Gerin, B., Chanteux, H., Depelchin, B. O., Dhalluin, S. and Atienzar, F. A. (2012). "Characterization of primary human hepatocytes, HepG2 cells, and HepaRG cells at the mRNA level and CYP activity in response to inducers and their predictivity for the detection of human hepatotoxins." Cell Biol Toxicol **28**(2): 69-87.

Gil Del Valle, L. (2010). "Oxidative stress in aging: Theoretical outcomes and clinical evidences in humans." Biomed Pharmacother.

Gille, C., Bolling, C., Hoppe, A., Bulik, S., Hoffmann, S., Hubner, K., Karlstadt, A., Ganeshan, R., Konig, M., Rother, K., Weidlich, M., Behre, J. and Holzhutter, H. G. (2010). "HepatoNet1: a comprehensive metabolic reconstruction of the human hepatocyte for the analysis of liver physiology." Mol Syst Biol **6**: 411.

Godoy, P., Hengstler, J. G., Ilkavets, I., Meyer, C., Bachmann, A., Muller, A., Tuschl, G., Mueller, S. O. and Dooley, S. (2009). "Extracellular matrix modulates sensitivity of hepatocytes to fibroblastoid dedifferentiation and transforming growth factor beta-induced apoptosis." Hepatology **49**(6): 2031-2043.

Gorman, A. M., Heavey, B., Creagh, E., Cotter, T. G. and Samali, A. (1999). "Antioxidant-mediated inhibition of the heat shock response leads to apoptosis." Febs Letters **445**(1): 98-102.

Gripon, P., Rumin, S., Urban, S., Le Seyec, J., Glaise, D., Cannie, I., Guyomard, C., Lucas, J., Trepo, C. and Guguen-Guillouzo, C. (2002). "Infection of a human hepatoma cell line by hepatitis B virus." P Natl Acad Sci USA **99**(24): 15655-15660.

Grizzi, F., Di Caro, G., Laghi, L., Hermonat, P., Mazzola, P., Nguyen, D. D., Radhi, S., Figueroa, J. A., Cobos, E., Annoni, G. and Chiriva-Internati, M. (2013). "Mast cells and the liver aging process." Immun Ageing **10**.

Group, B. D. W. (2001). "Biomarkers and surrogate endpoints: preferred definitions and conceptual framework." Clin Pharmacol Ther **69**(3): 89-95.

Grune, T., Shringarpure, R., Sitte, N. and Davies, K. (2001). "Age-related changes in protein oxidation and proteolysis in mammalian cells." J Gerontol a-Biol **56**(11): B459-B467.

Guerrieri, F., Kalous, M., Capozza, G., Muolo, L., Drahota, Z. and Papa, S. (1994). "Age-Dependent Changes in Mitochondrial F0f1 Atp Synthase in Regenerating Rat-Liver." Biochem Mol Biol Int **33**(1): 117-129.

Guevara, C. R., Philipp, O., Hamann, A., Werner, A., Osiewacz, H. D., Rexroth, S., Rogner, M. and Poetsch, A. (2016). "Global Protein Oxidation Profiling Suggests Efficient Mitochondrial Proteome Homeostasis During Aging." Mol Cell Proteomics **15**(5): 1692-1709.

Gunawardana, C. G., Kuk, C., Smith, C. R., Batruch, I., Soosaipillai, A. and Diamandis, E. P. (2009). "Comprehensive analysis of conditioned media from ovarian cancer cell lines identifies novel candidate markers of epithelial ovarian cancer." J Proteome Res **8**(10): 4705-4713.

Gygi, S. P., Rist, B., Gerber, S. A., Turecek, F., Gelb, M. H. and Aebersold, R. (1999). "Quantitative analysis of complex protein mixtures using isotope-coded affinity tags." Nat Biotechnol **17**(10): 994-999.

Hall, D. M., Sattler, G. L., Sattler, C. A., Zhang, H. J., Oberley, L. W., Pitot, H. C. and Kregel, K. C. (2001). "Aging lowers steady-state antioxidant enzyme and stress protein expression in primary hepatocytes." J Gerontol A Biol Sci Med Sci **56**(6): B259-267.

Hall, D. M., Xu, L., Drake, V. J., Oberley, L. W., Oberley, T. D., Moseley, P. L. and Kregel, K. C. (2000). "Aging reduces adaptive capacity and stress protein expression in the liver after heat stress." J Appl Physiol **89**(2): 749-759.

Halliwell, B. (1991). "Reactive oxygen species in living systems: source, biochemistry, and role in human disease." Am J Med **91**(3C): 14S-22S.

Halliwell, B. (2003). "Oxidative stress in cell culture: an under-appreciated problem?" Febs Lett **540**(1-3): 3-6.

Halliwell, B. (2006). "Reactive species and antioxidants. Redox biology is a fundamental theme of aerobic life." Plant Physiol **141**(2): 312-322.

Halliwell, B. (2008). "Are polyphenols antioxidants or pro-oxidants? What do we learn from cell culture and in vivo studies?" Arch Biochem Biophys **476**(2): 107-112.

Harman, D. (1956). "Aging: a theory based on free radical and radiation chemistry." J Gerontol **11**(3): 298-300.

Harrison, D. E., Strong, R., Sharp, Z. D., Nelson, J. F., Astle, C. M., Flurkey, K., Nadon, N. L., Wilkinson, J. E., Frenkel, K., Carter, C. S., Pahor, M., Javors, M. A., Fernandez, E. and Miller, R. A. (2009). "Rapamycin fed late in life extends lifespan in genetically heterogeneous mice." Nature **460**(7253): 392-395.

Harrold, J. A., Widdowson, P. S., Clapham, J. C. and Williams, G. (2000). "Individual severity of dietary obesity in unselected Wistar rats: relationship with hyperphagia." Am J Physiol-Endoc M **279**(2): E340-E347.

Hayflick, L. (1998). "How and why we age." Exp Gerontol **33**(7-8): 639-653.

Hayflick, L. and Moorhead, P. S. (1961). "The serial cultivation of human diploid cell strains." Exp Cell Res **25**: 585-621.

Herzog, A. P., Rogers, D. S., Brevick, J. L. and Boluyt, M. O. (2006). "Proteome Mapping of the Effects of Age, Pressure Overload, and Aldosterone Antagonism on Cardiac Fibrosis." Med Sci Sport Exer **38**(5): S417-S418.

Heydari, A. R., You, S., Takahashi, R., Gutsmann-Conrad, A., Sarge, K. D. and Richardson, A. (2000). "Age-related alterations in the activation of heat shock transcription factor 1 in rat hepatocytes." Exp Cell Res **256**(1): 83-93.

Hillenkamp, F., Karas, M., Beavis, R. C. and Chait, B. T. (1991). "Matrix-Assisted Laser Desorption Ionization Mass-Spectrometry of Biopolymers." Anal Chem **63**(24): A1193-A1202.

Hirano, T., Kaplowitz, N., Tsukamoto, H., Kamimura, S. and Fernandezcheca, J. C. (1992). "Hepatic Mitochondrial Glutathione Depletion and Progression of Experimental Alcoholic Liver-Disease in Rats." Hepatology **16**(6): 1423-1427.

Hiyoshi, M., Konishi, H., Uemura, H., Matsuzaki, H., Tsukamoto, H., Sugimoto, R., Takeda, H., Dakeshita, S., Kitayama, A., Takami, H., Sawachika, F., Kido, H. and Arisawa, K. (2009).

"D-Dopachrome tautomerase is a candidate for key proteins to protect the rat liver damaged by carbon tetrachloride." Toxicology **255**(1-2): 6-14.

Hohme, S., Hengstler, J. G., Brulport, M., Schafer, M., Bauer, A., Gebhardt, R. and Drasdo, D. (2007). "Mathematical modelling of liver regeneration after intoxication with CCl(4)." Chem Biol Interact **168**(1): 74-93.

Holmes, A. M., Creton, S. and Chapman, K. (2010). "Working in partnership to advance the 3Rs in toxicity testing." Toxicology **267**(1-3): 14-19.

Hung, C. H., Chan, S. H., Chu, P. M. and Tsai, K. L. (2015). "Quercetin is a potent anti-atherosclerotic compound by activation of SIRT1 signaling under oxLDL stimulation." Mol Nutr Food Res **59**(10): 1905-1917.

Hung, Y. C., Sava, V. M., Blagodarsky, V. A., Hong, M. Y. and Huang, G. S. (2003). "Protection of tea melanin on hydrazine-induced liver injury." Life Sci **72**(9): 1061-1071.

I, P., Listrat, A., Alliot, J., Chambon, C., Taylor, R. G. and Bechet, D. (2005). "Differential proteome analysis of aging in rat skeletal muscle." Faseb J **19**(6): 1143-+.

Ikwegbue, P. C., Masamba, P., Oyinloye, B. E. and Kappo, A. P. (2017). "Roles of Heat Shock Proteins in Apoptosis, Oxidative Stress, Human Inflammatory Diseases, and Cancer." Pharmaceuticals (Basel) **11**(1).

Iredale, J. P. and Arthur, M. J. (1994). "Hepatocyte-matrix interactions." Gut **35**(6): 729-732.

Jakubowicz-Gil, J., Rzymowska, J. and Gawron, A. (2002). "Quercetin, apoptosis, heat shock." Biochem Pharmacol **64**(11): 1591-1595.

James, P. (1997). "Protein identification in the post-genome era: the rapid rise of proteomics." Q Rev Biophys **30**(4): 279-331.

Jemnitz, K., Veres, Z., Monostory, K., Kobori, L. and Vereczkey, L. (2008). "Interspecies differences in acetaminophen sensitivity of human, rat, and mouse primary hepatocytes." Toxicol in Vitro **22**(4): 961-967.

Jeon, H., Lee, S., Lee, W. H. and Suk, K. (2010). "Analysis of glial secretome: the long pentraxin PTX3 modulates phagocytic activity of microglia." J Neuroimmunol **229**(1-2): 63-72.

Ji, L. L., Sheng, Y. C., Zheng, Z. Y., Shi, L. and Wang, Z. T. (2015). "The involvement of p62-Keap1-Nrf2 antioxidative signaling pathway and JNK in the protection of natural flavonoid quercetin against hepatotoxicity." Free Radical Bio Med **85**: 12-23.

Jin, K. L. (2010). "Modern Biological Theories of Aging." Aging Dis **1**(2): 72-74.

Johansen, J. S., Harris, A. K., Rychly, D. J. and Ergul, A. (2005). "Oxidative stress and the use of antioxidants in diabetes: Linking basic science to clinical practice." Cardiovasc Diabetol **4**(1): 5.

Johnson, S. C., Rabinovitch, P. S. and Kaeberlein, M. (2013). "mTOR is a key modulator of ageing and age-related disease." Nature **493**(7432): 338-345.

Jolly, C. and Morimoto, R. I. (2000). "Role of the heat shock response and molecular chaperones in oncogenesis and cell death." J Natl Cancer I **92**(19): 1564-1572.

Jun, J. E., Lee, S. E., Lee, Y. B., Jee, J. H., Bae, J. C., Jin, S. M., Hur, K. Y., Lee, M. K. and Kim, J. H. (2017). "Increase in serum albumin concentration is associated with prediabetes development and progression to overt diabetes independently of metabolic syndrome." PLoS One **12**(4).

Jungermann, K. and Kietzmann, T. (1996). "Zonation of parenchymal and nonparenchymal metabolism in liver." Annu Rev Nutr **16**: 179-203.

Kacew, S. and Festing, M. F. W. (1996). "Role of rat strain in the differential sensitivity to pharmaceutical agents and naturally occurring substances." J Toxicol Env Health **47**(1): 1-30.

Kaldas, M. I., Walle, U. K., Van der Woude, H., McMillan, J. M. and Walle, T. (2005). "Covalent binding of the flavonoid quercetin to human serum albumin." J Agr Food Chem **53**(10): 4194-4197.

Kaneto, H., Matsuoka, T. A., Katakami, N., Kawamori, D., Miyatsuka, T., Yoshiuchi, K., Yasuda, T., Sakamoto, K., Yamasaki, Y. and Matsuhisa, M. (2007). "Oxidative stress and the JNK pathway are involved in the development of type 1 and type 2 diabetes." Curr Mol Med **7**(7): 674-686.

Karas, M. and Hillenkamp, F. (1988). "Laser desorption ionization of proteins with molecular masses exceeding 10,000 daltons." Anal Chem **60**(20): 2299-2301.

Kayama, Y., Raaz, U., Jagger, A., Adam, M., Schellinger, I. N., Sakamoto, M., Suzuki, H., Toyama, K., Spin, J. M. and Tsao, P. S. (2015). "Diabetic Cardiovascular Disease Induced by Oxidative Stress." Int J Mol Sci **16**(10): 25234-25263.

Kendig, D. M. and Tarloff, J. B. (2007). "Inactivation of lactate dehydrogenase by several chemicals: Implications for in vitro toxicology studies." Toxicol in Vitro **21**(1): 125-132.

Kenyon, C. J. (2010). "The genetics of ageing." Nature **464**(7288): 504-512.

Kiang, J. G. and Tsokos, G. C. (1998). "Heat shock protein 70 kDa: Molecular biology, biochemistry, and physiology." Pharmacol Therapeut **80**(2): 183-201.

Kim, H. Y., Kim, J. H., Lee, S. A., Chang, H. E., Park, M. H., Hwang, S. J., Lee, J. Y., Mok, C. and Hong, S. G. (2008). "Saengshik, a formulated health food, prevents liver damage in

CCl4-induced mice and increases antioxidant activity in elderly women." J Med Food **11**(2): 323-330.

Kim, S. and Pevzner, P. A. (2014). "MS-GF+ makes progress towards a universal database search tool for proteomics." Nat Commun **5**: 5277.

Klee, E. W. and Sosa, C. P. (2007). "Computational classification of classically secreted proteins." Drug Discov Today **12**(5-6): 234-240.

Klingmuller, U., Bauer, A., Bohl, S., Nickel, P. J., Breitkopf, K., Dooley, S., Zellmer, S., Kern, C., Merfort, I., Sparna, T., Donauer, J., Walz, G., Geyer, M., Kreutz, C., Hermes, M., Gotschel, F., Hecht, A., Walter, D., Egger, L., Neubert, K., Borner, C., Brulport, M., Schormann, W., Sauer, C., Baumann, F., Preiss, R., MacNelly, S., Godoy, P., Wiercinska, E., Ciuclan, L., Edelmann, J., Zeilinger, K., Heinrich, M., Zanger, U. M., Gebhardt, R., Maiwald, T., Heinrich, R., Timmer, J., von Weizsacker, F. and Hengstler, J. G. (2006). "Primary mouse hepatocytes for systems biology approaches: a standardized in vitro system for modelling of signal transduction pathways." Syst Biol (Stevenage) **153**(6): 433-447.

Ko, H. S., Uehara, T. and Nomura, Y. (2002). "Role of ubiquilin associated with protein-disulfide isomerase in the endoplasmic reticulum in stress-induced apoptotic cell death." J Biol Chem **277**(38): 35386-35392.

Kokoszka, J. E., Coskun, P., Esposito, L. A. and Wallace, D. C. (2001). "Increased mitochondrial oxidative stress in the Sod2 (+/-) mouse results in the age-related decline of mitochondrial function culminating in increased apoptosis." P Natl Acad Sci-Biol **98**(5): 2278-2283.

Kondo, Y. and Ishigami, A. (2016). "Involvement of senescence marker protein-30 in glucose metabolism disorder and non-alcoholic fatty liver disease." Geriatr Gerontol Int **16 Suppl 1**: 4-16.

Koser, F., Hecker, M. and Drews, O. (2014). "The cardiac proteome changes with protein degradation in aging." Acta Physiol **210**: 156-158.

Kostadinova, R., Boess, F., Applegate, D., Suter, L., Weiser, T., Singer, T., Naughton, B. and Roth, A. (2013). "A long-term three dimensional liver co-culture system for improved prediction of clinically relevant drug-induced hepatotoxicity." Toxicol Appl Pharmacol **268**(1): 1-16.

Kowalski, G. M. and Bruce, C. R. (2014). "The regulation of glucose metabolism: implications and considerations for the assessment of glucose homeostasis in rodents." Am J Physiol Endocrinol Metab **307**(10): E859-871.

Krewski, D., Acosta, D., Andersen, M., Anderson, H., Bailar, J. C., Boekelheide, K., Brent, R., Charnley, G., Cheung, V. G., Green, S., Kelsey, K. T., Kerkvliet, N. I., Li, A. A., McCray, L., Meyer, O., Patterson, R. D., Pennie, W., Scala, R. A., Solomon, G. M., Stephens, M.,

Yager, J., Zeise, L. and Assess, S. C. T. T. (2010). "Toxicity Testing in the 21st Century: A Vision and a Strategy." J Toxicol Env Heal B **13**(2-4): 51-138.

Kuepfer, L. (2010). "Towards whole-body systems physiology." Mol Syst Biol **6**: 409.

Kuksal, N., Chalker, J. and Mailloux, R. J. (2017). "Progress in understanding the molecular oxygen paradox - function of mitochondrial reactive oxygen species in cell signaling." Biol Chem **398**(11): 1209-1227.

Kulasingam, V. and Diamandis, E. P. (2008). "Tissue culture-based breast cancer biomarker discovery platform." Int J Cancer **123**(9): 2007-2012.

Kumar, S. and Bandyopadhyay, U. (2005). "Free heme toxicity and its detoxification systems in human." Toxicol Lett **157**(3): 175-188.

Laemmli, U. K. (1970). "Cleavage of structural proteins during the assembly of the head of bacteriophage T4." Nature **227**(5259): 680-685.

Lambert, C. B., Spire, C., Claude, N. and Guillouzo, A. (2009). "Dose- and time-dependent effects of phenobarbital on gene expression profiling in human hepatoma HepaRG cells." Toxicol Appl Pharm **234**(3): 345-360.

Lamond, A. I. (2002). "Molecular biology of the cell, 4th edition." Nature **417**(6887): 383-383.

LeCluyse, E. L., Audus, K. L. and Hochman, J. H. (1994). "Formation of extensive canalicular networks by rat hepatocytes cultured in collagen-sandwich configuration." Am J Physiol **266**(6 Pt 1): C1764-1774.

Li, D. L., Wang, X., Liu, B., Liu, Y. Z., Zeng, Z. Y., Lu, L. L., Zheng, Z. Y., Li, B. and Zheng, Z. F. (2014). "Exercises in Hot and Humid Environment Caused Liver Injury in a Rat Model." PLoS One **9**(12).

Li, S., Tan, H. Y., Wang, N., Zhang, Z. J., Lao, L. X., Wong, C. W. and Feng, Y. B. (2015). "The Role of Oxidative Stress and Antioxidants in Liver Diseases." Int J Mol Sci **16**(11): 26087-26124.

Li, Y., Wongsiriroj, N. and Blaner, W. S. (2014). "The multifaceted nature of retinoid transport and metabolism." Hepatobiliary Surg Nutr **3**(3): 126-139.

Li, Y., Yao, J., Han, C., Yang, J., Chaudhry, M. T., Wang, S., Liu, H. and Yin, Y. (2016). "Quercetin, Inflammation and Immunity." Nutrients **8**(3): 167.

Lilienblum, W., Dekant, W., Foth, H., Gebel, T., Hengstler, J. G., Kahl, R., Kramer, P. J., Schweinfurth, H. and Wollin, K. M. (2008). "Alternative methods to safety studies in experimental animals: role in the risk assessment of chemicals under the new European Chemicals Legislation (REACH)." Arch Toxicol **82**(4): 211-236.

Lilley, K. S. and Friedman, D. B. (2004). "All about DIGE: quantification technology for differential-display 2D-gel proteomics." Expert Rev Proteomics **1**(4): 401-409.

Lipsky, M. S. (2015). "Biological theories of aging." Dm-Dis Mon **61**(11): 460-466.

Lipton, J. O. and Sahin, M. (2014). "The neurology of mTOR." Neuron **84**(2): 275-291.

Liu, J. X., Li, D., Zhang, T., Tong, Q., Ye, R. D. and Lin, L. G. (2017). "SIRT3 protects hepatocytes from oxidative injury by enhancing ROS scavenging and mitochondrial integrity." Cell Death Dis **8**.

Liu, S., Hou, W., Yao, P., Zhang, B., Sun, S., Nussler, A. K. and Liu, L. (2010). "Quercetin protects against ethanol-induced oxidative damage in rat primary hepatocytes." Toxicol In Vitro **24**(2): 516-522.

Liu, S., Hou, W., Yao, P., Zhang, B. Y., Sun, S. S., Nussler, A. K. and Liu, L. G. (2010). "Quercetin protects against ethanol-induced oxidative damage in rat primary hepatocytes." Toxicol in Vitro **24**(2): 516-522.

Lobo, V., Patil, A., Phatak, A. and Chandra, N. (2010). "Free radicals, antioxidants and functional foods: Impact on human health." Pharmacogn Rev **4**(8): 118-126.

Locksley, R. M., Killeen, N. and Lenardo, M. J. (2001). "The TNF and TNF receptor superfamilies: Integrating mammalian biology." Cell **104**(4): 487-501.

Lopez-Otin, C., Blasco, M. A., Partridge, L., Serrano, M. and Kroemer, G. (2013). "The Hallmarks of Aging." Cell **153**(6): 1194-1217.

Magdeldin, S., Enany, S., Yoshida, Y., Xu, B., Zhang, Y., Zureena, Z., Lokamani, I., Yaoita, E. and Yamamoto, T. (2014). "Basics and recent advances of two dimensional-polyacrylamide gel electrophoresis." Clin Proteom **11**.

Maher, J. J. and Friedman, S. L. (1993). "Parenchymal and Nonparenchymal Cell-Interactions in the Liver." Semin Liver Dis **13**(1): 13-20.

Mahmoudi, G. A., Astaraki, P., Mohtashami, A. Z. and Ahadi, M. (2015). "N-acetylcysteine overdose after acetaminophen poisoning." Int Med Case Rep J **8**: 65-69.

Mann, M. (2006). "Functional and quantitative proteomics using SILAC." Nat Rev Mol Cell Biol **7**(12): 952-958.

Manov, I., Hirsh, M. and Iancu, T. C. (2004). "N-acetylcysteine does not protect HepG2 cells against acetaminophen-induced apoptosis." Basic Clin Pharmacol **94**(5): 213-225.

Manthey, K. C., Chew, Y. C. and Zempleni, J. (2005). "Riboflavin deficiency impairs oxidative folding and secretion of apolipoprotein B-100 in HepG2 cells, triggering stress response systems." J Nutr **135**(5): 978-982.

Martignoni, M., Groothuis, G. M. M. and de Kanter, R. (2006). "Species differences between mouse, rat, dog, monkey and human CYP-mediated drug metabolism, inhibition and induction." Expert Opin Drug Met **2**(6): 875-894.

Medvedik, O., Lamming, D. W., Kim, K. D. and Sinclair, D. A. (2007). "MSN2 and MSN4 link calorie restriction and TOR to sirtuin-mediated lifespan extension in Saccharomyces cerevisiae." PLoS Biol **5**(10): e261.

Meister, A. (1988). "Glutathione Metabolism and Its Selective Modification." J Biol Chem **263**(33): 17205-17208.

Meng, C. K., Mann, M. and Fenn, J. B. (1988). "Of Protons or Proteins - a Beams a Beam for a That (Burns,O.S.)." Z Phys D Atom Mol Cl **10**(2-3): 361-368.

Mercado, N., Ito, K. and Barnes, P. J. (2015). "Accelerated ageing of the lung in COPD: new concepts." Thorax **70**(5): 482-489.

Merk, M., Zierow, S., Leng, L., Das, R., Du, X., Schulte, W., Fan, J., Lue, H., Chen, Y., Xiong, H., Chagnon, F., Bernhagen, J., Lolis, E., Mor, G., Lesur, O. and Bucala, R. (2011). "The D-dopachrome tautomerase (DDT) gene product is a cytokine and functional homolog of macrophage migration inhibitory factor (MIF)." Proc Natl Acad Sci U S A **108**(34): E577-585.

Michiels, C., Raes, M., Toussaint, O. and Remacle, J. (1994). "Importance of Se-Glutathione Peroxidase, Catalase, and Cu/Zn-Sod for Cell-Survival against Oxidative Stress." Free Radical Bio Med **17**(3): 235-248.

Mirzaei, M., Gupta, V. B., Chick, J. M., Greco, T. M., Wu, Y. Q., Chitranshi, N., Vander Wall, R., Hone, E., Deng, L. T., Dheer, Y., Abbasi, M., Rezaeian, M., Braidy, N., You, Y. Y., Salekdeh, G. H., Haynes, P. A., Molloy, M. P., Martins, R., Cristea, I. M., Gygi, S. P., Graham, S. L. and Gupta, V. K. (2017). "Age-related neurodegenerative disease associated pathways identified in retinal and vitreous proteome from human glaucoma eyes." Sci Rep **7**.

Miyata, M. and Smith, J. D. (1996). "Apolipoprotein E allele-specific antioxidant activity and effects on cytotoxicity by oxidative insults and beta-amyloid peptides." Nat Genet **14**(1): 55-61.

Mori, K., Blackshear, P. E., Lobenhofer, E. K., Parker, J. S., Orzech, D. P., Roycroft, J. H., Walker, K. L., Johnson, K. A., Marsh, T. A., Irwin, R. D. and Boorman, G. A. (2007). "Hepatic transcript levels for genes coding for enzymes associated with xenobiotic metabolism are altered with age." Toxicol Pathol **35**(2): 242-251.

Mujahid, A., Sato, K., Akiba, Y. and Toyomizu, M. (2006). "Acute heat stress stimulates mitochondrial superoxide production in broiler skeletal muscle, possibly via downregulation of uncoupling protein content." Poult Sci **85**(7): 1259-1265.

Müller, D., Kramer, L., Hoffmann, E., Klein, S. and Noor, F. (2014). "3D organotypic HepaRG cultures as in vitro model for acute and repeated dose toxicity studies." Toxicol In Vitro **28**(1): 104-112.

Muller, F. L., Lustgarten, M. S., Jang, Y., Richardson, A. and Van Remmen, H. (2007). "Trends in oxidative aging theories." Free Radical Bio Med **43**(4): 477-503.

Mustafi, S. B., Chakraborty, P. K., Dey, R. S. and Raha, S. (2009). "Heat stress upregulates chaperone heat shock protein 70 and antioxidant manganese superoxide dismutase through reactive oxygen species (ROS), p38MAPK, and Akt." Cell Stress Chaperon **14**(6): 579-589.

Nagai, N., Nakai, A. and Nagata, K. (1995). "Quercetin suppresses heat shock response by down regulation of HSF1." Biochem Biophys Res Commun **208**(3): 1099-1105.

Nakagawa, T., Lomb, D. J., Haigis, M. C. and Guarente, L. (2009). "SIRT5 Deacetylates carbamoyl phosphate synthetase 1 and regulates the urea cycle." Cell **137**(3): 560-570.

Natarajan, S. S., Krishnan, H. B., Lakshman, S. and Garrett, W. M. (2009). "An efficient extraction method to enhance analysis of low abundant proteins from soybean seed." Anal Biochem **394**(2): 259-268.

Nathan, C. and Ding, A. H. (2010). "SnapShot: Reactive Oxygen Intermediates (ROI)." Cell **140**(6).

Neumann, C. A., Krause, D. S., Carman, C. V., Das, S., Dubey, D. P., Abraham, J. L., Bronson, R. T., Fujiwara, Y., Orkin, S. H. and Van Etten, R. A. (2003). "Essential role for the peroxiredoxin Prdx1 in erythrocyte antioxidant defence and tumour suppression." Nature **424**(6948): 561-565.

Nickel, W. and Seedorf, M. (2008). "Unconventional mechanisms of protein transport to the cell surface of eukaryotic cells." Annu Rev Cell Dev Biol **24**: 287-308.

Nkuipou-Kenfack, E., Koeck, T., Mischak, H., Pich, A., Schanstra, J. P., Zurbig, P. and Schumacher, B. (2014). "Proteome analysis in the assessment of ageing." Ageing Res Rev **18**: 74-85.

Nussler, A., Konig, S., Ott, M., Sokal, E., Christ, B., Thasler, W., Brulport, M., Gabelein, G., Schormann, W., Schulze, M., Ellis, E., Kraemer, M., Nocken, F., Fleig, W., Manns, M., Strom, S. C. and Hengstler, J. G. (2006). "Present status and perspectives of cell-based therapies for liver diseases." J Hepatol **45**(1): 144-159.

O'Farrell, P. H. (1975). "High resolution two-dimensional electrophoresis of proteins." J Biol Chem **250**(10): 4007-4021.

Omiya, S., Hikoso, S. and Otsu, K. (2009). "Downregulation of Ferritin Heavy Chain Increases Labile Iron Pool, Oxidative Stress and Cell Death in Cardiomyocytes." J Physiol Sci **59**: 315-315.

Ong, S. E., Blagoev, B., Kratchmarova, I., Kristensen, D. B., Steen, H., Pandey, A. and Mann, M. (2002). "Stable isotope labeling by amino acids in cell culture, SILAC, as a simple and accurate approach to expression proteomics." Mol Cell Proteomics **1**(5): 376-386.

Orsini, M., Sperber, S., Noor, F., Hoffmann, E., Weber, S. N., Hall, R. A., Lammert, F. and Heinzle, E. (2018). "Proteomic Characterization of Primary Mouse Hepatocytes in Collagen Monolayer and Sandwich Culture." J Cell Biochem **119**(1): 447-454.

Ortuno-Sahagun, D., Pallas, M. and Rojas-Mayorquin, A. E. (2014). "Oxidative Stress in Aging: Advances in Proteomic Approaches." Oxid Med Cell Longev **2014**(1): 573208.

Pan, C., Zhou, Y., Dator, R., Ginghina, C., Zhao, Y., Movius, J., Peskind, E., Zabetian, C. P., Quinn, J., Galasko, D., Stewart, T., Shi, M. and Zhang, J. (2014). "Targeted discovery and validation of plasma biomarkers of Parkinson's disease." J Proteome Res **13**(11): 4535-4545.

Pawlowska-Goral, K., Kurzeja, E. and Stec, M. (2013). "N-acetylcysteine protects against fluoride-induced oxidative damage in primary rat hepatocytes." Toxicol In Vitro **27**(8): 2279-2282.

Payne, B. A. I. and Chinnery, P. F. (2015). "Mitochondrial dysfunction in aging: Much progress but many unresolved questions." Bba-Bioenergetics **1847**(11): 1347-1353.

Perez-Vizcaino, F. and Duarte, J. (2010). "Flavonols and cardiovascular disease." Mol Aspects Med **31**(6): 478-494.

Perez, L. M., Milkiewicz, P., Ahmed-Choudhury, J., Elias, E., Ochoa, J. E., Sanchez Pozzi, E. J., Coleman, R. and Roma, M. G. (2006). "Oxidative stress induces actin-cytoskeletal and tight-junctional alterations in hepatocytes by a Ca2+ -dependent, PKC-mediated mechanism: protective effect of PKA." Free Radic Biol Med **40**(11): 2005-2017.

Perkins, D. N., Pappin, D. J., Creasy, D. M. and Cottrell, J. S. (1999). "Probability-based protein identification by searching sequence databases using mass spectrometry data." Electrophoresis **20**(18): 3551-3567.

Pertoft, H., Laurent, T. C., Laas, T. and Kagedal, L. (1978). "Density gradients prepared from colloidal silica particles coated by polyvinylpyrrolidone (Percoll)." Anal Biochem **88**(1): 271-282.

Pessayre, D., Fromenty, B., Berson, A., Robin, M. A., Letteron, P., Moreau, R. and Mansouri, A. (2012). "Central role of mitochondria in drug-induced liver injury." Drug Metab Rev **44**(1): 34-87.

Phaniendra, A., Jestadi, D. B. and Periyasamy, L. (2015). "Free Radicals: Properties, Sources, Targets, and Their Implication in Various Diseases." Indian J Clin Biochem **30**(1): 11-26.

Pillay, C. S., Hofmeyr, J. H. S., Olivier, B. G., Snoep, J. L. and Rohwer, J. M. (2009). "Enzymes or redox couples? The kinetics of thioredoxin and glutaredoxin reactions in a systems biology context." Biochem J **417**: 269-275.

Poisson, J., Lemoinne, S., Boulanger, C., Durand, F., Moreau, R., Valla, D. and Rautou, P. E. (2017). "Liver sinusoidal endothelial cells: Physiology and role in liver diseases." J Hepatol **66**(1): 212-227.

Poljsak, B., Suput, D. and Milisav, I. (2013). "Achieving the Balance between ROS and Antioxidants: When to Use the Synthetic Antioxidants." Oxid Med Cell Longev **2013**(1): 956792.

Poon, H. F., Castegna, A., Farr, S. A., Thongboonkerd, V., Lynn, B. C., Banks, W. A., Morley, J. E., Klein, J. B. and Butterfield, D. A. (2004). "Quantitative proteomics analysis of specific protein expression and oxidative modification in aged senescence-accelerated-prone 8 mice brain." Neuroscience **126**(4): 915-926.

Powers, R. W., 3rd, Kaeberlein, M., Caldwell, S. D., Kennedy, B. K. and Fields, S. (2006). "Extension of chronological life span in yeast by decreased TOR pathway signaling." Genes Dev **20**(2): 174-184.

Prestes, C. C., Sgaravatti, A. M., Pederzolli, C. D., Sgarbi, M. B., Zorzi, G. K., Wannmacher, C. M., Wajner, M., Wyse, A. T. and Dutra Filho, C. S. (2006). "Citrulline and ammonia accumulating in citrullinemia reduces antioxidant capacity of rat brain in vitro." Metab Brain Dis **21**(1): 63-74.

Prewit, E. B. (2018). "The effect of gestational diabetes mellitus on the plasma proteome of children at 5-10 years of age." Am J Obstet Gynecol **218**(1): S57-S57.

Priesnitz, C., Sperber, S., Garg, R., Orsini, M. and Noor, F. (2016). "Fluorescence based cell counting in collagen monolayer cultures of primary hepatocytes." Cytotechnology **68**(4): 1647-1653.

Qian, L. J., Song, X. L., Ren, H. R., Gong, J. B. and Cheng, S. Q. (2004). "Mitochondrial mechanism of heat stress-induced injury in rat cardiomyocyte." Cell Stress Chaperon **9**(3): 281-293.

Qian, W. J., Monroe, M. E., Liu, T., Jacobs, J. M., Anderson, G. A., Shen, Y. F., Moore, R. J., Anderson, D. J., Zhang, R., Calvano, S. E., Lowry, S. F., Xiao, W. Z., Moldawer, L. L., Davis, R. W., Tompkins, R. G., Camp, D. G., Smith, R. D. and Injury, I. H. R. (2005). "Quantitative proteome analysis of human plasma following in vivo lipopolysaccharide administration using O-16/O-18 labeling and the accurate mass and time tag approach." Mol Cell Proteomics **4**(5): 700-709.

Qin, X., Swertfeger, D. K., Zheng, S., Hui, D. Y. and Tso, P. (1998). "Apolipoprotein AIV: a potent endogenous inhibitor of lipid oxidation." Am J Physiol **274**(5 Pt 2): H1836-1840.

Rahman, I., Kode, A. and Biswas, S. K. (2006). "Assay for quantitative determination of glutathione and glutathione disulfide levels using enzymatic recycling method." Nat Protoc **1**(6): 3159-3165.

Ray, P. D., Huang, B. W. and Tsuji, Y. (2012). "Reactive oxygen species (ROS) homeostasis and redox regulation in cellular signaling." Cell Signal **24**(5): 981-990.

Rhee, S. G., Kang, S. W., Chang, T. S., Jeong, W. and Kim, K. (2001). "Peroxiredoxin, a novel family of peroxidases." IUBMB Life **52**(1-2): 35-41.

Richert, L., Binda, D., Hamilton, G., Viollon-Abadie, C., Alexandre, E., Bigot-Lasserre, D., Bars, R., Coassolo, P. and LeCluyse, E. (2002). "Evaluation of the effect of culture configuration on morphology, survival time, antioxidant status and metabolic capacities of cultured rat hepatocytes." Toxicol in Vitro **16**(1): 89-99.

Ricoult, S. J. H. and Manning, B. D. (2013). "The multifaceted role of mTORC1 in the control of lipid metabolism." Embo Reports **14**(3): 242-251.

Robida-Stubbs, S., Glover-Cutter, K., Lamming, D. W., Mizunuma, M., Narasimhan, S. D., Neumann-Haefelin, E., Sabatini, D. M. and Blackwell, T. K. (2012). "TOR signaling and rapamycin influence longevity by regulating SKN-1/Nrf and DAF-16/FoxO." Cell Metab **15**(5): 713-724.

Rowe, C., Goldring, C. E., Kitteringham, N. R., Jenkins, R. E., Lane, B. S., Sanderson, C., Elliott, V., Platt, V., Metcalfe, P. and Park, B. K. (2010). "Network analysis of primary hepatocyte dedifferentiation using a shotgun proteomics approach." J Proteome Res **9**(5): 2658-2668.

Rubiolo, J. A., Mithieux, G. and Vega, F. V. (2008). "Resveratrol protects primary rat hepatocytes against oxidative stress damage: Activation of the Nrf2 transcription factor and augmented activities of antioxidant enzymes." Eur J Pharmacol **591**(1-3): 66-72.

Sakurai, K. and Cederbaum, A. I. (1998). "Oxidative stress and cytotoxicity induced by ferric-nitrilotriacetate in HepG2 cells that express cytochrome P450 2E1." Mol Pharmacol **54**(6): 1024-1035.

Sanchez-Hidalgo, J. M., Naranjo, A., Ciria, R., Ranchal, I., Aguilar-Melero, P., Ferrin, G., Valverde, A., Rufian, S., Lopez-Cillero, P., Muntane, J. and Briceno, J. (2012). "Impact of Age on Liver Regeneration Response to Injury After Partial Hepatectomy in a Rat Model." J Surg Res **175**(1): E1-E9.

Santus, P., Corsico, A., Solidoro, P., Braido, F., Di Marco, F. and Scichilone, N. (2014). "Oxidative Stress and Respiratory System: Pharmacological and Clinical Reappraisal of N-Acetylcysteine." Copd **11**(6): 705-717.

Sanz, N., Diez-Fernandez, C., Alvarez, A. and Cascales, M. (1997). "Age-dependent modifications in rat hepatocyte antioxidant defense systems." J Hepatol **27**(3): 525-534.

Sato, Y., Amano, A., Kishimoto, Y., Takahashi, K., Handa, S., Maruyama, N. and Ishigami, A. (2014). "Ascorbic acid prevents protein oxidation in livers of senescence marker protein-30/gluconolactonase knockout mice." Geriatr Gerontol Int **14**(4): 989-995.

Scarmeas, N., Luchsinger, J. A., Mayeux, R. and Stern, Y. (2007). "Mediterranean diet and Alzheimer disease mortality." Neurology **69**(11): 1084-1093.

Schanstra, J. P. and Mischak, H. (2015). "Proteomic urinary biomarker approach in renal disease: from discovery to implementation." Pediatr Nephrol **30**(5): 713-725.

Schmucker, D. L. (1990). "Hepatocyte fine structure during maturation and senescence." J Electron Microsc Tech **14**(2): 106-125.

Schriner, S. E., Linford, N. J., Martin, G. M., Treuting, P., Ogburn, C. E., Emond, M., Coskun, P. E., Ladiges, W., Wolf, N., Van Remmen, H., Wallace, D. C. and Rabinovitch, P. S. (2005). "Extension of murine life span by overexpression of catalase targeted to mitochondria." Science **308**(5730): 1909-1911.

Schug, M., Heise, T., Bauer, A., Storm, D., Blaszkewicz, M., Bedawy, E., Brulport, M., Geppert, B., Hermes, M., Follmann, W., Rapp, K., Maccoux, L., Schormann, W., Appel, K. E., Oberemm, A., Gundert-Remy, U. and Hengstler, J. G. (2008). "Primary rat hepatocytes as in vitro system for gene expression studies: comparison of sandwich, Matrigel and 2D cultures." Arch Toxicol **82**(12): 923-931.

Selvaratnam, J. and Robaire, B. (2016). "Overexpression of catalase in mice reduces age-related oxidative stress and maintains sperm production." Exp Gerontol **84**: 12-20.

Sena, L. A., Li, S., Jairaman, A., Prakriya, M., Ezponda, T., Hildeman, D. A., Wang, C. R., Schumacker, P. T., Licht, J. D., Perlman, H., Bryce, P. J. and Chandel, N. S. (2013). "Mitochondria Are Required for Antigen-Specific T Cell Activation through Reactive Oxygen Species Signaling." Immunity **38**(2): 225-236.

Sesso, H. D., Buring, J. E., Christen, W. G., Kurth, T., Belanger, C., MacFadyen, J., Bubes, V., Manson, J. E., Glynn, R. J. and Gaziano, J. M. (2008). "Vitamins E and C in the prevention of cardiovascular disease in men: the Physicians' Health Study II randomized controlled trial." JAMA **300**(18): 2123-2133.

Shambaugh, G. E., 3rd (1977). "Urea biosynthesis I. The urea cycle and relationships to the citric acid cycle." Am J Clin Nutr **30**(12): 2083-2087.

Sharov, V. S. and Schoneich, C. (2007). "Proteomic approach to aging research." Exp Rev Proteomic **4**(2): 309-321.

Shen, S. Q., Zhang, Y., Xiang, J. J. and Xiong, C. L. (2007). "Protective effect of curcumin against liver warm ischemia/reperfusion injury in rat model is associated with regulation of heat shock protein and antioxidant enzymes." World J Gastroentero **13**(13): 1953-1961.

Shenvi, S. V., Dixon, B. M., Petersen Shay, K. and Hagen, T. M. (2008). "A rat primary hepatocyte culture model for aging studies." Curr Protoc Toxicol **Chapter 14**: Unit 14 17.

Si-Tayeb, K., Lemaigre, F. P. and Duncan, S. A. (2010). "Organogenesis and development of the liver." Dev Cell **18**(2): 175-189.

Slany, A., Haudek, V. J., Zwickl, H., Gundacker, N. C., Grusch, M., Weiss, T. S., Seir, K., Rodgarkia-Dara, C., Hellerbrand, C. and Gerner, C. (2010). "Cell characterization by proteome profiling applied to primary hepatocytes and hepatocyte cell lines Hep-G2 and Hep-3B." J Proteome Res **9**(1): 6-21.

Slimen, I. B., Najar, T., Ghram, A., Dabbebi, H., Ben Mrad, M. and Abdrabbah, M. (2014). "Reactive oxygen species, heat stress and oxidative-induced mitochondrial damage. A review." Int J Hyperther **30**(7): 513-523.

Soldatow, V. Y., Lecluyse, E. L., Griffith, L. G. and Rusyn, I. (2013). "In vitro models for liver toxicity testing." Toxicol Res (Camb) **2**(1): 23-39.

Song, G., Cui, Y., Zhong, N. and Han, J. (2009). "Proteomic characterisation of pancreatic islet beta-cells stimulated with pancreatic carcinoma cell conditioned medium." J Clin Pathol **62**(9): 802-807.

Speakman, J. R. and Selman, C. (2011). "The free-radical damage theory: Accumulating evidence against a simple link of oxidative stress to ageing and lifespan." Bioessays **33**(4): 255-259.

Sperber, S. (2016). "Metabolic and proteomic characterization of primary hepatocytes in different in vitro cultivation conditions " Naturwissenschaftlich-Technische Fakultät der Universität des Saarlandes **PhD**(Dissertation): p. 46-47.

Srisomsap, C., Sawangareetrakul, P., Subhasitanont, P., Chokchaichamnankit, D., Chiablaem, K., Bhudhisawasdi, V., Wongkham, S. and Svasti, J. (2010). "Proteomic studies of cholangiocarcinoma and hepatocellular carcinoma cell secretomes." J Biomed Biotechnol **2010**: 437143.

Stanfel, M. N., Shamieh, L. S., Kaeberlein, M. and Kennedy, B. K. (2009). "The TOR pathway comes of age." Biochim Biophys Acta **1790**(10): 1067-1074.

Starkov, A. A. (2008). "The Role of Mitochondria in Reactive Oxygen Species Metabolism and Signaling." Ann Ny Acad Sci **1147**: 37-52.

Steinberg, T. H. (2009). "Protein Gel Staining Methods: An Introduction and Overview." G Prot Pur **463**: 541-563.

Swardfager, W., Lanctot, K., Rothenburg, L., Wong, A., Cappell, J. and Herrmann, N. (2010). "A Meta-Analysis of Cytokines in Alzheimer's Disease." Biol Psych **68**(10): 930-941.

Szatrowski, T. P. and Nathan, C. F. (1991). "Production of Large Amounts of Hydrogen-Peroxide by Human Tumor-Cells." Cancer Res **51**(3): 794-798.

Tabak, C., Arts, I. C. W., Smit, H. A., Heederik, D. and Kromhout, D. (2001). "Chronic obstructive pulmonary disease and intake of catechins, flavonols, and flavones - The MORGEN Study." Am J Resp Crit Care **164**(1): 61-64.

Tang, Y. H., Li, J., Gao, C., Xu, Y. Y., Li, Y. Y., Yu, X., Wang, J., Liu, L. G. and Yao, P. (2016). "Hepatoprotective Effect of Quercetin on Endoplasmic Reticulum Stress and Inflammation after Intense Exercise in Mice through Phosphoinositide 3-Kinase and Nuclear Factor-Kappa B." Oxid Med Cell Longev **2016**(4): 1-12.

Tarnus, E., Wassef, H., Carmel, J. F., Rondeau, P., Roche, M., Davignon, J., Bernier, L. and Bourdon, E. (2009). "Apolipoprotein E limits oxidative stress-induced cell dysfunctions in human adipocytes." FEBS Lett **583**(12): 2042-2048.

Tjalsma, H., Bolhuis, A., Jongbloed, J. D., Bron, S. and van Dijl, J. M. (2000). "Signal peptide-dependent protein transport in Bacillus subtilis: a genome-based survey of the secretome." Microbiol Mol Biol Rev **64**(3): 515-547.

To, Y., Ito, K., Kizawa, Y., Failla, M., Ito, M., Kusama, T., Elliott, W. M., Hogg, J. C., Adcock, I. M. and Barnes, P. J. (2010). "Targeting phosphoinositide-3-kinase-delta with theophylline reverses corticosteroid insensitivity in chronic obstructive pulmonary disease." Am J Respir Crit Care Med **182**(7): 897-904.

Toda, T. (2001). "Proteome and proteomics for the research on protein alterations in aging." Ann Ny Acad Sci **928**: 71-78.

Troen, B. R. (2003). "The biology of aging." Mt Sinai J Med **70**(1): 3-22.

Unlü, M., Morgan, M. E. and Minden, J. S. (1997). "Difference gel electrophoresis: a single gel method for detecting changes in protein extracts." Electrophoresis **18**(11): 2071-2077.

Urquiaga, I. and Leighton, F. (2000). "Plant polyphenol antioxidants and oxidative stress." Biol Res **33**(2): 55-64.

Verbeke, P., Clark, B. F. and Rattan, S. I. (2000). "Modulating cellular aging in vitro: hormetic effects of repeated mild heat stress on protein oxidation and glycation." Exp Gerontol **35**(6-7): 787-794.

Vina, J., Borras, C. and Miquel, J. (2007). "Theories of ageing." IUBMB Life **59**(4-5): 249-254.

Vinchi, F., Gastaldi, S., Silengo, L., Altruda, F. and Tolosano, E. (2008). "Hemopexin prevents endothelial damage and liver congestion in a mouse model of heme overload." Am J Pathol **173**(1): 289-299.

Vinken, M., Papeleu, P., Snykers, S., De Rop, E., Henkens, T., Chipman, J. K., Rogiers, V. and Vanhaecke, T. (2006). "Involvement of cell junctions in hepatocyte culture functionality." Crit Rev Toxicol **36**(4): 299-318.

Wach, A., Pyrzynska, K. and Biesaga, M. (2007). "Quercetin content in some food and herbal samples." Food Chem **100**(2): 699-704.

Wasinger, V. C., Cordwell, S. J., Cerpapoljak, A., Yan, J. X., Gooley, A. A., Wilkins, M. R., Duncan, M. W., Harris, R., Williams, K. L. and Humpherysmith, I. (1995). "Progress with Gene-Product Mapping of the Mollicutes - Mycoplasma-Genitalium." Electrophoresis **16**(7): 1090-1094.

Westerink, W. M. A. and Schoonen, W. G. E. J. (2007). "Phase II enzyme levels in HepG2 cells and cryopreserved primary human hepatocytes and their induction in HepG2 cells." Toxicol in Vitro **21**(8): 1592-1602.

Wiemann, S. U., Satyanarayana, A., Tsahuridu, M., Tillmann, H. L., Zender, L., Klempnauer, J., Flemming, P., Franco, S., Blasco, M. A., Manns, M. P. and Rudolph, K. L. (2002). "Hepatocyte telomere shortening and senescence are general markers of human liver cirrhosis." Faseb J **16**(9): 935-942.

Wong-Ekkabut, J., Xu, Z. T., Triampo, W., Tang, I. M., Tieleman, D. P. and Monticelli, L. (2007). "Effect of lipid peroxidation on the properties of lipid bilayers: A molecular dynamics study." Biophys J **93**(12): 4225-4236.

Wu, G. Y., Fang, Y. Z., Yang, S., Lupton, J. R. and Turner, N. D. (2004). "Glutathione metabolism and its implications for health." J Nutr **134**(3): 489-492.

Yamaguchi, M. (2014). "Regucalcin as a potential biomarker for metabolic and neuronal diseases." Mol Cell Biochem **391**(1-2): 157-166.

Yamaguchi, M. and Yoshida, H. (1985). "Regulatory effect of calcium-binding protein isolated from rat liver cytosol on activation of fructose 1,6-diphosphatase by Ca2+-calmodulin." Chem Pharm Bull (Tokyo) **33**(10): 4489-4493.

Yasueda, A., Urushima, H. and Ito, T. (2016). "Efficacy and Interaction of Antioxidant Supplements as Adjuvant Therapy in Cancer Treatment: A Systematic Review." Integr Cancer Ther **15**(1): 17-39.

Yoon, J. S., Chae, M. K., Jang, S. Y., Lee, S. Y. and Lee, E. J. (2012). "Antifibrotic effects of quercetin in primary orbital fibroblasts and orbital fat tissue cultures of Graves' orbitopathy." Invest Ophthalmol Vis Sci **53**(9): 5921-5929.

Zanatta, A., Viegas, C. M., Hickmann, F. H., de Oliveira Monteiro, W., Sitta, A., de Moura Coelho, D., Vargas, C. R., Leipnitz, G. and Wajner, M. (2015). "Ornithine In Vivo Administration Disrupts Redox Homeostasis and Decreases Synaptic Na(+), K (+)-ATPase Activity in Cerebellum of Adolescent Rats: Implications for the Pathogenesis of

Hyperornithinemia-Hyperammonemia-Homocitrullinuria (HHH) Syndrome." Cell Mol Neurobiol **35**(6): 797-806.

Zanger, U. M. and Schwab, M. (2013). "Cytochrome P450 enzymes in drug metabolism: Regulation of gene expression, enzyme activities, and impact of genetic variation." Pharmacol Therapeut **138**(1): 103-141.

Zaragoza, A., Diez-Fernandez, C., Alvarez, A. M., Andres, D. and Cascales, M. (2000). "Effect of N-acetylcysteine and deferoxamine on endogenous antioxidant defense system gene expression in a rat hepatocyte model of cocaine cytotoxicity." Biochim Biophys Acta **1496**(2-3): 183-195.

Zeeh, J. and Platt, D. (2002). "The aging liver - Structural and functional changes and their consequences for drug treatment in old age." Gerontology **48**(3): 121-127.

Zeilinger, K., Freyer, N., Damm, G., Seehofer, D. and Knospel, F. (2016). "Cell sources for in vitro human liver cell culture models." Exp Biol Med **241**(15): 1684-1698.

Zhang, H. J., Xu, L. J., Drake, V. J., Xie, L. T., Oberley, L. W. and Kregel, K. C. (2003). "Heat-induced liver injury in old rats is associated with exaggerated oxidative stress and altered transcription factor activation." Faseb J **17**(12): 2293-+.

Zhang, Y. Q., Liu, Y. H., Walsh, M., Bokov, A., Ikeno, Y., Jang, Y. C., Perez, V. I., Van Remmen, H. and Richardson, A. (2016). "Liver specific expression of Cu/ZnSOD extends the lifespan of Sod1 null mice." Mech Ageing Dev **154**: 1-8.

Zhao, L., Buxbaum, J. N. and Reixach, N. (2013). "Age-related oxidative modifications of transthyretin modulate its amyloidogenicity." Biochemistry **52**(11): 1913-1926.

Zhao, P., Mao, J. M., Zhang, S. Y., Zhou, Z. Q., Tan, Y. and Zhang, Y. (2014). "Quercetin induces HepG2 cell apoptosis by inhibiting fatty acid biosynthesis." Oncol Lett **8**(2): 765-769.

Zhao, Q. L., Fujiwara, Y. and Kondo, T. (2006). "Mechanism of cell death induction by nitroxide and hyperthermia." Free Radic Biol Med **40**(7): 1131-1143.

Zhou, Y., Hileman, E. O., Plunkett, W., Keating, M. J. and Huang, P. (2003). "Free radical stress in chronic lymphocytic leukemia cells and its role in cellular sensitivity to ROS-generating anticancer agents." Blood **101**(10): 4098-4104.

Zhuang, Y. L., Ma, Q. Y., Guo, Y. and Sun, L. P. (2017). "Protective effects of rambutan (Nephelium lappaceum) peel phenolics on H2O2-induced oxidative damages in HepG2 cells and D-galactose induced aging mice." Food Chem Toxicol **108**: 554-562.

10. Supplementary Material

10.1 Chapter 3

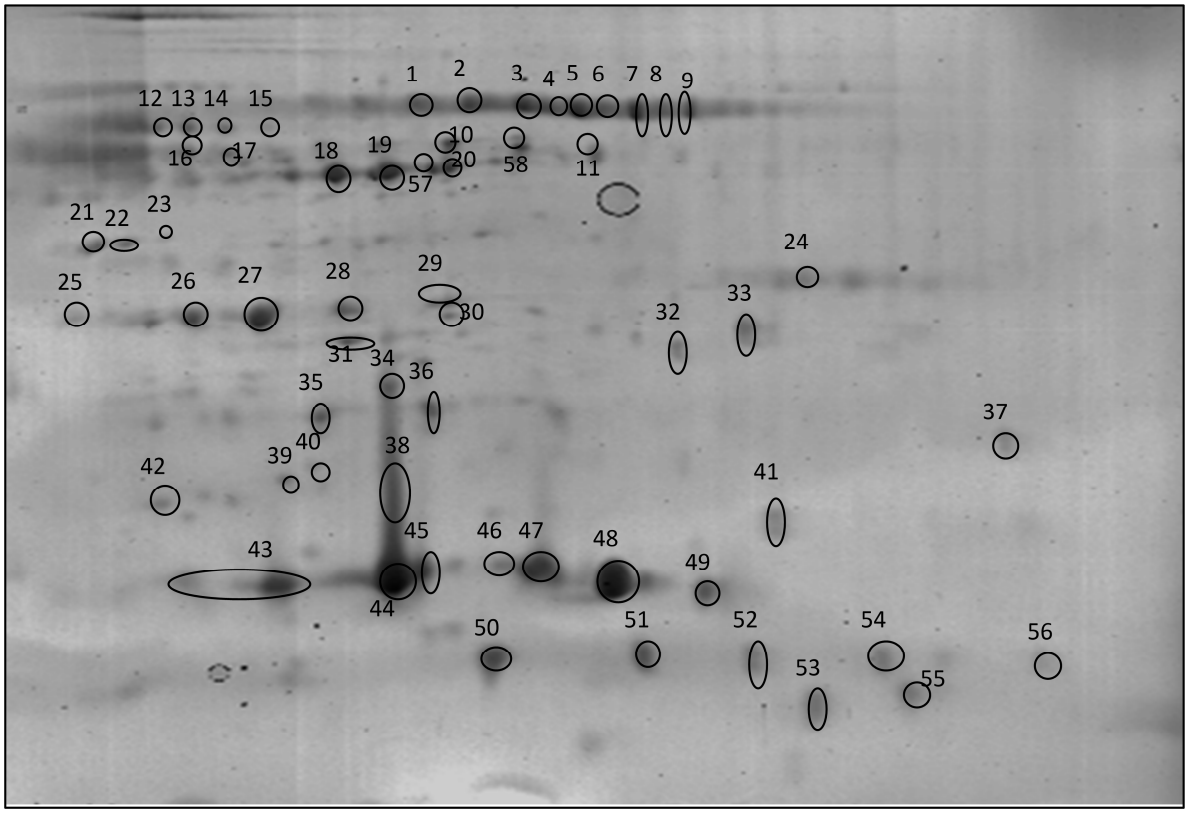

Supplementary Figure 3-1: 2-D gel electrophoresis of the extracellular proteome of primary rat hepatocytes. Protein separation was carried out with: 1. dimension - IPG strip 7 cm, pH 5-8, 2. dimension – 12.5% SDS gel. In total 58 proteins and protein isoforms could be identified with MALDI ToF MS/MS. Each spot is assigned to a protein in Supplementary Table 3-1.

Supplementary Table 3-1: List of all extracellular proteins of primary rat hepatocytes identified with MALDI ToF MS/MS. Spot numbers correlate to Supplementary Figure 3-1. Listed are protein name, Swiss-Prot accession number, secretion status and GO molecular function.

Spot no.	Swiss-Prot Accession no.	Protein	Secretion status	GO molecular function
1-9	P20059	**Hemopexin**	secreted	GO:0015232: heme transporter activity
10	Q9QX79	**Fetuin B**	secreted	GO:0008191: endopeptidase inhibitor activity
11	P04276	**Vitamin D-binding protein**	secreted	GO:0003779: actin binding GO:0005499: vitamin D-binding
12-15	Q6IMF3	**Keratin, Typ II cytoskeletal 1**	contamination from liver perfusion	GO:0005198: structural molecule activity
16	P01015	**Angiotensinogen**	secreted	GO:0005179: hormone activity GO:0007568: aging
17	Q4FZU2	**Keratin, Typ II cytoskeletal 6A**	contamination from liver perfusion	GO:0005198: structural molecule activity
18/19	Q03336	**Regucalcin**	secreted	GO:1901671: positive regulation of SOD activity GO:0030234: enzyme regulator activity GO:0007568: aging
20/57	P04276	**Vitamin D-binding protein**	secreted	GO:0003779: actin binding GO:0005499: vitamin D-binding
21	P00763	**Anionic trypsin-2**	secreted	GO:0004252: serine-type endopeptidase activity
22	P02651	**Apolipoprotein A-IV**	secreted	GO:0017127: cholesterol transporter activity
23	P00763	**Anionic trypsin-2**	secreted	GO:0004252: serine-type endopeptidase activity
24	P32755	**4-hydroxyphenylpyruvate dioxygenase**	not secreted	GO:0006559: L-phenylalanine catabolic process
25/26	P02650	**Apolipoprotein E**	secreted	GO:0005319: lipid transporter activity GO:0001315: age-dependent response to oxidative stress
27	P04276	**Vitamin D-binding protein**	secreted	GO:0003779: actin binding GO:0005499: vitamin D-binding

28	P46953	**3-hydroxyanthranilate 3,4-dioxygenase**	not secreted	GO:0009435: NAD biosynthetic process
29/30	P00762	**Anionic trypsin-1**	secreted	GO:0004252: serine-type endopeptidase activity
31	P46953	**3-hydroxyanthranilate 3,4-dioxygenase**	not secreted	GO:0009435: NAD biosynthetic process
32	Q03336	**Regucalcin**	not secreted	GO:1901671: positive regulation of SOD activity GO:0030234: enzyme regulator activity GO:0007568: aging
33	Q02974	**Ketohexokinase**	extracellular exosomes	GO:0016052: carbohydrate catabolic process
34	P02761	**Major urinary protein**	secreted	GO:0005550: pheromone binding
35/36	Q64240	**Protein AMBP**	secreted	GO:0004867: serine-type endopeptidase inhibitor activity
37	P70619	**Glutathione reductase**	extracellular exosomes	GO:0006979: response to oxidative stress
38	P02761	**Major urinary protein**	secreted	GO:0005550: pheromone binding
39	P31044	**Phosphatidylethanolamine-binding protein 1**	secreted	GO:0004252: serine-type endopeptidase activity GO:0007568: aging
40	P30152	**Neutrophil gelatinase-associated lipocalin**	secreted	GO:0006979: response to oxidative stress GO:0005215: transporter activity
41	P04916	**Retinol-binding protein 4**	secreted	GO:0005215: transporter activity
42	P02650	**Apolipoprotein E**	secreted	GO:0005319: lipid transporter activity GO:0007568: aging
43-47	P02761	**Major urinary protein**	secreted	GO:0005550: pheromone binding
48	P07632	**Superoxide dismutase [Cu-Zn]**	evidence for secretion via exosomes	GO:0006979: response to oxidative stress
49	D4A5I9	**Myosin-6**	extracellular exosomes	GO:0003774: motor activity
50	P80254	**D-dopachrome decarboxylase**	secreted	GO:0006954: inflammatory response GO:0042438: melanin biosynthetic process
51/52	P02767	**Transthyretin**	secreted	GO:0042562: hormone binding
53	P80254	**D-dopachrome decarboxylase**	secreted	GO:0006954: inflammatory response GO:0042438: melanin biosynthetic

				process
54/55	P02661	**Alpha-S1-casein**	secreted	GO:0005215: vitamin transporter activity
56	P52759	**Ribonuclease UK 114**	extracellular exosomes	GO:0016892:endoribonuclease activity
58	P53812	**Phosphatidylinositol transfer protein beta isoform**	not secreted	GO:0008289: lipid binding

Supplementary Table 3-2: List of all extracellular proteins of primary rat hepatocytes after 24 h of cultivation identified with MALDI ToF MS/MS. Listed are protein name, Swiss-Prot accession number, gene name, protein score and total ion score.

Swiss-Prot Accession no.	Protein Name	Gene Name	Protein Score	Ion Score
P46953	**3-hydroxyanthranilate 3,4-dioxygenase**	**HAAO**	210	108
P32755	**4-hydroxyphenylpyruvate dioxygenase**	**HPD**	256	127
P02661	**Alpha-S1-casein**	**CSN1S1**	348	340
P01015	**Angiotensinogen**	**AGT**	151	117
P00762	**Anionic trypsin-1**	**PRSS1**	92	87
P00763	**Anionic trypsin-2**	**PRSS2**	162	7
P02651	**Apolipoprotein A-IV**	**APOA4**	97	78
P02650	**Apolipoprotein E**	**APOE**	115	102
P80254	**D-dopachrome decarboxylase**	**DDT**	468	376
Q9QX79	**Fetuin B**	**FETUB**	86	62
P70619	**Glutathione reductase**	**GSR**	464	373
P20059	**Hemopexin**	**HPX**	619	551
Q6IMF3	**Keratin, Typ II cytoskeletal 1**	**KRT1**	98	89
Q4FZU2	**Keratin, Typ II cytoskeletal 6A**	**KRT6a**	72	65
Q02974	**Ketohexokinase**	**KHK**	391	323
P02761	**Major urinary protein**	**MUP**	329	226
D4A5I9	**Myosin-6**	**MYO6**	97	86
P30152	**Neutrophil gelatinase-associated lipocalin**	**LCN2**	187	173
P31044	**Phosphatidylethanolamine-binding protein 1**	**PEBP1**	355	295

P53812	**Phosphatidylinositol transfer protein beta isoform**	**PITPB**	83	78
Q64240	**Protein AMBP**	**AMBP**	205	124
Q03336	**Regucalcin**	**RGN**	303	166
P04916	**Retinol-binding protein 4**	**RBP4**	269	248
P52759	**Ribonuclease UK 114**	**RIDA**	200	149
P07632	**Superoxide dismutase [Cu-Zn]**	**SOD1**	363	319
P02767	**Transthyretin**	**TTR**	177	105
P04276	**Vitamin D-binding protein**	**GC**	455	373

10.2 Chapter 4

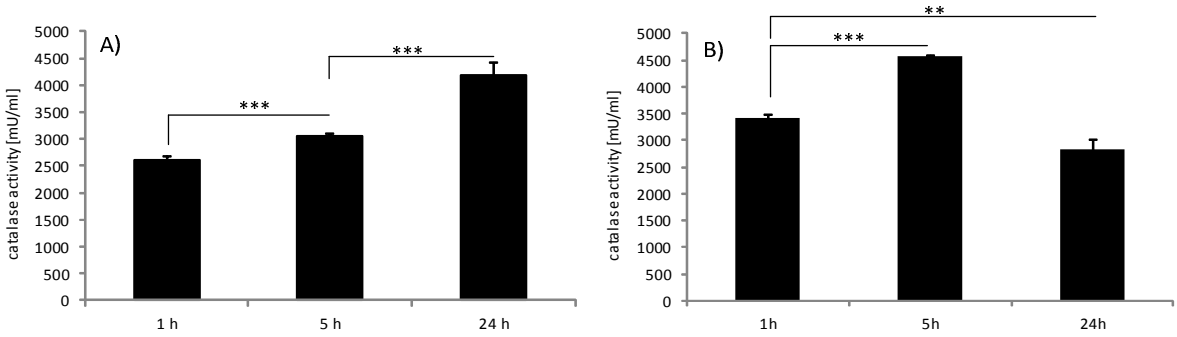

Supplementary Figure 4-1: Catalase activity in [mU/ml] of A) middle-aged Wistar PRH and B) *HepG2*, 1 h, 5 h and 24 h after the start of the cultivation at 37 °C. Error bars indicate standard deviation (PRH N=2, n=6; *HepG2*: n=3). Statistical significance was determined with student's t-test. *, ** and *** indicate significance at p=0.05, p=0.01 and p=0.001. All results were correlated to the living cell number after 1 h, 5 h and 24 h of cultivation determined using calcein AM staining.

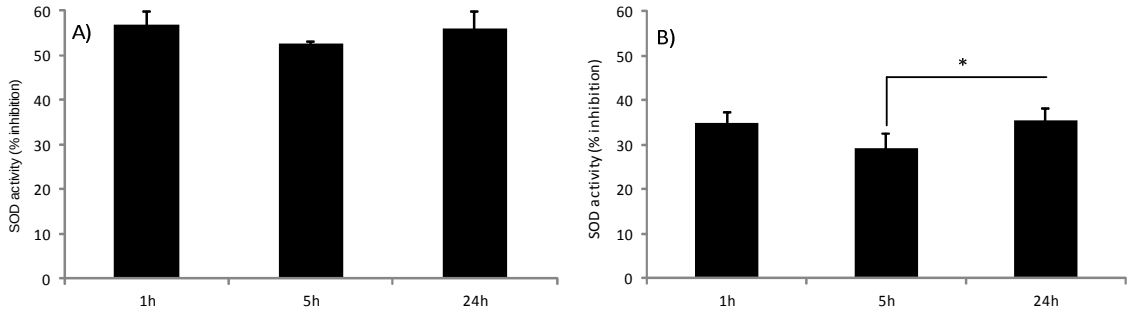

Supplementary Figure 4-2: SOD activity in [% inhibition [a]] of A) middle-aged Wistar PRH and B) HepG2, 1 h, 5 h and 24 h after the start of the cultivation at 37 °C. Error bars indicate standard deviation (PRH N=2, n=6; HepG2: n=3). Statistical significance was determined with student's t-test. *, ** and *** indicate significance at p=0.05, p=0.01 and p=0.001. All results were correlated to the living cell number after 1 h, 5 h and 24 h of cultivation determined using calcein AM staining.

[a] The SOD activity assay uses a xanthine/xanthine oxidase (XOD) system to generate superoxide anions. The included chromagen produces a water-soluble formazan dye upon reduction by superoxide anions. The activity of SOD is determined as the inhibition of chromagen reduction.

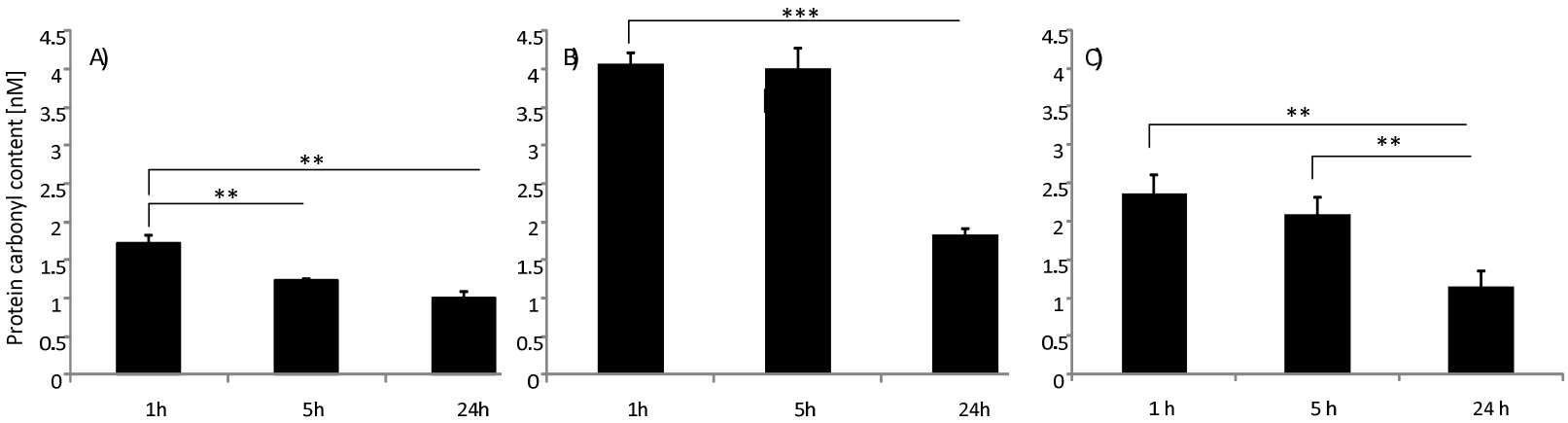

Supplementary Figure 4-3: Protein carbonyl content in A) Wistar 1, B) Wistar 2, C) *HepG2*, 1 h, 5 h and 24 h after the start of the cultivation at 37 °C. Error bars indicate standard deviation (PRH Wistar 1: n=3; PRH Wistar 2: n=3; *HepG2*: n=3). Statistical significance was determined with student's t-test. *, ** and *** indicate significance at p=0.05, p=0.01 and p=0.001. All results were correlated to the living cell number after 1 h, 5 h and 24 h of cultivation determined using calcein AM staining.

Supplementary Table 4-1: GSH/GSSG content [nmol/mg protein] of *HepG2* measured for control, heat stress (HS), hydrogen peroxide (H_2O_2) and the respective pre-treated cells with (Q) and NAC (N-acetylcysteine) 1 h, 5 h and 24 h after start of the experiment. The values represent average and standard deviation (SD) from 3 technical replicates (n = 3).

	1h		**5h**		**24h**	
	average	SD	average	SD	average	SD
control	37.6	1.2	35.5	2.7	36.7	1.7
control + Q	49.5	5.6	45.8	1.650	65.5	1.4
control + NAC	25.0	2.5	19.3	2.352	15.6	0.3
HS	6.8	0.6	14.0	2.0	11.9	1.0
HS + Q	16.7	2.0	23.3	3.9	14.5	0.8
HS + NAC	10.7	1.3	17.2	3.5	11.9	2.6
H_2O_2	46.8	6.6	61.2	1.3	61.7	3.9
H_2O_2 + Q	22.2	2.6	26.7	1.4	28.8	3.3
H_2O_2 + NAC	11.4	1.8	24.3	0.9	28.4	0.5

Supplementary Table 4-2: LDH leakage [mU/1E6 cells] of Wistar 2 measured for control, heat stress (HS) and hydrogen peroxide (H_2O_2) 1 h, 5 h and 24 h after start of the experiment. The values represent average and standard deviation from 3 technical replicates (n = 3).

	1h		**5h**		**24h**	
	Wistar 1	Wistar 2	Wistar 1	Wistar 2	Wistar 1	Wistar 2
control	5.63 ± 0.92	27.80 ± 1.22	10.40 ± 2.21	46.58 ± 2.66	16.86 ± 1.56	135.47 ± 17.80
HS	7.13 ± 1.98	33.42 ± 3.93	21.27 ± 4.42	68.18 ± 7.20	31.60 ± 4.46	152.19 ± 8.48
H_2O_2	7.58 ± 0.55	27.23 ± 2.47	10.22 ± 0.16	60.50 ± 11.48	17.19 ± 0.40	176.58 ± 20.42

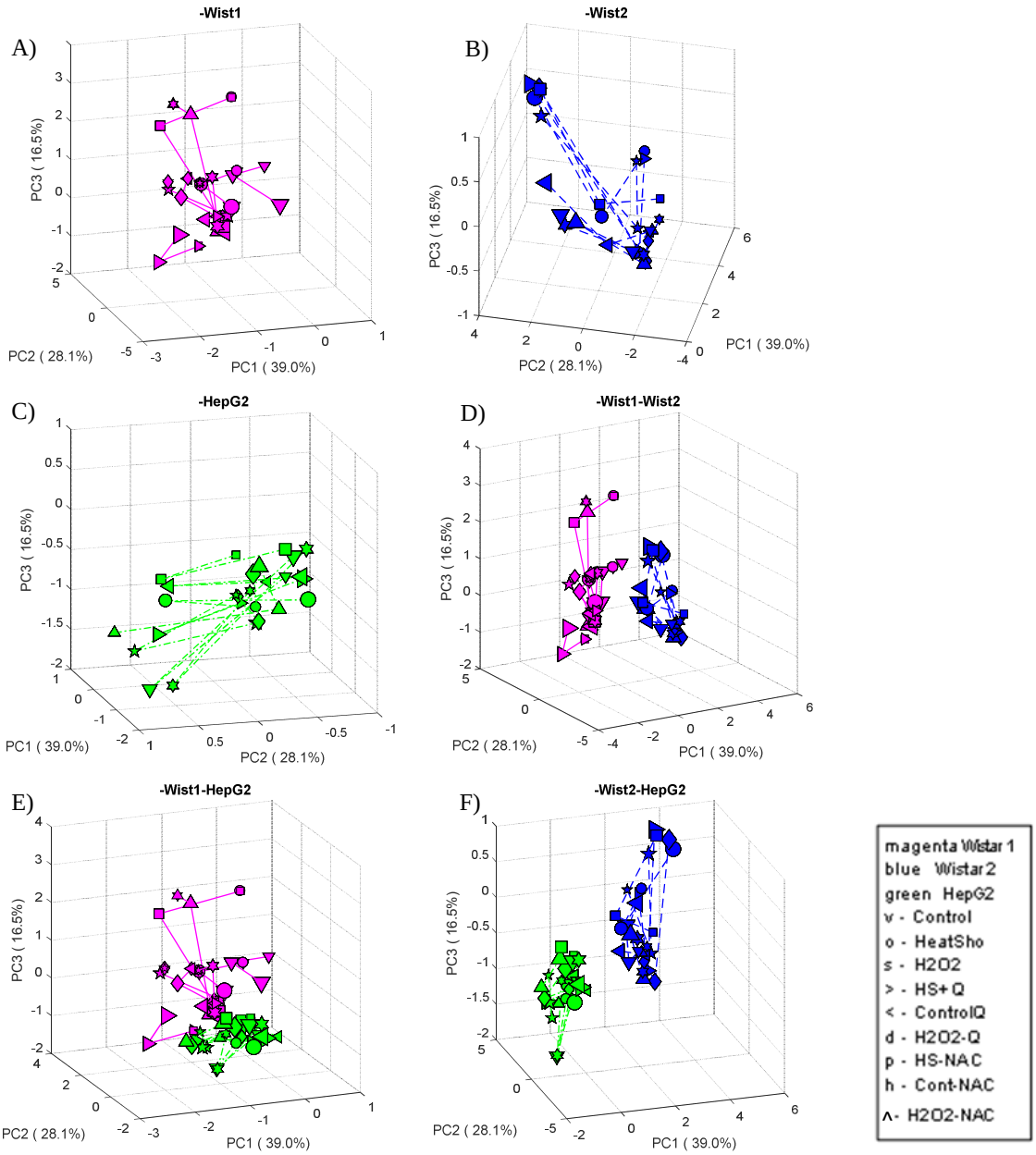

Supplementary Figure 4-4: Principal component analysis of the assay data for albumin, LDH, ROS, protein oxidation, GSH/GSSG, catalase and SOD from PRH of A) Wistar 1, B) Wistar 2 and C) *HepG2* (green) (n=3). D) shows the direct comparison of Wistar 1 and Wistar 2, E) the comparison between Wistar 1 and *HepG2* and F) the comparison between Wistar 2 and *HepG2*. Increasing size of the data symbol represents the progressing time after treatment.

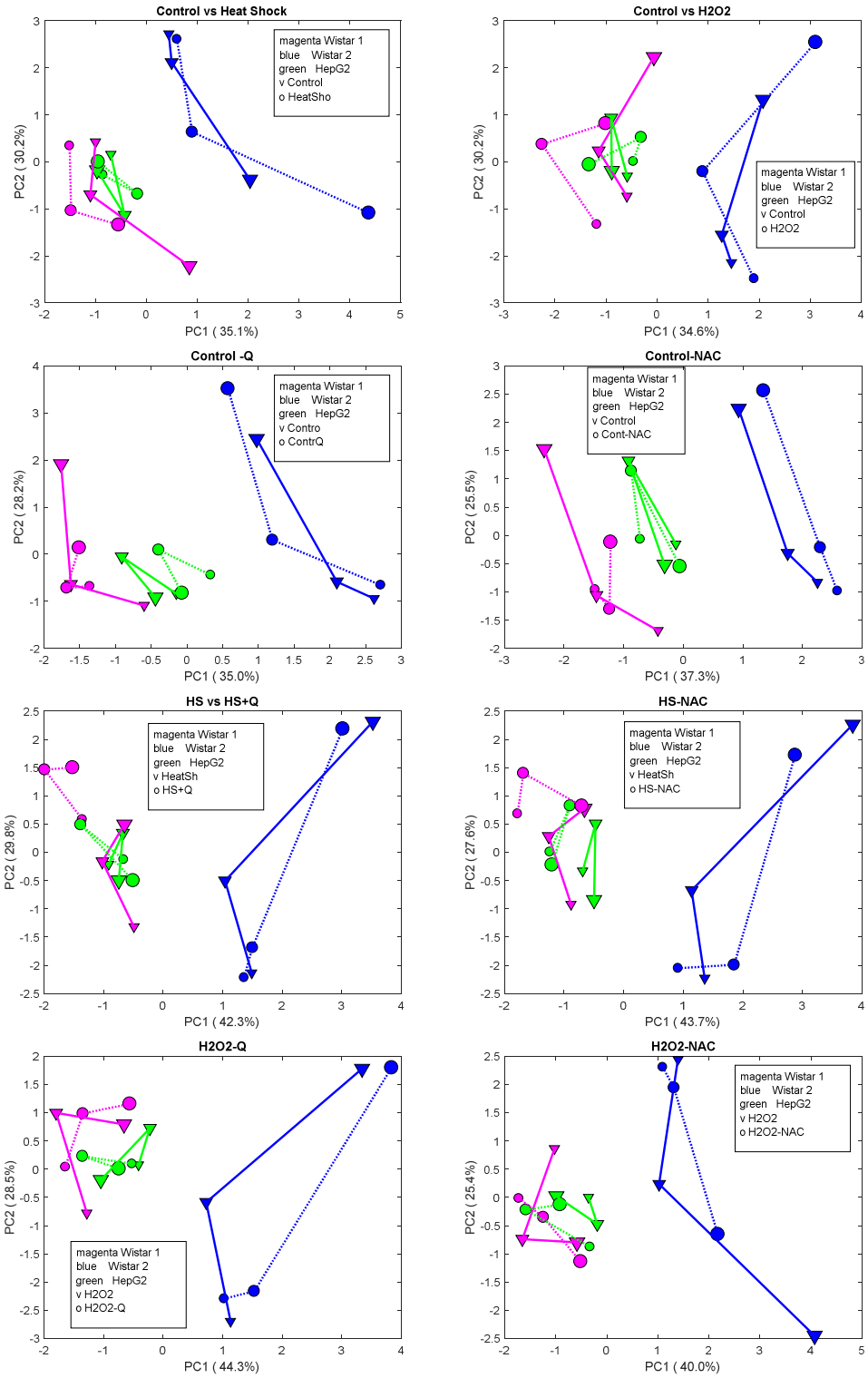

Supplementary Figure 4-5: Principal component analysis of the assay data for albumin, LDH, ROS, protein oxidation, GSH/GSSG, catalase and SOD from PRH of two individual Wistar rats (magenta: Wistar1, blue: Wistar2) and *HepG2* (green) (n=3). Hepatocytes were exposed to oxidative stress by heat or H_2O_2. Antioxidant effect of NAC and quercetin (dashed line) was estimated in relation to the respective control (solid line). Increasing size of the data symbol represents the progressing time after treatment.

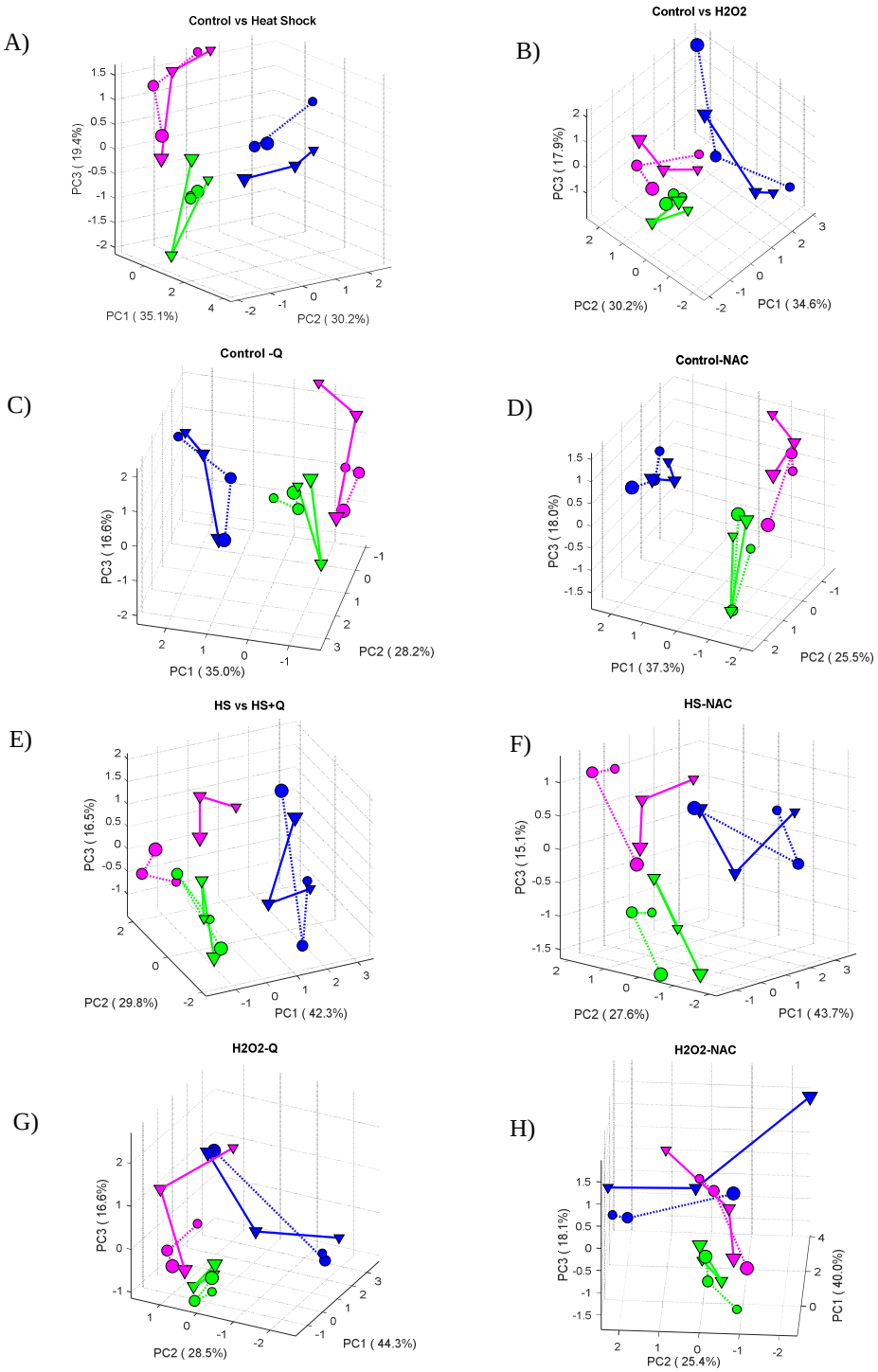

Supplementary Figure 4-6: 3D plots for the principal component analysis of the assay data for albumin, LDH, ROS, protein oxidation, GSH/GSSG, catalase and SOD from PRH of two individual Wistar rats (magenta: Wistar1, blue: Wistar2) and *HepG2* (green) (n=3). Hepatocytes were exposed to oxidative stress by heat or H_2O_2. Antioxidant effect of NAC and quercetin (dashed line) was estimated in relation to the respective control (solid line). Data symbols: v: respective control condition, ○: treated condition. Increasing size of the data symbol represents the progressing time after treatment.

10.3 Chapter 5

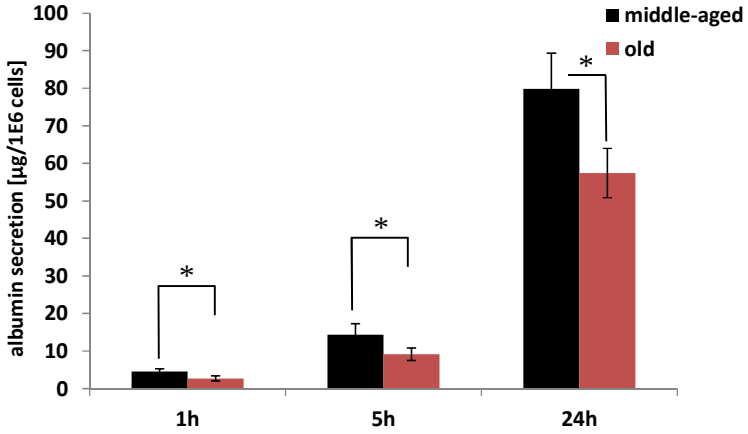

Supplementary Figure 5-1: Albumin secretion in [µg/1E6 cells] of middle-aged and old Sprague Dawley PRH 1 h, 5 h and 24 h after the start of the cultivation at 37 °C. Error bars indicate standard deviation (N=3, n=9). Statistical significance was determined with student's t-test. *, ** and *** indicate significance at p=0.05, p=0.01 and p=0.001. All results were correlated to the living cell number after 1 h, 5 h and 24 h of cultivation determined using calcein AM staining.

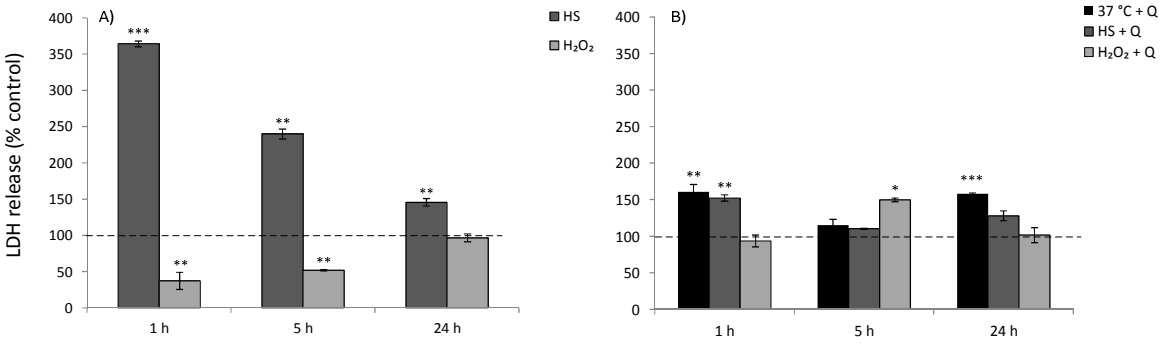

Supplementary Figure 5-2: LDH release of A) primary hepatocytes from middle-aged Sprague Dawley rat 3 under heat stress and H_2O_2 stress related to untreated control, B) primary hepatocytes from middle-aged Sprague Dawley rat 3 after 4 h pre-incubation with 50 µM quercetin in relation to the corresponding untreated and treated cells. Error bars indicate standard deviation (N=1, n=3). The dashed line represents the 100% marking. Statistical significance was determined with student's t-test. *, ** and *** indicate significance at p=0.05, p=0.01 and p=0.001. All results were correlated to the living cell number after 1 h, 5 h and 24 h of cultivation determined using calcein AM staining. Abbreviations: HS: heat stress; Q: quercetin.

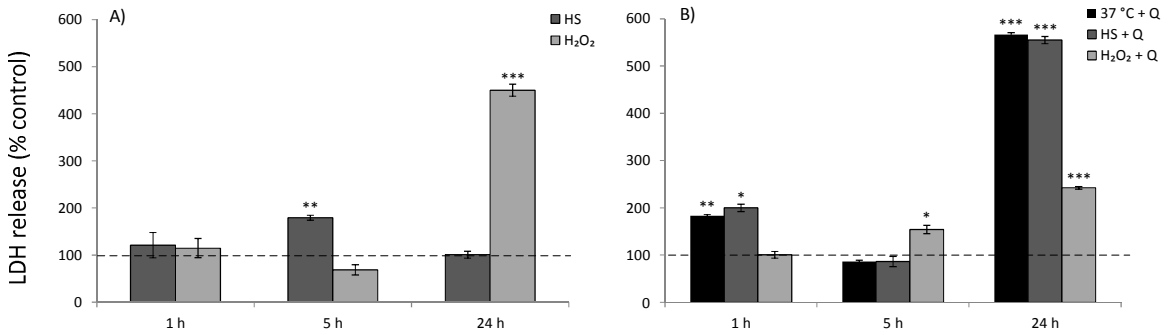

Supplementary Figure 5-3: LDH release of A) primary hepatocytes from old Sprague Dawley rat 3 under heat stress and H_2O_2 stress related to untreated control, B) primary hepatocytes from old Sprague Dawley rat 3 after 4 h pre-incubation with 50 µM quercetin in relation to the corresponding untreated and treated cells. Error bars indicate standard deviation (N=1, n=3). The dashed line represents the 100% marking. Statistical significance was determined with student's t-test. *, ** and *** indicate significance at p=0.05, p=0.01 and p=0.001. All results were correlated to the living cell number after 1 h, 5 h and 24 h of cultivation determined using calcein AM staining. Abbreviations: HS: heat stress; Q: quercetin.

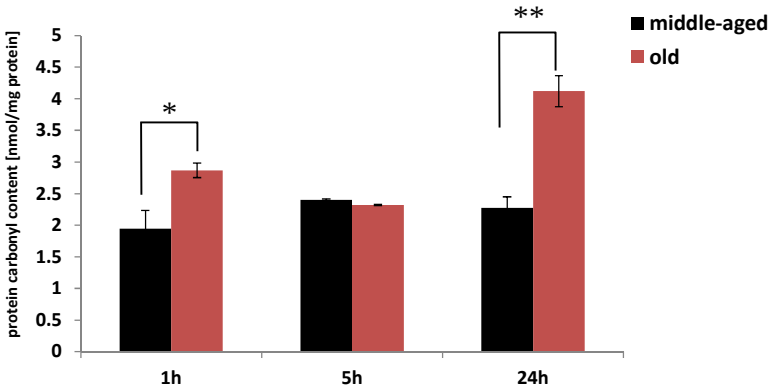

Supplementary Figure 5-4: Protein carbonyl content in [nmol/mg protein] of middle-aged and old Sprague Dawley PRH 1 h, 5 h and 24 h after the start of the cultivation at 37 °C. Error bars indicate standard deviation (N=3, n=9). Statistical significance was determined with student's t-test. *, ** and *** indicate significance at p=0.05, p=0.01 and p=0.001. All results were correlated to the living cell number after 1 h, 5 h and 24 h of cultivation determined using calcein AM staining.

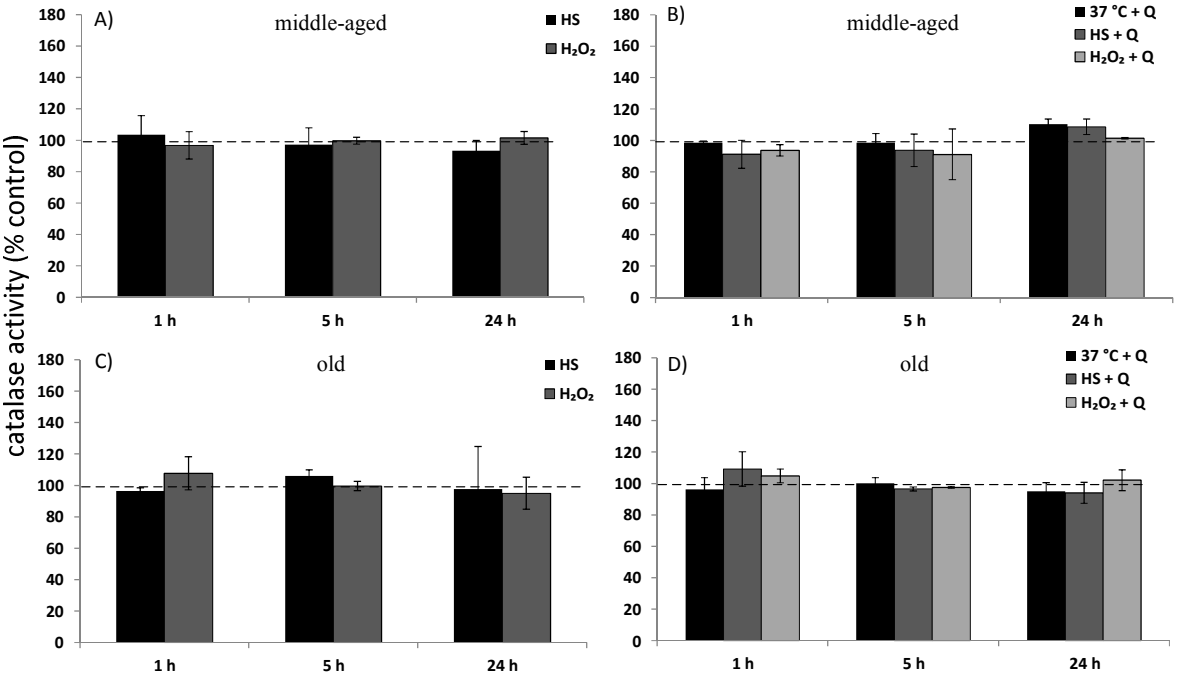

Supplementary Figure 5-5: Catalase activity of A) primary hepatocytes from middle-aged Sprague Dawley rats under heat stress and H_2O_2 stress related to untreated control, B) primary hepatocytes from middle-aged Sprague Dawley rats after 4 h pre-incubation with 50 µM quercetin in relation to the corresponding untreated and treated cells, C) primary hepatocytes from old Sprague Dawley rats under heat stress and H_2O_2 stress related to untreated control and D) primary hepatocytes from old Sprague Dawley rats after 4 h pre-incubation with 50 µM quercetin in relation to the corresponding untreated and treated cells. Error bars indicate standard deviation (N=3, n=3). The dashed line represents the 100% marking. Statistical significance was determined with student's t-test. *, ** and *** indicate significance at p=0.05, p=0.01 and p=0.001. All results were correlated to the living cell number after 1 h, 5 h and 24 h of cultivation determined using calcein AM staining. Abbreviations: HS: heat stress; Q: quercetin.

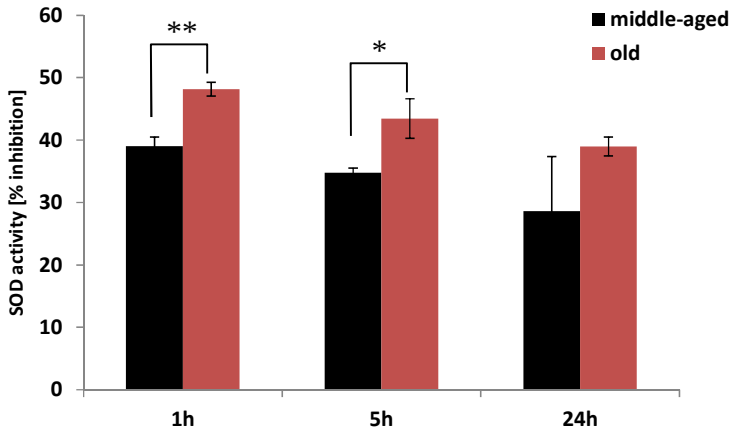

Supplementary Figure 5-6: SOD activity in [% inhibition [a]] of middle-aged and old Sprague Dawley PRH 1 h, 5 h and 24 h after the start of the cultivation at 37 °C. Error bars indicate standard deviation (N=3, n=9). Statistical significance was determined with student's t-test. *, ** and *** indicate significance at p=0.05, p=0.01 and p=0.001. All results were correlated to the living cell number after 1 h, 5 h and 24 h of cultivation determined using calcein AM staining.

[a] The SOD activity assay uses a xanthine/xanthine oxidase (XOD) system to generate superoxide anions. The included chromagen produces a water-soluble formazan dye upon reduction by superoxide anions. The activity of SOD is determined as the inhibition of chromagen reduction.

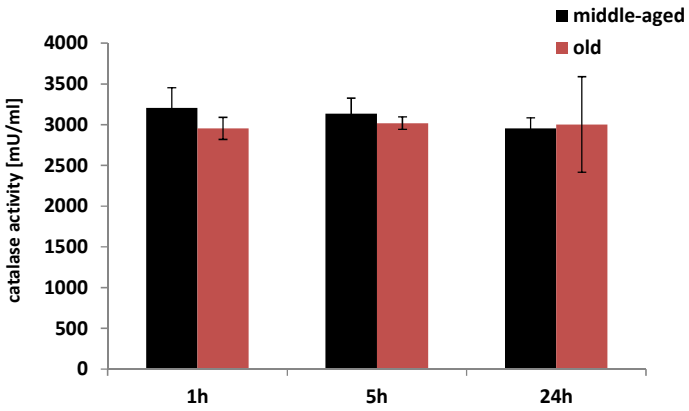

Supplementary Figure 5-7: Catalase activity in [mU/ml] of middle-aged and old Sprague Dawley PRH 1 h, 5 h and 24 h after the start of the cultivation at 37 °C. Error bars indicate standard deviation (N=3, n=9). Statistical significance was determined with student's t-test. All results were correlated to the living cell number after 1 h, 5 h and 24 h of cultivation determined using calcein AM staining.

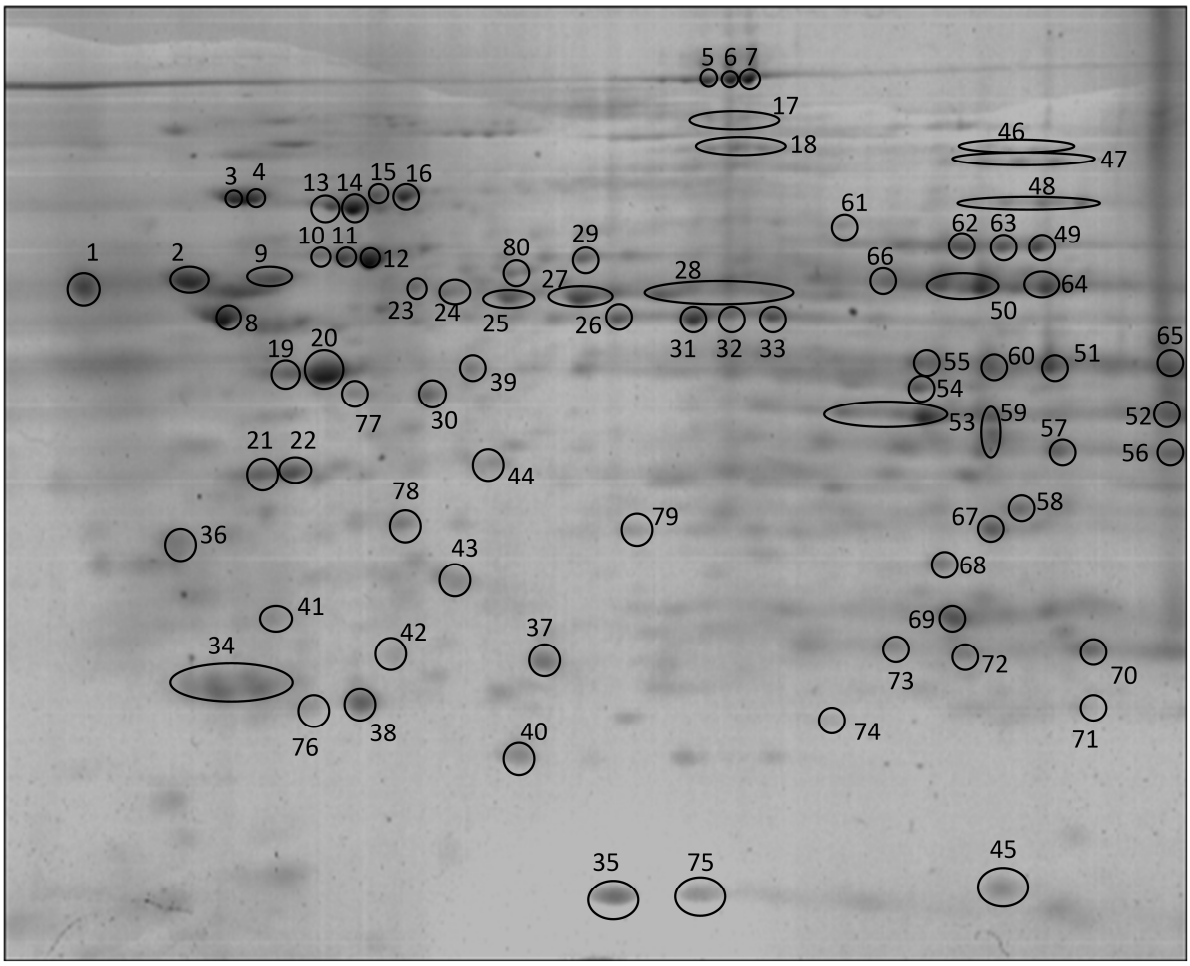

Supplementary Figure 5-8: 2-D gel electrophoresis of the intracellular proteome of PRH from SD rats. In total 80 proteins and protein isoforms could be identified with MALDI ToF MS/MS. Each spot is assigned to a protein in Supplementary Table 5-1.

Supplementary Table 5-1: List of all intracellular proteins of primary hepatocytes from SD rats identified with MALDI ToF MS/MS. Spot numbers correlate to Supplementary Figure 5-8.

Spot no.	Swiss-Prot Accession no.	Protein	Protein Function
1	P18418	Calreticulin	GO:0051082: unfolded protein binding
2	P04785	Protein disulfide-isomerase 1	GO:0019899: enzyme binding
3	P06761	78 kDa glucose-regulated protein	GO:0051787: misfolded protein binding GO:0034976: response to ER stress
4	P06761	78 kDa glucose-regulated protein	GO:0051787: misfolded protein binding GO:0034976: response to ER stress
5	P07756	Carbamoyl-phosphate synthase [ammonia]	GO:0000050: urea cycle GO:0042493: response to drug GO:0070365: hepatocyte differentiation
6	P07756	Carbamoyl-phosphate synthase [ammonia]	GO:0000050: urea cycle GO:0042493: response to drug GO:0070365: hepatocyte differentiation
7	P07756	Carbamoyl-phosphate synthase [ammonia]	GO:0000050: urea cycle GO:0042493: response to drug GO:0070365: hepatocyte differentiation
8	P10719	ATP synthase subunit beta, mitochondrial	GO:0006754: ATP biosynthetic process
9	D3ZZ80	Obscurin-like protein 1	GO:0051015: actin filament binding
10	P63039	60 kDa heat shock protein, mitochondrial	GO:0051787: misfolded protein binding GO:0009408: response to heat GO:0043065: positive regulation of apoptotic process
11	P63039	60 kDa heat shock protein, mitochondrial	GO:0051787: misfolded protein binding GO:0009408: response to heat GO:0043065: positive regulation of apoptotic process
12	P63039	60 kDa heat shock protein, mitochondrial	GO:0051787: misfolded protein binding GO:0009408: response to heat GO:0043065: positive regulation of apoptotic process
13	P63018	Heat shock cognate 71 kDa protein	GO:0051787: misfolded protein binding GO:0009408: response to heat GO:0043065: positive regulation of apoptotic process
14	P63018	Heat shock cognate 71 kDa	GO:0051787: misfolded protein binding

		protein	GO:0009408: response to heat GO:0043065: positive regulation of apoptotic process
15	P48721	Stress-70 protein, mitochondrial	GO:0009636 : response to toxic substance GO:0051787: misfolded protein binding
16	P48721	Stress-70 protein, mitochondrial	GO:0009636 : response to toxic substance GO:0051787: misfolded protein binding
17	P52873	Pyruvate carboxylase, mitochondrial	GO:0006094: gluconeogenesis
18	Q64380	Sarcosine dehydrogenase, mitochondrial	GO:0016491:oxidoreductase activity
19	P02651	Apolipoprotein A-IV	GO:0017127: cholesterol transporter activity
20	P60711	Actin, cytoplasmic 1	GO:0043044 :ATP-dependent chromatin remodeling
21	Q03336	Regucalcin	GO:1901671: positive regulation of SOD activity GO:0030234: enzyme regulator activity GO:0007568: aging
22	Q03336	Regucalcin	GO:1901671: positive regulation of SOD activity GO:0030234: enzyme regulator activity GO:0007568: aging
23	Q8VIF7	Selenium-binding protein 1	GO:0015031: protein transport
24	Q8VIF7	Selenium-binding protein 1	GO:0015031: protein transport
25	Q8VIF7	Selenium-binding protein 1	GO:0015031: protein transport
26	Q8VIF7	Selenium-binding protein 1	GO:0015031: protein transport
27	P11598	Protein disulfide-isomerase A 3	GO:0045471: response to ethanol GO:0008233: peptidase activity
28	P11884	Aldehyde dehydrogenase, mitochondrial	GO:0043066: negative regulation of apoptotic process
30	Q64640	Adenosine kinase	GO:0005524: ATP binding GO:0046872: metal ion binding
31	P04764	Alpha-enolase	GO:0031072: heat shock protein binding GO:2001171: positive regulation of ATP biosynthetic process
32	P10760	Adenosylhomocysteinase	GO:0071268: homocysteine biosynthetic process
33	P04764	Alpha-enolase	GO:0031072: heat shock protein binding GO:2001171: positive regulation of ATP biosynthetic process
34	P02761	Major urinary protein	GO:0005550: pheromone binding
35	P07632	Superoxide dismutase [Cu-Zn]	GO:0006979: response to oxidative stress

36	P22734	Catechol O-methyltransferase	GO:0032502: developmental process
37	O35244	Peroxiredoxin-6	GO:0098869: cellular oxidant detoxification
39	P13444	S-adenosylmethionine synthase, isoform type 1	GO:0016597: amino acid binding
40	P04916	Retinol-binding protein 4	GO:0005215: transporter activity
41	P04639	Apolipoprotein A-I	GO:0005319: lipid transporter activity
42	P02793	Ferritin light chain 1	GO:0006879: cellular iron ion homeostasis
43	P19132	Ferritin heavy chain	GO:0006879: cellular iron ion homeostasis
44	Q02974	Ketohexokinase	GO:0006000: fructose metabolic process
45	P19804	Nucleoside diphosphate kinase B	GO:0034599: cellular response to oxidative stress GO:0009142: nucleoside triphosphate biosynthetic process
46	Q9ER34	Aconitate hydratase, mitochondrial	GO:0006101: citrate metabolic process
47	P12346	Serotransferrin	GO:0006879: cellular iron ion homeostasis GO:0006953: acute-phase response
48	P50137	Transketolase	GO:0046390: ribose phosphate biosynthetic process
49	P04762	Catalase	GO:0034599: cellular response to oxidative stress
50	P10860	Glutamate dehydrogenase 1, mitochondrial	GO:0006537: glutamate biosynthetic process
51	P09034	Argininosuccinate synthase	GO:0000050: urea cycle GO:0007568: aging
52	P00884	Fructose bisphosphate aldolase B	GO:0006000: fructose metabolic process
53	P07824	Arginase-1	GO:0000050: urea cycle GO:0007568: aging
54	P25093	Fumarylacetoacetase	GO:0006527: arginine catabolic process
55	P15650	Long chain specific acyl-CoA dehydrogenase	GO:0044242: cellular lipid catabolic process
56	P04797	Glyceraldehyde-3-phosphate dehydrogenase	GO:0006096: glycolytic process
57	P04797	Glyceraldehyde-3-phosphate dehydrogenase	GO:0006096: glycolytic process
58	P13255	Glycine N-methyltransferase	GO:0005977: glycogen metabolic process
59	P00481	Ornithine carbamoyltransferase, mitochondrial	GO:0000050: urea cycle
60	P41562	Isocitrate dehydrogenase, cytoplasmic	GO:0006099: tricarboxylic acid cycle GO:0034599: cellular response to oxidative stress

61	P12928	Pyruvate kinase PKLR	GO:0006096: glycolytic process
62	P04762	Catalase	GO:0034599: cellular response to oxidative stress
63	P0C2X9	Delta-1-pyrroline-5-carboxylate dehydrogenase	GO:0010133: proline catabolic process to glutamate
64	Q4V8I9	UTP—glucose-1-phosphate uridylyltransferase	GO:0005977: glycogen metabolic process
65	P22791	Hydroxymethylglutaryl-CoA synthase, mitochondrial	GO:0006695: cholesterol biosynthetic process
66	P20673	Argininosuccinate lyase	GO:0000050: urea cycle GO:0007568: aging
67	P13803	Electron transfer flavoprotein subunit alpha	GO:0009055: electron transfer activity
68	Q497B0	omega amidase NIT2	GO:0006541: glutamine metabolic process
69	P14604	2 Enoyl-CoA hydratase	GO:0006635: fatty acid beta-oxidation
70	P04906	Glutathione S-transferase P 1	GO:0034599: cellular response to oxidative stress
71	Q63716	Peroxiredoxin-1	GO:0034599: cellular response to oxidative stress
72	P48500	Triosephosphate isomerase	GO:0006096: glycolytic process
73	B0BNN3	Carbonic anhydrase 1	GO:0006730: one-carbon metabolic process
74	P04041	Glutathione peroxidase 1	GO:0034599: cellular response to oxidative stress GO:0007568: aging
75	P07632	Superoxide dismutase [Cu-Zn]	GO:0006979: response to oxidative stress
76	P35704	Peroxiredoxin-2	GO:0034599: cellular response to oxidative stress
78	P02650	Apolipoprotein E	GO:0005319: lipid transporter activity GO:0007568: aging
79	D3ZNJ5	Thioether S-methyltransferase	GO:0009308: amine metabolic process
80	P04785	Protein disulfide isomerase associated 3, isoform CRA-a	GO:0045454: cell redox homeostasis GO:1902175: regulation of oxidative stress-induced intrinsic apoptotic signaling pathway

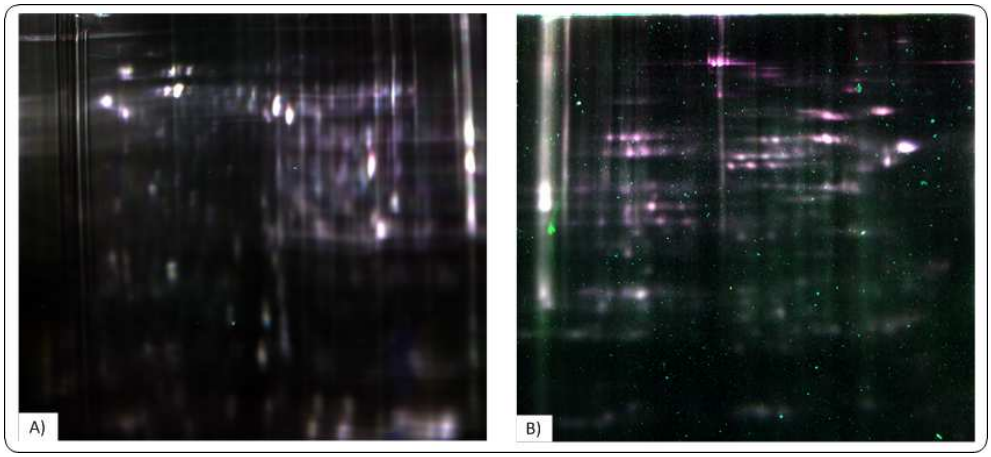

Supplementary Figure 5-9: Overlay of representative DIGE gels (pH 3-10) showing differential protein abundance in the intracellular proteome of old Sprague Dawley PRH after heat exposure. Comparison between control (37 °C) and heat-stressed (42 °C) PRH samples after (A) 5 h of cultivation and (B) 24 h of cultivation. Spots that are only present in control: green; heat-stressed: red; same abundance: white; (N=2, n=6).

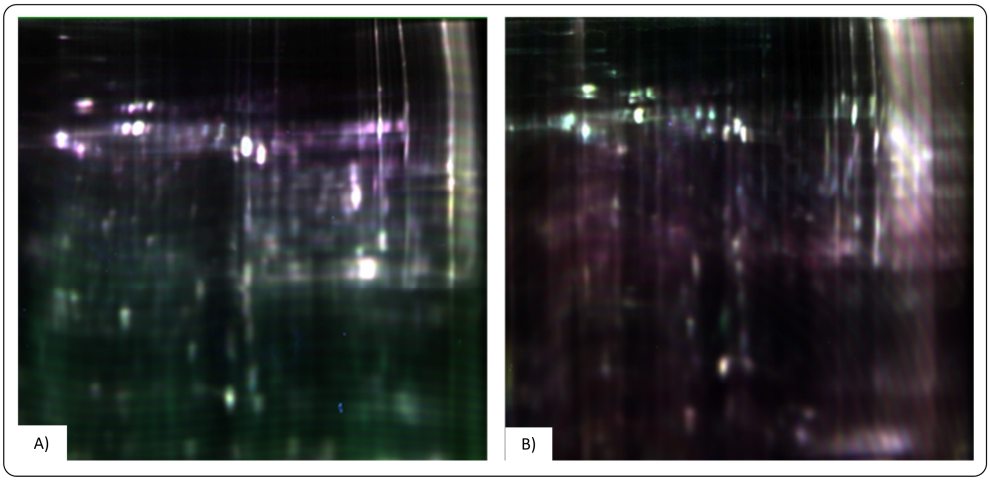

Supplementary Figure 5-10: Overlay of representative DIGE gels (pH 3-10) showing differential protein abundance in the intracellular proteome of Sprague Dawley PRH under heat stress conditions compared to PRH treated with 50 µM quercetin prior to heat stress. Proteome of A) middle-aged PRH after 1 h and B) old PRH after 5 h of cultivation (N=2, n=6).

10.4 Chapter 6

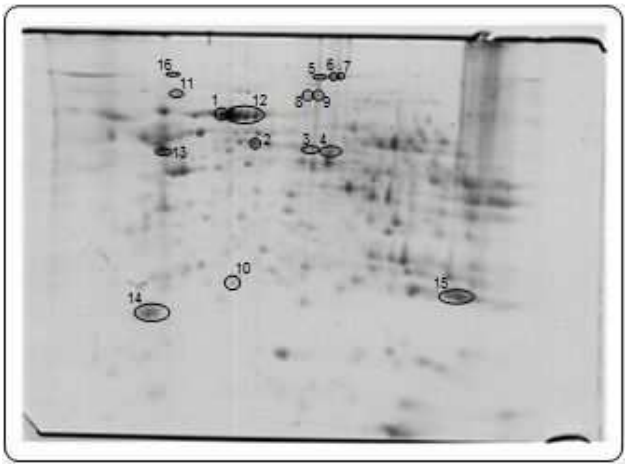

Supplementary Figure 6-1: 2-D gel electrophoresis of the intracellular proteome of PMH in ML culture at day 1 of cultivation. 1) 75 kDa glucose regulated protein 2) Selenium-binding protein 3 and 4) Aldehyde dehydrogenase 5, 6 and 7) Carbamoyl-phosphate synthase 8 and 9) Sarcosine dehydrogenase 10) Ferritin 11) Transitional ER ATPase 12) serum albumin 13) ATP synthase 14) Major urinary protein 16) Argininosuccinate synthase.

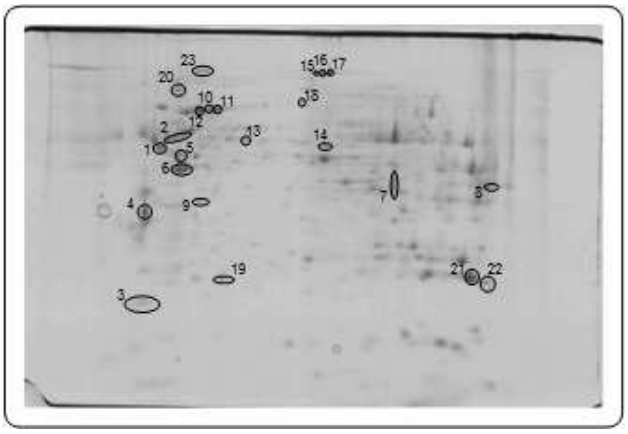

Supplementary Figure 6-2: 2-D gel electrophoresis of the intracellular proteome of PMH in ML culture at day 5 of cultivation. 1 and 2) ATP synthase, 3) Major urinary protein, 4) Regucalcin, 5 and 6) Actin, 7) Ornithine carbamoyltransferase, 8) Fructose bisphosphate aldolase, 9) Apolipoprotein E, 10 and 11) Serum albumin, 12) 75 kDa glucose regulated protein, 13) Selenium binding protein, 14) Aldehyde dehydrogenase, 15, 16 and 17) Carbamoyl-phosphate synthase, 18) Sarcosine dehydrogenase, 19) Ferritin, 20) Transitional ER, ATPase 21 and 22) Glutathione -S transferase.

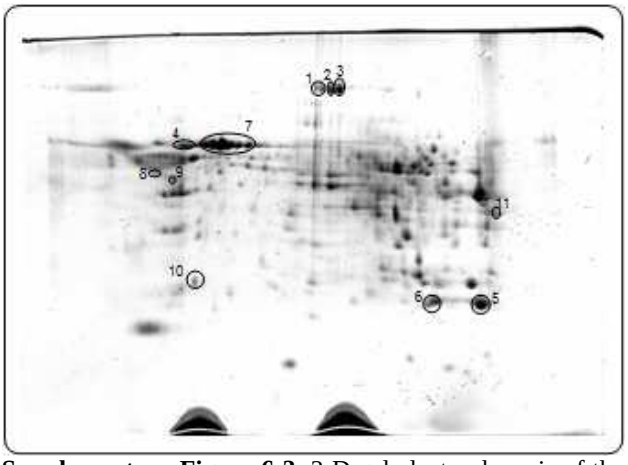

Supplementary Figure 6-3: 2-D gel electrophoresis of the intracellular proteome of PMH in SW culture at day 1 of cultivation. 1, 2 and 3) Carbamoyl phosphate synthase, 4) Protein disulfate isomerase, 5) Glutathione S transferase, 6) Superoxide dismutase, 7) Serum albumin, 8 and 9) ATP synthase, 10) Regucalcin, 11) Fructose-bisphosphate aldolase

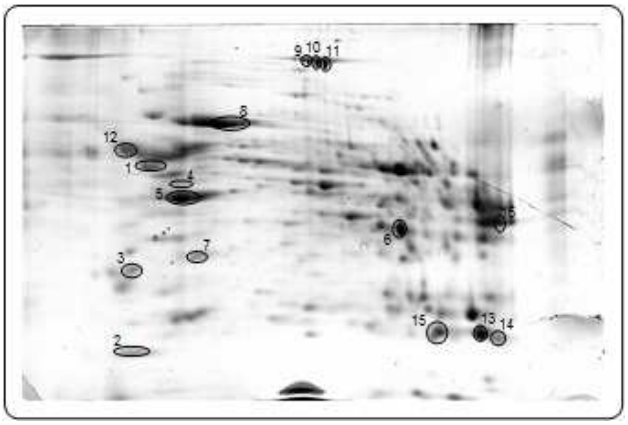

Supplementary Figure 6-4: 2-D gel electrophoresis of the intracellular proteome of PMH in SW culture at day 5 of cultivation. 1) ATP synthase, 2) Major urinary protein, 3) Regucalcin, 4 and 5) Actin, 6) Ornithine carbamoyltransferase, 7) Apolipoprotein E, 8, 9, 10 and 11) Carbamoylphosphate synthase, 12) Protein disulfate isomerase, 13 and 14) Glutathione S-transferase, 15) Superoxide dismutase, 16) Fructose-bisphosphate aldolase.

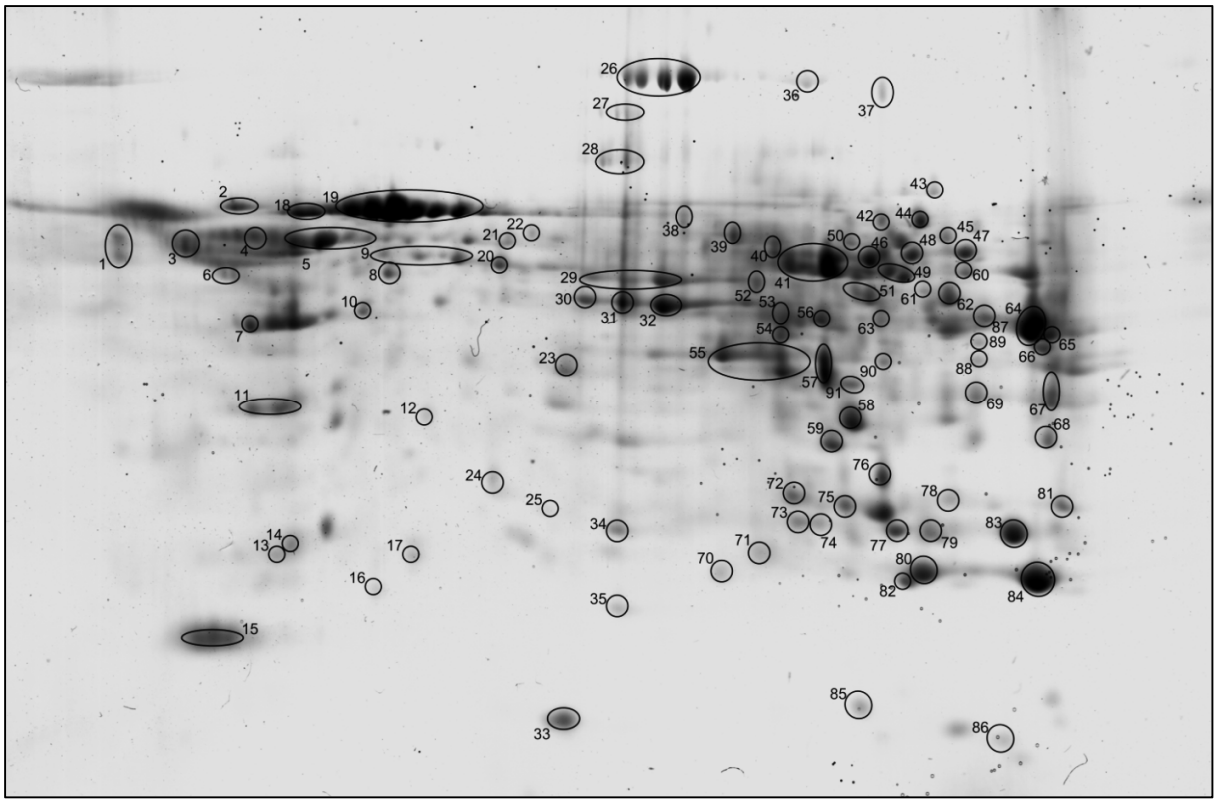

Supplementary Figure 6-5: 2-D gel electrophoresis of the intracellular proteome of PMH. In total 91 proteins and protein isoforms could be identified with MALDI ToF MS/MS. Each spot is assigned to a protein in Supplementary Table 6-1.

Supplementary Table 6-1: List of all intracellular proteins of primary mouse hepatocytes identified with MALDI ToF MS/MS. Spot numbers correlate to Supplementary Figure 6-5.

Spot no.	Protein
1	Calreticulin
2	78 kDa glucose-regulated protein
3	Protein disulfide-isomerase
4	Obscurin-like protein 1
5	60 kDa heat shock protein, mitochondrial
6	ATP synthase subunit beta, mitochondrial
7	Apolipoprotein A-IV
8	S-adenosylmethionine synthase isoform type-1
9	Selenium-binding protein 2
10	Adenosine kinase
11	Regucalcin

12	Ketohexokinase
13	Lactoylglutathione lyase
14	Apolipoprotein A-I
15	Major urinary protein
16	Ferritin light chain 1
17	Ferritin heavy chain
18	Heat shock cognate 71 kDa protein
19	Serum albumin
20	Selenium-binding protein 1
21	Bifunctional epoxide hydrolase 2
22	Carboxylesterase 3A
23	Fructose-1,6-bisphosphatase 1
24	Indolethylamine N-methyltransferase
25	Peroxiredoxin-4
26	Carbamoyl-phosphate synthase [ammonia],
27	Pyruvate carboxylase, mitochondrial
28	Sarcosine dehydrogenase, mitochondrial
29	Aldehyde dehydrogenase, mitochondrial
30	Alpha-enolase
31	Adenosylhomocysteinase
32	Alpha-enolase
33	Superoxide dismutase [Cu-Zn]
34	Peroxiredoxin-6
35	Retinol-binding protein 4
36	Keratin, type II cytoskeletal 73
37	Carbonic anhydrase 3
38	FAST kinase domain-containing protein 2
39	Triokinase/FMN cyclase
40	Pyruvate kinase PKLR
41	Glutamate dehydrogenase 1, mitochondrial
42	Transketolase
43	Aconitate hydratase, mitochondrial
44	Transketolase
45	Non-specific lipid-transfer protein
46	Catalase

47	Catalase
48	Delta-1-pyrroline-5-carboxylate dehydrogenase,
49	UTP--glucose-1-phosphate uridylyltransferase
50	Delta-1-pyrroline-5-carboxylate dehydrogenase,
51	Hydroxymethylglutaryl-CoA synthase, mitochondrial
52	Argininosuccinate lyase
53	Long-chain specific acyl-CoA dehydrogenase,
54	Fumarylacetoacetase
55	Arginase-1
56	Isocitrate dehydrogenase [NADP] cytoplasmic
57	Ornithine carbamoyltransferase, mitochondrial
58	Glycine N-methyltransferase
59	Electron transfer flavoprotein subunit alpha,
60	Retinal dehydrogenase 1
61	4-aminobutyrate aminotransferase, mitochondrial
62	Hydroxymethylglutaryl-CoA synthase, mitochondrial
63	Argininosuccinate synthase
64	Betaine--homocysteine S-methyltransferase 1
65	3-ketoacyl-CoA thiolase, mitochondrial
66	Acetyl-CoA acetyltransferase, mitochondrial
67	Glyceraldehyde-3-phosphate dehydrogenase
68	Hydroxyacyl-coenzyme A dehydrogenase,
69	Glyceraldehyde-3-phosphate dehydrogenase
70	Glutathione peroxidase 1
71	Glutathione S-transferase P 1
72	Phosphoglycerate mutase 1
73	Triosephosphate isomerase
74	Glutathione S-transferase Mu 1
75	Carbonic anhydrase 3
76	Carbonic anhydrase 3
77	Triosephosphate isomerase
78	Electron transfer flavoprotein subunit beta
79	Glutathione S-transferase Mu 1
80	Glutathione S-transferase
81	Electron transfer flavoprotein subunit beta

82	Superoxide dismutase [Mn], mitochondrial
83	Glutathione S-transferase Mu 1
84	Glutathione S-transferase P 1
85	Nucleoside diphosphate kinase B
86	Peptidyl-prolyl cis-trans isomerase A
87	Betaine--homocysteine S-methyltransferase 1
88	Fructose-bisphosphate aldolase B
89	Glutaryl-CoA dehydrogenase, mitochondrial
90	Ornithine carbamoyltransferase, mitochondrial
91	Alcohol dehydrogenase [NADP(+)]

Supplementary Table 6-2: Identified proteins, which were not significantly different in PMH cultivated in collagen ML culture and SW culture after 1 or 5 days of cultivation. DIGE analysis showed mean fold changes between – 1.5 and +1.5. Spot numbers correlate to Supplementary Figure 6-5. Swiss-Prot database information (http://www.uniprot.org).

Spot no.	Swiss-Prot Accession no.	Protein	Protein function
1	P14211	**Calreticulin**	response to hormones, cell cycle arrest
2	P20029	**78 kDa glucose-regulated protein**	protein folding, stress response
3	P09103	**Protein disulfide-isomerase**	oxidative stress response
4	D3YYU8	**Obscurin-like protein 1**	regulation of mitotic nuclear division
5	P63038	**60 kDa heat shock protein**	protein folding, stress response
7	P06728	**Apolipoprotein A-IV**	oxidative stress response
8	Q91X83	**S-adenosylmethionine synthase**	S-adenosylmethionine biosynthesis
10	P55264	**Adenosine kinase**	AMP synthesis from adenosine
12	P97328	**Ketohexokinase**	fructose catabolic process
13	Q9CPU0	**Lactoylglutathione lyase**	glutathione metabolic process
14	Q00623	**Apolipoprotein A-I**	lipid transport
16	P63017	**Heat shock cognate 71 kDa protein**	protein folding, inflammatory

			response
21	P34914	**Bifunctional epoxide hydrolase 2**	xenobiotic metabolism, lipid phosphatase activity
22	Q63880	**Carboxylesterase 3A**	xenobiotic metabolism
23	Q9QXD6	**Fructose-1,6-bisphosphatase**	gluconeogenesis
24	P40936	**Indolethylamine N-methyltransferase**	response to toxic substances
25	O08807	**Peroxiredoxin-4**	oxidative stress response
27	Q05920	**Pyruvate carboxylase**	gluconeogenesis
30	P17182	**Alpha-enolase**	glycolytic process
31	P50247	**Adenosylhomocysteinase**	amino-acid biosynthesis
34	O08709	**Peroxiredoxin-6**	oxidative stress response
35	Q00724	**Retinol-binding protein 4**	response to insulin
37/75/76	P16015	**Carbonic anhydrase 3**	oxidative stress response
38	Q922E6	**FAST kinase domain-containing protein 2**	assembly of the mitochondrial large ribosomal subunit
39	Q8VC30	**Triokinase/FMN cyclase**	cellular carbohydrate metabolic process
40	P53657	**Pyruvate kinase PKLR**	glycolysis
41	P26443	**Glutamate dehydrogenase 1, mitochondrial**	TCA cycle
42	P40142	**Transketolase**	binds cofactors and metal ions
43	Q99KI0	**Aconitate hydratase**	TCA cycle
45	P32020	**Non-specific lipid-transfer protein**	steroid biosynthetic process
46/47	P24270	**Catalase**	oxidative stress response
48/50	Q9Z110	**Delta-1-pyrroline-5-carboxylate dehydrogenase**	cellular amino acid biosynthetic process
49	Q91ZJ5	**UTP-glucose-1-phosphate uridylyltransferase**	glucosyl donor in cellular metabolic pathways
52	Q91YI0	**Argininosuccinate lyase**	L-arginine biosynthesis, urea cycle
53	P51174	**Long-chain specific acyl-CoA dehydrogenase**	mitochondrial fatty acid beta-oxidation
54	P35505	**Fumarylacetoacetase**	amino-acid degradation
55	Q61176	**Arginase-1**	urea cycle

56	O88844	**Isocitrate dehydrogenase [NADP] cytoplasmic**	TCA cycle
58	Q9QXF8	**Glycine N-methyltransferase**	gluconeogenesis
59	Q99LC5	**Electron transfer flavoprotein subunit alpha**	fatty acid beta-oxidation
60	P24549	**Retinal dehydrogenase 1**	retinol metabolic process
61	P61922	**4-aminobutyrate aminotransferase, mitochondrial**	response to ethanol and hypoxia
52/62	P54869	**Hydroxymethylglutaryl-CoA synthase, mitochondrial**	response to various stress stimuli
63	P16460	**Argininosuccinate synthase**	urea cycle
64/87	O35490	**Betaine-homocysteine S-methyltransferase 1**	amino-acid biosynthesis
65	Q921H8	**3-ketoacyl-CoA thiolase, mitochondrial**	lipid metabolism
66	Q8QZT1	**Acetyl-CoA acetyltransferase, mitochondrial**	response to hormones and starvation
67/69	P16858	**Glyceraldehyde-3-phosphate dehydrogenase**	glycolysis
68	Q61425	**Hydroxyacyl-coenzyme A dehydrogenase**	lipid metabolism
70	P11352	**Glutathione peroxidase 1**	response to oxidative stress
72	Q9DBJ1	**Phosphoglycerate mutase 1**	glycolysis regulation
73/77	P17751	**Triosephosphate isomerase**	glycolysis
78/81	Q9DCW4	**Electron transfer flavoprotein subunit beta**	fatty acid beta-oxidation
85	Q01768	**Nucleoside diphosphate kinase B**	Nucleotide metabolism
86	P30416	**Peptidyl-prolyl cis-trans isomerase A**	response to mitochondrial oxidative stress
89	Q60759	**Glutaryl-CoA dehydrogenase, mitochondrial**	amino-acid metabolism
91	Q9JII6	**Alcohol dehydrogenase [NADP(+)]**	response to xenobiotics and drugs

Danksagung

Prof. Dr. Elmar Heinzle danke ich vielmals für die Möglichkeit meine Dissertation in seiner Arbeitsgruppe durchführen zu können und die Bereitstellung dieses äußerst interessanten Themas. Vielen Dank für die vielen hilfreichen Diskussionen und die konstruktive Kritik, die meine Arbeit vorangebracht haben.
Ich danke Prof. Dr. Gert-Wieland Kohring vielmals für die Übernahme der Zweitkorrektur dieser Arbeit. Dr. Fozia Noor danke ich für ihre Betreuung und die Leitung des „Zoiga-Labs“. Ein besonderer Dank gilt Dr. Saskia Sperber für die tolle Zusammenarbeit beim Thema Proteomanalyse in Sandwich-Kulturen, die zu unserer gemeinsamen Publikation geführt hat. Ebenfalls danken möchte ich Esther Hoffmann, die ebenfalls einen großen Beitrag zu dieser Arbeit geleistet hat. Vielen lieben Dank!
Allen Partnern des BMBF Projektes „Oxisys“ danke ich für die gute Kooperation über den gesamten Projektzeitraum hinweg. Dr. Kathrin Zeilinger danke ich für die hervorragende Koordination des Projektes und Dr. Ursula Müller-Vieira für die Versorgung mit primären Rattenhepatozyten.
Dr. Klaus Hollemeyer danke ich für seine Unterstützung rund um das Thema MALDI und seine zahlreichen Anekdoten in den Mittagspausen. Dr. Susanne Kohring möchte ich herzlichst für ihre allgegenwärtige Unterstützung in allen organisatorischen Fragen danken.
Der gesamten Arbeitsgruppe der Technischen Biochemie möchte ich für das gute Arbeitsklima während der letzten Jahre danken! Richa Garg danke ich für ihre Unterstützung im Team „Oxisys“. Ein großer Dank gebührt meinen Freunden Judith Wahrheit, Saskia Sperber, Christian Priesnitz, Sebastian Klein, Esther Hoffmann, Mirjam Selzer und Inês Miranda Santos für die schöne Zeit und die gemeinsam verbrachten Feierabende! Besonders möchte ich hier noch meinen Freunden Christian Weyler, Lisa Schuh und Yeda Kaminski danken, die mich immer unterstützt haben und auch die Arbeit in kleiner Runde zu einer unvergesslichen Zeit gemacht haben!
Zum guten Schluss danke ich meiner Mutter, Isa Orsini, die immer an mich geglaubt hat und ohne die diese Dissertation nicht möglich gewesen wäre. Vielen Dank!